Acetylation Control of the Retinoblastoma Tumour Suppressor Protein.

Douglas James Markham

To

The Institute of Biomedical and Life Sciences,

University of Glasgow

for the degree of

Doctor of Philosophy

January 2006

Division of Biochemistry and Molecular Biology

Institute of Biomedical and Life Sciences

University of Glasgow

Abstract

The work presented in this thesis concentrates on the functional consequences of acetylation upon the retinoblastoma tumour suppressor protein (pRb), the activity of which is frequently, if not universally, de-regulated in tumour cells. This study has shown that the acetylation of pRb at lysine (K) residues 873/874 reduces the interaction of E2F-1 with the carboxyl terminal (C-terminal) region of pRb. In turn this acetylation event promotes the association of the C-terminal region of pRb with its amino terminal (N-terminal) domain (residues 1-378). A further aspect of this study suggests that acetylation may result in a change of pRb localization from the nucleus to the cytoplasm. Moreover it is also shown that the N-terminal of pRb is acetylated *in vitro* and in cells. These results suggest a model whereby the acetylation of pRb at E2F-1 target genes results in a reduced interaction between the C-terminal of pRb and E2F-1. Another ramification of the model implies that the N-terminal region of pRb interacts with the C-terminal region in response to DNA damage induced acetylation of pRb. This interaction may influence the bipartite nuclear localization signal (NLS) within the C-terminal domain, thus providing a possible mechanism for retaining pRb localised to the cytoplasm. These results highlight a new mechanism through which pRb may mediate tumour suppressor activity, and in addition define a previously undescribed pathway through which acetylation can influence growth control.

Acknowledgements

I am greatly indebted to the Medical Research Council for providing me with funding to make this study possible.

I would also like to thank Prof. Robert White and Prof. Gordan Lindsay for their advice and guidance during my studies. Also my sincere thanks to Dr Costas Demonacos, Dr Marija Kristic-Demonacos, Dr Amanda Coutts and Mrs Linda Smith, and for those who assisted this study and taught me in many aspects.

My most sincere thanks and gratitude are due to Prof. Nicholas B. La Thangue, who supervised my research project during the last 4 years. I thank him for the advice, guidance, and encouragement he gave at crucial times. Through his generosity, understanding and support, I am able to present this thesis.

I would also like to thank all the people who assisted this study, giving their time to help teach me techniques, or to offer advice. Firstly I would like to thank Judith Soloway who helped me a lot when I started my study in the Cathcart Laboratory. Also thanks go to Dr Sheila Harris, Dr Darran O'Connor, Dr Craig Stevens, Dr Oonagh Laughran, Dr Sharon Sheehan, Dr Laurent Delavaine, Dr Houda Boulahbel, Dr Alastair Milton, Dr Shonagh Munro, Dr Carmel O'Riley, Dr Nandkumar Khaire, Martin Jansson, Adam Inche, Kaisa Luoto, and Anne Graham who taught me various aspects of molecular biology. I would also like to thank other colleagues who contributed through their advice and support including; Dr Steven France, Dr Sarah Mason, Nicola Logan, Julia Dunlop, Susan Fotheringham, Danmei Xu, Dr Xiujie Zhao and Rebecca Fisher.

Special thanks go to Dr Alan Vereaux (CRUK) whose advice on insect cell lines and baculovirus expression systems were priceless.

Abbreviations

A	Alanine
Ac	Acetylated
ActD	Actinomycin D
Ad	Adenovirus
AML	Acute myeloid leukaemia
β-gal	β-galactosidase
bp	Base pair
BSA	Bovine serum albumin
C	Cysteine
CAK	Cdk-activating kinase
cAMP	Cyclic adenosine mono-phosphate
CAT	Chloramphenicol acetyltransferase
CBP	CREB-binding protein
Cdk	Cyclin dependent Kinase
CDKI	Cdk inhibitors
C/EBP	CCAAT-box/enhancer-binding protein
CH	Casein Kinase
Chk	Check-point kinase
CKI	Cyclin dependent kinase inhibitor
CMV	Cytomegalovirus
CNS	Central Nervous System
Co-IP	Co-immunoprecipitation
CR	Conserved region (in the adenovirus E1A protein)
C-pRb	The carboxyl terminal region of pRb (residues 763-928)
CRE	cAMP-response element
CREB	CRE-binding protein
CtIP	C-terminal binding protein (CtBP) interacting protein
DHFR	Dihydrofolate reductase
DMEM	Dublecco's modified Eagle's medium
Dox	Doxorubicin
dNTP	Deoxy-nucleoside triphosphate
DTT	Dithiothreitol
E	Glutamic acid
EDTA	Ethylene diamine tetra-acetic acid
E2F-1	Early-region-2 transcription-factor-1
EGF	Epidermal growth factor
ER	Oestrogen receptor
Et	Etoposide
FCS	Foetal calf serum
FITC	Fluorescein isothiocyanate
FL	Full Length
FL-pRb	Full length retinoblastoma protein (residues 1-928)
FPLC	Fast protein liquid chromatography
GST	Glutathione-S-transferase
HA	Hemaglutinin protein (derived from influenza virus)
HA-C-pRb (wt)	HA tagged pRb (residues 763-928)
HA-C-pRb QQ	HA-C-pRb mutated at K residues 873/874 to Q
HA-C-pRb RR	HA-C-pRb mutated at K residues 873/874 to R
HA-N-pRb	HA tagged pRb (residues 1-376)
HA-pRb (wt)	HA tagged pRb (residues 1-928)

HA-pRb QQ	HA-pRb mutated at K residues 873/874 to Q
HA-pRb RR	HA-pRb mutated at K residues 873/874 to R
HAT	Histone acetyl-transferase
HBP	High mobility group (HMG)-box protein
HDAC(s)	Histone deacetylase(s)
Hdm2	Human double minute 2
HEPES	N-[2-Hydroxethyl]piperazine-N'-[2-ethanesulfonic acid]
His	Histidine tag
HPV	Human papilloma virus
IB	Immunoblotting
IP	Immunoprecipitation
IPTG	Isopropyl-β-D-thiogalactopyranoside
IR	Ionising irradiation
IVT	In vitro translated
JMY	Junction-mediating and regulatory protein
K	Lysine
KIX	Kinase inducible domain
L	Leucine
LB	Luria-Bertani medium
LOH	Loss of heterozygosity
LT	Large T antigen
Luc	Luciferase
M	Methionine
MAPK	Mitogen-activated protein kinases
Mdm2	Murine double minute 2
MEF's	Mouse embryonic fibroblasts
MOI	Multiplicity of infection
MOZ	Monocytic leukemia zinc-finger
Mut	Mutant
MyoD	Myogenic helix-loop-helix (HLH) transcription factor
NLS	Nuclear localization signal
nm	Nano metres
NP-40	Nonidet P-40
N-pRb	N-terminal of pRb residues 1 to 379
P	Proline
PP	Pocket protein
PAGE	Polyacrylamide gel electrophoresis
PBS	Phosphate buffered saline
P/CAF	p300/CBP-associated factor
PcG	Polycomb group protein
PCR	Polymerase chain reaction
PI3K	Phosphoinositol, 3, Kinase.
PMSF	Phenylmethylsulfonyl fluoride
PNS	Peripheral Nervous System
Pol	RNA polymerase
pRb	Retinoblastoma protein
ptm	Post-translational modification
Q	Glutamine
QQ	pRb derivative (mutated at K873/874 to Q873/874)
Rb	Retinoblastoma gene 1
Rpm	Revolutions per minute
R	Arginine
RR	pRb derivative (mutated at K873/874 to R873/874)
Rb	Rb gene

S	Serine
SCF	Skp-Cullin-F box
SDS	Sodium dodecyl sulfphate
SRC-1	Steroid receptor co-activator 1
STAT	Signal transducer and activator of transcription
SV40	Simian virus 40
T	Threonine
TAD	Trans-activation domain
TAF	TBP-associated factor
TBP	TATA binding protein
TCF	T-cell factor
TGFβ	Transforming growth factor β
TNF	Tumour necrosis factor
TSA	Trichostatin A
TK	Thymidine kinase
TR	Thyroid hormone
Tris	Tris (hydroxymethyl)methylamine
Tween 20	Polyoxyethylene sorbitan monolaurate
UBF	Upstream binding factor
UV	Ultraviolet light
VP16	Virion protein 16 trans-activation domain
W	Tryptophan
wt	Wild-type
w/v	Weight per volume
YY1	Ying yang 1
(+/+)	Wild-type
(+/-)	Hetrozygous mutant
(-/-)	Homozygous mutant

Publications

The following publication was submitted and published during the course of the work presented in this thesis.

Markham, D., Munro, S., Soloway, J., O'Connor D, P., La Thangue, N. B. 2005. DNA-damage-responsive acetylation of pRb regulates binding to E2F-1. EMBO Reports (Accepted and available online at http://www.nature.com/embor/index.html)

Table of Contents

Table of Figures

INTRODUCTION

CHAPTER 3

CHAPTER 5

PREFACE:

It is apparent that many transcription factors have multiple roles, often in different cellular processes. In particular, some transcription factors appear to have roles in two opposing processes. In order to coordinate cellular processes, protein function is regulated by post-translational modification. This thesis is concerned with the later. Post-translational modification can affect a protein in different ways. Modification of amino acid residues alters the chemical reactivity and the physical characteristics of the amino acid residue. This can affect the secondary or tertiary structure of the protein, or simply affect the local binding surface around the site of the modification. Many proteins interact with each other via specific peptide consensus sequences. Post-translational modification of a protein can therefore alter its affinity for binding partners.

As an analogy, changes in our hormone levels (triggered by shock) can transiently effect changes in our mood and physiology. Similarly post-translational modification can affect protein function in response to external factors in the cells microenvironment. Proteins can change their partners, their location, and their function as a result of posttranslational modifications. Upstream signalling pathways directly transmit stimuli emanating from the cell membrane to effect changes in post-translational modification and hence gene expression in the nucleus [8].

The transcription factors pRb, E2F-1 and p53 all have multiple functions that are tightly regulated by post-translational modification. These proteins play key roles in processes such as tumour suppression, control of proliferation, apoptosis, differentiation, foetal development and DNA repair. If a cell loses its ability to control the post-translational modification of these proteins, the resulting change in cellular physiology can augment the process of tumour formation and progression. Conversely, certain drugs that

control post-translational modification are now being utilized to treat cancers, in particular HDAC inhibitors [271].

My studies have centred on post-translational modification of proteins involved in controlling the cell cycle, particularly concentrating on the affect of acetylation on the retinoblastoma tumour suppressor protein (pRb), and the effect on the E2F-1 transcription factor. This study has uncovered some new insights into the functional consequence of pRb acetylation in response to DNA damage. Damage responsive acetylation of pRb appears to affect the interaction between the carboxyl terminal region of pRb and E2F-1. It is possible that damage-responsive acetylation of pRb releases E2F-1 to activate specific genes that promote apoptosis.

The N-terminal domain of pRb is the single largest domain of the protein, spanning the first 378 amino acids. Until recently, this domain was thought to be involved in processes not related to the role of pRb tumour suppression and control of proliferation. My study suggests that the N-terminal region of pRb may play an important regulatory role by facilitating various changes in the conformation of pRb bought about by acetylation. Overall, this study has illuminated new levels of control in pRb, and defined previously unrecognized pathways influenced by acetylation.

INTRODUCTION

THE PATH TO NEOPLASIA

A cell becomes cancerous due to a combination of factors; excessive proliferation (the loss of cell cycle control), an ability to survive (loss of apoptotic control), and an ability to modify its environment (its supply of blood and nutrients). The development of neoplasia (cancer) is therefore a multistage process, each step characterised by distinct genetic changes (mutations). Many of the oncogenes mutated in the initiation and promotion of healthy cells to cancerous cells are involved in controlling progression through the cell cycle (Figure 1a).

THE CELL CYCLE

The cell cycle is divided into four phases (Growth phase 1 (G1) → Synthetic (S)-phase→ Growth phase 2 (G2)→ Mitosis (M)-phase) [1]. There are two basic events in cell division; generation of a single copy of its genetic material (S-phase), and the partition of the cellular components between two identical daughter cells (M-phase). The two other phases of the cycle, G1 and G2, represent gap periods during which cells prepare themselves for the successful completion of the S- and M- phases. Cells may also enter a quiescent state (G0) in response to specific anti-mitogenic signals, or to the absence of proper mitogenic signalling (Figure 1b) [2].

CONTROLLING PROGRESSION THROUGH THE CYCLE

In order to ensure controlled progression through the cell cycle, cells have developed a series of checkpoints that prevent them from entering into a new cell cycle phase until they have successfully completed the previous one [3].

Figure 1

a)

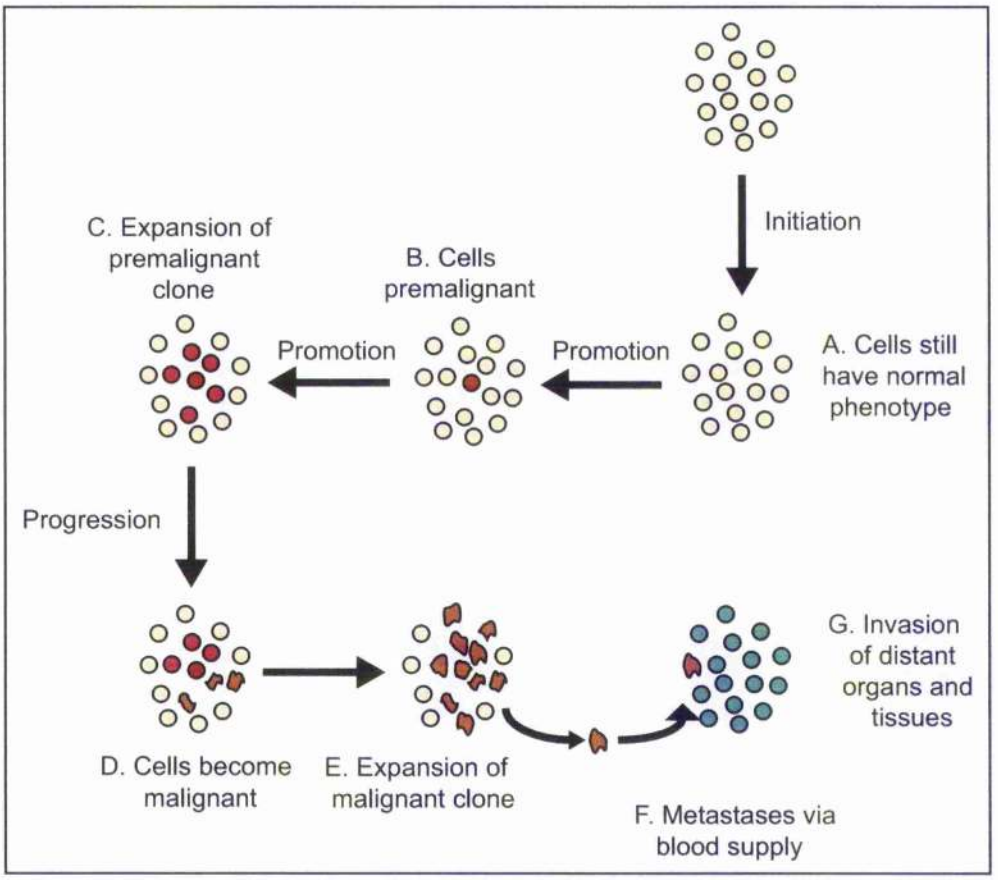

Adapted from [2], and [25]

Figure 1

b)

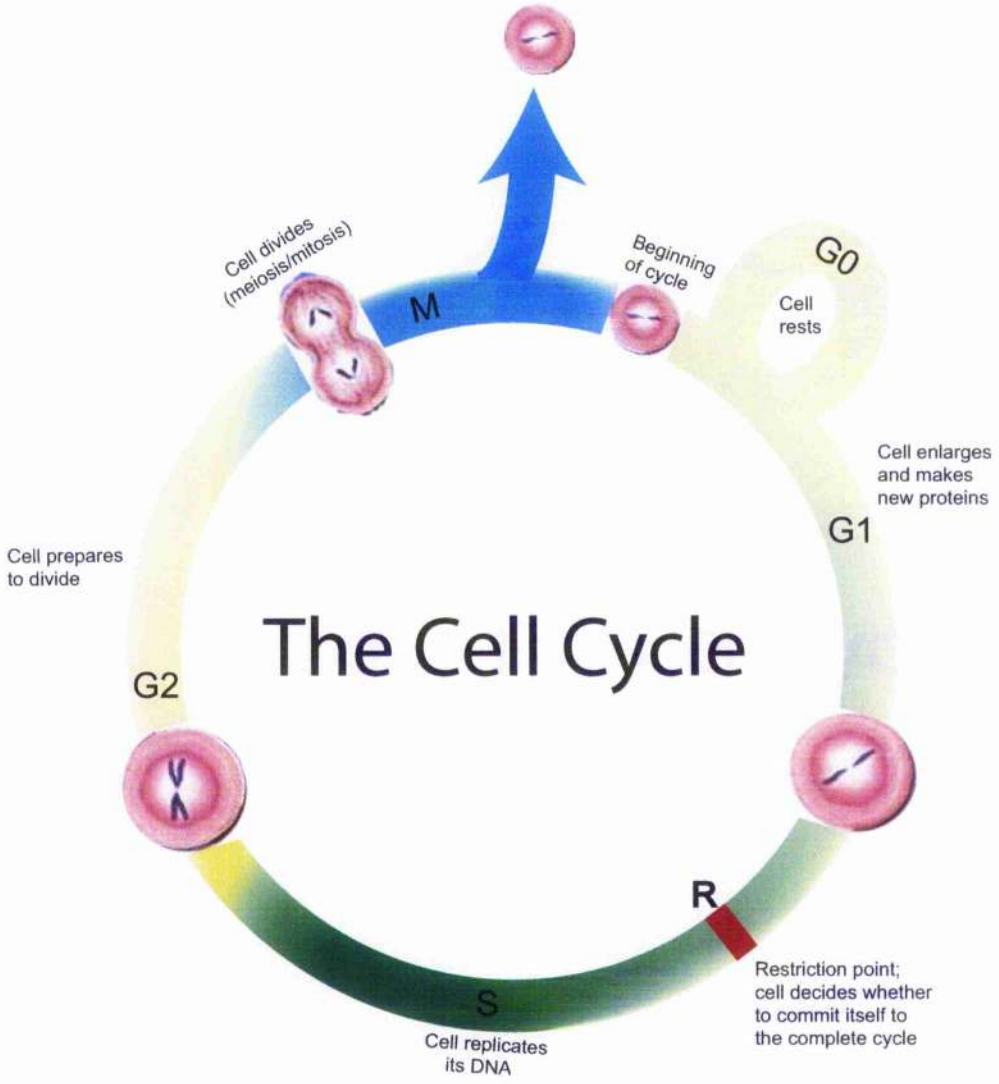

Adapted from the website: http://learninglab.co.uk/headstart/cycle3.htm
Authors: Gresty, K., & Dryden, R.

Figure 1: The cancer cell cycle

a) The pathway to neoplasia

In order to transform and become malignant, pre-cancerous cells develop progressive mutations in genes whose protein products regulate cellular processes (such as proliferation and apoptosis). As mutations accumulate (Steps A to B to C), premalignant cells develop into a small tumour mass. Further mutation enables the premalignant cells to bypass all controls on proliferation and apoptosis (Steps C to D) and hence they become malignant. Malignant cells replicate and dominate the tumour mass (Steps D to E). Malignant cells mutate further still and become capable of existing without local survival factors. Mutation occurs in genes that control cell/cell adhesion, and malignant cells detach from the tumour mass (Steps E to F). Metastasis of the tumour occurs through the blood and lymphatic systems, and migrating tumours may find their way into other organs where they develop further (Step G).

b) Depicts the cell cycle

There are 4 phases of the cell cycle, G1 (Growth phase) in which cells grow and prepare for S-phase, S-phase (DNA synthesis) in which DNA is duplicated, G2 (Growth phase 2) in which the cell prepares for mitosis, and M-phase (Mitosis phase) in which cells divide their nuclear and cytoplasmic content to create 2 daughter cells.

Quiescent cells and newly divided cells must pass certain checkpoints to progress through the cycle. These checkpoints function to make sure that cells reach their homeostatic size, otherwise cells would decrease in size with each round of division [2]. A cell's passage through checkpoints can be influenced by any incurred DNA damage, the availability of nutrients, or the intensity of mitogenic information that cells receive at any given time.

After mitosis, cells undergo a period of mitogen dependence, before deciding whether or not to enter the cell cycle. A transition then occurs when cells are no longer dependent on mitogenic signals. The transition between the two states was coined the 'Restriction Point' by Arthur Pardee in 1974 (Figure 1b) [4]. The restriction point (R) represents the point of no return that commits cells to a new round of cell division. The molecular events that allow cells to pass through the (R) have not been thoroughly elucidated. It has been shown that members of the retinoblastoma (Rb) family of proteins play key roles. Indeed ablation of this gene family eliminates (R) [5].

MITOGENIC STIMULATION DURING THE G1/S PHASE TRANSITION OF THE CELL CYCLE

Extra-cellular ligands trigger various processes such as proliferation and differentiation through receptor activation. Differentiation is triggered by neurotrophic factors, such as nerve growth factor (NGF). On the other hand, proliferation is triggered by mitogenic factors, such as epidermal growth factors (EGF). Other anti-mitogenic factors such as TGFβ are released in response to contact inhibition [6]. Cellular stress such as those generated by inflammatory cytokines mediates inflammation response, apoptosis, and developmental pathways (Figure 2a).

Upon ligand binding, cell surface receptors activate their particular cell signalling cascade. These cascades eventually signal through to the nucleus and affect changes in

Figure 2

a)

Stimulus	Growth Factors	Inflamatory cytokines cellular stress	???	Serum stress
MAPKKK	Mos Raf TPL2	TPL2 MEKK MLK/DLK TAK ASK	???	???
MAPKK	MEK1/2	MKK4/7 MKK3/6	???	MKK5
MAPK	ERK1/2	JNK P38 MAPK	ERK3	ERK5
Response	Proliferation Differentiation Development	Inflamation, Apoptosis, Development	???	Proliferation

b)

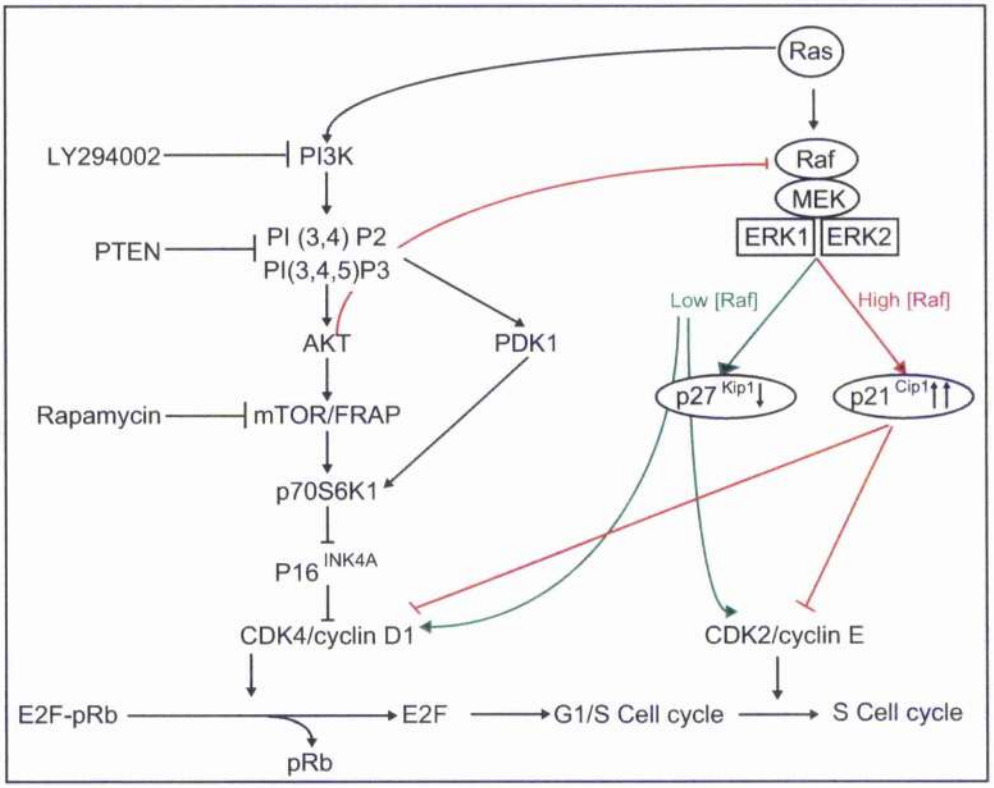

c)

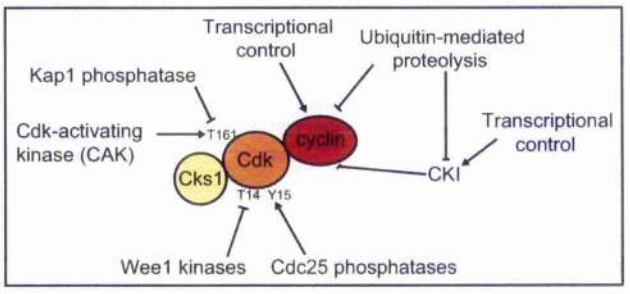

Reproduced from; a) [7], b) [14], and c) [21].

Figure 2: Mitogenic growth factor signalling pathways affect the cell cycle

a) Table showing various mammalian MAPK signalling pathways.

A variety of signalling pathways respond to various extracellular signals. Mitogen activated protein kinase (MAPK) pathways are shown here as an example. Growth factors such as EGF activate Ras signalling through Raf. Other MAPK kinase pathways respond to inflammatory signals and serum stress.

b) Ras and PI3K signalling pathways both regulate the activity of cyclin/Cdk complexes.

The Ras/Raf and phosphoinositide 3-kinase (PI3K) signalling pathways both converge to regulate cyclin/Cdk activity. The type of regulation is dependent on the level of mitogenic signalling. High levels of Ras activation lead to increases in $p21^{Cip1}$ expression, a protein which inhibits cyclin/Cdk activation. Moderate levels of Ras signalling lead to decreased expression of $p27^{Kip1}$ thereby activating cyclin/Cdk heterodimers. Ras can also activate the PI3K pathway which eventually lead to the inhibition of $p16^{INK4A}$ and the corresponding activation of cyclin D/Cdk4/6.

c) Cyclin/Cdk complexes are regulated by multiple mechanisms

Cdk enzymes are not active unless bound to their cognate cyclin. Activation of cyclin/Cdk complexes requires increased cyclin transcription, and the inhibition

of CKIs. Cdks themselves are activated by phosphorylation and de-phosphorylation events. Cdks are activated by phosphorylation of T161 by Cdk-activating kinase (CAK), and by the de-phosphorylation of Y15 by CDC25A phosphatase.

gene expression. There are numerous signalling cascades, which feed through and effect the cell cycle (both positively and negatively). I describe here the mitogen activated protein kinase (MAPK) signalling pathway as one example (Figure 2a and 2b).

The basic arrangement of the MAPK kinase cascade begins with receptor activation of a G-protein (that recruits the upstream kinase to the cell membrane upon receptor stimulation by the ligand). The G-protein works upstream of a core module consisting of three kinases; a MAPK kinase kinase (MAPKKK) that phosphorylates and activates a MAPK kinase (MAPKK), which in turn activates MAPK [7, 8]. There are presently four known MAPK signalling pathways observed in mammals (Figure 2a).

These include the extra-cellular signal-regulated kinase 1 and 2 (ERK1/2) cascade, which preferentially regulates cell growth and differentiation, as well as the c-Jun N-terminal kinase (JNK) and p38 MAPK cascades (which function mainly in stress responses like inflammation and apoptosis) [9-11].

The effect of Ras/Raf/MEK/ERK pathway on the cell cycle

The G1/S phase transition requires cyclin dependent kinases (Cdks) to facilitate the expression of genes involved in DNA synthesis and proliferation. Cdks are inactive without their cyclin binding partners (see below). Researchers studying the mitogenic stimulation of macrophages by colony-stimulating factor 1 first cloned cyclin D1. In this macrophage model, colony-stimulating factor 1 is required for continuous expression of cyclin D1 [12]. Mitogens stimulate the induction of cyclin D1 expression via signalling cascades. These involve tyrosine kinase receptors and G-proteins known to transmit signals through the Ras/Raf/MAPK/ERK pathway (Figure 2b) [13]. Activated Ras or Raf are known to induce cyclin D1 expression (Figure 2b and 2c) [14-16]. Furthermore, stimulation of cells in response to growth factors or Ras signalling requires cyclin D/Cdk4/6 [17-20].

Studies carried out using NIH3T3 cells show that mitogenic stimulation causes a sustained activation of MAPK, lasting until cells begin progressing through the G1/S phase boundary. The activation of Cdk2 and hence DNA synthesis was inhibited by treating NIH3T3 cells with a MEK inhibitor (PD98059). The MEK inhibitor also ablated Cdk2 Thr-161 activating phosphorylation, indicating a role for the Ras/Raf/MEK/ERK pathway in the regulation of Cdk activating kinase (CAK) (Figure 2c) [21, 22]. Raf despatches signals into different down-stream pathways that promote proliferation, cellular differentiation and inhibit cell cycle arrest/apoptosis. A recent report has also implicated Raf-1 as a pRb kinase contributing to pRb inactivation [23]. Mitogen stimulation induces the binding of pRb to Raf-1, and pRb inactivation was dependent on Raf-1 binding.

CYCLIN DEPENDENT KINASES (Cdks)

Cdks are promoters of the cell cycle

Cdks phosphorylate serine/threonine (S/T) residues of key proteins controlling the cell cycle, thus driving forward the cell cycle. Cdks are a group of S/T kinases that form active heterodimeric complexes upon binding cyclin regulatory subunits. Cdk3 is involved in driving cells through quiescence into G1 (Figure 3). Cdk4 and Cdk6 are involved in driving cells through early G1 phase, whereas Cdk2 is required to complete G1 and initiate S-phase (Figure 3). Cdks are only active when bound in complex with cyclins [24]. Cdk3 form complexes with C type cyclins. Cdk4/6 form complexes with D type cyclins (D1-D3). Cdk2 is activated by forming complexes with cyclin E1 and E2 during G1/S transition, and by cyclins A1 and A2 during S-phase [25].

Cdk regulation

Cdks are not active unless they are bound to their cognate cyclin. Also, Cdks need to be phosphorylated on T residues (T172 in Cdk4 and T160 in Cdk2) located in their T loop for proper catalytic activity (Figure 2c) [24, 26, 27]. This phosphorylation is carried out by the cyclin K/Cdk7 complex (CAK). This S/T kinase is also involved in transcription and DNA repair [27].

Cdk activity can also be regulated during G2/M transition. This is achieved by phosphorylation of a (T) residue and the de-phosphorylation of the adjacent tyrosine (Y) residue (T14/Y15) in Cdk1. Wee1/Myt1 phosphorylates T14 and T15 (Figure 2c). This allows cyclin B to complex with Cdk1. Cyclin B is then phosphorylated on T161. The complex is activated by the de-phosphorylation of Y15 by CDC25A [24, 26]. Regulation of CDC25A is critical for the G1 response to DNA damage. Mammalian cells respond to UV or ionizing radiation by rapid ubiquitin/proteasome-mediated degradation of CDC25A [28].

Cdks are also regulated by inhibitors coined Cdk inhibitors (CKIs), and were initially proposed to accumulate in response to a cells need to cease dividing. There are two types of CKIs; the complex inhibitors (INKs) and the kinase inhibitors (Cip1, Kip). The four members of the INK4 family are $p16^{INK4a}$, $p15^{INK4b}$, $p18^{INK4c}$ and $p19^{INK4d}$. The INK4 family members exert their inhibitory activity by binding to the Cdk4 and Cdk6 kinases, preventing their association with D type cyclins (Figure 2b)[29]. The kinase inhibitors of the Cip1/Kip family bind and inhibit Cdk kinases and cyclins. The Cip/Kip family is composed of three members; $p21^{CIP1}$, $p27^{KIP1}$, and $p57^{KIP2}$. The Cip/Kip family block kinase activity by interfering with both substrate recognition and ATP binding [30]. The Cip/Kip family preferentially inhibit Cdk1/2. Cip1/Kip inhibition of cyclin D/Cdk4/6 complexes is relatively inefficient [30].

Figure 3

a)

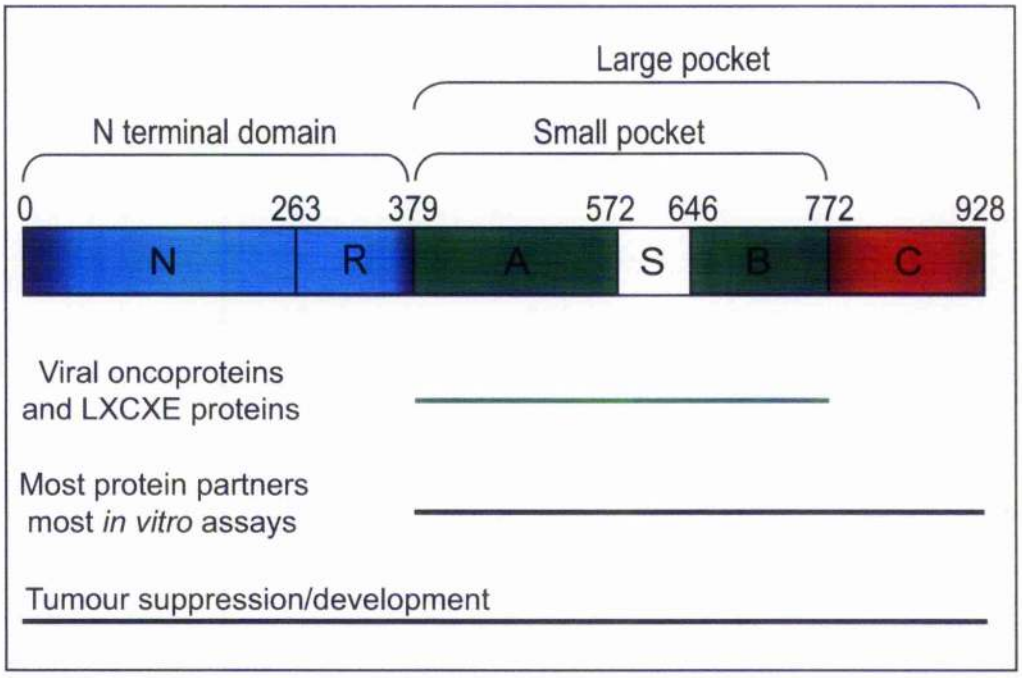

b)

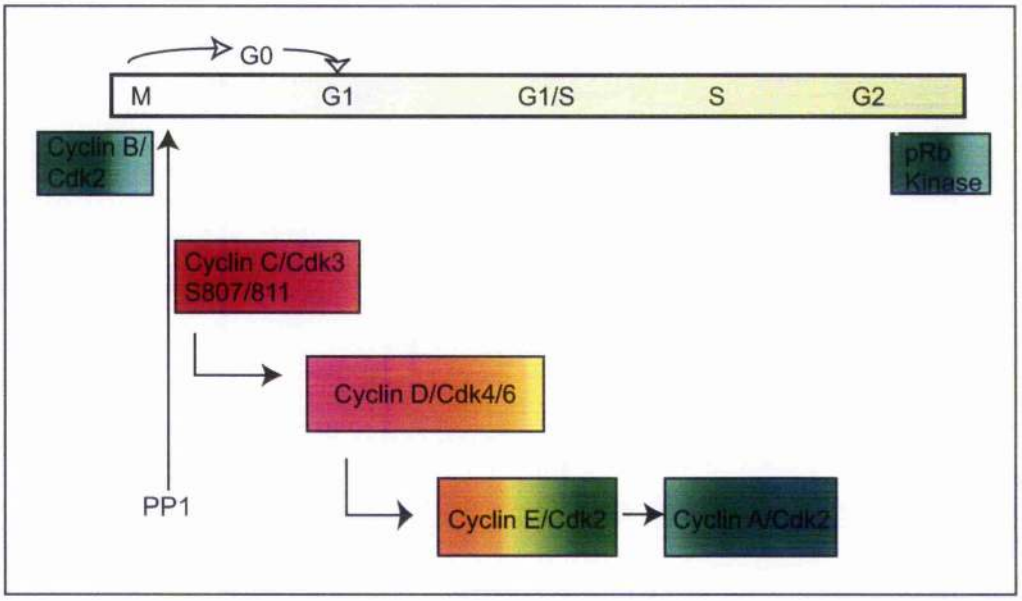

a) Reproduced from [111], b) Generated using data from [24],[25],[26],[34],[104].

Figure 3: The phosphorylation of pRb by Cdks through the cell cycle

a) The structural and functional protein domains of pRb.

pRb contains five protease resistant sub domains (N, R, A, Spacer 'S', and B domains). There is a sixth sub domain which is sensitive to proteases coined the'C terminal domain'. The A, B, and C sub domains correspond to functional domains that have been mapped genetically. Beneath the pRb schematic are listed some identified functional properties of pRb. The line shown next to the listed properties indicates the extent of the protein that is sufficient for function. The A, S and B sub domains comprise the small pocket, and are sufficient for viral oncoprotein binding and for interaction with pRb binding partners that utilize an LXCXE amino acid motif. The A, S, B and C sub domains comprise the large pocket and are sufficient for most pRb-binding partners. The amino terminal domain is required for normal tumour suppression and embryonic development.

b) Phosphorylation events through the cell cycle.

Exit from cell cycle arrest initiates when pRb is phosphorylated by cyclin C/Cdk3. Mitogenic stimulation results in the sequential phosphorylation of pRb by cyclin D/Cdk4/6 which induces conformational change in pRb, thus allowing cyclin E/Cdk2 to further phosphorylate pRb. This promotes the gradual release of E2F-1 from pRb. Once inhibition of E2F-1 is lifted, cells can progress through S-phase. When S-phase is completed, further phosphorylation of E2F-1 by cyclin A/Cdk2 causes E2F-1 to leave its promoter. A further pRb kinase that is not under the control of cyclins has been shown to be active during late G2/M phase. During mitosis, cyclin B/Cdk2 is activated. At the end of mitosis, pRb is de-phosphorylated by Protein Phosphatase 1 (PP1).

The Cip/Kip family act to promote the complex formation between cyclin D and Cdk 4/6. The Cip/Kip family also stimulate the nuclear import of cyclin D/Cdk4/6 and increase the half life ($t_{1/2}$) of cyclin D [24].

In contrast to their affects on cycin D/Cdk4/6, Cip1/Kip inhibitors block phosphorylation by cyclin E/Cdk2, and promote cyclin E/Cdk2 ubiquitination and degradation. Increases in protein levels of cyclin D (following mitogenic stimulation) may increase cyclin E/Cdk2 activity via Cdk inhibitor exchange. On the formation of cyclin D/Cdk4/6 dimer, Cip1 from cyclin E/Cdk2 may dissociate and complex with cyclin D/Cdk4/6 [24]. Increases in INK4 protein levels (following differentiation or other signals promoting cell cycle withdrawal) may decrease both cyclin E/Cdk2 and cyclin D/Cdk4/6 by Cdk inhibitor exchange [24].

RETINOBLASTOMA PROTEIN

The pRb/E2F pathway

Approximately seventeen years ago, the retinoblastoma tumour suppressor gene *(Rb)* was molecularly cloned [31]. Later on, Knudson's two-hit hypothesis [32] was validated by demonstration that mutational inactivation of both alleles of *Rb* induces cancer of the retina. Patients with one allele of *Rb* have a high chance of developing sporadic retinoblastoma by loss-of-heterozygosity [33]. pRb controls cell growth and proliferation, and will facilitate cell cycle arrest upon DNA damage to allow repair to take place.

Mutation or deregulation of pRb has been observed in nearly every type of human cancer examined [2]. The protein sequence is well conserved across five disparate species (bird, human, rodent, fish and amphibian) (Figure 4a). Deregulation of pRb is so frequent in cancer, that some have argued it is a prerequisite for all human cancers [25]. Although pRb can physically interact with well over one hundred different cellular proteins [34], the most studied interaction is that of the pRb large pocket with the E2F-1 protein.

Figure 4

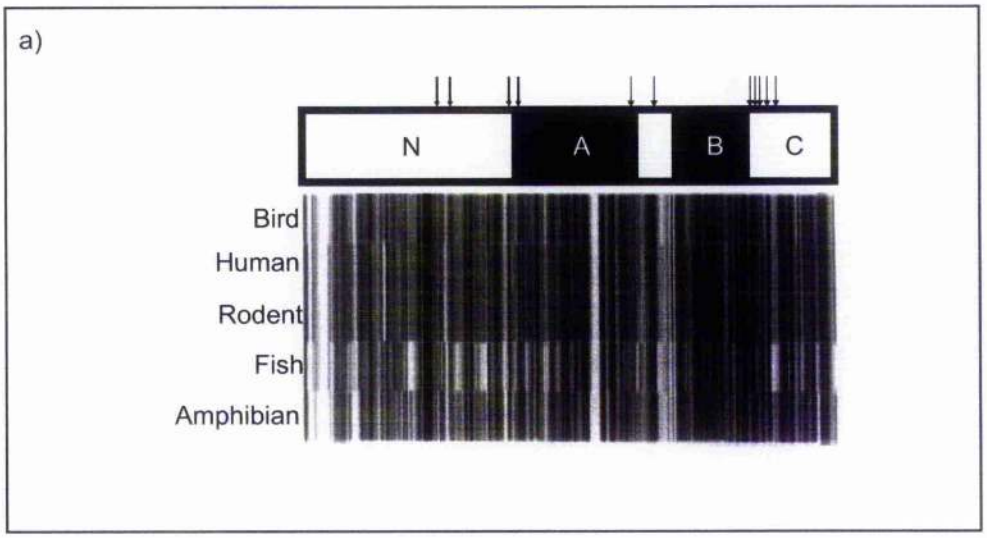

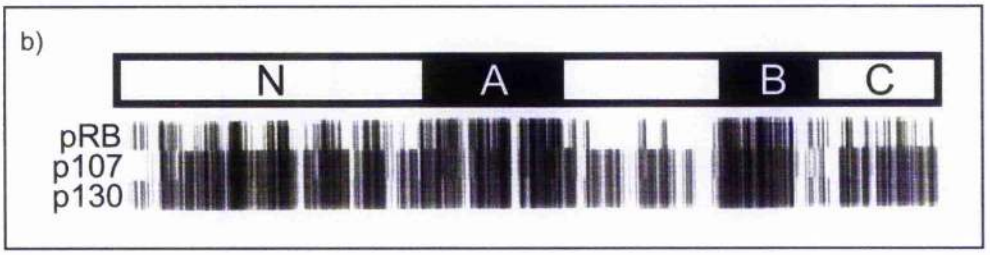

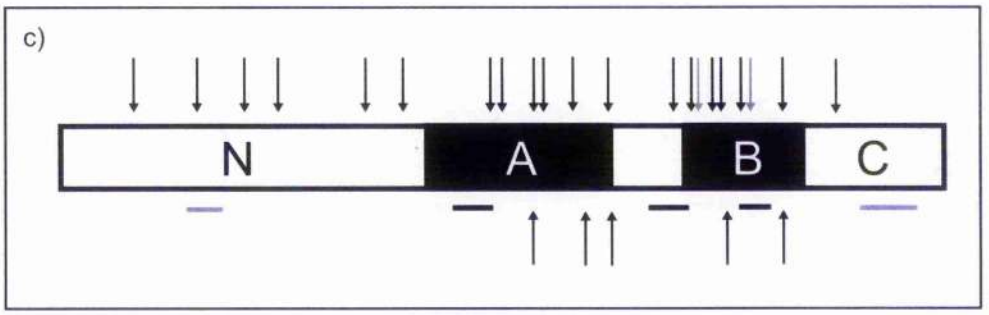

a), b) and c) reproduced from [111].

Figure 4: The conservation of amino acids between the pocket protein family members

a) The N, A, B and C domains are depicted schematically.

The arrows above the map highlight the position of phosphorylation sites that are present in the 5 indicated vertebrate species. Below the schematic are barcodes depicting multiple protein sequence alignments of pRb homologues from chicken, human, mouse, trout, and newt.

The barcode for each species consists of a series of vertical lines representing each amino acid within the linear sequence of the relevant protein. The shading of the vertical lines is proportional to the sequence identity/similarity at the given position. An amino acid that is identical at a particular position in the alignment is shaded black. Dissimilar amino acids are shaded white. Patches of dark shading indicates regions of conservation, while lightly shaded patches indicate non-conserved regions.

b) Sequence similarity between pRb, p107 and p130.

A schematic of human pocket proteins is shown indicating the 4 major domains (N, A, B, and C). Multiple sequence alignment is depicted as in (a) above. The schematic of pRb depicts the four major domains (N, A, B and C domains). Arrows above the schematic represent mis-sense mutations identified in the *Rb* gene. Black arrows indicate fully penetrating inactivating mutations. Grey arrows indicate mutations in tumours from patients with low

penetrating retinoblastoma families. Arrows below the map indicate in-frame deletion mutants identified in *Rb*. The arrows represent less than or equal to 5 amino acid deletions. The bars indicate the extent of larger in-frame deletions. As above, lightly shaded arrows and bars indicate mutations identified in partially penetrant retinoblastoma families.

The Rb tumour suppressor protein (pRb) binds to the E2F-1 transcription factor preventing it from interacting with the cells transcription machinery. In the absence of pRb, E2F-1 (along with its binding partner DP-1) mediates the *tran-activation* of E2F-1 target genes that facilitate the G1/S transition and S-phase. E2F target genes encode proteins involved in DNA replication (for example DNA polymerase α, thymidine kinase (TK), dihydrofolate reductase (DHFR) and cdc6), and chromosomal replication (replication origin-binding protein HsOrc1 and MCM 5). When cells are not proliferating, E2F DNA binding sites contribute to transcriptional repression. *In vivo* footprinting experiments obtained on *Cdc2* and *B-myb* promoters demonstrated E2F DNA binding site occupation during G0 and early G1, when E2F is in transcriptional repressive complexes with the pocket proteins [35, 36].

The family of pocket proteins

p107 and *p130* are genes which encode proteins with similar structure to pRb [37]. Comparison of the amino acid sequences of pRb, p107, and p130 indicates substantial amino acid similarity (Figure 4b). Overall, pRb shares approximately 21 % sequence homology with p107 and p130. However, it is clear that p107 and p130 (47 % identity) are more closely related to each other than either one is to pRb. Most of the conserved sequences lie within the small pocket region (residues 379-792) sharing 30-40 % identity. Viral oncoproteins, Simian virus 40 large T antigen (SV40 LT), adenovirus early gene A (ad E1A) and 'high risk' Human papillomavirus E7 (HPVs E7) all target the pocket domain. Viral oncoprotein binding to the pocket domain displaces cellular proteins which interact with the pocket, thereby de-activating the pocket proteins (PP) through preventing them from interacting with E2F-1 [38] [39-41]. The N- and C-terminal domains of pRb are not well conserved (10-20 % identity). Key sub domains within the N-terminal domain are also shared with a high degree of sequence homology between pocket proteins. For

example, the spacer region of pRb lacks a cyclin/Cdk binding motif shared by p107 and p130 and is considerably shorter.

It is likely that the pocket regions of pRb, p107 and p130 have similar function. The main functional differences between the pocket proteins are likely to relate to differences in their N-terminal and C-terminal domains. Despite being closely related, only *pRb* is frequently mutated in tumour cells (Figure 4c). *p107* and *p130* are not frequently mutated in naturally occurring tumour cells. Indeed, mutation of *p107* has only been detected in a B cell lymphoma cell line [42] and possibly human myelogenous leukemias [43]. While still relatively uncommon, mutation or alteration of p130 expression is detected more frequently in cancer than mutation or alteration of p107 expression. Potentially inactivating mutations of *p130* have been discovered in lung cancer [44, 45] and Burkitt's lymphoma [46]. Levels of p130 are lower in tumours of higher stage and grade in lung, endometrial, oral squamous cell carcinoma, and uveal melanoma [47-50]. It is clear that *Rb* is more frequently mutated in human cancer than *p107* or *p130*.

The unique tumour suppressor function of pRb is reinforced in mouse models containing inactivating mutations of the various pocket proteins. Mice lacking either *p107* or *p130* are viable, whereas mice lacking *Rb* are not [51, 52]. Inactivating both *p107* and *p130* causes severe defects in bone development, resulting in death shortly after birth. This suggests that these two genes are either redundant or can functionally compensate for one another in a way that *Rb* cannot. It seems that pRb has a different function to p107/p130 in foetal development.

pRb is known to be required for cells to enter permanent cell cycle arrest prior to differentiation [53]. Murine cells lacking *Rb* are compromised in their ability to differentiate into adipocytes, whereas cells lacking in *p107* or *p107/p130* actually differentiate into adipocytes more efficiently [54, 55]. Importantly, neither *p107* null nor *p130* null mice are tumour prone. Although tumour phenotypes cannot be assessed in double $p107^{-/-}/p130^{-/-}$ knockout mice, $p107^{-/-}/p130^{+/-}$ and $p107^{+/-}/p130^{-/-}$ genotypes are

viable and have been examined. Unlike $Rb^{+/-}$ mice, these genotypes do not exhibit a tumour prone phenotype [52]. Hence sporadic loss of the remaining *p107* or *p130* wild-type allele does not initiate tumourigenesis. Interestingly, $Rb^{+/-}$ mice do not suffer from retinoblastoma, but instead develop tumours of pituitary and thyroid origin. This difference may be attributable to the physiology of humans as compared to mice.

E2F proteins

pRb, p107 and p130 have their own preference for binding to different E2F family members [56]. The E2F family presently consists of eight members (E2F-1 to 8) [57]. E2F-1, 2 and 3 are activating E2F family members and prefer to bind pRb (Figure 5a). In contrast, E2F-4 and 5 are repressive E2F and prefer to bind p107/p130 (Figure 5a and 5b). In general, p130/E2F complexes are mainly found in quiescent or differentiated cells, whereas p107/E2F complexes predominate in S-phase cells. pRb/E2F complexes form during G1 and G1/S phase transition, but also exist in quiescent or differentiated cells [58]. E2F-6 also acts as a transcriptional repressor, but through a distinct, pocket protein independent manner. E2F-6 mediates repression by direct binding to polycomb group proteins or via the formation of a large multimeric complex containing Mga and Max proteins [59].

E2F-7 recognises and binds E2F sites utilizing two distinct DNA binding domains, and does not require a DP-subunit to effectively bind to DNA. E2F-7 has no transcriptional activation domain and no pRb binding domain [60, 61]. The most recently discovered E2F, E2F-8 is very similar in structure and sequence to E2F-7, with its two distinct DNA binding domains.

Figure 5

a)

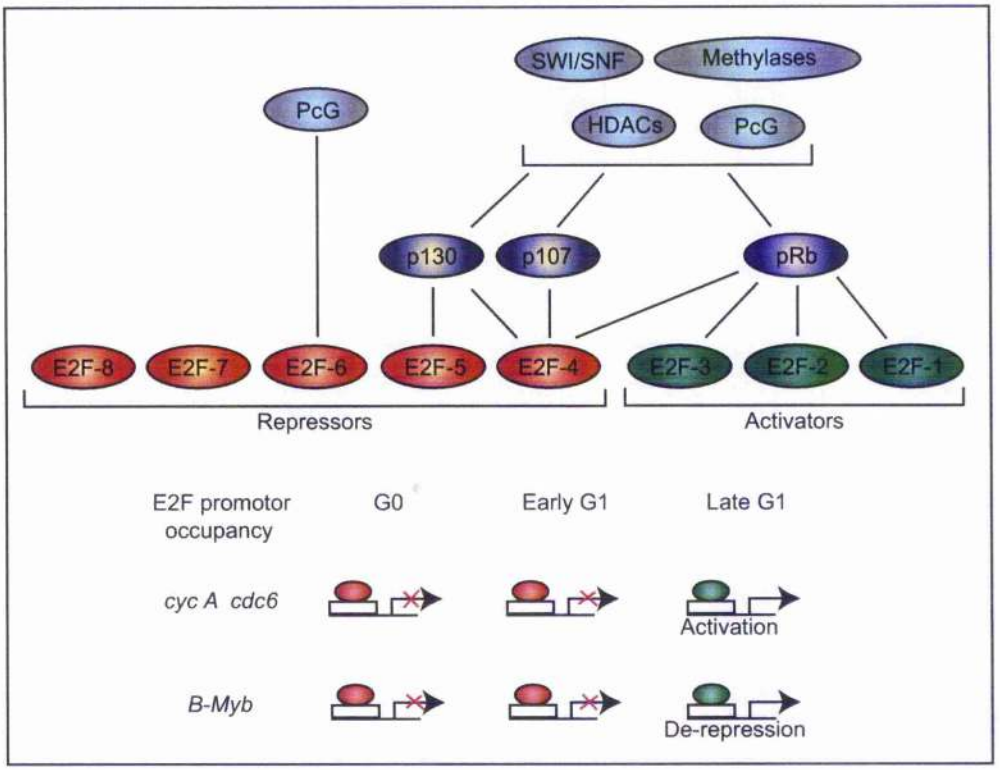

b)

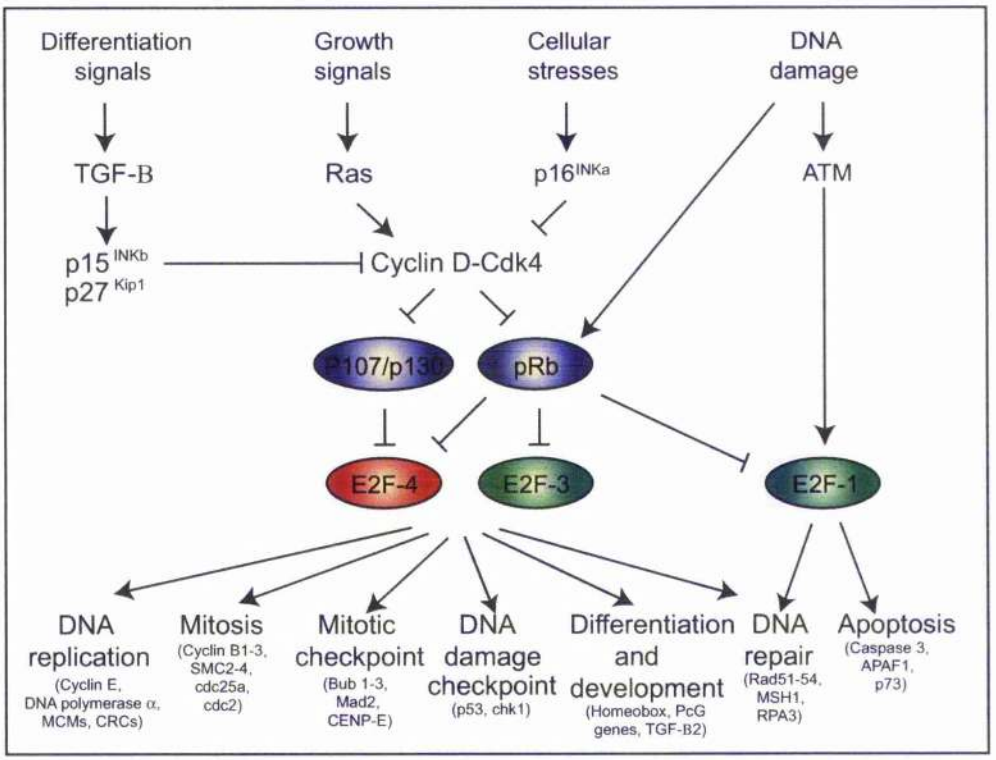

Adapted and reproduced from a) [57], [61] and [63], b) [57].

Figure 5: Pocket proteins and their E2F partners can activate or repress transcription

a) Promoter occupancy of E2F target genes

The E2F family of transcription factors is divided into activator and repressor E2Fs. Repressor E2F (E2F-4 to 6) occupy E2F promoters in G0 and early G1, and recruit chromatin remodeling factors directly (E2F6) or indirectly through p107 and p130 (E2F-4, 5). As cells enter into late G1 phase, the repressor E2F complexes are replaced by activator E2Fs (E2F-1 to 3). Two types of E2F-regulated promoters were uncovered, based on whether activator E2F remained at the promoter throughout late G1 and S-phase (*cyclin A*, *cdc6*), or whether they were only detected transiently during late G1 (*b-myb*). These binding differences correlate with other studies identifying promoters essentially regulated by transcriptional activation, and those regulated mainly through repression. pRb was not localized on most E2F-regulated promoters, despite the fact that it forms *in vivo* complexes with 'E2F-1 to 4' (dashed lines).

b) Proposed transcriptional program of the E2F/pocket protein pathway

The E2F/pRb pathway acts down-stream of several important signaling cascades that trigger cell cycle arrest. Cellular senescence and the transforming growth factor β pathway induce cell cycle inhibitors such as $p16^{INK4a}$, $p27^{Kip1}$ and $p15^{INKb}$, which inactivate cyclin D/cdk4 and trigger pocket protein-dependent cell cycle arrest. Alternatively, the MAPK pathway induces cyclin

D expression and leads to E2F transcriptional activation. DNA damage can induce two types of response depending on the context and intensity of DNA damage: a cell cycle arrest requiring pRb, or a pro-apoptotic response mediated through ATM and E2F-1. Recent microarray studies suggest that the network of E2F-regulated genes is vastly broader than previously suspected. For many of these new targets however, it remains to be shown if their regulation by E2F is important for the biological processes in which they participate. E2F functions beyond the G1/S transition of the cell cycle to regulate DNA replication, DNA repair and DNA damage checkpoint genes. It also controls the transcription of genes that function during mitosis, in mitotic checkpoints, and in apoptosis. Finally, E2F induces genes that are involved in differentiation and development. ATM, ataxiatelangiectasia protein; MCM, mini chromosome maintenance protein; PcG, Polycomb group protein.

E2F-8 expression is induced at the G1/S phase transition, and does not require DP subunits to bind and repress E2F promoters. Over-expression of E2F-8 in diploid human fibroblasts reduces expression of E2F-target genes and inhibits cell growth consistent with a role for repressing E2F transcriptional activity [62, 63].

pRb/E2F complexes

Genes that encode proteins involved in regulation of DNA synthesis and proliferation need to be tightly regulated. The cell needs to switch on these genes during the G1/S-phase transition, and switch them off again when S-phase is complete. As mentioned above, E2F-1 to 3 bind promoters and are able to activate transcription, whilst E2F-4 to 8 repress transcription (Figure 5a) [64]. The pocket proteins bind both activating and repressing E2Fs, and by doing so inhibit any *trans*-activation mediated by the E2F [65]. This is known as non-active (or static) repression (reviewed in [66]). This repression is lifted by Cdk phosphorylation (Figure 3). Pocket proteins that are bound to E2F are also able to bind other proteins via the small pocket. It has been shown that pRb/E2F complexes can form repressor complexes at promoters that actively repress transcription (Figure 6) [67-69]. Histone deacetylases such as HDAC1 can bind pRb

and recruit repressor complexes that serve to deacetylate histones. This process is labelled active repression [66]. On the other hand, histone acetyl-transferases can acetylate histones and activate transcription. This process is dynamic activation, which is distinct from pocket protein phosphorylation by Cdks (reviewed in [66]). An E2F controlled gene whose expression is silent but requires activation must remove the repressing E2F/pocket protein complex and replace it with an activating E2F/Pocket protein complex (Figure 6).

Figure 6

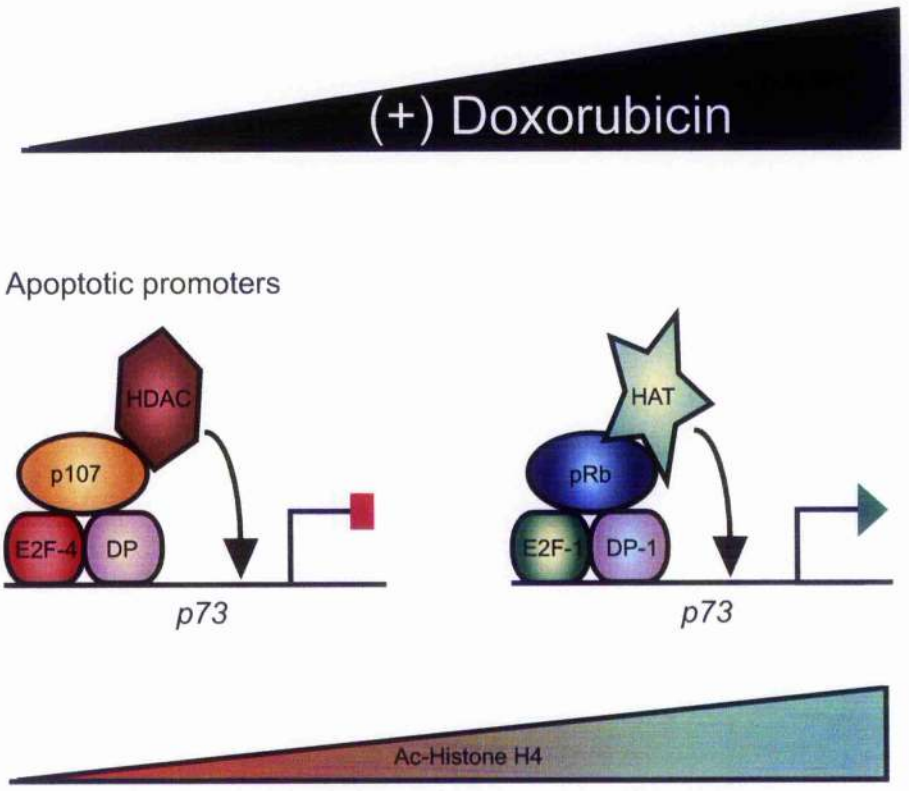

Adapted from [75]

Figure 6: The re-localization of E2F/DP complexes during DNA damage

Double stranded DNA damage is relayed through to the E2F/DP heterodimer through the ATM/Chk2 pathway. In response to DNA damage, activating E2F (E2F-1) present at TK/DHFR promoters re-localizes to the p73 promoter. There, they swap places with repressive E2F (E2F-4), which relocates to the TK/DHFR promoter. This changing place of E2F/DP complexes affects the transcriptional activity at the promoters. E2F-1/DP-1 complexes facilitate an increase in acetylation of histone H4 by recruiting HAT enzymes, which facilitate the unwinding of condensed chromatin leading to an increase in transcription. E2F-4/DP complexes recruit HDAC enzymes that result in a decrease in acetyl histone H4 and a corresponding drop in transcription resulting from chromatin condensation.

pRb/E2F complexes are found during G1 and G1/S phase transition, p107/E2F complexes predominate during S-phase, and p130/E2F complexes are mainly found in quiescent differentiated cells. Using chromatin immunoprecipitation assays (ChIP), it was found that repression on E2F-responsive promoters was associated with the recruitment of E2F-4 and p130, and coincided with low level of histone acetylation [70]. In late G1 phase, the E2F-4/p130 complex is replaced by E2F-1 and E2F-3, together with enhanced level of acetylation of histones H3 and H4 (Figure 5a). These studies indicate that distinct E2F heterodimers recruit enzymes to deacetylate or acetylate core histones, therefore repressing or activating E2F-responsive genes [71].

Double stranded DNA damage such as that induced by irradiation (IR) or DNA damage inducing chemicals (such as etoposide or doxorubicin) cause the recruitment of DNA damage homologous recombination and repair (HRR) response proteins such as TIP60. TIP60 is able to acetylate ATM kinase, thus activating the ATM DNA damage response pathway [72]. One of the down-stream targets of ATM kinase is Chk2. ATM activates Chk2 kinase by phosphorylating it. ATM and Chk2 phosphorylate E2F-1 at S31 and S364 respectively [73, 74]. The result is an increase in protein stability of E2F-1. Its phospho form undergoes an intra-cellular localization change.

Using ChIP assays, studies showed that E2F-4 (present on the p73 E2F promoter) and E2F-1 (present on the TK and DHFR responsive E2F promoter) swap promoter in response to doxorubicin induced DNA damage [75]. This swap induced a corresponding drop in histone H4 acetylation at the TK/DHFR gene, and a corresponding increase in histone H4 acetylation at the p73 gene (Figure 6). Phospho-E2F-1 can be seen to re-localise into distinct nuclear speckles after cells were treated with etoposide to induce DNA damage [74]. It seems likely that those genes whose functions oppose each other (such as TK and p73) might swap their E2F/pocket protein complexes upon a change in conditions such as DNA damage (as in this case) or cell cycle progression from G1-S phase (as in the first example).

Organization of pRb

Domains A and B of pRb are highly conserved, and they interact with each other along an extended inter-domain interface to form the central "pocket" [41], which is crucial to the tumour suppressor function of pRb [76]. The pocket is disrupted by most naturally occurring germ-line mutations in hereditary retinoblastoma patients [77], and by most tumour-derived mutations [78]. Viral oncoproteins and a number of endogenous pRb binding proteins contain and LXCXE motif that allows them to bind pRb [38, 41, 79, 80]. The LXCXE sequence motif is found in certain cellular pRb binding proteins, such as the D-type cyclins, but not in the E2F transcription factors, which share a distinct eighteen residue pRb binding motif [81, 82].

An LXCXE peptide binds a highly conserved groove on the B-box portion of the pocket [41]. However, domain A is required for domain B to assume active conformation, thus explaining the conservation of both domains [40, 41]. A number of endogenous proteins that interact with pRb also contain an LXCXE like sequence, including HDAC1 and HDAC2, and the ATPase BRG1, from the SWI/SNF nucleosome remodelling complex [83]. In contrast to experiments *in vitro*, transfection assays in cultured cells have suggested that interaction with HDAC is required for the inhibition of E2F-1 by pRb [83, 84]. Other studies have shown a partial requirement for HDAC activity in the pRb-mediated inhibition of E2F activity [85, 86]. E2F-1 has been shown to interact with the HAT p300/CBP and P/CAF [87]. It is possible that pRb-mediated recruitment of HDAC to E2F acts to offset this HAT activity.

It has been shown that E2F-1 can be acetylated, which increases the binding of the E2F/DP complex to DNA [88]. The recruitment of HDAC to E2F via pRb may inhibit E2F activity by deacetylation of the protein, further decreasing its binding to DNA. Binding of pRb and other PP complex to E2F does not simply inhibit E2F activity. The resulting

pRb/E2F complex binds to promoters and actively represses transcription by blocking the activity of surrounding enhancers on the promoter [67-69, 83, 89-95].

Phosphorylation control of pRb

Mitogenic and growth factor signalling pathways activate Cdks in a sequential manner (Figure 2b and 3). It was thought that pRb represses E2F-1 via its pocket interaction with the E2F-1 *trans*-activation domain (Figure 7), and that this interaction was sufficient. Recent reports have shown that the C-terminal domain of pRb binds E2F-1, and that this interaction is similar in strength to the pRb pocket interaction with the *trans*-activation domain of E2F-1 [96-98]. Models suggested that phosphorylation of the C-terminal domain of pRb allowed for further phosphorylation of S/T residues in the A/B pocket and spacer domains thereby reducing affinity of pRb small pocket for the E2F-1 *trans*-activation.

Thus it was demonstrated that cyclin D/Cdk4/6 sequentially phosphorylates pRb causing its partial dissociation with E2F, and facilitating cyclin E/Cdk2 interaction with pRb [98]. Cyclin E/Cdk2 then further phosphorylates pRb completely freeing E2F-1 from pRb and allowing the host transcription machinery to bind to E2F/DP-1 [98]. There are sixteen consensus phosphorylation sites for Cdk phosphorylation across pRb (Figure 8). Studies have characterized the residues across pRb which phosphorylated, by cyclin/Cdk complexes (Figure 8) [99-102] also reviewed in [103, 104]. Sequential phosphorylation of pRb not only removes E2F-1 binding, but also controls the binding of proteins like HDACs (containing the LXCXE binding motif) to the B domain [40, 41, 105] also reviewed in [66, 104]. Reports have indicated that phosphorylation of pRb alters its intra-nuclear localization thereby preventing pRb from inhibiting E2F-1 *trans*-activation [106, 107].

Figure 7

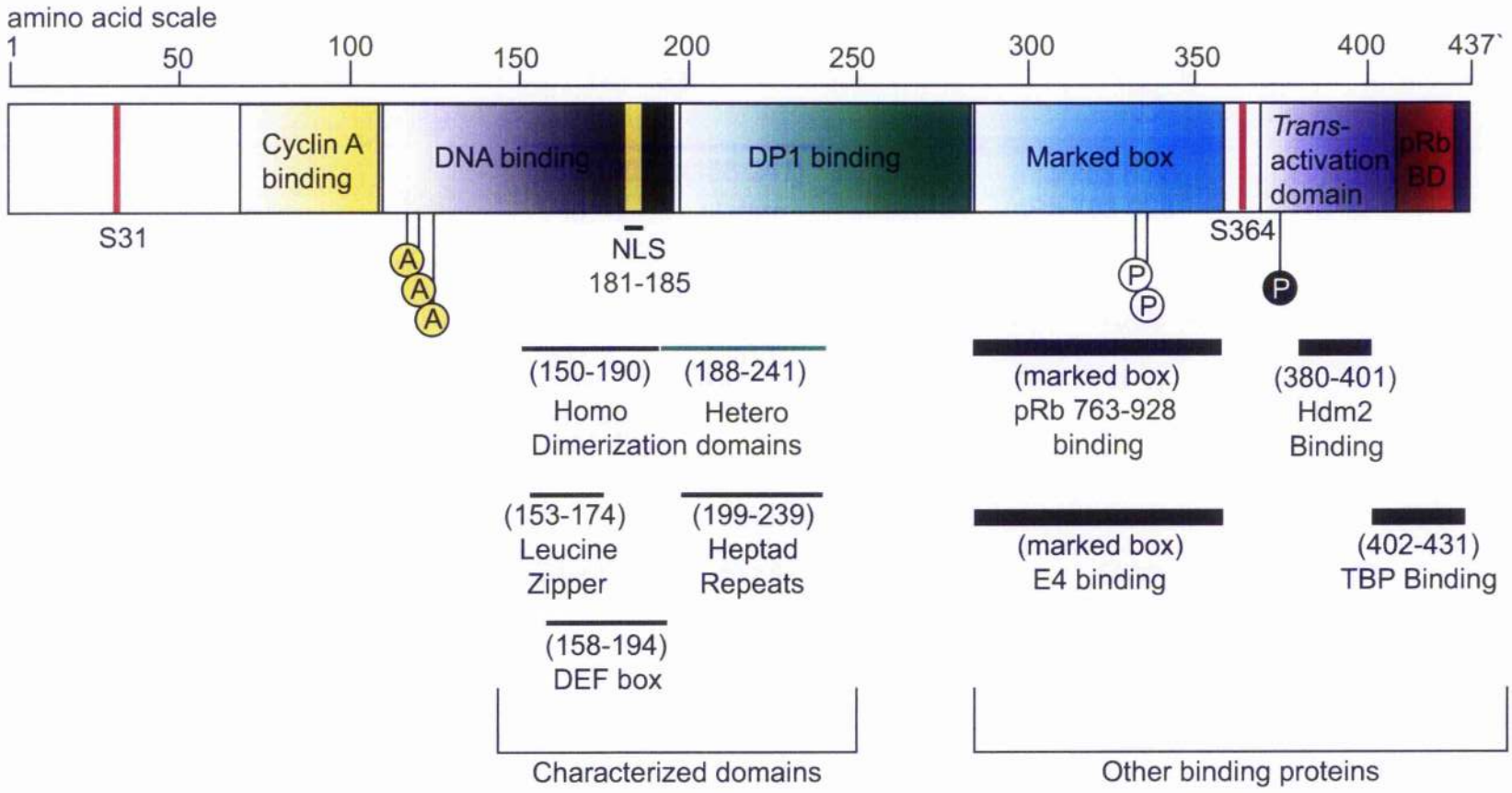

Adapted from [64], [65], [88], [93] and [229].

Figure 7: Schematic representation of E2F-1 showing domains and binding proteins

The E2F-1 protein is made up of 437 amino acids. The schematic depicts the main domains so far characterized. Relevant domains include; the DNA binding and DP-1 binding domains (that are required for stable binding to DNA), the marked box domain (MB) required for interactions with the C-terminal domain of pRb, and the *trans*-activation domain (required for binding the small pocket region of pRb, and for promoting transcription).

Below the main schematic; relevant post-translational modifications, characterized domains, and other binding proteins are displayed. Post-translational modifications; yellow circle with A = Acetylated K residues (K117/K120/K125) which are acetylated in response to induced double strand DNA damage, white circle with P = Serine residues phosphorylated during the G1 to S phase transition, black circle with P = Serine residue phosphorylated during the G2 to M phase transition by cyclin A/Cdk2 causing the release of E2F-1 from the DNA. S31 and S364 marked by a red line on the schematic are represented because these residues are phosphorylated by ATM kinase and Chk2 kinase respectively in response to etoposide induced DNA damage.

The role of the pRb in tumour suppression

Mutation of the *Rb* allele predisposes patients to develop other tumours, such as osteosarcomas and fibrosarcomas. Almost two-thirds of the secondary tumours arising in patients with retinoblastoma are mesenchymal in origin. The *Rb* gene was cloned and shown to contain twenty seven exons, spanning across 180kb on chromosome 13 [31, 108]. Mutations to the *Rb* gene may result in premature termination of protein translation. A huge variety of mutations have been observed in tumours derived from patients over the last twenty years (http://rb1-lsdb.d-lohmann.de). It is important to note that inactivation of pRb can occur indirectly by inactivation of proteins that inhibit Cdk phosphorylation, or the amplification of proteins that lead to the stimulation of Cdk activation and phosphorylation.

Figure 8

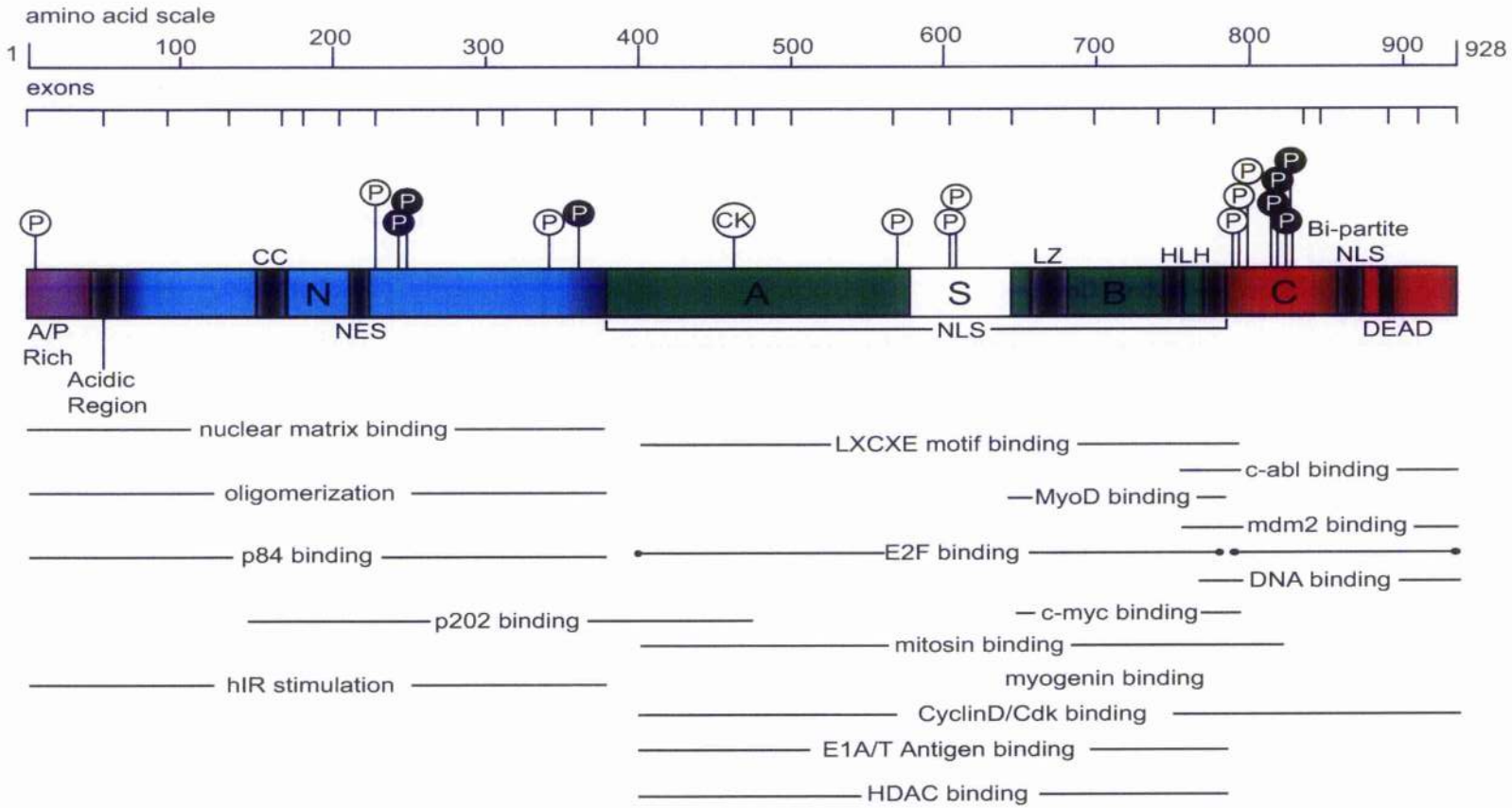

Adapted and reproduced from [122]

Figure 8: Schematic representation of pRb depicting its domains and binding partners

The pRb tumour suppressor protein (shown mapped) is a 928 amino acid phospho-protein. The map shows regions in the protein that have been implicated in specific protein interactions. A/P rich region, CC-coiled coil protein motif, NES-nuclear export motif, CK-casein kinase II phosphorylation recognition site, LZ-leucine zipper motif, HLH putative motif, NLS motif (pRb contains a mono partite NLS spanning the A/B pocket, a bipartite NLS in the C-terminal domain (residues 860-877), and the DEAD box (residues 883-887). Filled circles at sites of known phosphorylation and open circles at possible sites of phosphorylation denote the S/T phosphorylation sites. The A and B domains of pRb are connected by a Spacer region (S).

THE N-TERMINAL REGION OF pRb

Factors that interact with the N-terminal region of pRb

Hsc73

Heat shock cognate protein Hsc73 and Hsp75 are related proteins have been reported to co-immunoprecipitate with pRb. It was hypothesised that they are required to fold pRb into an active conformation. Hsp75 binds to the C-terminal domain of pRb. However, Hsc 73 (heat shock cognate protein) was shown to bind to the N-terminal/ domain/A domain of pRb using an *in vitro* kinase assay, and this binding was not affected by the addition of E1A (which binds the pRb small pocket domain). A GST fusion protein containing amino acids 1-515 of pRb was the smallest fragment that retained binding activity (Inoue et al., 1995). It was reported that Hsc 73 preferentially associates with hypophosphorylated pRb and that Hsc 73 might act as a molecular stabilizer of hypophosphorylated pRb [109].

Microchromosome maintenance protein-7 (MCM7)

MCM7 is a DNA replication factor required for DNA synthesis. A two-hybrid screen was used to probe for proteins that interact with the first 400 amino acids of pRb, yielding MCM7 [110]. GST pull downs using GST-MCM7 as bait were found to bind N-terminal domain fusion proteins of pRb, p107 and p130 as well as full length pRb *in vitro*. Studies showed that small deletions in the N-terminal domain had no effect on MCM7 binding, suggesting that MCM7 interacts with a large surface of the N-terminal domain of pRb. This is indeed likely, as the N-terminal domains of p107 and p130 only share 12 % homology with the amino acid sequence of N-terminal domain of pRb [111]. Endogenous MCM7 was shown to interact with pRb in co-immunoprecipitation experiments in myeloblastic leukemia (ML-1) cells. The function of the interaction between N-terminal

domain of pRb and MCM7 was illuminated by experiments using the *Xenopus* cell free DNA replication system. Studies demonstrated that human N-terminal domain pRb (which binds *Xenopus* MCM7) was able to ablate DNA replication. This effect could be reversed by the addition of the C-terminal domain of MCM7 (which binds the N-terminal domain of pRb) [110]. These data suggest that pRb might function to suppress pre-replication initiation at origins of replication through interactions with MCM proteins, including MCM7. This model has been bolstered by the finding that pRb co-localizes with MCM proteins in perinucleolar foci in G1 and early S-phase [112].

The human insulin receptor (*hIR*) promoter

The vast majority of literature on pRb concentrates on its repressive inhibitory functions in relation to the cell cycle and tumour suppression. In a study by Wen-jun Shen *et al* [113], pRb was shown to activate the transcription of the human insulin receptor (*hIR*) thus increasing the cells sensitivity to insulin. pRb regulates cellular proliferation and cell cycle control by activating several cellular genes, through a conserved cis-activating element termed the retinoblastoma control element (RCE). As well as pRb, Sp1 activates transcription through binding the RCE motif [114-119].

Using the human hepatoma cell line (HepG2), Shen *et al* demonstrated that pRb stimulated the expression of the *hIR* gene through RCE sites in the *hIR* promoter. pRb N-terminal domain deletion mutants showed dramatically reduced ability to activate the hIR promoter, whilst deletion mutants that ablate the binding of viral oncoproteins (such as E1A) increased promoter activity. In addition, over-expression of Sp1 was shown to augment *hIR* promoter activity, suggesting that Sp1 can also augment the hIR promoter. This is significant because hyperphosphorylated pRb can out compete Sp1 for binding to its inhibitor Sp1-I, leaving Sp1 to activate hIR [113].

Three regions in the N-terminal domain of pRb were shown to be important for stimulation of the *hIR* promoter (amino acids 37-89, 89-140, and 343-389), although the

actual residues in the N-terminal domain that are required for binding to the *hIR* promoter have not been determined. It is also interesting that the spacer region of pRb is required for *hIR* promoter stimulation. Therefore perhaps protease sensitive linking regions such as the spacer between the A and B domains in pRb (that are not required for E2F and viral oncoprotein binding) serve some function in regulating the ability of pRb to elicit *hIR* promoter activation.

This study suggested a model where pRb not only releases E2F-1 upon its phosphorylation by Cdks, but also then actively promotes the expression of genes that facilitate growth and proliferation. It is possible that functional A and B domains of pRb are not involved in regulating the pRb activation of the *hIR* promoter. Instead, post-translational modification (such as phosphorylation) of the spacer region might be required. The spacer region is phosphorylated by Cdks during G1/S phases of the cell cycle. Phosphorylation of pRb may facilitate the interaction of pRb with Sp1-I and/or promote the recruitment and binding of pRb to the *hIR* promoter. The N-terminal domain has three regions of protein sequence containing kinase recognition sites [76, 120] and has been proposed to be important for hyperphosphorylation of pRb [120]. A requirement for pRb hyperphosphorylation in order to mediated *hIR* promoter stimulation is consistent with the observation that pRb N-terminal domain deletion mutants fail to stimulate the *hIR* promoter [113].

Nuclear Death Domain Protein p84N5

p84N5 (p84) was isolated as a pRb binding protein in a two-hybrid screen using GST-pRb (1-300) as bait [121]. Over-expression of p84 leads to increased apoptosis. Incidently, over-expression of the N-terminal domain of pRb led to increased apoptosis in MV1-Lu cells [122]. p84 contains a death domain consensus sequence in its C-terminal domain that shows sequence similarity to death domains in the tumour necrosis factor receptor 1 (TNFR1), TNFRSF1A-associated via death domain (TRADD) and Fas/Apo1.

Mutations in the conserved death domain region of p84 ablate its ability to induce apoptosis. GST-p84 fusion proteins have been shown to bind preferentially to hypophosphorylated pRb in cell lysates. Whereas p84 is present throughout the cell cycle, p84 could only be co-precipitated with pRb from G1 phase Monkey kidney BSC-1 (CV-1) cell extracts [123]. p84 is a component of the nuclear matrix and immunostaining experiments suggest that a high proportion of p84 is co-localized with centers of RNA processing. pRb is also known to localize to the nucleolus, and can interact with nuclear-associated proteins and Mdm2 [124, 125]. Enrichment of pRb in the nucleolus could represent a means of attenuating RNA polymerase I/III transcription [126]. Over-expression of cyclin E (forcing pRb hyperphosphorylation) in SAOS2 cells causes the removal of pRb from the nucleolus. This effect is dependent on the phosphorylation of the pRb large pocket domain. Localization of pRb to the nucleolus requires the N-terminal domain [106]. It seems therefore that pRb inhibits p84-induced apoptosis during G1 phase. p84 association to pRb is lost after Cdk phosphorylation of pRb and its subsequent expulsion from the nucleolus [123].

pRb interacts with SRC/p160 and NGF1B facilitating the *trans*-activation of pro-opiomelanocortin (POMC)

pRb can actively enhance the activity of some nuclear receptor transcription factors (such as Glucocorticoid receptor nuclear (GR)) by the recruitment of activator complexes such as Brm/GRG1 subunits of the SWI/SNF complex [127]. In the pituitary gland, cells express the pro-opiomelanocortin (POMC) and HNF-4 genes during enterocyte differentiation. Enterocyte differentiation is triggered through the action of the hypothalamic hormone 'corticotrophin-releasing hormone' (CRH) that binds to receptors in the cell membrane. Signal cascades are activated by CRH/receptor interaction. The down-stream consequence leads to ligand activation of nuclear receptors (NR) in the nuclear membrane.

Mutant mice heterozygous for the *Rb* gene ($Rb^{+/-}$) develop tumours of pituitary POMC expressing cells [52]. Humans do not develop pituitary tumours as a direct result of *Rb* inactivation. Comparing adenomas to poorly differentiated carcinomas, loss of *Rb* expression was linked to pituitary corticotroph tumour progression in humans [128]. Batsche *et al* investigated whether pRb regulates the transcription of the POMC gene [129].

A subset of three NR (Nur factors) are targeted by pRb including; Nur77, Nur-related factor (Nurr1) and neuron-derived orphan receptor 1 (NOR-1) [130-132]. Nur77 and NOR-1 are implicated in the control of thymocyte apoptosis, while Nurr1 plays an essential role in the development of the midbrain dopaminergic neurons (reviewed in [132]). Nur factors contribute to basal and CRH-induced POMC transcription. The pituitary POMC promoter target of Nur homodimer action is the Nur response element (NurRE) [130, 132].

The N-terminal activation domain (AF-1) recruits co-activators of the steroid receptor co-activator SRC/p160 family [133]. The C-terminal activation domain (AF-2) contains a ligand-binding domain (LBD), the direct target of CRH signalling. The AF-1 and AF-2 domains require co-activators such as SRCs to mediate their transcriptional effects. SRCs have HAT activity and are able to recruit CBP/p300 to enhance transcription [134].

Batsche *et al* [129] demonstrate that pRb acts as a potentiator of SRC/p160 co-activator function and that this action is mediated by direct interactions between pRb, Nurr 77 and SRCs. Their data demonstrated strong activation of the POMC promoter upon over-expression of pRb in AtT-20 corticotropin-secreting cells (AtT-20 cells), and that this effect was NurRE dependent. Interestingly, the N-terminal domain of pRb was required for the enhancement of NGFI-B/SRC activity. Co-transfection of the POMC promoter with a truncated pRb mutant (containing amino acids 379-928) exhibited markedly decreased POMC expression [129].

Studies into the structural domains of the N-terminal region of pRb

Two major studies on pRb domain structure presently exist. The initial study used tryptic digest to reveal protease resistant domains [135]. Later studies utilised caspases to reveal caspase resistant domains that roughly mirrored protease resistant domains [136]. Digestion of $p110^{Rb}$ (full length pRb) occurred in a stepwise fashion with transient fragments giving way to more stable proteolysis-resistant fragments. $p110^{Rb}$ yielded four protease-resistant fragments designated R (10kDa), N (30kDa), Λ (24KDa) and B (19.5KDa). The C-terminal domain of pRb is the least well defined. It is predicted that the C-terminal domain of pRb is highly flexible containing many turns and is therefore highly protease susceptible [136]. Sequence analysis of the N-termini of the recovered peptides revealed the exact location of these domains in pRb. The N-terminal domain of pRb was further digested and found to consist of 2 protease resistant sub-domains, N (1-263) and R (263-378).

This study was followed by the observation that pRb is cleaved by caspases into two fragments (p48 and p68) corresponding to N-terminal domain of pRb (1-378) and the large pocket (379-928) [136]. This cleavage is likely facilitated by caspases on one of four Aspartic acid (D) residues in the N-terminal domain of pRb (D 349, 363, 394, and 421). Over-expression of Bcl-2 (which blocks caspase activation) prevented the cleavage. This cleavage happens shortly before apoptosis, and results in p48 re-localising to the cytoplasm, and p68 releasing E2F-1.

Oncogenic mutations in the N-terminal domain of pRb

The IIA-N-pRb construct (1-376) is coded for by exons 1 to 12 in the *Rb* gene. Mutations that have been found in the N-terminal domain of the *Rb* gene (http://rb1-lsdb.d-lohmann.de) include point mutations, small deletions and insertions, large deletions, and small deletion/insertion complex mutations. Most mutations of the *Rb* gene in human

cancers lead to either splicing errors or premature termination of translation. Presently there are only six in-frame mutations identified in the sequence coding for the N-terminal domain of pRb in the *Rb* gene, and no in-frame deletion mutants [111]. That said, a deletion at 638 bp of the *Rb* gene leads to the altering of a splice donor site, causing the in-frame deletion of exon 4 [137]. Exon 4 covers amino acids 127-166. This mutant protein retains partial or complete large pocket activity in a number of *in vitro* assays of pRb function [138, 139].

At a general level, one might expect cancer-derived mutations affecting the N-terminal domain to correlate with highly conserved regions, or in regions important for the structural conformation of the protein. Among distantly related vertebrate species, pRb orthologues share 33 % amino acid identity over the entire length of the protein. The highest degree of structural similarity is in the A and B domains, but the N-terminal domain has identical amino acids at about 20 % of the positions. Within the N-terminal domain, the level of similarity varies considerably. Several sub-regions within the N-terminal domain (amino acid positions 195-235, 270-289, and 317-343 of human pRb) all exhibit greater than 50 % amino acid identity among the 5 disparate vertebrate species. Within these sub domains, there are stretches of amino acids that exhibit nearly complete similarity [111]. It is notable also that the N-terminal domain of pRb is unique and shares only 12 % homology to the N-terminal domains in p107 and p130 [111].

The affect of the N-terminal domain of pRb in relation to the tumour suppressor function of full length pRb.

Over the last two decades, the published literature on pRb has concentrated on the characterisation of the small and large pockets (379-792 and 379-928) respectively. This is not surprising considering that research on pRb tends to concentrate on its tumour suppression functions. Further, the N-terminal domain of pRb was thought to be

dispensable for pRb-mediated tumour suppression, and an N-terminal truncated pRb protein exerts more potent cell growth suppression than wild-type pRb [140]. The authors proposed that truncated pRb proteins could be produced by alternative translation from the second in-frame AUG codon of the *Rb* mRNA [140]. Alternative splicing at exon 2 has more recently been found in normal human placenta, various tumour cells, and rat tissues [141]. The resultant *Rb* transcript should be translated exclusively into a truncated Rb protein lacking the N-terminal 112 amino acid residues [141]. Viable N-terminal domain truncated pRb proteins have also been shown to accumulate in growth-arrested or differentiated human leukaemia cell lines after addition of retinoic acid, phorbol 12-myristate 13-acetate, or α-interferon [142-144].

In 1997, a study brought into serious question the assumption that the N-terminal region is dispensable for tumour suppression [145]. Although the entire deletion of the N-terminal domain leaves a truncated protein that growth suppresses more efficiently than wild-type pRb, mutation of specific regions in the N-terminal domain does compromise pRb-mediated tumour suppression. Studies were carried out in transgenic mice expressing human pRb with different deletions in the N-terminal domain (RbΔN). None of the deletions compromised Cdk2 consensus phosphorylation sites. The mutant mice were compared with mice expressing identically regulated wild-type pRb. Expression of both pRb and RbΔN caused developmental growth retardation, but the wild-type protein was more potent. In contrast to wild-type pRb, the RbΔN proteins were unable to rescue $Rb^{-/-}$ mice completely from embryonic lethality. Embryos survived until gestational day 18.5 but displayed defects in the terminal differentiation of erythrocytes, neurons, and skeletal muscle. Thus, the N-terminal domain is important for complete tumour suppression, as the *RbΔN* transgenes failed to prevent pituitary melanotroph tumours in $Rb^{+/-}$ mice. This study strongly suggests that the N-terminal domain of pRb is required for embryonic and post-natal development, tumour suppression, and the functional integrity of the entire Rb protein.

The N-terminal domain of pRb can be phosphorylated

There are presently two publications reporting the phosphorylation of the N-terminal domain of pRb. The first showed that pRb 1-378 is phosphorylated during G2/M phases by a novel pRb/histone H1 kinase (RbK) [100] and the second found that pRb is phosphorylated by cyclin D/Cdk4/6 and cyclin (A/E)/Cdk2 and that several residues in the N-terminal domain of pRb are phosphorylated during G1/S transition [146].

RbK was discovered during GST-pull down experiments using GST-pRb (1-378) bound to glutathione-agarose beads and used as affinity reagents in an *in vitro* protein-binding assay followed by an *in vitro* kinase assay. It was further discovered that part of the N-terminal domain of pRb (amino acids 89-202 [100]) associated with RbK in metaphase-arrested cells, and that RbK enzymatic activity peaks during G2/M phases of synchronised human caucasian, lung carcinoma cells (A549) and ML1 cells.

In 1992, a study reported that a variety of subtle N-terminal domain *Rb* mutations abrogate pRb-mediated growth suppression and block pRb phosphorylation *in vivo* despite the retention of E2F-binding activity within the pRb pocket[120]. The N-terminal domain consists of three regions that contain kinase recognition sites [76, 120] and have been proposed to be important for phosphorylation of pRb [120]. There are two clusters of phosphorylation sites within the N-terminal domain of pRb (S230/S250/T252 and T356/T373), efficiently phosphorylated by Cdks [146]. These sites may be crucial to pRb function because they are conserved in rodents, fish, birds, and amphibians. Since phosphorylation can alter binding to pRb, phosphorylation can alter the spectrum of pRb protein complexes formed.

THE P53 TUMOUR SUPPRESSOR PROTEIN

The p53 tumour suppressor is a DNA binding transcription factor often found mutated in cancer. In response to DNA damage and conditions that require growth arrest

(such as cell density) p53 is activated [147]. Through inducing $p21^{WAF/CIP}$, p53 regulates the G1/S DNA damage checkpoint, where the cells arrest prior to S phase to allow DNA repair to be performed. Central to this process is Mdm2 (human Hdm2), an E3 ligase that targets both p53 and itself for ubiquitination. This function of Mdm2 has been shown to play a role in allowing export of p53 from the nucleus to the cytoplasm and degradation of p53 by the proteosome [148]. Mdm2 is a transcriptional target of p53, creating a negative feedback loop where p53 activates expression of Mdm2. This keeps p53 levels low during normal growth and development. Activation of the p53 response to cellular stress such as DNA damage, oncogene activation, telomere erosion and hypoxia is mediated, at least in part, by inhibition of Mdm2 and rapid stabilisation of the p53 protein [148].

Several oncogenes can induce stabilisation of p53 by enlisting the activity of ARF, a protein that functions by binding directly to Mdm2, inhibiting the ubiquitination of p53 and allowing accumulation of p53 in the nucleus [148]. ARF expression can be directly activated by the transcription factors DMP1 and E2F-1. In normal cells, a proliferative signal that activates the Ras/Raf/MEK/MAPK pathway will result in the activation of the transcription factors E2F, Ets and AP-1. Stabilization of E2F-1 leads to activation of ARF, which leads to activation of p53 and apoptosis. Ets and AP-1 bind to the *Mdm2* promoter and stimulate its production. These increased levels of Mdm2 balance the increase in ARF [149].

P300 AND CROSS-TALK IN THE CELL CYCLE

The p300/CBP family of proteins includes p300, CBP, p270 and potentially other proteins [150]. Evidence indicates that p300/CBP genes are altered in various human tumours [151-155], which is consistent with studies on $Cbp^{+/-}$ mice that suggest CBP possesses tumour suppressor activity in the haematopoietic system [156]. Thus p300/CBP proteins may be regarded as having some of the hallmarks expected of a classical tumour suppressor protein. The p300/CBP family are involved in processes including proliferation,

differentiation and apoptosis (reviewed by [157-159]. p300/CBPfunction as transcriptional co-activators and are involved in multiple, signal-dependent transcriptional events [160].

Viral oncoproteins (such as E1A and SV40 large T antigen) specifically target p300/CBP family proteins (Figure 9) [161-165]; reviewed by [166, 167]. p300/CBP interaction with viral oncoproteins causes a loss of cellular growth control [168, 169], enhances DNA synthesis [170] and blocks cellular differentiation [164, 171-173], reviewed by [159]. It is thought that p300/CBP proteins regulate transcription by directly remodelling chromatin through the acetylation of histones, facilitating the decondensation of chromatin, which allows the transcription machinery to access promoters [174-177]. p300/CBP family proteins are endowed with histone acetyl-transferase (HAT) activity [178] [179]. They are able to facilitate the transfer of an acetyl group to the ε-amino group of a K residue. The acetylation level of chromatin has been established as the key mechanism in regulating transcription, reviewed by [180].

Figure 9

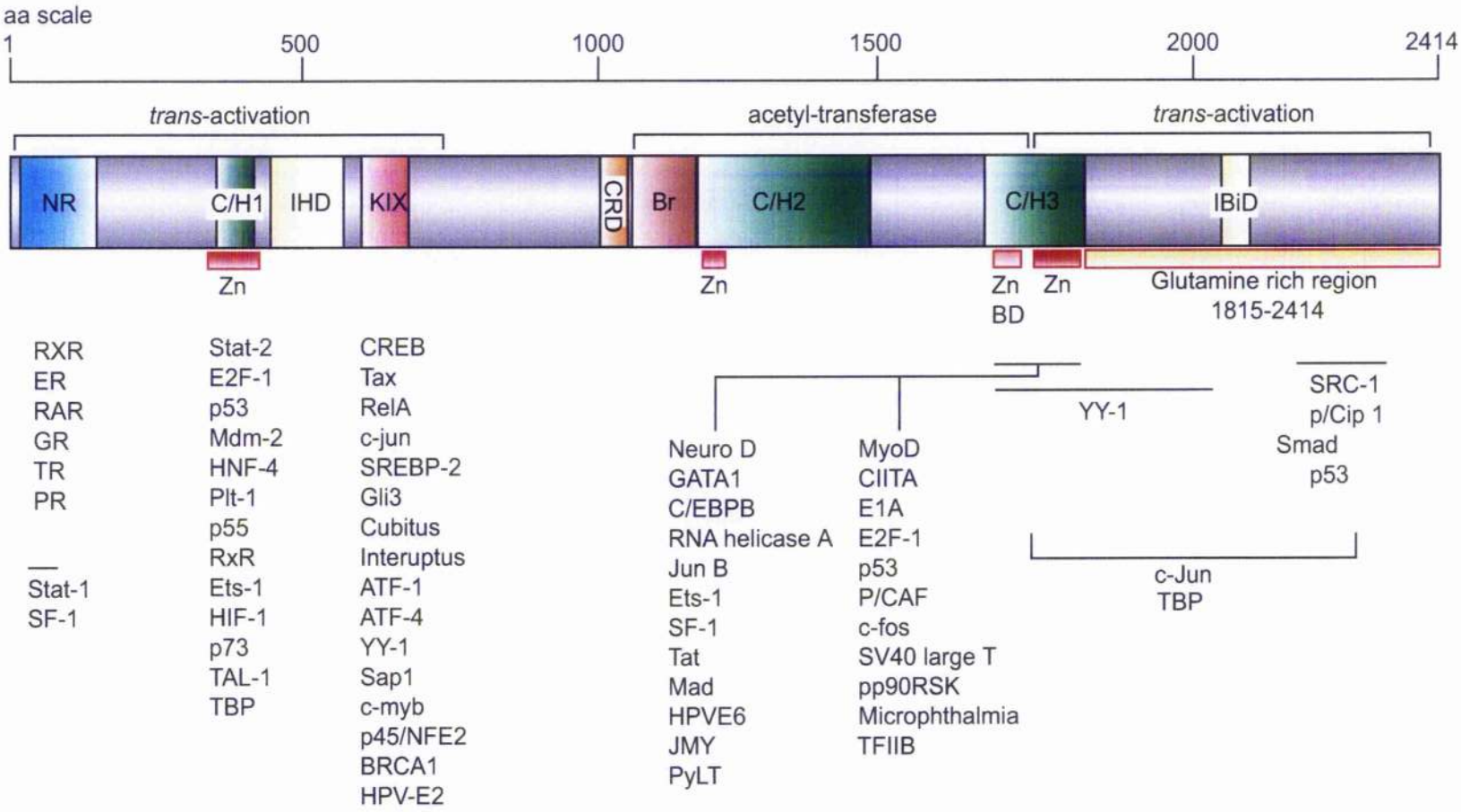

Adapted from [150], [160], and [178].

Figure 9: Schematic representation of the p300 protein depicting its domains and binding partners

The full length p300 contains all of the following defined domains; Nuclear receptor binding domain (NR), 3 cysteine-histidine domains (C/H1) (C/H2) (C/H3), CREB binding domain (KIX), the CRD domain, the Bromo-domain, the IBiD, and the N-terminal phosphopeptide-binding domains with homology to IBiD (IHD). The N-terminal and C-terminal domains are *trans*-activation domains that bind a variety of transcription factors to facilitate gene expression. The acetyl-transferase region (residues 1135 to 1673) recognises its substrates through the bromo-domain.

Underneath the schematic, known transcription factors that bind p300 are shown in relation to the region of p300 they bind.

The identification of p300/CBP

p300 and CBP were identified as proteins that bind to the adenoviral E1A and the cAMP-response-element-binding protein (CREB), respectively [181]. *p300/CBP* genes are conserved in a variety of multicellular organisms. *p300* is present in chromosome 22 (22q13) [163] and *CBP* resides in chromosome 16 (16p13.3) [182]. Curiously, the 22q13 region shares significant homology to 16p13.3, which is also implicated in Rubinstein-Taybi syndrome (RTS; [151]. Apart from *p300/CBP*, these two regions may contain eight other pairs of paralogous genes [183].

p300 and CBP share several conserved regions, which constitute most of the known functional domains in the proteins (Figure 9) [161]. The main conserved regions include the bromo-domain (conserved through out mammalian HATs), three cysteine-histidine rich (CH)-rich domains (CH1, CH2 and CH3), and a KIX domain. The CH1, CH3 and the KIX domains are likely to be important in mediating protein-protein interactions, and a number of cellular and viral proteins bind to these regions (Figure 9). Crystallographic studies show that the bromo-domain recognises acetylated residues [184]. p270 shares some common antigenic determinants with p300, and has been reported to be a component of mammalian SWI/SNF complexes (involved in chromatin remodelling) [185].

p300/CBP have many overlapping functions but also a number of unique functions. Most sequence specific transcription factors can be activated by p300/CBP in transfection-based assays. Knockout mice have been utilised to study the unique and connected functions of *p300/CBP*. Mice were generated that exhibited $p300^{-/-}$ or $Cbp^{-/-}$ genotypes. Both show similar embryonic lethal phenotypes [186]. Examination revealed defects in growth and neural tube closure [186]. Further more, some $p300^{+/-}$ mice and $Cbp^{+/-}$ mice suffer early lethality [186]. It is thought to be important for the protein levels of p300 and CBP to be maintained above a threshold (hence explaining $p300^{-/-}$ or $Cbp^{+/-}$ lethality) [186].

CBP and p300 also have unique functions. Patients suffering from the haplo-insufficient RTS are heterozygous for a mutation in the *Cbp* allele [151], and $Cbp^{+/-}$ mice also show skeletal abnormalities similar to sufferers of RTS [187]. $p300^{-/-}$ fibroblasts have specific defects in retinoic-acid dependent transcription but retain normal CREB activity [186].

p300/CBP and the cell cycle

E1A mutants that cannot bind to p300 exhibit defective cellular transformation [39]. This suggests that p300 and CBP are important in cell cycle regulation, reviewed by [167]. Studies of $p300^{-/-}$ and $Cbp^{-/-}$ knockout mice have provided direct evidence that p300/CBP proteins are important for cell cycle regulation and differentiation [186]. Consistent with this idea is the observation that in cell-based assays p300/CBP can cooperate with members of the MyoD family of muscle-differentiation regulating transcription factors in modulating the expression of down-stream myogenic factors, including myogenin and MEF2, and promote cell cycle withdrawal in myoblasts induced to differentiate [172].

The p300/CBP-P/CAF protein complex can arrest cell cycle progression [169]. Cell cycle arrest is required for cells to begin differentiation, and acetylation of pRb by P/CAF is required for C2C12 cells to arrest and undergo myogenic differentiation [53]. Mutation in the HAT domain of P/CAF impairs MyoD-dependent *trans*-activation [188]. It is interesting that the over-expression of E1A (which antagonises P/CAF binding to p300/CBP), drives cells into S-phase [169]. In *Caenorhabditis elegans (C. elegans)*, inactivating the *Cbp-1* gene blocks most aspects of differentiation. Evidence that acetylation by p300/CBP/P/CAF promotes differentiation was observed indirectly by the observation that components of the HDAC complexes which antagonize HAT activity, rescues some of the *Cbp-1* phenotype [189], providing evidence that p300/CBP/P/CAF

HAT activity is required for differentiation, at least in *C. elegans*, to counteract the role of HDACs.

Cell growth and proliferation are influenced by p300/CBP activity [170]. It was observed that *p300*$^{-/-}$ mouse embryonic fibroblasts MEFs grow more slowly compared to wild-type cells and have a phenotype reminiscent of senescence. The binding of E1A to p300 correlates with E1A-induced DNA synthesis [170], so the E1A-p300 complex might play an active role in stimulating cellular growth and proliferation.

There are other ways in which p300/CBP promotes cell growth and proliferation. p300 forms a ternary complex with p53 and Mdm2. Mdm2 mutants that fail to bind p300 are unable to degrade p53, hence p300 is required to degrade p53 [190]. In E2F-5, a Cdk-phosphorylation consensus site in the transcription activation domain is phosphorylated by cyclin E/Cdk2 as cells approach S-phase [191]. This phosphorylation was shown to augment interaction of p300 with E2F thereby enhancing the transcription of E2F genes [191].

p300/CBP proteins are also involved in mediating apoptosis. p300 can interact with the hypoxia-inducible factor (HIF1α) [192], which binds to and stabilizes p53 during hypoxia [193]. The HIF1α-p300/CBP-p53 pathway is thought to play an important role in regulating apoptosis under hypoxic conditions and may prevent tumour development. *In vitro* studies in mammalian cell-based assays have provided evidence that p300/CBP is involved in apoptosis [194]. Cells lacking p300 but not CBP have impaired ionising radiation (IR) sensitivity [195], and functional sequestration of p300/CBP activity by E1A, or a dominant negative version of p300, reduces p53-dependent apoptosis [194]. *In vivo* p300 also interacts in complex with JMY (junction-mediating and regulatory protein), and p53 in response to stress [196]. This complex up-regulates a variety of target genes including *bax*, which may account for its pro-apoptotic ability [196].

p300 is also involved in controlling cell adhesion [197]. The nuclear proto-oncoprotein SYT can associate with p300 and this association occurs predominantly in

contact inhibited cells [198]. SYT is an SH2/SH3 domain containing protein that becomes mutated in synovial sarcomas and certain other cancers. SYT mutant cells are believed to exhibit deficient cell adhesion control [197]. The mechanisms by which the p300-SYT interaction affects cell adhesion remains unclear.

Transcriptional regulation by p300/CBP

The initiation of transcription by RNA polymerase II requires sequence-specific promoter/enhancer-binding transcription factors as well as the basal transcription machinery. Unless transcription factors can directly interact with the basal transcription machinery, other proteins must act as bridges that connect them to the basal machinery. p300/CBP is known to interact both with a wide variety of transcription factors and with components of the basal transcriptional machinery, including TBP, TFIIB, TFIIE and TFIIF [196].

Therefore, in one model, p300/CBP provides such a bridge. Since p300/CBP proteins are involved in numerous signal transduction pathways, Kamei and colleagues have proposed that a coordinated re-distribution of p300/CBP activity among different classes of factor in a signal-dependent manner imparts specificity in transcriptional regulation [199]. For example, the engagement of p300/CBP by various hormone receptors inhibits AP-1 transcription [199], and over-expression of E2F-1 can hinder p53 *trans*-activation in a p300/CBP-dependent manner [200].

p300/CBP has been frequently found in complex with other HATs, including P/CAF [201], SRC-1 [202] and P/CIP/ACTR/AIB1 [203]. p300/CBP proteins might nucleate the assembly of diverse cofactor proteins into multi-component co-activator complexes [202]. p300/CBP may function as a scaffolding protein that binds a variety of transcription cofactors thereby facilitating protein-protein and protein-DNA interactions that make up the transcription machinery. Studies of the human interferon β (IFNβ) enhancer have shown that the surface of p300/CBP provides a scaffold for different

components of the transcription apparatus [204]. The recruitment of p300/CBP, together with transcription factors such as ATF2/JUN, p50/p65 of NF-kB and interferon regulatory factor 1, alongside architectural proteins including high mobility group (HMG) proteins, may be important for cooperativity and transcriptional activation [205].

p300/CBP HAT activity acts upon transcription factors, and the basal transcriptional apparatus, to influence transcription. Many transcription factors are acetylated by p300/CBP such as p53 [206], E2F-1, E2F-2 and E2F-3[88, 207], Myb [208], MyoD [188], GATA-1 [176], EKLF [209], HNF-4 [210] and NF-Y [211] (Figure 10). In almost all cases, acetylation enhances their DNA-binding activity. Acetylation at the p53 C-terminal domain may cause a conformational change that relieves the inhibitory effect of this region towards p53 DNA-binding, leading to increased DNA-binding activity [206].

It is also possible that acetylation creates a surface that facilitates protein-DNA recognition; this idea is consistent with the observation that many transcription factors have enhanced DNA-binding activity upon acetylation. Protein acetylation can also regulate protein-protein interaction; acetylation of *Drosophila* TCF inhibits its binding to Armadillo, thereby leading to down-regulation of transcription [212]. The viral oncoprotein E1A is also acetylated, and acetylation of K239 in E1A regulates its binding to CtBP (C-terminal binding protein), which is capable of interacting with various transcription repressors [213]. The pRb is acetylated in a fashion that influences subsequent phosphorylation of pRb, and E1A can stimulate pRb acetylation [214]. pRb is also acetylated during early stages of differentiation by P/CAF [53]. Components of the basal transcription apparatus (for example, TFIIE and TFIIF, and TAF(I)68), can also be acetylated [175]. Acetylation of these factors enhances DNA-binding activity and consequently stimulates gene activity [215]. Many more transcription factors are known to be acetylated and with various functional outcomes (listed in Figure 10).

Acetylation of multiple sites in the core histone tails is associated with transcriptional activity. An important question is whether the p300/CBP HAT activity

targets nucleosomal histones directly and regulates transcription by chromatin remodelling. Although p300/CBP can acetylate all four core histone *in vitro* [179, 216], it is not clear whether histones are the *bona fide* targets of p300/CBP HAT activity *in vivo* and, if so, which K residues in the histone tails are specifically modified by p300/CBP HAT. Biochemical and genetic experiments have demonstrated the importance of histone tails as key targets of acetylation, which has a significant impact in regulating transcription [177] reviewed by [217]. Specifically, by mutating the N-terminal tail of histone H4, Durrin *et al* showed that conditionally active genes, such as *Gal1* or *Pho5*, become less inducible [218]. Furthermore, mutation of certain K residues in the H3 and H4 tails may bypass the need for GCN5 (a key yeast HAT) for transcriptional activation [177]. Acetylation may be responsible for transcriptional repression, because deletion or K substitution in the histone H3 tails leads to higher basal levels of *Gal1* and *Pho5* transcription in budding yeast [219].

Figure 10

	Protein	References
Acetylation increases DNA binding affinity	p53	Gu and Roeder, 1997
	SRY	Thevenet et al., 2004
	STAT3	Yuan et al., 2005
	GATA1	Boyes et al., 1998
	GATA2	Hayakawa et al., 2004
	E2F-1	Martinez-Balbas et al., 2000; Marzio et al., 2000
Acetylation decreases DNA binding affinity	YY-1	Yao et al., 2001
	HMG-A1	Munshi et al., 1998
	HMG-N2	Luhrs et al., 2002
	p65	Kiernan et al., 2003
Acetylation increases transcriptional activation	p53	Gu and Roeder, 1997; Luo et al., 2004
	HMG-A1	Munshi et al., 2001
	STAT3	Wang et al., 2005; Yuan et al., 2005
	AR	Fu et al., 2000; Gaughan et al., 2002
	ERα (basal)	Wang et al., 2001
	GATA1	Boyes et al., 1998
	GATA2	Hayakawa et al., 2004
	GATA3	Yamagata et al., 2000
	EKLF	Zhang and Bieker, 1998
	MyoD	Sartorelli et al., 1999; Polesskaya et al., 2000
	E2F-1	Martinez-Balbas et al., 2000; Marzio et al., 2000
Acetylation decreases transcriptional activation	ERα (ligand dependent)	Wang et al., 2001
	HIF1α	Jeong et al., 2002
Acetylation increases protein stability	p53	Ito et al., 2002
	c-MYC	Patel et al., 2004
	AR	Gaughan et al., 2005
	ERα	Kawai et al., 2003
	E2F-1	Martinez-Balbas et al., 2000
	Smad7	Gronroos et al., 2002
Acetylation decreases protein stability	HIF1α	Jeong et al., 2002
Acetylation promotes protein protein interaction	STAT3	Wang et al., 2005; Yuan et al., 2005
	AR	Fu et al., 2002
	EKLF	Zhang et al., 2001
	Importin α	Bannister et al., 2000
Acetylation disrupts protein protein interaction	NF-κB	Chen et al., 2001
	Ku70	Cohen et al., 2004
	Hsp90	Kovacs et al., 2005

Figure 10: The ramifications of acetylation of non-histone cellular proteins

This table lists the non-histone proteins presently known to undergo acetylation. Shown here is a summary of transcription factors and other non-histone proteins are acetylated. In each case the purported function of acetylation is listed in the left column.

Biochemical analysis indicated that the removal of H2A/H2B from nucleosomal arrays enhances gene activity, at least in part by decreasing the level of chromatin folding [220, 221]. More recently, a functional interaction between p300/CBP and a family of proteins involved in nucleosome assembly, the nucleosome assembly proteins (NAP), has been documented [222]. NAP is involved in the assembly of regularly spaced nucleosomal arrays [223]. Ito *et al* demonstrated that acetylation of histones by p300 helps the transfer of H2A-H2B dimers from nucleosomes to NAP-1 [222], such a mechanism might directly couple acetylation of nucleosomes to nucleosome remodelling in transcriptional regulation.

HATs might then play roles in both transcription activation and inactivation [205]. Hypo-acetylation generally (but not always) correlates with transcriptional repression, and hyper-acetylation correlates with transcriptional activation, reviewed by [180]. Mechanistically, acetylation of K residues within the histone tails may have several outcomes: (1) it may promote transcription factor access to DNA in chromatin [224], possibly by neutralising the positive charge associated with the K ε-amino group (reviewed by [225]); (2) it may weaken inter-nucleosomal interactions and de-stabilise higher-order chromatin structure [220, 221]; and (3) it may promote the processivity of RNA polymerase through nucleosome arrays [226].

Li *et al* elegantly demonstrated the requirement of p300 HAT activity in stimulating transcription from the thyroid hormone receptor bA (*tr* b*a*) promoter and *hsp70* promoter. Importantly, these studies suggested that p300 facilitates transcription from a disrupted chromatin template but is not itself involved in disrupting chromatin structure and instead stabilises a remodelled chromatin state [211, 227].

Objectives

pRb was first discovered to be acetylated by Chan *et al* [214]. pRb acetylated at residues K873/874 was shown to prevent *in vitro* phosphorylation of pRb by cyclinE/Cdk2. Thus, acetylation of K873/874 was predicted to induce cell cycle arrest at the G1/S phase boundary. Flow cytometry studies confirmed that the pRb mutant derivative pRb (379-928) 873/874 QQ, caused an increase in the percentage of cells in G1-phase as a proportion of the total asynchronous cell population [214].

Further to this, acetylation of pRb was observed to be induced by differentiation in 'human leukemic monocyte lymphoma cell line' (U937 cells) [214]. This has been followed by a recent study that confirms pRb acetylation at residues K873/874 is required for the initial stages of differentiation in C2C12 cells [53]. Using a specific antibody raised against acetylated K873/874, acetylation of pRb was shown to be induced by etoposide treatment in a variety of cell lines [97]. Consequently, a corresponding change in the intra-nuclear localization of acetylated pRb was observed in response to DNA damage [74, 97]. One of the aims of this study is to trace some of the down-stream functional consequences of K873/874 acetylation, in relation to the control of E2F-1.

Analogous studies on E2F-1 and p53 revealed they are acetylated in response to DNA damage [75, 228]. Similar studies found that E2F-1 is phosphorylated and stabilized by ATM kinase and Chk2 kinase in response to DNA damage [73, 229], and that phospho-E2F-1 (phosphorylated at S364) also undergoes a nuclear redistribution in response to DNA damage. Exogenous expression of E2F-1 is known to induce apoptosis by *trans*-activation of apoptotic genes such as *p73* and *apaf-1* [75]. As pRb is acetylated in response to DNA damage, it follows that the acetylation of pRb might be involved in regulating E2F-1-dependent apoptosis. A further objective of this study was to address how the acetylation of pRb might influence E2F-1 activity, and to test whether acetylation of pRb at residues K873/874 could facilitate nuclear redistribution in response to DNA damage.

pRb was shown to be *in vitro* acetylated by p300 in four out of its six domains; only the spacer and the N-terminal demain remained left to study [214]. An additional aim of this study was to address whether the N-terminal demain of pRb is acetylated both *in vitro* and *in vivo*, and under what control. A key question concerned whether or not the N-terminal domain of pRb can impact on the well-characterized properties of pRb (for instance, its interaction with E2F-1) through interacting with the C-terminal domain.

CHAPTER 2

MATERIALS AND METHODS

PLASMIDS

pGEX2T-Rb (379-928) has been described in Bandara *et. al.* 1991 [230]. pGEX2T 763-928, and pcDNA3-9B10 Rb (1-928) were kind gifts from Robert White and Sybille Mittnacht. pSG5L-HARb 1-928 was kindly provided by Bill Sellers. pGEX2T GST-Rb 10-330 was provided by Paul Robins [231]. Flag-p300 1134-2414, and His-p300 1195-1673 have been described previously [214]. Flag-p300 (FL) baculovirus was also provided by Nakatani [216]. pHA-E2F-1 and pCMV-βgal plasmids have been described in Lee *et. al.* [232]. pE2F-1 and pDP-1 have been described in Bandara *et. al.* [233]. The mammalian expression vector for Mdm2 has been described [234].

pGEXKG-Rb 1-376 and pcDNA3HA-Rb 1-376 were PCR cloned from pSG5L-HARb 1-928 using the Advantage® –GC2 PCR kit (Clontech) as per supplied protocol.

Plasmids	5'-Primer	3'-Primer
pGEXKG-Rb 1-376 and pCDNA3HA-Rb 1-376	TAATTACCATGGCCTACCCCTACGACGTG	TTCTAGCTCGAGTGACCTAACTGGAGTGTGTG

The 'Quick change multi site-directed mutagenesis kit' (Stratagene) was utilised to generate pGEX2T-Rb 763-928 $^{K873Q/K874Q}$ and pGEX2T-Rb 763-928$^{K873R/K874R}$ from pGEX2T-Rb 763-928. The 2HA-pcDNA3-Rb 763-928, 2HA-pcDNA3-Rb 763-928$^{K873Q/K874Q}$, and 2HA-pcDNA3-Rb 763-928 $^{K873R/K874R}$ were subcloned from pGEX2T 763-928, pGEX2T 763-928$^{K873Q/K874Q}$ and the pGEX2T 763-928$^{K873R/K874R}$ bacterial expression vectors respectively by restriction digest using *Bam* H1, and *Eco*R1 restriction

enzymes (Promega). The resulting vectors were sequenced by Lark technologies using the universal pGEX reverse primer to confirm the mutant's identity. pSG5L-HARb 1-928$^{K873Q/K874Q}$ and pSG5L-HARb 1-928 $^{K873R/K874R}$ were subcloned by restriction digest from pcDNA3 9E10 Myc-Rb 1-928.

SITE-DIRECTED MUTAGENESIS

pGEX2T-C-pRb 763-928 point mutants were generated using Quick change site-directed mutagenesis kit (Stratagene). Primer pairs encoding Rb K873/874 to Q (QQ) or R (RR) were generated (using specifically designed software on the Stratagene website http://labtools.stratagene.com/QC). The primer properties match those listed in the manual; ie 25 to 45 bases in length, with a melting temperature (TM) of ≥ 78 °C, and with the desired mutation in the middle of the primer, with 10-15 bases of the correct sequence on both sides. Primers were manufactured by Sigma-Genosys. Briefly; these primers were annealed to the circular double-stranded template (pGEX2T-C-pRb 763-928) and extended by PCR reaction in a thermal cycler with PfuTurbo® DNA polymerase to produce two nicked circular strands. The parent template DNA was then digested using Dpn1 (which only recognises methylated template DNA). The mutated product was then transformed into XL1-Blue super competent cells. These cells repair nicks in the mutated DNA strands. The resulting cells were grown on Terrific Broth (TB) (Sigma-Aldrich)/agar plates containing ampicillin at 50 µg/ml final concentration (Sigma-Aldrich). Colonies were cultured overnight in TB/amp growth media and the DNA was harvested using the mini prep kit (Qiagen). The resulting DNA was sequenced using the universal pGEX reverse primer to confirm the mutations and the accuracy of the PCR product (Lark technologies).

Plasmids	Primer pair
873/874RR	Sense 5'-ccctcctaaaccactgagaaga ctacgctttgatattgaag-3' αSense 5'-cttcaatatcaaagcgtagtcttct cagtggtttaggaggg-3'
873/874QQ	Sense 5'-caaccctcctaaaccactgcagcaa ctacgctttgatattgaag-3' αSense 3'-cttcaatatcaaagcgtagttgctg cagtggtttaggagggttg-3'

TISSUE CULTURE AND TRANSFECTION

The C33A, U2OS, HEK 293, and HeLa cells were cultured in Dulbecco modified Eagle medium (GIBCO) supplemented with 10 % foetal calf serum (FCS) and 0.1 % penicillin/streptomycin (GIBCO) at 37 °C in 5 % CO_2. These human cancer cell lines were purchased from the European Tissue Culture Collection (ECACC). High Five (HI5) and SF9 insect cells were utilised for the protein expression and baculovirus amplification respectively. Insect cells were maintained in TC100 medium (GIBCO) supplemented with 5 % FCS and 0.1 % gentamycin (GIBCO) at 26 °C. HI5 and SF9 cells were purchased from Cancer Research UK (CRUK). Detection of acetyl-N-pRb was aided by treating cells with 10 μM TSA, which was purchased from Sigma Aldrich. Transfections were carried out using both Effectene transfection reagent (Qiagen) and Genejuice transfection reagent (Novagen) according to manufacturer's guidelines. pCMV-β galactosidase (β-gal) 0.5 μg was included in all transfections to compare transfection efficiency between samples. The amount of DNA in each transfection in an experiment was equalised by the addition of the appropriate amount of empty vector DNA.

IMMUNOBLOTTING AND IMMUNOPRECIPITATION

Primary Antibodies

The 'Acetylated-Lysine Polyclonal Antibody' (Anti-Ac-K poly) and the 'Acetylated-Lysine Monoclonal Antibody' (Anti-Ac-K mono) were both purchased from Cell Signalling. Anti-HA monoclonal antibody αHAII (ascites form) was purchased from Covance, and the anti-HA polyclonal antibody αHA-Y11 was purchased from Santa Cruz. The monoclonal E2F-1 antibody KH95 along with the E2F-1 polyclonal antibody C20 were purchased from Santa Cruz. The pRb antibodies IF8 (monoclonal) and C15 (polyclonal) were purchased from Santa Cruz. The pRb antibody G3-245 mouse monoclonal antibody was purchased from BD biosciences. Anti-DP-1 polyclonal antibody K20 was purchased from Santa Cruz. The anti-Mdm2/Hdm2 monoclonal antibody SMP14 was purchased from Santa Cruz. The anti-Flag antibody (M2) was purchased from Sigma. The anti-GST antibody B14 was purchased from Santa Cruz.

Secondary antibodies

The following secondary antibodies were used for immunoblotting at 1 in 5000 dilution from manufacture's stock: Goat anti-mouse antibody and goat anti-rabbit antibody were purchased from Dako.

The following fluorescent secondary antibodies were used during immunostaining at 1 in 400 dilution from manufacture's stock: The 'Alexa Fluor ® 488 (green) goat anti-mouse antibody (2 mg/ml)', the 'Alexa Fluor ® 594 (Red) goat anti-mouse antibody (2 mg/ml)', and the 'Alexa Fluor ® 595 (Red) donkey anti-rabbit antibody (2 mg/ml)' were purchased from Invitrogen.

Preparing cell lysate with IPH buffer

Cells were incubated for 48 h post-transfection. The cells were then washed twice in ice-cold PBS purchased from Sigma (supplemented with protease inhibitor cocktail ((Calibiochem) at 1 in 1000 dilution). Cells were harvested by scraping cells into 1 ml of fresh ice-cold PBS. Cell pellets were collected by centrifugation at 1200 rpm in a Sorvall bench top centrifuge. Pellets underwent lysis by rotation on a wheel at 4 °C in IPH buffer (50 mM Tris pH 8.0, 150 mM NaCl, 5 mM EDTA, 1 mM PMSF, protease inhibitor cocktail ((Calibiochem) at 1 in 1000 dilution), 10 µM TSA (Sigma)), supplemented with 0.5 % NP-40. Cells underwent lysis for 45 min before being centrifuged at 13000 rpm for 20 min (in a Sorvall bench top micro centrifuge) to separate the required supernatant from the waste cell debris. Supernatant was kept on ice whilst the protein concentration was determined using the Bradford assay (Biorad).

Preparation of separate nuclear and cytoplasmic extracts.

Separate nuclear and cytoplasmic extract was prepared using a slightly modified version of the Dignam method [235]. After transfection, cells were incubated for 48 h. The cells were washed twice in ice-cold PBS (containing protease inhibitor cocktail (Calibiochem) at 1 in 1000 dilution). Cells were scraped into 1 ml of ice-cold hypotonic buffer (20 mM HEPES pH 7, 10 mM KCL, 1 mM $MgCl_2$, 0.5 mM DTT, 0.1 % Triton X-100, 20 % Glycerol, 2 mM PMSF, 10 µM TSA) supplemented with protease inhibitor cocktail ((Calibiochem) at 1 in 1000 dilution). Cells were disrupted using 15 strokes of a Dounce Homogeniser. Following this, samples were centrifuged at 3000 rpm for 5 min. The supernatant was removed and stored as the cytoplasmic fraction. The remaining pellet was resuspended in 2/3-pellet volume of extraction buffer (hypotonic buffer supplemented with 420 mM NaCl). Nuclear lysis was achieved by incubating samples (under rotation) at 4 °C for 20 min. The nuclear extract was separated from the nuclear matrix by centrifuging

samples for 10 min at 13,000 rpm. Cytoplasmic and nuclear extract was kept on ice whilst the protein concentration was determined using the Bradford assay (BioRad). Extract was used right away or else stored at -80 °C.

Immunoprecipitation

In order to ensure equal loading of exogenous protein for each IP, the transfection efficiency of each sample was determined by measuring the relative expression of β-galactosidase (β-gal). To measure the β-gal activity, 20 µl of cell extract was mixed with 20 µl of 2x β-gal buffer (200 mM Na phosphate buffer pH 7.3, 2 mM $MgCl_2$, 100 mM β-mercaptoethanol (Sigma), 1.33 mg/ml o-nitrophenyl-beta-d-galactopyranoside (ONPG) (Sigma)). The reaction mixtures were incubated at 37 °C until a yellow colour developed. The reactions were stopped by the addition of 960 µl of 0.5 M Na_2CO_3 to each sample, and the relative absorbances were measured at 420 nm.

In some experiments it was necessary to measure the difference in binding affinity of various mutants of the C-terminal domain of pRb for E2F-1. In order to ensure the equal loading of mutant proteins, 100 µg of input for each transfected mutant were first run on a sodium dodecyl sulphate-polyacrylamide gel electrophoresis (SDS-PAGE) gel. Immunoblotting facilitated visualisation of relative protein levels. Relative protein levels were ascertained by measuring the band intensity of the exogenous protein in each sample using densitometric analysis software (Image J).

Protein-G-agarose was incubated with 3 µl of primary antibody (2.5 µg/µl) for 2-4 h at 4 °C. The resulting beads were washed 6 times with IPH buffer (supplemented with 0.5 % NP-40) to remove excess antibody. Each protein extract sample was first pre-incubated for 1 h at 4 °C with antibody free Protein-G-agarose in order to remove that bound non-specifically to the agarose beads. Pre-cleared extract was incubated with antibody bound Protein-G-agarose for 2-5 h at 4 °C rotating on a wheel. After incubation,

the beads were extensively washed (approximately 6 to 10 times) with IPH buffer (supplemented with 0.5 % NP-40). Proteins bound to the beads were eluted with 3X SDS loading buffer (150 mM Tris pH 6.8, 6 % SDS, 0.3 % Bromophenyl Blue, 30 % glycerol, and 2 mM β-mercaptoethanol) and visualised by immunoblotting using the appropriate antibodies.

All other immunoprecipitations described were carried out in the same manner as above, with slight modifications of the NP-40 concentrations.

STRIPPING AND RE-PROBING OF BLOTS

In order to re-probe blots, bound antibodies were removed by immersing the blotting membrane in 15 ml of stripping buffer (0.2 M Glycine, 1 % SDS, HCL to pH 2.5) for 45 min at room temperature. The stripped membrane was rinsed with dH_20 over and over for a period of about 5 min. Removal of any residual stripping buffer was ensured by 3 (5 min) washes in PBS (supplemented with 0.1 % Triton-X-100). The membrane was then re-blocked in 5 % milk (Marvel) diluted in PBS (Sigma) for 30 min before re-applying the primary antibody.

IMMUNOSTAINING

The following immunostaining protocol is a modified version previously published by Gonzales *et al* [236]. Cells were transfected and fixed 48 h after transfection. Cells were washed twice in ice-cold PBS to remove growth media. Cells were then fixed in PBS (supplemented with 3.7 % formaldehyde) for 15 min. Residual formaldehyde was removed by washing the cells 3 times (5 min washes) with PBS. Cells were permeabilized by immersion in PBS (supplemented with 0.5 % Triton-X-100) for 5 min at room temperature. Cells were treated with PBS (supplemented with 10 % FCS) for 30 min at room temperature. The blocking solution was aspirated and the cells were treated with 100 µl of primary antibody solution (antibody added to PBS at the appropriate dilution) for 1 h

at room temperature. During primary antibody incubation, cells were stored in a humid box. Following this, the primary antibody solution was aspirated. The cells are washed 4 times (4 min washes) in PBS (supplemented with 0.025 % Tween 20). Cells were then treated with 100 µl of the appropriate Alexa Fluor® secondary antibody (diluted 1 in 400 in PBS) for 30 min in a covered humid box. The cells were washed 4 times (4 min washes) in PBS (supplemented with 0.025 % Tween 20). The cover slips were drained and mounted in Vectashield mounting medium with DAPI (Vector Labs H-1200) on a glass microscope slide. The slides were sealed with nail varnish. The cells were viewed on an Olympus BX60 fluorescent microscope. Images were taken using the Hamamatsu Digital CCD camera, and digitally manipulated using the Open lab computer software.

PROTEIN PREPARATION

Expression and Purification of Glutathione-S-Transferase-tagged fusion proteins.

Glutathione-S-Transferase fusion protein expression and purification were performed as described in the company protocol (Amersham, formerly Pharmacia). Fresh overnight starter cultures (50 ml) of BL21 (DE3) pLys (Invitrogen) were transformed with the appropriate pGEX-recombinants diluted 1 in 10 in TB media (supplemented with 0.8 % glycerol and ampicillin (100 µg/ml)). The bacterial cultures were incubated for 16 h at 37 °C with shaking (225 rpm).

Cells were diluted 1 in 50 in the same growth media, and sub-cultured in the same conditions until the bacterial culture density (measured by a spectrophotometer) reached an absorbance of approximately 0.5-0.6 at 600 nm. Upon reaching this cell density, the culture was supplemented with 50 µM isopropyl-β-D-thiogalactopyranoside (IPTG, Sigma). The culture was subsequently incubated at 15 °C for 15 h to allow for the induction of protein expression before harvesting the cells.

Bacterial pellets were collected from the cultures by centrifugation at 13,000 rpm

for 10 min at 4 °C. The bacterial pellet was then re-suspended in 30 ml (or equal pellet volume) of PBS (supplemented with 200 μM PMSF, protease inhibitor cocktail (Calibiochem) at 1 in 1000 dilution and 1 % Triton-X-100 (Sigma)). Lysis of the re-suspended culture was achieved by passing the culture drop-wise through a pressure gradient of 995 psi (three times) in a French press machine. The soluble and insoluble fractions were separated by centrifugation at 13000 rpm for 30 min at 4 °C. The soluble supernatant was transferred to 50 ml falcon tubes. Glutathione-Sepharose beads (200 μl of beads per 100 ml bacterial culture) was added to the soluble fraction and incubated under rotation at 4 °C for 1 h. The glutathione-Sepharose beads were washed three times with 20 ml of ice-cold PBS supplemented with 1 % Triton, and once with cold PBS prior to the addition of soluble lysate.

GST beads were separated from the lysate by passing the mixture through a 5 ml polypropylene column (Qiagen). The beads were washed twice (30 min per wash) in 5 ml PBS (supplemented with 200 μM PMSF, protease inhibitor cocktail ((Calibiochem) at 1 in 1000 dilution) and 1 % Triton-X-100). The beads were washed for a further 40 min in PBS without Triton-X-100. Protein impurities were removed by a further 20 min wash step using PBS (supplemented with 200 μM PMSF, protease inhibitor cocktail (Calibiochem) at 1 in 1000 dilution and 10 μM reduced glutathione (Sigma)). Protein preparations produced for *in vitro* pull down assays were stored at -20 °C at this stage. For experiments requiring eluted protein, GST-tagged proteins were batch eluted by incubating the GST beads for 30 min in elution buffer (50 mM Tris-HCL (pH 8), 10 mM reduced glutathione, 120 mM NaCl) rotating at 4 °C. The ratio of bead volume to elution buffer volume ratio for elution was 1:1. All fusion proteins were subsequently dialysed into BC100 exchange buffer (20 mM Tris-HCL (pH 8), 0.5 mM EDTA, 100 mM KCl, 20 % glycerol, 0.5 mM DTT, 0.5 mM PMSF and protease inhibitor cocktail (Calibiochem) at 1 in 1000 dilution). Dialysis was facilitated by injecting eluted protein into 500 μl capacity dialysis slides (Pierce Slide-

A-Lyser® 0.5 ml dialysis cassettes) and immersing the cassettes into ice-cold BC100 exchange buffer. Cassettes were left rotating in buffer for approximately 3 h. All aliquots of protein were run through SDS-PAGE gels and visualised by Coomassie staining. Protein aliquots were stored at –80 °C.

Expression and purification of His-tagged fusion proteins

The procedure for His-tagged fusion protein expression was similar to that described for GST-fusion protein expression. Fresh overnight starter cultures (50 ml) of BL21 (DE3) pLys (Invitrogen) transformed with the appropriate pET28-recombinants were diluted 1 in 10 in TB media (supplemented with 0.8 % glycerol, containing kanamycin (10 μg/ml)) and incubated for 16 h at 37 °C with shaking (225 rpm). The bacterial culture was sub cultured, induced, pelleted and lysed using exactly the same procedures as those outlined in the GST-fusion protein expression protocol above. The buffers used to prepare His-tagged proteins were different. Pelleted bacteria were resuspended in Lysis buffer (10 mM Tris pH 7.9, 10 % glycerol, 0.5 M NaCl, 0.1 % NP-40, 0.5 mM PMSF, and protease inhibitor cocktail (Calibiochem) at 1 in 1000 dilution).

The soluble fraction of the lysate was supplemented with 1 mM Imidazole. At this stage, Ni-NBT agarose beads (Qiagen) were washed 3 times in lysis buffer. The Ni-NBT agarose beads (200 μl of beads/100 ml culture) were added to the extract and incubated under rotation at 4 °C for 1 h. Ni-NBT beads were separated from the lysate by passing the mixture through a 5 ml polypropylene column (Qiagen). The beads were washed 3 times in 5 ml volumes of BC100 (supplemented with 20 mM Imidazole) each wash lasting 30 min under rotation at 4 °C. The beads were then washed for 20 min in BC100 (supplemented with 40 mM Imidazole). Elutions of the bound His-tagged proteins were facilitated by the addition of a volume of BC100 (supplemented with 2 M Imidazole) equal to the Ni-NBT bead volume. The polypropylene column containing the beads and elution buffer were rotated at 4 °C for 1 h. Protein samples were dialysed in BC100 as described for GST

protein preparation, so removing the Imidazole.

Amplification of Flag-p300 FL baculovirus

SF9 insect cells were used to amplify the Flag-p300 baculovirus. SF9 cells were grown in 150 ml tissue culture flasks. The first step was to initially infect the cells with virus. The media was aspirated and 200 µl of virus along with 2 ml of serum free TC100 (GIBCO) were added to the flask. The flasks were covered from the light and left rocking for 1 h at room temperature. After initial infection, the flask was supplemented with 23 ml of TC100 (supplemented with 5 % FCS and 0.1 % gentamycin (GIBCO)). The SF9 cells were left until most of the cells had burst (between 10 to 14 days). The virus and media was aliquoted into sterile screw capped vials and stored at -80 °C (wrapped in tin foil to keep out the light).

Expression and purification of Flag-p300 FL baculovirus

The first step was to determine the optimal amount of virus and the optimal cell density for baculovirus expression in High Five (HI5) cells. HI5 cells were grown on 6 well tissue culture plates. The 6 well plates were infected at different levels of cell density (40 %, 50 %, 70 %, 80 %, and 90 % confluence). Each plate was then divided so each well was infected with increasing volumes of virus (10 µl, 20 µl, 50 µl, 100 µl, 150 µl and 200 µl). Infection procedure was identical to that described above. The HI5 cells were harvested 48 h post-transfection in 500 µl ice-cold PBS. The cells were pelleted by centrifugation at 1,500 rpm for 5 min. The supernatant was removed, and replaced with 100 µl of 3X SDS loading buffer. Cells were mixed and briefly sonicated for 10 sec before heat denaturing the proteins at 100 °C for 5 min. The samples were run on an SDS-PAGE gel and visualised by immunoblotting. Anti-Flag antibody was used to detect p300 levels. The virus concentration that gave the best expression was scaled up for infection of a T150

tissue culture flask.

Large-scale expression of Flag-p300 FL required 9 flasks of HI5 cells (T150 tissue culture flasks). Optimum cell density was determined to be approximately 70 % confluence. The growth media in the flasks was aspirated and the appropriate volume of virus was added with 2 ml of serum free media. The flasks were covered to keep out light and left rocking at room temperature for 1 h. After the infection period, the flasks were topped up with 23 ml of TC100 (supplemented with 5 % FCS, 0.1 % gentamycin). Cells were incubated at 26 °C for 48 h. Cells were removed by agitation. The cells and media were decanted into 50 ml falcon tubes and washed 3 times in ice-cold PBS (supplemented with 0.5 mM PMSF, and protease inhibitor cocktail (Calibiochem) at 1 in 1000 dilution). The cell pellets were combined so that they were shared between 2 falcon tubes. Cells were lysed by the addition of 5 ml lysis buffer (25 mM HEPES pH 7.8, 0.1 mM EDTA, 0.4 M KCL, 0.1 % NP-40, 5 mM β-mercaptoethanol, and protease inhibitor cocktail ((Calibiochem) at 1 in 1000 dilution). Pellets were lysed using 15 strokes of a dounce homogenizer (kept cold in ice throughout). Soluble lysate was recovered by centrifugation at 13000 rpm for 15 min at 4 °C.

Precipitation of Flag-p300 FL was accomplished by incubating the lysate with 1 ml of resuspended 'EZ view ^{TM} Red ANTI-FLAG ® M2 Affinity Gel' (Sigma). These 'Flag' beads were washed 3 times with 10 ml lysis buffer prior to incubation with the lysate in order to remove the preservative. The incubation mixture was rotated for 1 h at 4 °C. After binding, the Flag beads were washed 2 times with 10 ml of ice-cold wash buffer (50 mM Tris pH 8.6, 200 mM KCL, 2 mM β-mercaptoethanol) each wash rotating for 30 min at 4 °C. The Flag beads were transferred to 5 ml polypropylene columns (Qiagen). Flag-p300 FL was eluted into 300 µl fractions with elution buffer (50 mM diethanolamine, 1 M KCL, 1 mM EDTA, 50 % ethyleneglycol). Fractions were eluted into chilled eppendorf tubes containing 20 µl of 2 M NaI_2PO_4 to adjust the pH to 7. All samples were dialysed into

BC100 exchange buffer (supplemented with 0.5 mM PMSF and protease inhibitor cocktail ((Calibiochem) at 1 in 1000 dilution) using the same dialysis slides mentioned in the GST fusion protein purification protocol. Small aliquots (10 µl) of the fractions were run on an SDS-PAGE gel and visualised by immunoblotting. Anti-Flag antibody was used to detect p300 levels.

Protein concentration

If the protein preparations required concentrating, dialysed protein was placed into 'Viva spin columns' (Pierce). The columns contain an inner vessel with a porous membrane on one side, and an outer vessel that completely encloses the inner vessel. Protein samples were concentrated through centrifugation of the columns at 13,000 rpm on a bench top Sorval micro centrifuge. Spin columns with a MWCO of 10,000 Daltons were used to concentrate the various GST-pRb proteins for use in acetylation assays.

IN VITRO PROTEIN ACETYLATION ASSAY

Recombinant proteins (for use as substrate) were compared against known concentrations of BSA protein by visualisation on a Coomassie stained SDS-PAGE gel. Core histones purified from chicken erythrocytes were purchased from Upstate for use as positive control in p300 acetylation assays.

Reactions were prepared with 2-4 µg of substrate protein, 6 µl of 5x HAT buffer (260 mM Tris pH 8, 25 % glycerol, 0.5 mM EDTA), 3 µl of DTT (10 mM), 1 µl [^{3}H] Acetyl-Coenzyme A (50 µCi/ml) purchased from Amersham, 0.2 µg of HAT, and de-ionised water to bring the reaction volume to 30 µl. Reactions were mixed briefly by vortex, and centrifuged briefly at 13,000 rpm. Reactions were incubated in a 30 °C water bath for 30-45 min, and then briefly centrifuged (at 13,000 rpm). Samples were mixed by pipetting, and carefully spotted onto 2 cm diameter phosphocellulose filter paper circles (P81 grade chromatography paper purchased from Whatman). The filters (spotted

reactions) were then left to air dry for 15 min at room temperature. The filters were washed in 0.2 M sodium carbonate buffer (pH 9.2) 3 times (each wash lasting 5 min) at room temperature. The washed filters were briefly dipped into acetone and left to air dry for 1 h at room temperature. The dried filters were placed into scintillation vials containing 4 ml of scintillation fluid. Scintillation vials were mixed by inversion. Incorporation of [^{3}H] Acetyl-Coenzyme A was measured using a liquid scintillation counter.

IN VITRO PULL DOWN ASSAYS

In each experiment GST-tagged proteins (for use as bait) had their concentrations compared by visualisation on a Coomassie stained SDS-PAGE gel. Relative concentrations were determined by densitometric analysis of protein bands (using Image J software).

Cell extract (1 mg per pull down) was initially pre-cleared by incubation with 30 µl of GST sepharose beads (Amersham) rotating at 4 °C for 1 h. Pre-cleared extract was incubated at 4 °C for 1 h with 2 µg of GST tagged recombinant protein. Reaction volume was brought to 1 ml by addition of IVT buffer (50 mM Tris pH 7.5, 150 mM NaCl, 5 µM EDTA, 0.5 % v/v NP-40, supplemented with 0.8 mM DTT, 200 µM PMSF, 400 µM Sodium Orthovanadate, and protease inhibitor cocktail (Calibiochem) at 1 in 1000 dilution). Each reaction was then supplemented with 30 µl of GST beads and incubated for a further 3 h at 4 °C. Reactions were then washed 4 times (5 min per wash) with 700 µl of IVT buffer (0.5 % NP-40) to remove non-specifically bound proteins. All centrifugation steps were carried out at 2000 rpm for 2 min at 4 °C. Proteins bound to the beads were eluted with 40 µl of 3X SDS loading buffer and analysed by SDS-PAGE, followed by immunoblotting.

Listed are specific conditions and variations of the protocol for the different GST binding assays included in the thesis: *In vitro* translated (IVT) ^{35}S labelled pCMV E2F-1 was used for a source of target protein for the GST pRb (763-928) bait. Interaction was

therefore assessed using autoradiography to identify E2F-1, and coomassie staining to identify GST pRb (763-928). On establishing that E2F-1 bound GST pRb (763-928), the E2F-1 source for subsequent pull downs was derived from HEK 293 nuclear extract. Interaction was assessed as described in the main protocol (above). Levels of E2F-1 were detected by immunoblotting with anti-KH95 antibody (Santa Cruz). Levels of recombinant C-terminal domain of pRb were assessed by immunoblotting using anti C15 antibody (Santa Cruz), which binds to the C-terminal domain of pRb. Levels of recombinant GST-Gst Protein (used as a negative control) were detected using anti-GST B14 (Santa Cruz).

IVT Mdm2 was used as a source of target protein for accessing whether the pRb 763-928 $^{K873Q/K874Q}$ mutant derivative was able to bind other target proteins. IVT buffer used in the binding assay was supplemented with only 0.1 % NP-40. Mdm2 was detected by immunoblotting using anti-SMP14 antibody (Santa Cruz). Levels of recombinant C-terminal domain pRb were assessed by immunoblotting using anti-C15 antibody (Santa Cruz). Levels of recombinant GST-Gst Protein (used as a negative control) were detected using anti-GST B14 (Santa Cruz). HA-pSG5L-Rb 1-928 or 2HA-NRb 1-376 were transfected into HEK 293 cells.

Cells were lysed in IPH buffer (0.5 % NP-40). Following the GST pull down, levels of NRb and FL pRb were detected using mouse monoclonal HA11 antibody (Covance). Levels of recombinant C-terminal domain pRb were assessed by immunoblotting using anti-C15 antibody (Santa Cruz). Levels of recombinant GST-Gst Protein (used as a negative control) were detected using anti-GST B14 (Santa Cruz).

CHAPTER 3

INTRODUCTION: THE N-TERMINAL DOMAIN OF pRb IS ACETYLATED

THE N-TERMINAL DOMAIN OF pRB IS ACETYLATED *IN VITRO*.

Mutation or deregulation of pRb has been observed in nearly every type of human cancer examined [2]. Deregulation of pRb is so frequent in cancer that some have argued it is a prerequisite for all human cancer [25]. Although pRb can physically interact with well over 100 different cellular proteins [34], the most studied interaction is that of the pRb large pocket with the E2F-1 protein. Point mutations occurring in the N-terminal domain of pRb have been identified from cancer patients (reviewed in [111]). It is likely that point mutations would occur in locations close to important regulatory regions within protein domains.

Proteins have been found to specifically interact with the N-terminal domain of pRb. Proteins that interact with the N-terminal domain of pRb may have their binding regulated through the post-translational modification of the N-terminal domain. If K acetylation of the N-terminal domain of pRb affects its protein/protein interactions, one might expect potential acetylated K residues to be mutated in human tumours. In that regard, the only documented K residue undergoing point mutation in human tumours is K136. In the C-terminal domain, acetylation of pRb at K873/874 reduces phosphorylation of pRb, possibly through preventing cyclin E/A from docking [214]. Also, pRb can be phosphorylated by RbK, a mitotic pRb kinase [100], and Cdk enzymes [146]. There may be additional phosphorylation sites along the N-pRb that have not yet been defined.

I set out to address whether N-pRb is acetylated. For this study, I configured a robust *in vitro* acetylation assay that allowed an investigation into the acetylation of N-pRb. The assay demonstrated that GST-pRb 1-376 is acetylated by Flag-p300 FL but not

by the HAT domain constructs His-p300 1195-2414 and Flag-p300 1135-2414. These results indicate that the N-terminal domain of pRb is acetylated.

THE N-TERMINAL DOMAIN OF PRB IS ACETYLATED IN HEK 293 CELLS

The acetylation of the C-terminal domain in pRb has been shown to be damage responsive [97], and induced during differentiation of C2C12 cells [53]. This suggests that the N-terminal domain has a function in tumour suppression. Other transcription factors are acetylated. Presently, two other reports have described the DNA damage induced acetylation of the cell cycle transcription factors E2F-1 and p53 [75, 228]. These studies both report that treating cells with doxorubicin (for E2F-1) and IR (for p53) results in the induction of acetylation. Studies on E2F-1 demonstrate that residues 117, 121, and 125 are acetylated *in vivo* in response to doxorubicin treatment [53]. This induction of acetylation occurs between 8 h and 16 h post treatment (induction of pRb acetylation by etoposide occurs between 4 h and 24 h post treatment [97]).

A similar study on DNA damage inducible Chk1/2 phosphorylation of p53 has more closely studied the link between Chk phosphorylation and DNA damage inducible acetylation [228]. Importantly, Chk1 and Chk2 have roles in regulating p53 acetylation. Using siRNA to knockdown Chk1/2, it was observed that levels of C-terminal domain p53 phosphorylation and acetylation of K382 were reduced [228], leading to a reduced activation of *p21* and *Bax* in response to DNA damage. Reduced expression of Chk kinases leads to decreased DNA damage responsive acetylation of p53, and a corresponding drop in apoptosis. Therefore, perhaps DNA damage could induce N-terminal domain pRb acetylation in cells. To test this idea I sought to study the *in vivo* acetylation and the intra-cellular location of the N-terminal domain of pRb.

CHAPTER 3

RESULTS

THE N-TERMINAL DOMAIN OF PRB IS ACETYLATED *IN VITRO*.

His-p300 1195-1673 does not efficiently acetylate GST-pRb fusion proteins

Three recombinant p300 proteins were purified for *in vitro* acetylation assays (Figure 11). The catalytic domain of p300 stretches across residues 1195-1673 (Figure 12a), and was purified in BL21 cells (Figure 12b). This region contains the bromo-domain, two zinc binding domains and the cysteine-histidine domains C/H2 and CH3 (Figure 12a). His-p300 1195-1673 efficiently acetylates core histones, but does not maintain significant auto-acetylation. Increasing the concentration of His-p300 1195-1673 caused a linear increase in the acetylation of core histones (Figure 12c and d). His-p300 1195-1673 was repeatedly unable to efficiently acetylate either GST-pRb 379-928 or GST-pRb 1-376 *in vitro* (Figure 12c and d).

Flag-p300 1135-2414 does not efficiently acetylate GST-N-pRb 1-376

The p300 acetyl-transferase domain was not sufficient to acetylate GST-N-pRb, but was able to acetylate core histones. As well as the acetyl-transferase domain, Flag-p300 1135-2414 contains the p300 *trans*-activation region (1673-2414). Domains in this region are depicted (Figure 13a). Flag-p300 1135-2414 was purified from High five insect cells infected with baculovirus-Flag-p300 1135-2414 (Figure 13b). The resulting purified protein was visualised by coomassie staining. Flag-p300 1135-2414 resolved at approximately 140 KDa (Figure 13b).

Flag-p300 1135-2414 was used to acetylate either core histones or GST-N-pRb fusion proteins (Figure 13c). Flag-p300 1135-2414 was observed to have significant auto-acetylation (3.3 fold greater than His-p300 1195-1673, Figure 13d). Flag-p300 1135-2414 acetylated core histones as efficiently as the His-p300 1195-1673. However, despite an increase in auto-acetylation, Flag-p300 1135-2414 was not able to efficiently acetylate GST-N-pRb fusion proteins (Figure 13d).

Figure 11

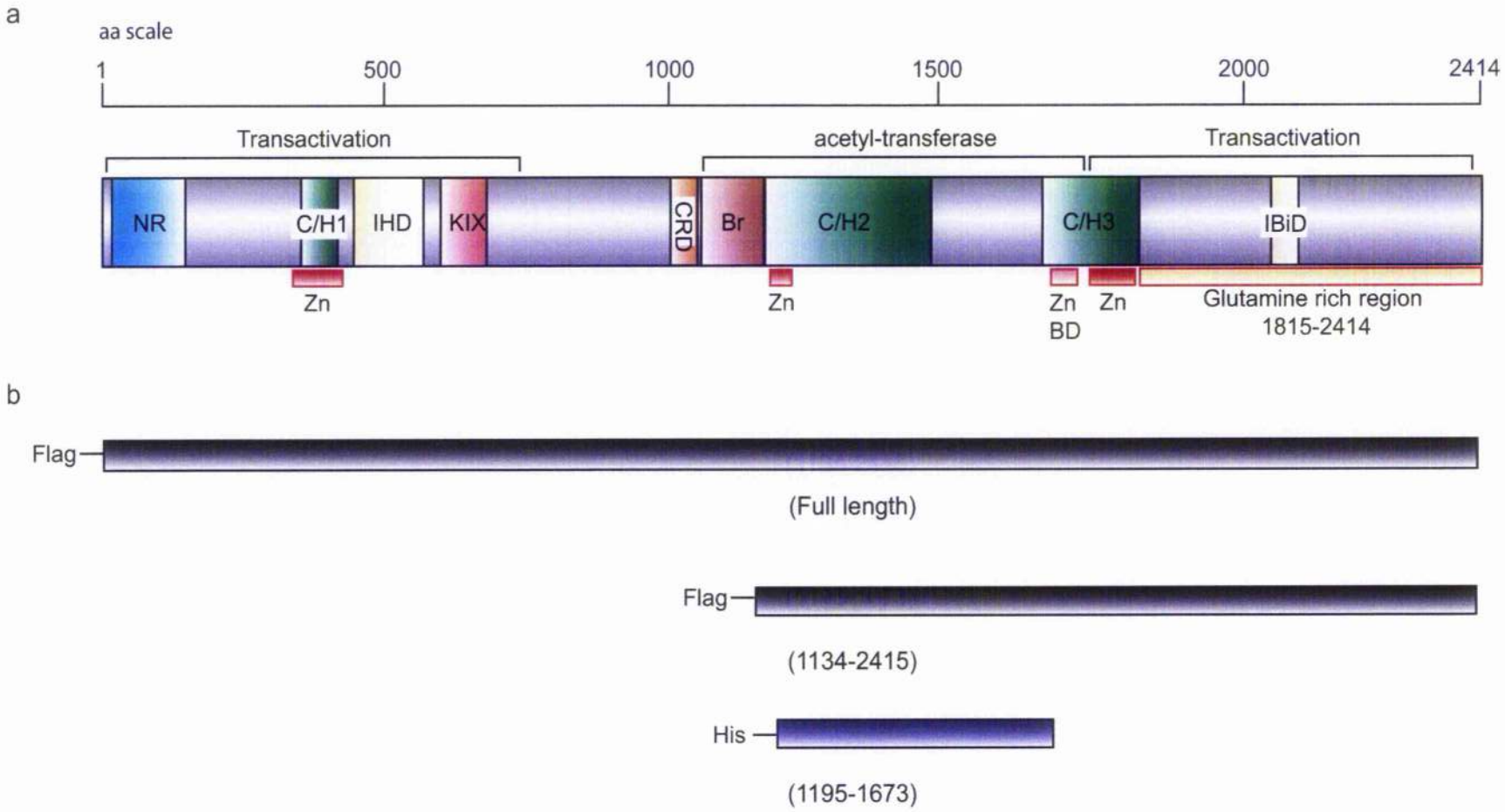
a
aa scale
1
500
1000
1500
2000
2414
Transactivation
acetyl-transferase
Transactivation
NR
C/H1
IHD
KIX
CRD
Br
C/H2
C/H3
IBiD
Zn
Zn
Zn
BD
Zn
Glutamine rich region
1815-2414
b
Flag
(Full length)
Flag
(1134-2415)
His
(1195-1673)

Figure 11: p300 HAT constructs

a) Three p300 constructs were used in HAT assays: The Flag-p300 FL construct contains the following domains; Nuclear receptor binding domain (NR), 3 cysteine-histidine domains (C/H1) (C/H2) (C/H3), CREB binding domain (KIX), Bromo-domain, IBiD, and N-terminal phosphopeptide-binding domain with homology to IBiD (IHD).

b) Flag p300 FL is able to acetylate GST-pRb (1-376), GST-pRb (10-330), GST-pRb (379-928), GST-pRb (763-928) and core histones (Upstate). Flag-p300 (1135-2415) contains the HAT domain and the C-terminal domain *trans*-activation region of p300, and can acetylate the core histones efficiently, but not the GST-N-pRb proteins. His-p300 (1195-1673) contains the HAT of p300, and can efficiently acetylate core histones but is unable to acetylate GST-N-pRb (1-376), GST-N-pRb (10-330), GST-pRb (379-928), or GST-C-pRb (763-928).

Figure 12

a)

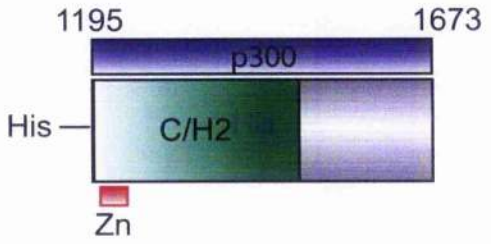
1195
1673
p300
His
C/H2
Zn

b)

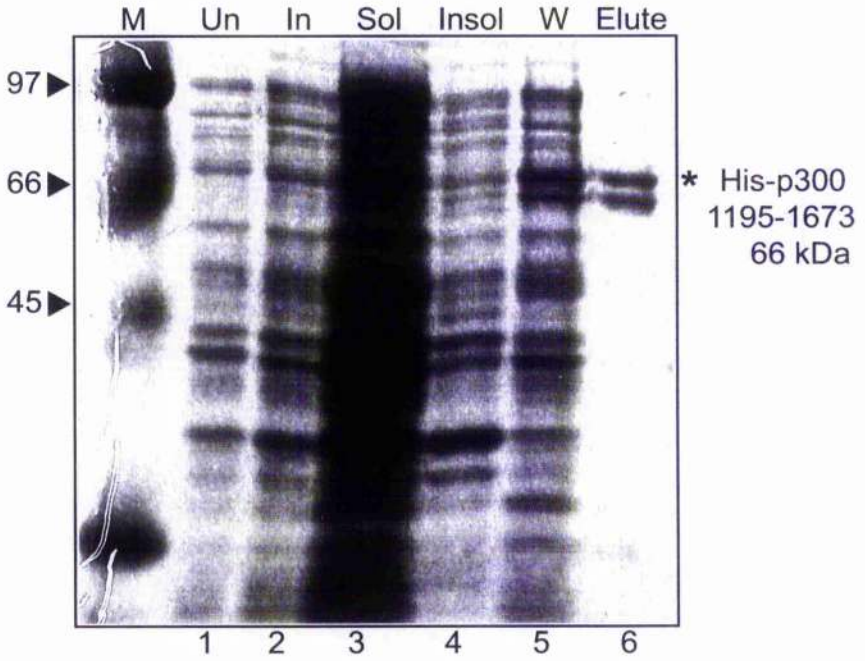
M
Un
In
Sol
Insol
W
Elute
97
66
45
1
2
3
4
5
6
* His-p300
1195-1673
66 kDa

Figure 12

c)

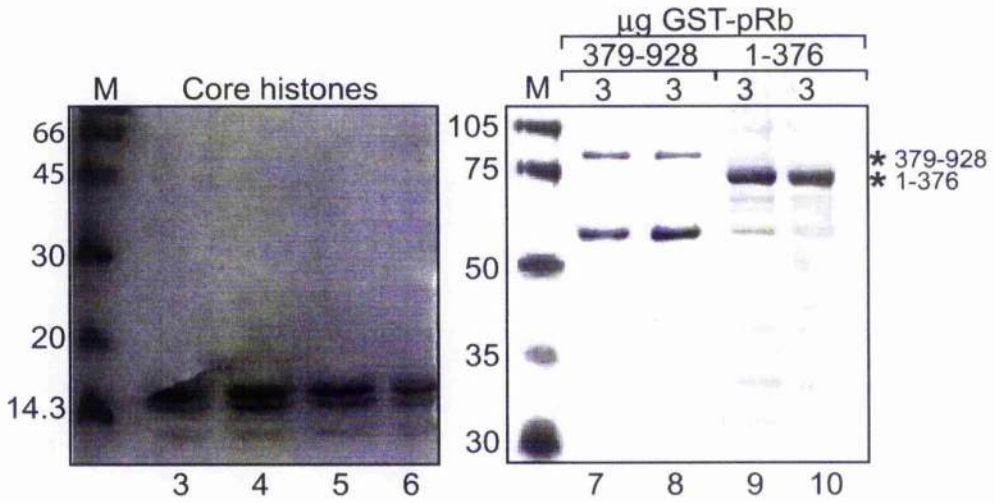
M
Core histones
66
45
30
20
14.3
3
4
5
6
µg GST-pRb
379-928
1-376
M
3
3
3
3
105
75
50
35
30
* 379-928
* 1-376
7
8
9
10

d)

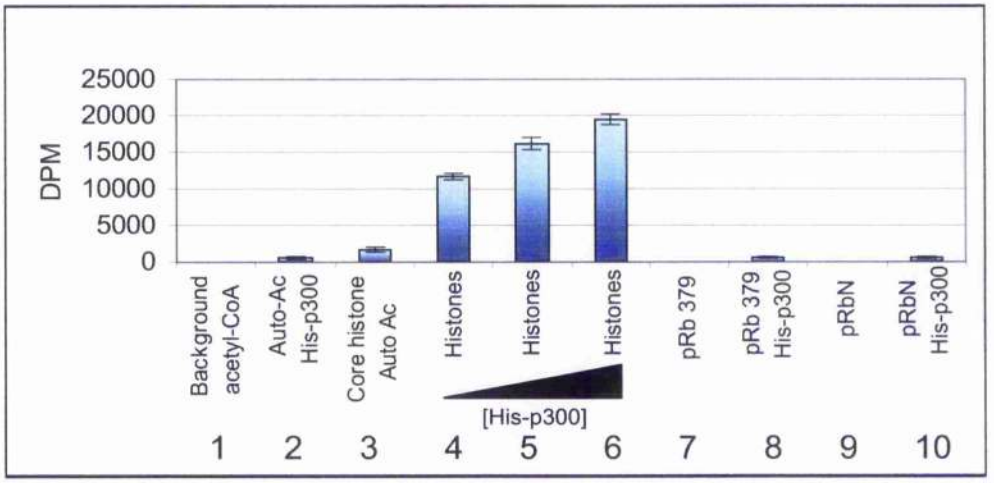
DPM
25000
20000
15000
10000
5000
0
Background acetyl-CoA
Auto-Ac His-p300
Core histone Auto Ac
Histones
Histones
Histones
[His-p300]
pRb 379
pRb 379 His-p300
pRbN
pRbN His-p300
1
2
3
4
5
6
7
8
9
10

Figure 12: His-p300 1195-1673 is sufficient to acetylate core histones but not GST-pRb fusion proteins

a) Schematic showing the region of purified His-p300. This region covers the catalytic domain of p300. Residues 1195-1673 contain the cysteine-histidine domain (C/H1), and a zinc finger domain shown in red. This derivative stops just short of the C/H2 domain.

b) The His-p300 1195-2414 construct was expressed in BL21 cells as described in Materials and Methods. Fractions from the various stages of purification were run on a 10 % SDS PAGE gel and visualised by coomassie staining. His-p300 1195-1673 resolves at a molecular weight of approximately 66 KDa (Lane 6).

Lanes	Fraction	
1	Un-induced BL21 cells	Pre bacterial lysis
2	Induced BL21 cells	
3	Soluble fraction	Post-bacterial lysis.
4	Insoluble fraction	
5	First wash fraction	
6	Elute	

c) The input levels of the proteins used are shown visualised by coomassie staining. Lanes 3 to 6 show 3μg core histones (≈10-22 KDa). Lanes 7 and 8 show 3μg of GST-pRb 379-928, and lanes 9 to 10 show 3 μg of GST-N-pRb 1-376.

d) *In vitro* acetylation reactions were incubated for 30 min and measured using a scintillation counter for incorporation of ^{3}H acetyl co-enzyme A. Values on the bar

graph represent an average of three independent experiments. Each experiment was carried out using the same batch of His-p300 1195-1673. Lanes 4 to 6 show a titration of His-p300 (Lane 4, 0.4 μg, Lane 5, 1 μg, Lane 6, 2 μg).

Figure 13

a)

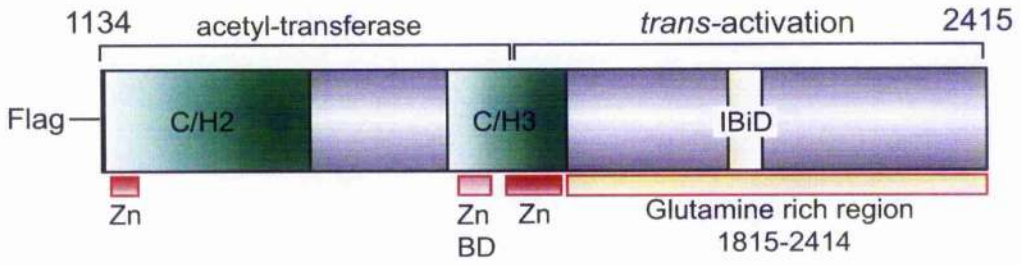
1134
acetyl-transferase
trans-activation
2415
Flag
C/H2
C/H3
IBiD
Zn
Zn
BD
Zn
Glutamine rich region
1815-2414

b)

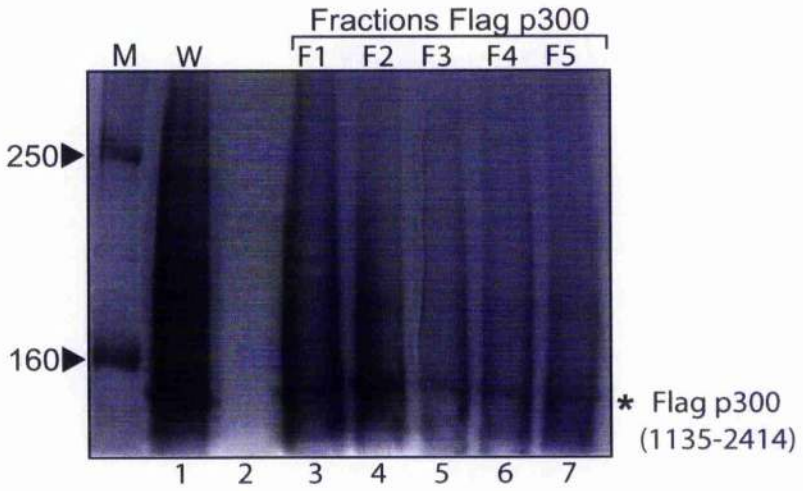
Fractions Flag p300
M
W
F1
F2
F3
F4
F5
250
160
* Flag p300
(1135-2414)
1
2
3
4
5
6
7

Figure 13

c)

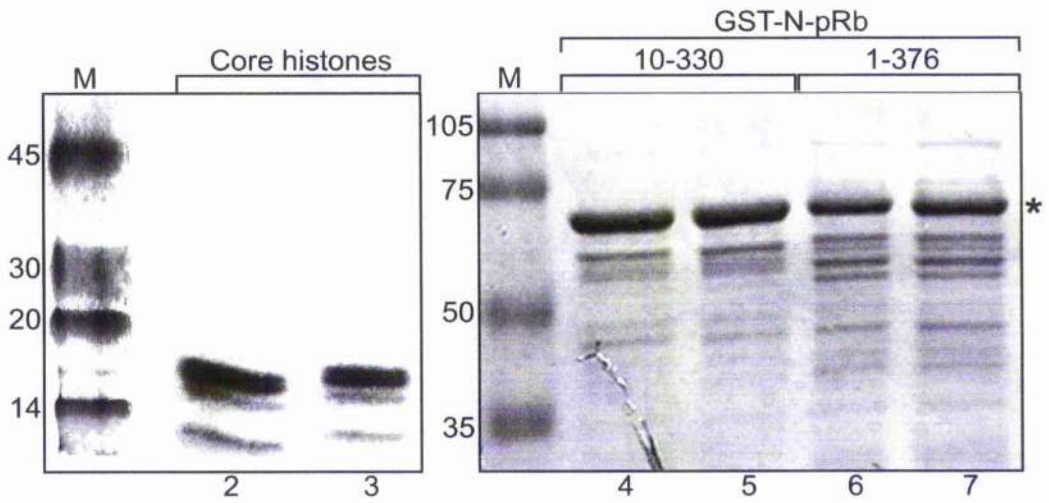
M
Core histones
45
30
20
14
2
3
M
GST-N-pRb
10-330
1-376
105
75
50
35
*
4
5
6
7

d)

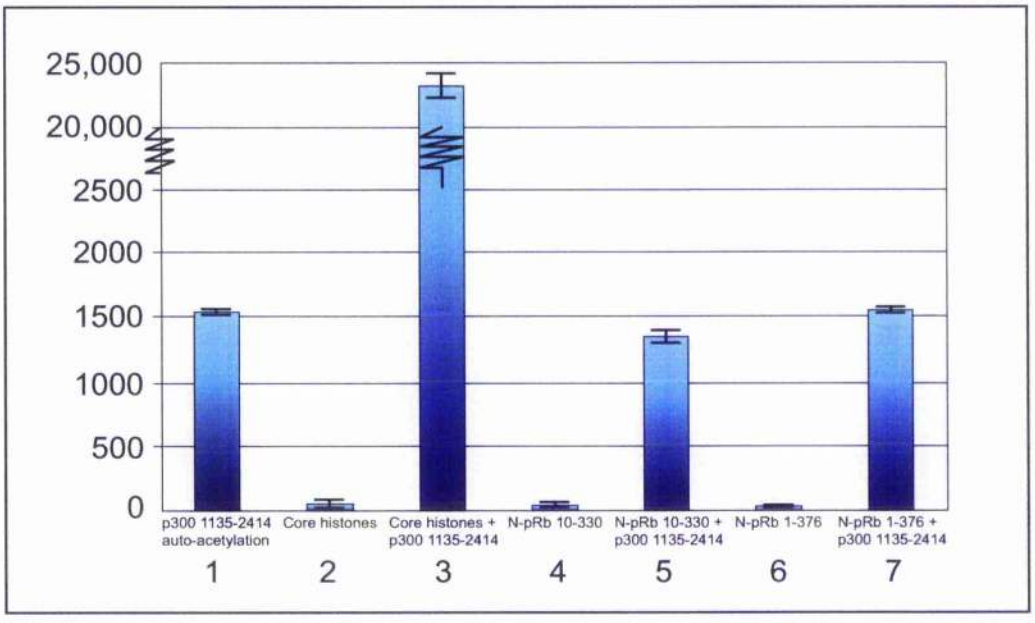
25,000
20,000
2500
2000
1500
1000
500
0
p300 1135-2414 auto-acetylation
Core histones
Core histones + p300 1135-2414
N-pRb 10-330
N-pRb 10-330 + p300 1135-2414
N-pRb 1-376
N-pRb 1-376 + p300 1135-2414
1
2
3
4
5
6
7

Figure 13: Flag-p300 1135-2414 is sufficient to acetylate core histones but not GST-N-pRb fusion proteins

a) Schematic showing the region of purified Flag-p300. This region covers the catalytic domain of p300 and also the neighbouring *trans*-activation domain (see also Figure 2). The Flag-p300 1135-2414 construct encodes all of the following domains: the acetyl-transferase domain (2 cysteine-histidine domains (C/H2, C/H3), 3 zinc-finger domains), and a *trans*-activation domain (the C-terminal glutamine rich region containing the IBiD domain).

b) Shows purified fractions of Flag-p300 1135-2414 (2 μg) separated by electrophoresis and visualised by staining with coomassie blue. Flag-p300 1135-2414 resolves at approximately 150 KDa. Lane 1 shows protein eluted in the wash buffer (W) prior to elution.

c) Core histones (10-17 KDa) acetylated by Flag-p300 1135-2414 were resolved on a 15 % SDS-PAGE gel (reactions 2 and 3). N-terminal domain pRb GST fusion proteins used in reactions 4 to 7 were resolved on a 10 % SDS-PAGE gel (protein position marked with asterix). Gels were visualised using coomassie staining.

d) *In vitro* acetylation of substrates was assessed by measuring the incorporation of ^{3}H acetyl co-enzyme A. Values on the bar graph represent an average of three independent experiments. Each experiment was carried out using the same fraction of Flag-p300 1135-2414 (fraction 2 shown in Figure 13 b).

Flag-p300 FL can efficiently acetylate GST N-pRb fusion proteins *in vitro*

The region spanning the first 1135 residues of p300 contains domains that are also important for the *trans*-activation capacity of p300 (Figure 11). This region contains the nuclear hormone receptor-binding domain, a cysteine-histidine domain (C/H1) containing a zinc-binding domain, the IHD domain (an N-terminal phosphopeptide-binding domain with homology to IBiD), the CREB binding domain (KIX), and the CRD domain (Figure 14a). Purified Flag-p300 FL (Figure 14b) was used to acetylate GST-pRb fusion proteins (visualised in Figure 14c). Flag-p300 FL exhibited approximately 2-fold greater auto-acetylation than the equivalent concentration of Flag-p300 1135-2414. Flag-p300 FL was repeatedly able to acetylate GST-pRb fusion proteins. The large pocket of pRb (GST pRb 379-928) and the C-terminal domain (GST-C-pRb 763-928) showed approximately twice the acetylation of GST-N-pRb fusion proteins (Figure 14d).

The effects of varying substrate and HAT concentration on *in vitro* acetylation

The catalytic activity of p300 is regulated by its auto-acetylation [237]. Hypo-acetylated p300 is less catalytically active than hyper-acetylated forms. The basal catalytic rate of p300-mediated acetylation is stimulated by the acetylation of key K residues in the activation loop of p300 spanning residues 1520 through 1560 [237]. Optimizing *in vitro* acetylation assays involves a carefull balancing act. Adding greater amounts of HAT to the acetylation reaction will cause a proportional increase in levels of substrate or auto-acetylation. *In vitro* acetylation reactions are inhibited by too much salt in the reaction mix. The auto-acetylation of various titrations of Flag-p300 FL was measured to assess the optimal amount of Flag-p300 required.

Figure 14

a)

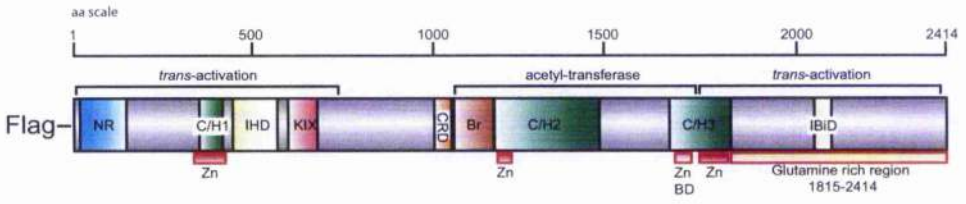
aa scale
1
500
1000
1500
2000
2414
trans-activation
acetyl-transferase
trans-activation
Flag–
NR
C/H1
IHD
KIX
CRD
Br
C/H2
C/H3
IBiD
Zn
Zn
Zn
BD
Zn
Glutamine rich region
1815-2414

b)

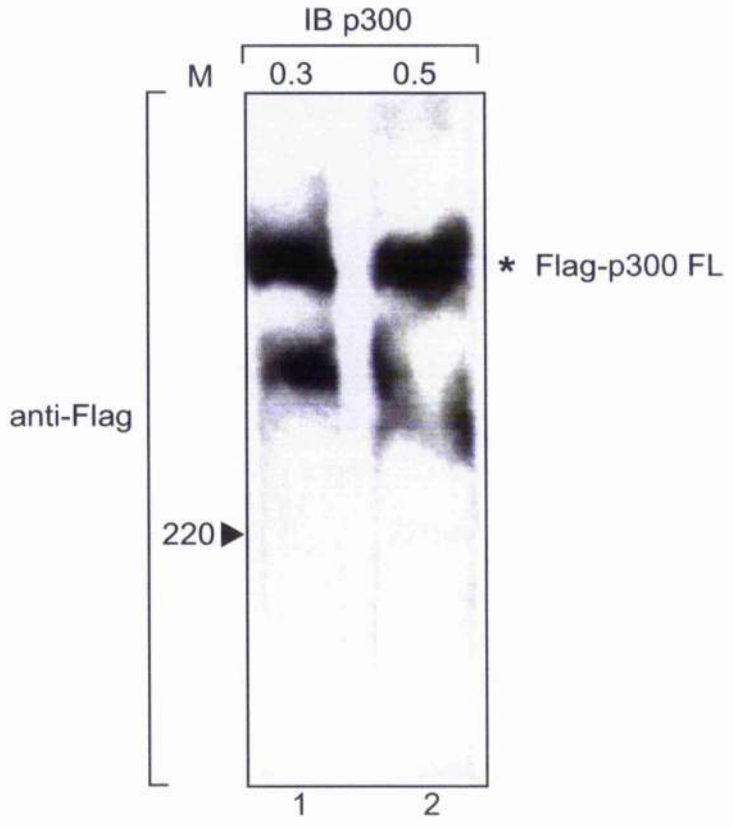
IB p300
M
0.3
0.5
* Flag-p300 FL
anti-Flag
220
1
2

Figure 14

c)

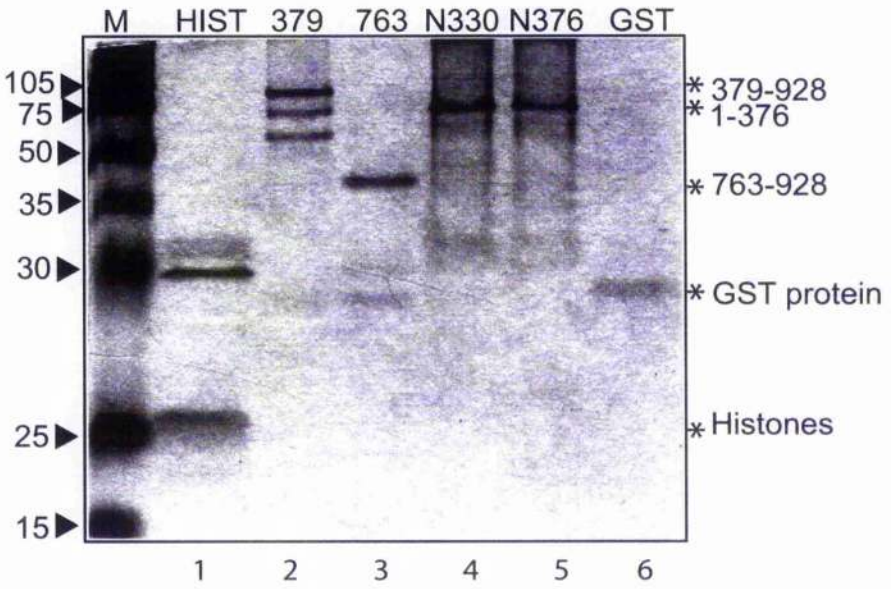
M
HIST
379
763
N330
N376
GST
105
75
50
35
30
25
15
1
2
3
4
5
6
* 379-928
* 1-376
* 763-928
* GST protein
* Histones

d)

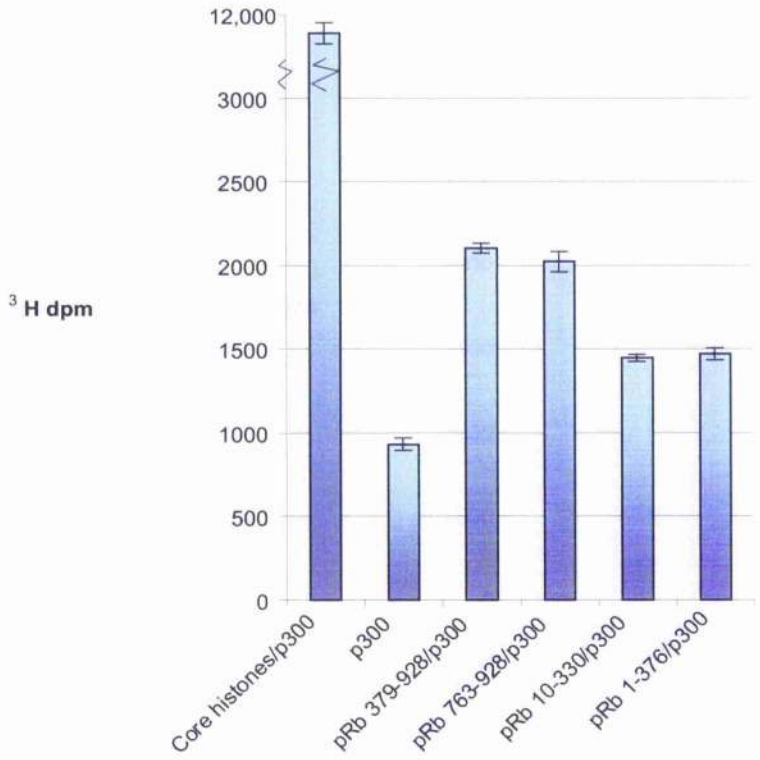
^{3}H dpm
12,000
3000
2500
2000
1500
1000
500
0
Core histones/p300
p300
pRb 379-928/p300
pRb 763-928/p300
pRb 10-330/p300
pRb 1-376/p300

Chapter 3

Figure 14: Flag-p300 FL acetylates the N-terminal domain of pRb

a) Schematic showing Flag-p300 FL (see also Figure 9).

b) Purified Flag-p300 FL (0.3 μg and 0.5 μg) was run on a 6 % SDS-PAGE gel, and immunoblotted with anti Flag antibody. Flag-p300 FL resolves at 265 KDa.

c) Reactions contained 4 μg of substrate protein (Lane 1 Core histones, lane 2 GST-pRb 37 9-928, Lane 3 GST-pRb 763-928, Lane 4 GST-pRb 10-330, Lane 5 GST-pRb 1-376, and Lane 6 GST protein) for acetylation by 1 μg of Flag-p300 FL (50 ng/μl). Substrates for the six reactions are shown resolved on a 12.5 % SDS-PAGE gel stained with coomassie.

d) The bar graph shows the acetylation of proteins visualised in a). GST protein was not acetylated. Each bar in the graph plots the average of three independent experiments. Background levels of acetylation for the substrates, and the level of acetylation of GST protein are all less than 70 dpm.

Figure 15

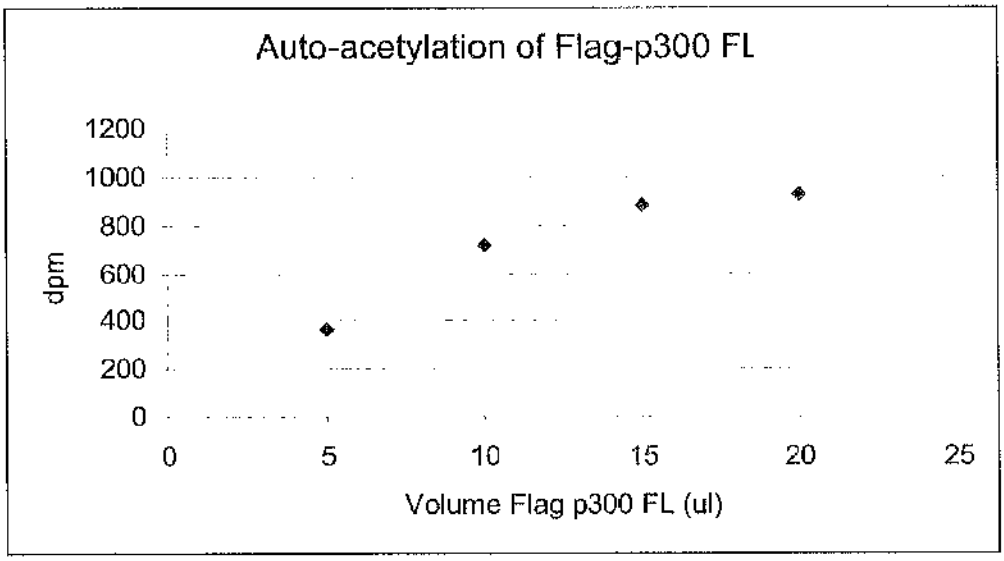
Auto-acetylation of Flag-p300 FL
dpm
1200
1000
800
600
400
200
0
0
5
10
15
20
25
Volume Flag p300 FL (ul)

Figure 15 Auto-acetylation of Flag-p300 FL

In this experiment, the amount of Flag-p300 FL added to the standard 30 µl reaction was titrated (0.25 µg, 0.5 µg, 0.75 µg and 1 µg). The resulting changes in the auto-acetylation of p300 were measured using a scintillation counter. Values plotted on the graph represent an average of three independent experiments.

The amount of auto-acetylation appeared to be proportional to the concentration of Flag-p300 FL when the total volume of p300 in the reaction is less than 10 µl (representing a final concentration of 20 ng/µl Flag-p300 FL in the reaction).

Adding more than 20 ng/µl Flag-p300 FL into the reaction causes further increases in the level of auto-acetylation, but the rate of increase declined (perhaps due to higher salt concentration in the reaction mix). A similar effect was observed when varying the concentration of Flag-p300 FL in the presence of a constant amount of core histones (Figure 16), and when varying the concentration of Flag-p300 FL in the presence of constant GST-pRb 1-376 (Figure 18). Varying the amount of substrate protein acetylated by Flag-p300 FL gave a linear increase in the acetylation of histones (Figure 17) and GST-pRb 1-376 (Figure 19).

Figure 16

a)

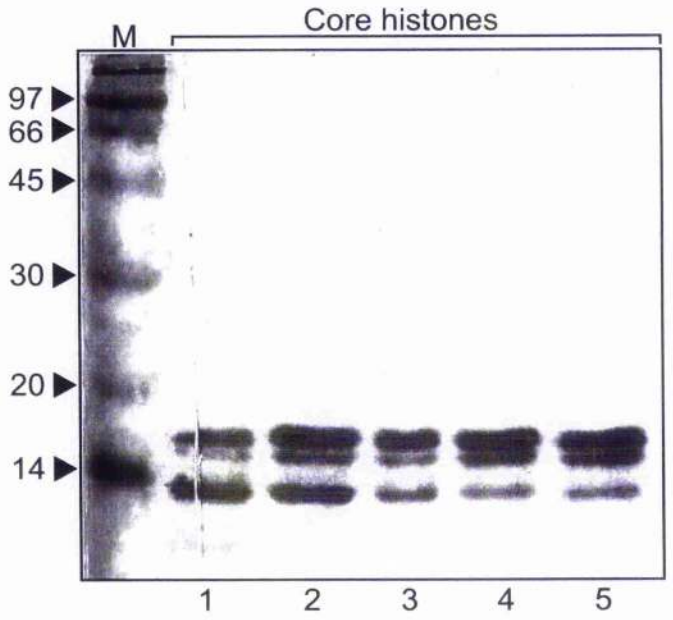
M
Core histones
97
66
45
30
20
14
1
2
3
4
5

b)

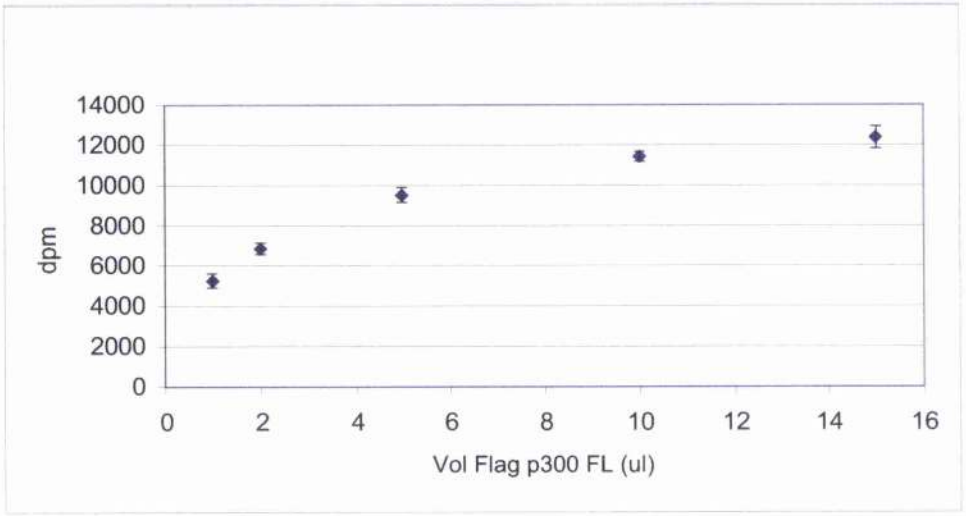
14000
12000
10000
8000
6000
4000
2000
0
dpm
0
2
4
6
8
10
12
14
16
Vol Flag p300 FL (ul)

Figure 16: The affect of titrating Flag-p300 FL on the acetylation of 2 µg core histones

Core histones (2 µg) were added to each acetylation assay. Varying amounts of Flag-p300 FL were added to the reactions.

a) The figure shows the amount of core histones in the acetylation assay visualised by coomassie staining.

b) The change in acetylation of 2 µg of core histones by titration of p300 (50 ng, 100 ng, 250 ng, 500 ng, and 750 ng of Flag-p300 FL) is plotted. Values on the graph represent an average of three independent experiments.

Figure 17

a)

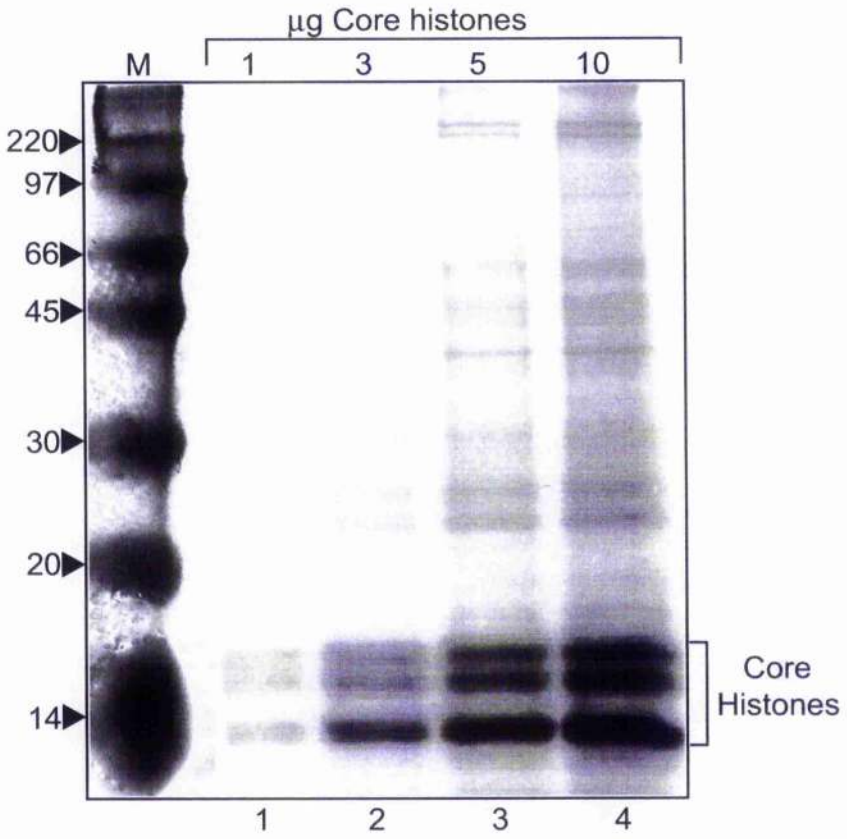
µg Core histones
M
1
3
5
10
220
97
66
45
30
20
14
Core Histones
1
2
3
4

b)

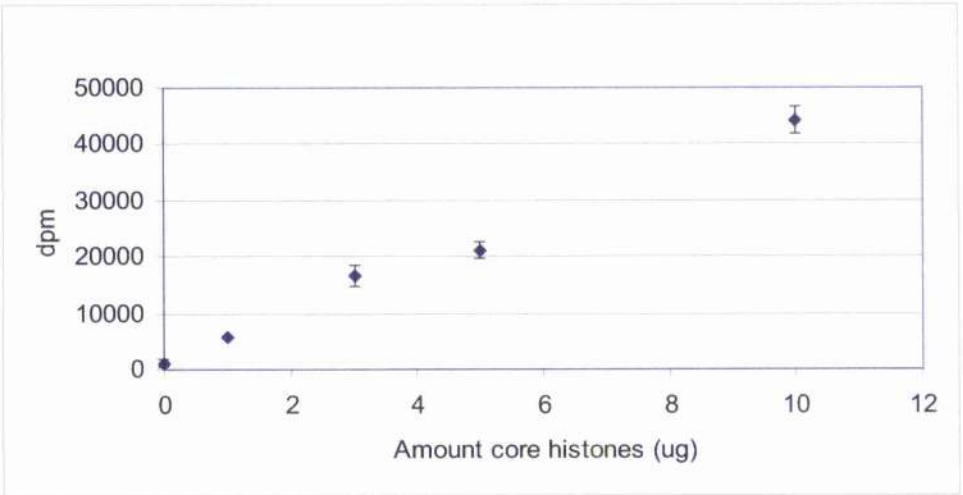
50000
40000
30000
20000
10000
0
dpm
0
2
4
6
8
10
12
Amount core histones (ug)

Figure 17: Titration of the amount of core histones affects the level of *in vitro* acetylation by Flag-p300 FL

Flag-p300 FL (0.5 μg) was added to each 30 μl acetylation assay. Varying amounts of core histones were added to the reactions.

a) The figure shows the amount of core histones in the acetylation assay visualised by coomassie staining.

b) The change in acetylation of core histones (1 μg, 3 μg, 5 μg, and 10 μg of core histones) facilitated by 0.5 μg of Flag-p300 FL is plotted. Values represented on the graph an average of three independent experiments.

Figure 18

a)

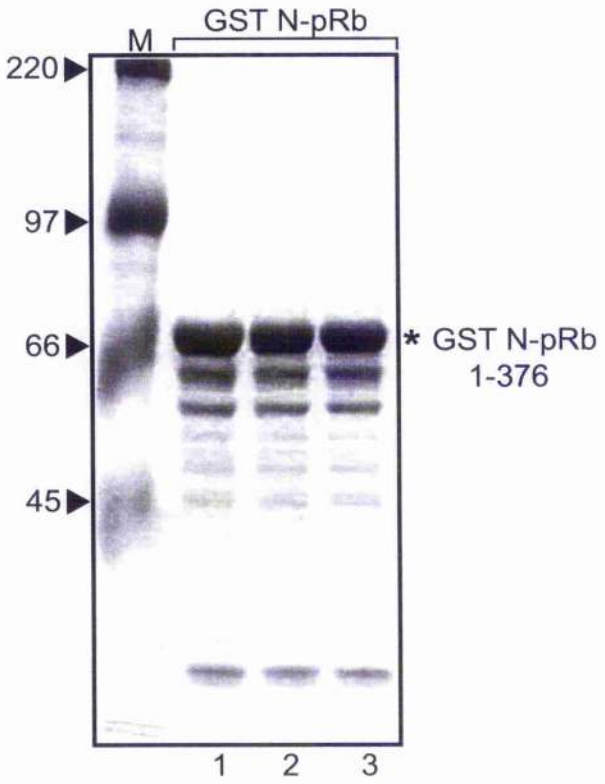
M
GST N-pRb
220
97
66
45
* GST N-pRb
1-376
1
2
3

b)

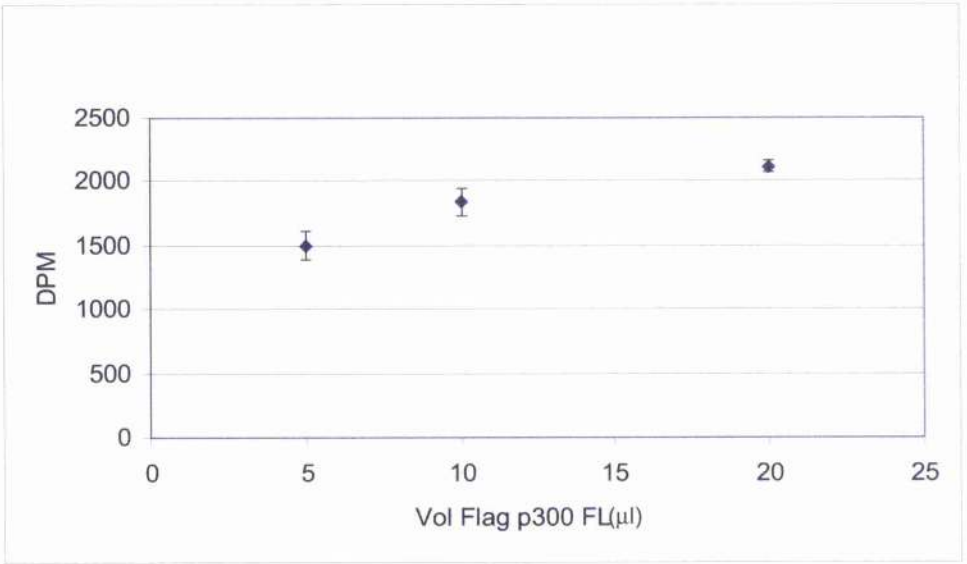
2500
2000
1500
1000
500
0
DPM
0
5
10
15
20
25
Vol Flag p300 FL(µl)

Figure 18: The effect on the acetylation of GST-N-pRb by the titration of Flag-p300 FL

GST-N-pRb 1-376 (4 μg) was added to each 30 μl acetylation assay. Varying amounts of Flag-p300 FL were added to the reactions.

a) The figure shows the amount of GST-N-pRb fusion protein in the acetylation assays visualised by coomassie staining. The asterix highlights the position of GST N-pRb (67.4 KDa).

b) The change in acetylation of 4 μg of GST-N-pRb by titration of p300 (0.25 μg, 0.5 μg and 1 μg of Flag-p300 FL) is plotted. Values on the graph represent an average of three independent experiments.

Figure 19

a)

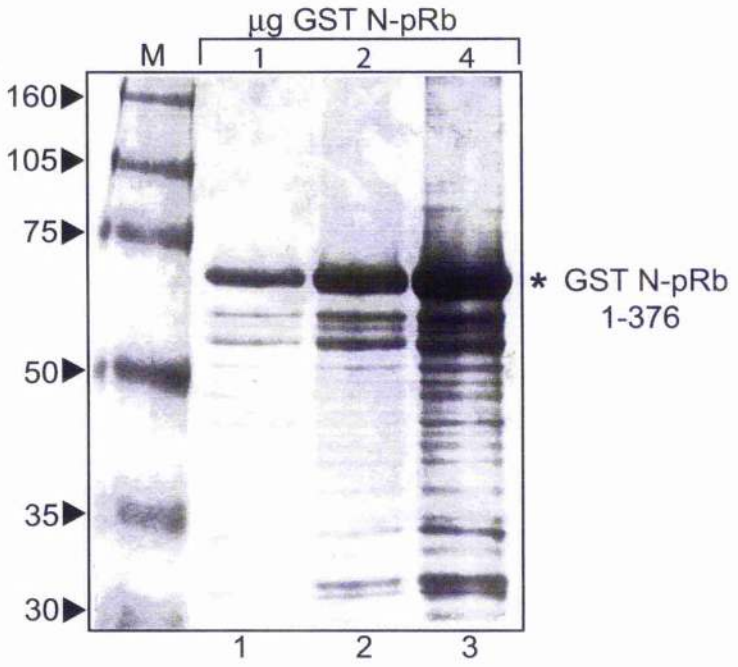
µg GST N-pRb
M
1
2
4
160
105
75
50
35
30
1
2
3
* GST N-pRb
1-376

b)

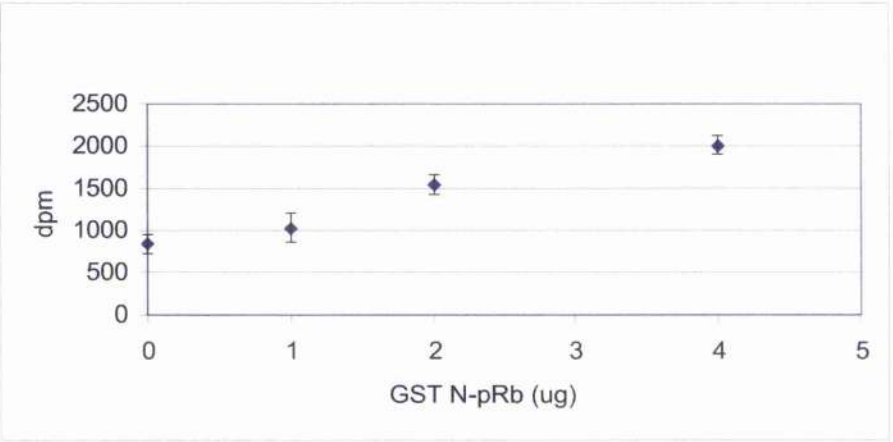
2500
2000
1500
1000
500
0
dpm
0
1
2
3
4
5
GST N-pRb (ug)

Figure 19: ***In vitro*** **acetylation of GST-N-pRb by Flag-p300 FL is affected by the titration of GST-N-pRb.**

Flag-p300 FL (0.5 μg) was added to each 30 μl acetylation assay. Varying amounts of GST-N-pRb were added to the reactions.

a) The figure shows the amount of GST-N-pRb in the acetylation assay visualised by coomassie staining. The asterix highlights the position of GST-N-pRb (67.4 KDa).

b) The change in acetylation of GST-N-pRb (1 μg, 2 μg and 4 μg of GST-N-pRb) facilitated by 0.5 μg of Flag-p300 FL was plotted. Values on the graph represent an average of three independent experiments.

HA-pRb 1-376 is acetylated *in vivo*

Many cancer cell lines do not express active pRb, but instead express truncated proteins resulting from frameshift mutations in *Rb* that lead to premature stop codons. I used the Dignam method of lysing cells in order to study the nuclear/cytoplasmic distributions of Ha-pRb 1-376 in HEK 293 cells ($Rb^{+/+}$ cells where pRb is functionally inactivated) and C33A cells (in which the *Rb* is genetically inactivated), to study how N-terminal truncated pRb proteins might localise in tumours that have or do not have active endogenous pRb.

In order to explore whether the *in vitro* acetylation of pRb 1-376 reflect events that occur in cells, I used a pan-acetyl lysine antibody to assess acetylation of the N-terminal domain of pRb in cells. The approach involved treating cells with agents that induce double-stranded DNA damage, in order to test whether DNA damage induces the acetylation of the N-terminal domain in a similar way that has been shown for the C-terminal domain [97]. The anti-acetyl lysine antibody has been previously characterised as specifically recognising acetyl-GST pRb 379-928 and HA-Rb FL [214]. Since this antibody can recognise a great number of nuclear and cytoplasmic polypeptides (that contain acetylated K consensus sites found in histones), it was necessary to immunoprecipitate HA-pRb 1-376 to reduce the level of other acetylated proteins.

Prior to harvesting, cells were treated with TSA to prevent HDAC enzymes from reversing acetylation, thus aiding detection. HEK 293 cells were utilised because they have previously been shown to contain endogenous acetylated pRb. Immunoblots confirmed the presence of acetylated HA-pRb 1-376 (Figure 20, Lanes 3 to 10) that was specific (as no bands were detected in immunoprecipitates from non-transfected extracts,

Figure 20

a)

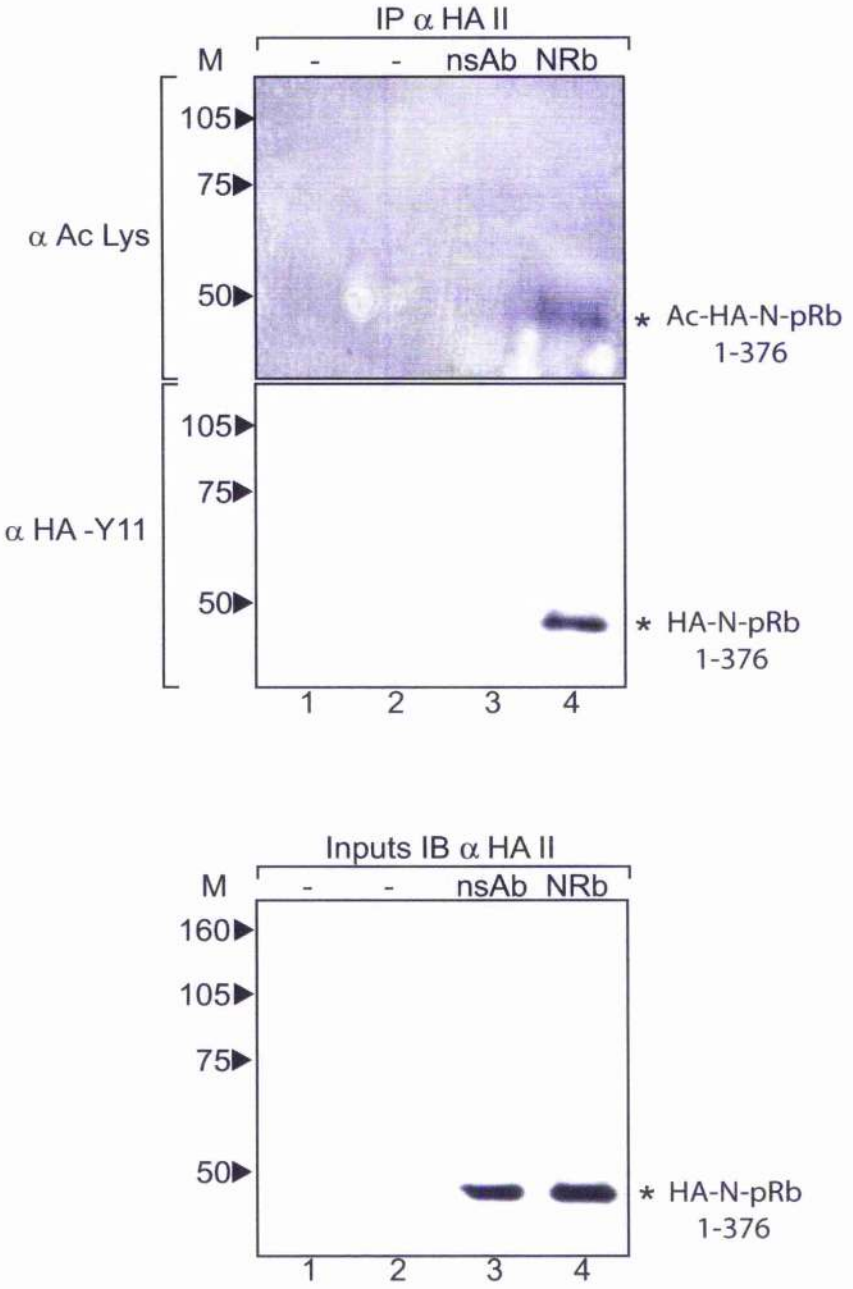
IP α HA II
M
-
-
nsAb
NRb
105
75
50
α Ac Lys
* Ac-HA-N-pRb
1-376
105
75
50
α HA -Y11
* HA-N-pRb
1-376
1
2
3
4
Inputs IB α HA II
M
-
-
nsAb
NRb
160
105
75
50
* HA-N-pRb
1-376
1
2
3
4

Figure 20

b)

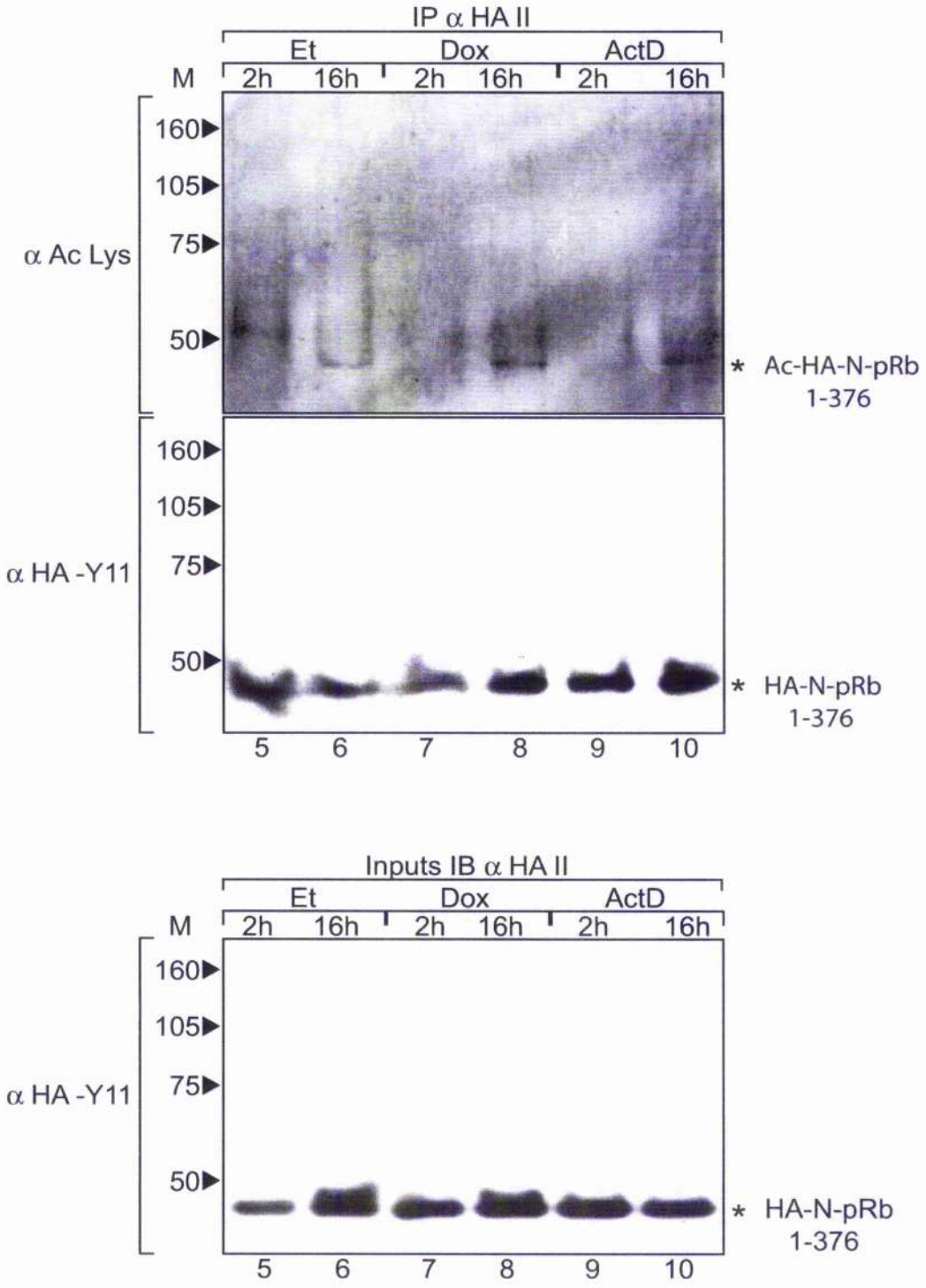
IP α HA II
Et
Dox
ActD
M
2h
16h
2h
16h
2h
16h
160
105
75
50
α Ac Lys
* Ac-HA-N-pRb 1-376
α HA -Y11
* HA-N-pRb 1-376
5
6
7
8
9
10
Inputs IB α HA II
Et
Dox
ActD
M
2h
16h
2h
16h
2h
16h
160
105
75
50
α HA -Y11
* HA-N-pRb 1-376
5
6
7
8
9
10

Figure 20: The N-terminal domain of pRb is acetylated in HEK 293 cells

HEK 293 cells were transfected with 2 μg pcDNA3 2HA-pRb 1-376 and immunoprecipitated with the anti-HAII antibody. Cells from all the samples (lanes 1 to 10) were harvested 48 h post transfection.

a) Un-treated cell extracts were immunoblotted with anti-acetylated-lysine polyclonal antibody (Ac Lys) (top panel), anti-HA Y11 polyclonal antibody (middle panel). Input (10 %) was immunoblotted with anti-HAII monoclonal antibody (bottom panel). pcDNA3 2HA-pRb 1-376 migrates to 47 KDa on an SDS-PAGE gel. Lane 1 is the mock control, and Lane 2 is transfected with 2 μg of empty pcDNA3 vector (as a transfection control). In Lane 3, extract was immunoprecipitated with goat anti-rabbit secondary antibody (used as the non-specific antibody control). Lane 4 shows Ha-pRb 1-376 immunoprecipitated by anti-HAII.

b) Cell extracts treated with etoposide, doxorubicin and actinomycin D were immunoblotted with anti-acetylated-lysine polyclonal antibody (Ac Lys) (top panel), anti-HA Y11 polyclonal antibody (middle panel). Input (10 %) was immunoblotted with anti-HAII monoclonal antibody (bottom panel). In Lanes 5 to 10, cells were transfected with 2 μg pcDNA3 2HA-pRb 1-376. Prior to harvesting, Lanes 5 and 6 were treated with 50 μM etoposide for 2 h and 16 h respectively. Lanes 7 and 8 were treated with 2 μM doxorubicin for 2 h and 16 h respectively. Lanes 9 and 10 were treated with 20 nM actinomycin D for 2 h

and 16 h respectively.

Figure 21

a)

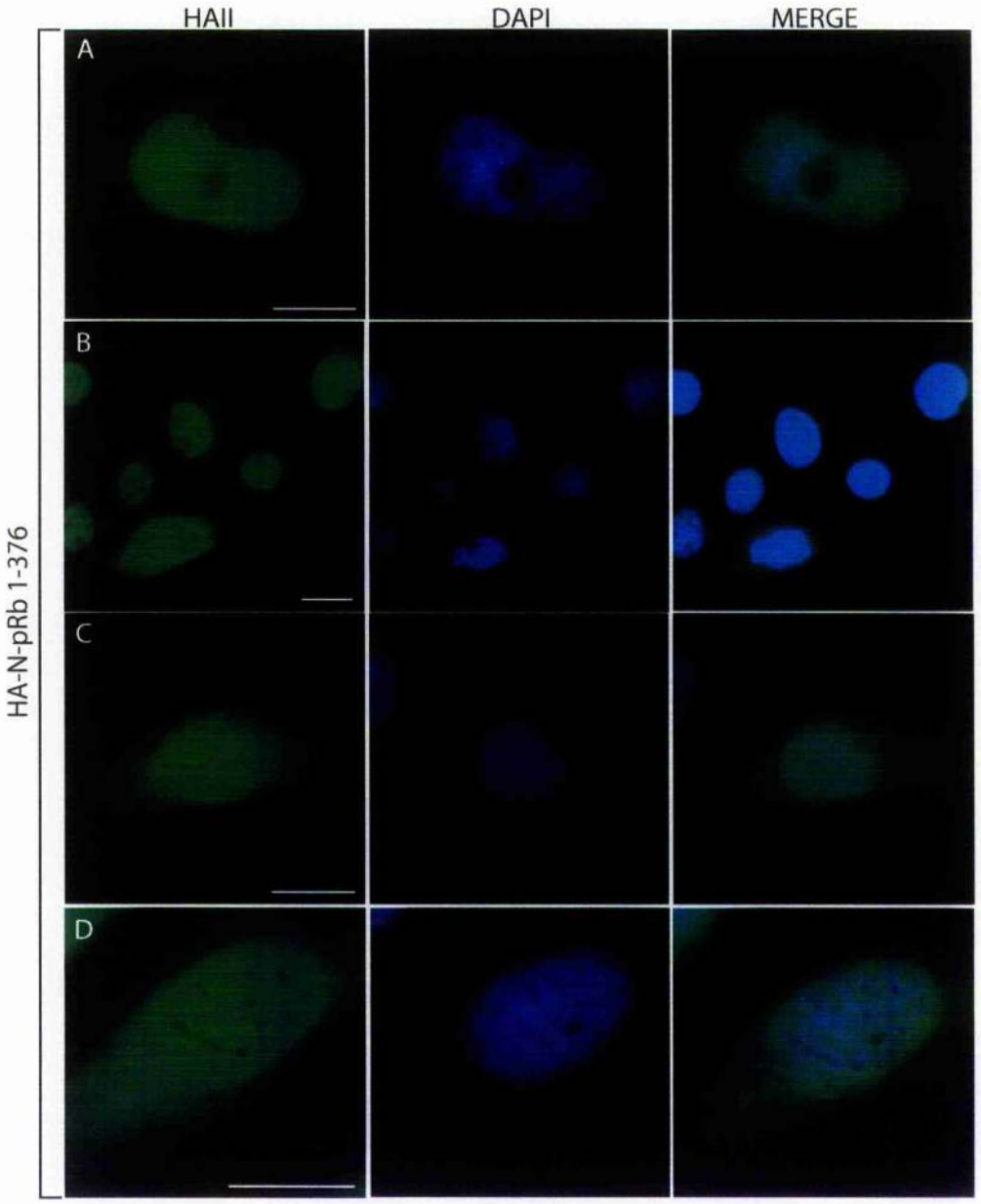

Figure 21

b)

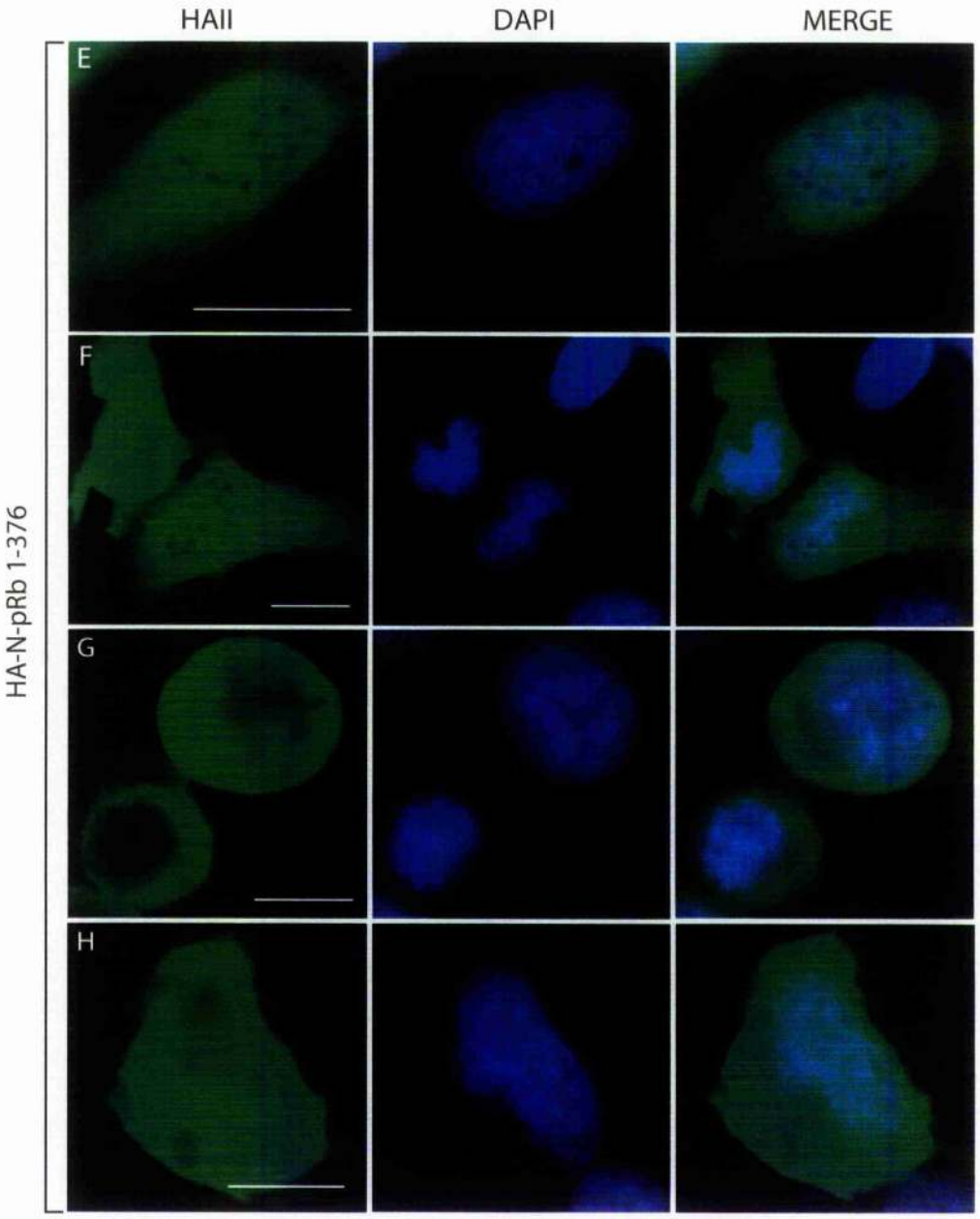

Figure 21 C

	Treatments	Transfected cells scored	% Nuclear	% Cytoplasmic	% Nuclear/ Cytoplasmic	% Cyto-plasmic
A	N/A	140	62	0	38	≈ <10 %
B	N/A	156	69	0	31	≈ <10 %
C	10 μM Etoposide	135	33	0	67	≈ <20 %
D	100 μM Etoposide	120	29	0	71	≈ <20 %
E	20 nM Actinomycin D	116	25	0	75	≈ <20 %
F	50 Jm^{-2} UV light	70	0	0	100	≈ <50 %
G	100 μM DFO (Hypoxia)	76	0	0	100	≈ < 35%
H	43 °C (2 h) (Heat Shock)	66	0	0	100	≈ <50 %

Figure 21: The localization of pcDNA3 HA-N-Rb 1-376 in response to DNA damage

U2OS cells were transfected with either 1μg or 3μg (B) of pcDNA3 HA-N-pRb 1-376. Prior to immunostaining, cells were treated with DNA damaging agents. Part a) shows samples A to D, and part b) Shows samples E to H. All images were taken at 630X magnification and later computer manipulated to enlarge images for presentation. The white line at the bottom right corner of images stained with anti-HAII represents 10μm.

a) Cells in samples A and B were not treated prior to immunostaining. Cells in sample C were treated with 10 μM etoposide and incubated for 16 h prior to immunostaining. Cells in sample D were treated with 100 μM etoposide and incubated for 8 h prior to immunostaining.

b) Cells in sample E were treated with 20 nM actinomycin D and incubated for 16 h prior to immunostaining. Cells in sample F were exposed to 50 Jm^{-2} of UVB light and incubated for 16 h prior to immunostaining. Cells in sample G were treated with 100 μM DFO and incubated for 24 h prior to immunostaining. Cells in sample H were incubated at 43 °C for 2 h to heat shock the cells, followed by 16 h incubation at 37 °C prior to immunostaining.

c) The table shows the number of transfected cells scored per treatment and the percentage of transfected cells (in each treatment A to H) that contain either only nuclear, only cytoplasmic or both nuclear and cytoplasmic staining. Five

fields of view (at X630 magnification) were scored for each treatment.

nor from extract derived from cells that were transfected with empty vector (Figure 20, Lanes 1 and 2). Protein G beads that were incubated with Goat anti-Rabbit secondary antibody failed to immunoprecipitate acetylated proteins or HA-pRb 1-376) (Figure 20, Lane 3).

Cells that were treated with DNA damaging agents (dissolved in DMSO) prior to harvest showed an increased level of acetylated HA-pRb 1-376 (Figure 20, Lanes 5 to 10). Cells were treated with DNA damaging agents that mimic the effects resulting from double stranded breaks in DNA. Cells were treated with etoposide (Figure 20, Lanes 5 and 6), with doxorubicin (Figure 20, Lanes 7 and 8), or with actinomycin D (Figure 20, Lanes 9 and 10). Extract was run on SDS-PAGE gels and blotted to visualise the levels of HA-N-pRb 1-376 prior to carrying out the immunoprecipitation in order to ensure that each immunoprecipitation contained the same level of exogenous protein. Immunoprecipitated levels of HA-N-pRb 1-376 were observed to be approximately equal in all lanes by re-blotting the membranes with anti-HA antibody. Previous studies on DNA damage inducible acetylation of K residues 873/874 in the C-terminal domain of pRb demonstrated that induction of acetylation occurred between 6 h and 24 h post treatment with etoposide, but peaked by 16 h post treatment [97]. With that in mind, cells were harvested 2 h and 16 h post treatment with the above-mentioned agents (to show a clear affect of the treatment). Any effect on the cells caused by the addition of DMSO (in the damaging agents) was mitigated by normalizing for volume of DMSO in all the samples both 16 h and 2 h prior to harvesting the cells. All three DNA damaging agents induced acetylation of HA-N-pRb 1-376 after 16 h incubation, but not after 2 h.

HA-N-pRb 1-376 localises to the nucleus in U2OS cells

U2OS cells transfected HA-N-pRb 1-376 showed substantial nuclear localisation (Figure 21 a), samples A and B). Approximately 40 % of cells showed weak cytoplasmic

Figure 22

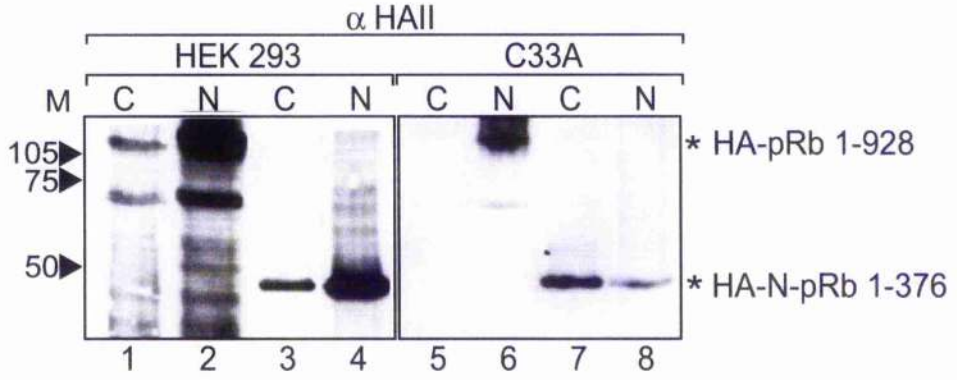
α HAII
HEK 293
C33A
M
C
N
C
N
C
N
C
N
105
75
50
* HA-pRb 1-928
* HA-N-pRb 1-376
1
2
3
4
5
6
7
8

Figure 22: The localization of exogenous N-terminal domain pRb

HEK 293 (human embryonic kidney cells) and C33A cells (a cell line propagated by extracting tumour cells from a human cervical carcinoma) were transfected with either 2 μg of HA-pRb 1-928 or 2 μg of 2HA-pRb 1-376. Cells were incubated for 48h. Once harvested, the cells were lysed using the Dignam method to isolate nuclear and cytoplasmic protein fractions. The gel shows 100 μg of both cytoplasmic and nuclear extract. Samples of both FL-pRb and N-terminal domain pRb were run on SDS-PAGE gel, and immunoblotted with anti-HAII antibody.

staining (Figure 21c). I decided to characterise the stained cells as entirely nuclear, entirely cytoplasmic or nuclear/cytoplasmic (Figure 21c). The percentage of the total cells counted in samples that were nuclear, cytoplasmic or nuclear/cytoplasmic was calculated. The localization of HA-N-pRb 1-376 was assessed in response to treatment with etoposide (Figure 21a, sample C and D), actinomycin D (Figure 21b, sample E), ultra violet light (UVB) (Figure 21b, sample F), desferrioxamine (DFO) (mimics hypoxia) (Figure 21 b, sample G), or heat shock (Figure 21 b, sample H). Etoposide activates mainly the ATM/Chk2 arm of the DNA damage response pathway by inhibiting DNA topoisomerase II, thereby inhibiting DNA synthesis, causing double stranded breaks in DNA. Actinomycin D creates DNA damage through inhibiting RNA polymerase III. Cells given these treatments displayed similar cellular morphologies. In these samples, most stained cells showed nuclear/cytoplasmic staining (≈70 % of cells counted). The degree of cytoplasmic staining was quite low, with approximately 80 % of total staining being retained in the nucleus. In short, double-stranded DNA damage promoted the cytoplasmic staining of 20 % of the HA-N-pRb 1-376 in 70 % of cells counted.

U2OS cells were treated with UVB light (Figure 21b, sample F), DFO (Figure 21b, sample G) and heat shock (Figure 21b, sample H). All three of these treatments resulted in greater cytoplasmic staining levels of HA-N-pRb 1-376 than treating cells with etoposide or actinomycin D. The UVB treatment resulted in the greatest level of cytoplasmic HA-N-pRb 1-376 (≥50 % of staining appeared to be cytoplasmic in Figure 21b, sample F). DFO treated cells showed limited nuclear staining (Figure 21b, sample G). Although not as effective as UVB light or heat shock, DFO caused approximately 30-40 % of the cells to exhibit cytoplasmic staining. Cells treated with heat shock (Figure 21b, sample H) all showed total nuclear/cytoplasmic localisation of HA-N-pRb 1-376 in U2OS cells. Again like UVB treatment greater than 50 % of total staining was observed to be cytoplasmic.

Cell type may influence the distribution of HA-N-pRb 1-376

HA-pRb 1-928 and HA-N-pRb 1-376 were transfected into both HEK 293 cells (*Rb* $^{+/+}$ cells) and C33A cells (which express a truncated pRb that locates to the cytoplasm) (Figure 22). Cells were separated into cytoplasmic and nuclear fractions. Protein concentration of the extracts was measured by Bradford assay. Extract from both fractions was run on an SDS-PAGE gel, and proteins were immunoblotted with anti-HAII antibody. It was observed that in HEK 293 cells and C33A cells that HA-pRb 1-928 was extracted mainly in the nuclear fraction. In contrast, HA-N-pRb 1-376 was predominantly localized in nuclear fractions of HEK 293 cells, but mostly in cytoplasmic fractions of C33A cells (Figure 22).

CHAPTER 3

DISCUSSION

THE N-TERMINAL DOMAIN OF PRB IS ACETYLATED *IN VITRO*.

The acetylation of the N-terminal domain of pRb described here suggests an additional level of regulation of pRb activity. Using limiting amounts of p300 in the *in vitro* assay, it was found that both His-p300 1195-1673 and Flag-p300 1135-2414 do not efficiently acetylate GST-pRb fusion proteins. Flag-p300 FL was able to acetylate GST-pRb 379-928 and GST-pRb 1-376 approximately 8-fold less than it acetylates core histones. Previous work has shown that Flag-p300 1135-2414 can acetylate pRb *in vitro*, but these reactions were carried out using high concentrations of Flag-p300 1135-2414 [214]. There are many possibilities as to why FL p300 is more effective at acetylating pRb.

It is possible that the N-terminal and C-terminal *trans*-activation domains of p300 might help facilitate p300 auto-acetylation. His-p300 1195-1673 showed very little auto-acetylation comparative to Flag-p300 (1135-2414 and FL), despite being able to acetylate core histones effectively. Flag-p300 1135-2414 contains a *trans*-activation domain in its C-terminal domain (1673-2414), whilst Flag-p300 FL contains a further *trans*-activation region in its N-terminal domain (1-1195). The difficulty in using Flag-p300 FL purified from insect cells is the possibility of contamination resulting from the immunoprecipitation of other HAT enzymes. The extent of such contamination could be assessed by comparing levels of auto-acetylation from purified Flag-p300 FL with the levels of auto-acetylation observed using catalytically dead Flag-p300 FL.

Flag-p300 FL displays approximately 6-fold greater auto-acetylation than His-p300 1195-1673, and approximately 2-fold greater auto-acetylation than Flag-p300 1135-2414.

However, this observation would be more significant if the p300 enzymes were purified using 'fast protein liquid chromatography' (FPLC) to remove any possible contaminating HATs that could potentially be responsible for the observed auto-acetylation.

Recent studies suggest that hyper-acetylated p300 carries a higher basal catalytic activity than hypo-acetylated forms. Indeed, auto-acetylation of a proteolytically sensitive loop region of p300 (residues 1520 to 1560) greatly enhances p300 acetyl-transferase activity [237]. Perhaps the *trans*-activation domains in p300 aid interaction between p300 proteins thereby increasing auto-acetylation. It may be possible that the other regions of p300 have a stabilising effect on the overall tertiary structure of the p300 protein, and in that way augment its own auto-acetylation.

If this were the case why would the His-p300 1195-1673 acetylate core histones efficiently? Core histones are relatively small (less than 18KDa) compared with GST-pRb 379-928 (97 KDa) and GST-pRb 1-376 (76KDa). At similar concentrations, the molar ratio of core histones to GST-pRb 379-928 and GST-N-pRb 1-376 would be very high, and an individual core histone contains many more acetylated sites than pRb. Thus, there is a higher probability that the small histones (present in a greater molar ratio) might access the active site of His-p300 1195-1673 easier than the bulky GST-pRb fusion proteins. Regardless, Flag-p300 FL is able to acetylate GST-pRb fusion proteins at quite low concentrations (20 ng/µl). GST-N-pRb 1-376 showed approximately half the acetylation of GST-C-Rb 763-928 and GST-pRb 379-928.

Whilst *in vitro* acetylation was demonstrated with p300, it is likely other proteins also influence *in vivo* acetylation. A recent report has shown that pRb is acetylated at residues 873/874 during differentiation. Further, both p300 and P/CAF were able to *in vitro* acetylate pRb at K residues 873/874, and *in vivo* acetylation during early differentiation required P/CAF [53]. It is therefore possible that other HAT enzymes like P/CAF could contribute to pRb acetylation, or help p300 target pRb for acetylation.

Cyclin D/Cdk4 and cyclin (A/E)/Cdk2 phosphorylate the N-terminal domain of

pRb and several residues in the N-terminal domain of pRb are phosphorylated during G1/S transition [146]. It will be necessary to use mass spectroscopy to identify the K residues acetylated *in vitro* by Flag-p300 FL. It will be interesting to study whether the acetylation of the N-terminal domain of pRb affects cyclin D/Cdk4 and cyclin (A/E)/Cdk2 mediated phosphorylation, in a similar fashion to the influence of acetylation in the C-terminal domain on phosphorylation by Cdks.

In summary, using an *in vitro* acetylation assay, I was able to show that the N-terminal domain of pRb can be acetylated by p300. In combination with the previously documented acetylation of the C-terminal domain of pRb, these results suggest that acetylation may regulate diverse aspects of pRb tumour suppressor activity.

THE N-TERMINAL DOMAIN OF PRB IS ACETYLATED IN HEK 293 CELLS

E2F-1 and p53 are both acetylated in response to DNA damage [75, 228], as is the C-terminal domain of pRb [97]. It is interesting that treating cells with etoposide, doxorubicin and actinomycin D induced acetylation of the N-terminal domain of pRb. DNA damage induced acetylation of p53 is known to be dependent on Chk2 [228] and preliminary work suggests that C-terminal domain pRb acetylation is also Chk2 dependent (Judith Soloway, personal communication). Both E2F-1 and p53 are phosphorylated in response to DNA damage by Chk2 kinase [74, 228].

Interestingly, there are a number of potential Chk2 consensus phosphorylation sites present in the N-terminal domain of pRb (Figure 36, part e). Perhaps Chk2 is the upstream kinase responsible for influencing the DNA damage induced acetylation of pRb at both N-terminal and C-terminal domains? If that were the case, would phosphorylation have any other consequences for pRb function (such as a change in localization)? Therefore the next step would be to mutate potential Chk2 phosphorylation sites in the N-terminal domain to see any affect acetylation. Mutating Chk2 phosphorylation sites 'Ser residues to Asp' (mimicking phosphorylated-Ser residues) or 'Ser to Ala' (preventing phosphorylation)

could be employed to ascertain if Chk2 phosphorylation is required for the induction of acetylation.

A change in localization was observed for acetyl-pRb in U2OS cells in response to DNA damage [97]. It would be interesting to investigate whether DNA damage induced acetylation of the N-terminal domain of pRb impacts on pRb localization in response to DNA damage. Perhaps the N-terminal domain of pRb is involved in regulation of the C-terminal domain of pRb. HA-pRb 1-376 localises predominantly to the cytoplasm in C33A cells, but conversely localises to the nucleus in HEK 293 cells (Figure 22).

It is possible therefore that the interaction between the N-terminal and the C-terminal domains of pRb requires the presence of the pocket domain as a binding intermediary. However, there are limitations in drawing conclusions from this experiment. For example, there could be other genetic differences between HEK 293 and C33A cells that account for the different intra-cellular localization of N-pRb. This could be resolved by repeating the experiment in $Rb^{+/+}$ and $Rb^{-/-}$ MEF cells. I will improve future experiments by immunoblotting for PCNA and GAPDH as positive controls. PCNA is an entirely nuclear protein [238]. Immunoblotting the cytoplasmic extract for PCNA will show the efficiency of the nuclear extraction process used. GAPDH is an entirely cytoplasmic protein [239], which could be immunoblotted to determine the level of cytoplasmic contamination in the nuclear extract. Damaging U2OS cells using UV light, DFO or heat shock caused a change in the nuclear/cytoplasmic distribution of HA-N-pRb 1-376 (Figure 21b, samples F and G). Cells damaged with UV had less nuclear HA-N-pRb than cells damaged by treatment with etoposide or actinomycin D (compare Figure 21b, sample E with sample F). At the onset of apoptosis, pRb is cleaved by caspases in the internal region, resulting in the production of two major protein fragments, p48 and p68 [136]. In cells treated with DNA damaging agents, caspase cleavage of pRb proteins may result in the dissociation of the N-terminal domain from the A domain of the small pocket and in the translocation of the p48 protein and the exogenous HA-pRb 1-376 to the cytoplasm.

This may explain the observation that in C33A cells (containing genetically inactivated pRb), the HA-N-pRb 1-376 protein localizes mostly to the cytoplasm. HEK 293 cells and U2OS cells (which express pRb) trap the HA-pRb 1-376 in the nucleus, and only during apoptosis does HA-N-pRb 1-376 escape (Figure 21b, samples F to H).

In summary, pRb is acetylated *in vivo* in response to DNA damage at both the N-terminal and C-terminal domains. The N-terminal domain derivative HA-N-pRb-1-376 used here localized to the nucleus in U20S cells, but an altered nuclear/cytoplasmic staining occurred in response to UV treatment. In C33A cells, the majority of HA-N-pRb-1-376 occurs in the cytoplasm, whereas in HEK 293 cells the majority of HA-N-pRb 1-376 is present in the nucleus.

CHAPTER 4

INTRODUCTION: DNA DAMAGE-RESPONSIVE ACETYLATION OF pRB REGULATES BINDING TO E2F-1.

GST-C-pRb 763-928 INTERACTS WITH E2F-1 *IN VITRO*.

pRb has multiple roles in various cellular processes, including the repression of E2F-1 dependent apoptosis [240]. Exogenous E2F-1 can cause quiescent cells to re-enter the cell cycle [91]. Despite this, other studies have shown that E2F-1 has the ability to induce apoptosis when expressed in the absence of proliferative signals [241-243]. The assertion that E2F-1 can induce apoptosis was bolstered by studies carried out on E2F-1 knockout mice. E2F-1$^{-/-}$ mice develop thymic hyperplasia, likely due to a lack of thymocyte apoptosis during the development of the mouse [244].

E2F-1 *trans*-activation domain deletion mutants are still capable of inducing apoptosis [96]. Further, it was found that pRb mutants (which fail to repress *trans*-activation of other E2F-1 genes) could still bind E2F-1. Other E2F proteins did not interact with the mutant pRb. Indeed, chimeric proteins made by substituting the marked box/marked box adjacent region of E2F-1 (MB/MBA) with that of E2F-4 failed to interact with mutant pRb [96]. This interaction was found to require an intact E2F-1 DNA binding domain and the MB/MBA region of E2F-1. This mutant pRb/E2F-1 interaction was not pRb pocket dependent. The C-terminal domain of pRb residues (792-928) could still bind to E2F-1, and with equal affinity to wild-type pRb. These studies led to the possibility that post-translational modifications of the C-terminal domain of pRb might regulate this C-pRb/E2F-1 MB interaction.

Recent studies have shown that the C-pRb/E2F-1 MB interaction is dependent on

two sub-domains in the C-terminal domain of pRb and DP-1. The C-pRb core domain (residues 829-864) contributes to the majority of the binding energy, binding to E2F-1 with a Kd of 5 μM. The C-pRb N-terminal domain (residues 786-800) also interacts with the E2F-1 MB segment increasing the affinity of C-pRb for E2F-1 MB by 36 fold (corresponding to a Kd of 110 nM) [98].

The damage-induced acetylation of pRb occurs in the C-terminal domain at residues K873/874, close to the C-pRb core sub-domain [97]. It was therefore hypothesised that acetylation at residues K873/874 might interfere with the C-pRb/E2F MB interaction, facilitating the release of pRb and induction of apoptosis. In addressing this question, GST-C-pRb 763-928 was mutated at K873/874. Mutant derivatives were engineered, one where residues K873/874 were substituted with R, and another for Q. Mutating K to Q has been shown to phenotypically mimic acetylation in histones [177], E2F-1 [75], and pRb [214]. Here I found that E2F-1 binds to the C-terminal domain of pRb (amino acids 763-928). Furthermore, mutating K873/874 reduced binding to E2F-1. These results suggest that acetylation influences the binding affinity of the C-terminal domain of pRb for E2F-1.

THE ACETYLATION OF PRB AT RESIDUES K873/874 REDUCES THE E2F-1 INTERACTION IN CELLS.

The C-terminal domain of pRb (residues 792 to 928 and 763 to 928) binds to E2F-1 *in vitro* [96, 97], and interacts with the marked box region of E2F-1[96]. The marked box region of E2F-1 (Figure 7) influences the *trans*-activation function of E2F-1 [240]. Cells transfected with marked box deletion mutants of E2F-1 show no difference in levels of apoptosis over control cells, whereas over-expression of wild-type E2F-1 induces apoptosis [240].

pRb has anti-apoptotic functions (reviewed in [245]), which are likely mediated through the binding of the C-terminal domain of pRb with the marked box region of E2F-1

[96]. I have demonstrated that the binding of E2F-1 to the C-pRb is prevented *in vitro* by mutating residues K873/874 of pRb to Q residues (which mimic acetylation). Consequently, it was important to address whether the effect could be recapitulated *in vivo*, to test whether DNA damage responsive acetylation of pRb at residues 873/874 would affect the interaction between the C-pRb and E2F-1.

HEK 293 cells used in these experiments were transformed using adenovirus, and therefore they express the E1A and E1B oncoproteins [246]. E1A binds pRb small pocket region via its LXCXE motif [41]. One of the consequences of the pRb/E1A interaction is the loss of binding between the small pocket of pRb and the *trans*-activation domain of E2F-1 [40]. Therefore, HEK 293 cells were utilised to address whether the C-terminal domain of pRb bound to E2F-1 *in vivo*, and whether mutating pRb residues 873/874 to Q residues affects this interaction. Wild-type pRb was also expressed in HEK 293 cells to address whether mutating residues 873/874 in context with the FL pRb protein affected the interaction with E2F-1.

ACETYLATION AT RESIDUES K873/874 OF PRB INCREASES THE INTERACTION BETWEEN THE C- AND N-TERMINAL DOMAINS OF PRB.

Residues K873/874 are acetylated *in vivo* during differentiation and in response to etoposide induced DNA damage [53, 97, 214]. In Chapter 3 of this study the N-terminal domain of pRb was shown to be acetylated by Flag-p300 FL *in vitro*, and observed to be acetylated in HEK 293 cells in response to etoposide-induced DNA damage.

Despite a battery of publications specifically on the N-terminal domain of pRb (reviewed in [34]), not much is known about its main functions and how it interacts with the rest of the protein. However, studies using the yeast two-hybrid system confirmed that the pRb could self-associate and that this association is mediated by interactions between the N-terminal and C-terminal domains of the protein [135]. I wished to address whether the N-terminal domain of pRb is involved in regulation of the C-terminal domain of pRb,

which might affect the localization of pRb and perhaps also its binding affinity for E2F-1.

Here I present data that suggests post-translational modification of pRb regulates the binding of the N-terminal domain to the C-terminal domain of pRb. Overall, the result is consistent with a role for the N-terminal domain of pRb in the localization of pRb during response to DNA damage through the interaction with the C-terminal domain of pRb.

CHAPTER 4

RESULTS

GST-C-pRb 763-928 INTERACTS WITH E2F-1 *IN VITRO*.

The C-terminal domain of pRb binds to E2F-1

It was necessary to clarify that the C-terminal domain of pRb could interact with E2F-1. GST-C-pRb 763-928 was used in a GST pull down assay. It was observed that GST-C-pRb 763-928 bound E2F-1 *in vitro*, whereas GST protein failed to interact with ^{35}S-methionine E2F-1 (Figure 23a). IVT ^{35}S-methionine labelled E2F-1 was used for the GST pull down (Figure 23b).

The GST-C-pRb 763-928 QQ mutant showed much reduced binding to E2F-1

A study using the pRb (378-928) QQ mutant derivative showed that the exogenously expressed QQ mutant could arrest cells in G1 as efficiently as wild-type pRb that had been acetylated by the addition of exogenous p300 [214]. I wished to assess whether pRb acetylation at residues K873/874 might alter the binding affinity of pRb 763-928 for E2F-1. Two mutant pRb 763-928 derivatives, GST-C-pRb 763-928 QQ and GST-C-pRb 763-928 RR, were engineered to create a recombinant GST-C-pRb 763-928 that mimics K residue acetylation (QQ mutant), and one that could not be acetylated (RR mutant) (Figure 24a). The substitutions were selected based on their physical and chemical similarities to K residues. R and Q residues were selected because they have a similar physical mass (Da) and van der waals volume (A^3) as K residues (Figure 24b). K, Q and R residues are characteristically polar, but Q residues are neutral in charge mimicking

acetylated K residues (Figure 25a, and 25b). Both Q and R make acceptable substitutions for K residues when they are solvent exposed (Figure 25c) [247-249]. GST-C-pRb 763-928 mutants (Figure 26a) were combined with HEK 293 extracts containing E2F-1. It was a concern that mutating the pRb 763-928 at K residues 873/874 might have inactivated the mutant protein. In order to assess the integrity of the QQ and RR mutant proteins, each mutant was tested for binding with *in vitro* translated Mdm2 (Figure 26b), a known target for the C-terminal domain of pRb [125]. Each GST-pRb derivative bound Mdm2 with equal efficiency (Figure 26b). HEK 293 cells were used as a source of endogenous E2F-1 (Figure 26c). It was found that whilst the wild-type and RR mutant proteins efficiently bound E2F-1, the QQ mutant protein showed a significant loss of affinity. GST did not show affinity for E2F-1. Thus acetylation of K873/874 may influence binding to E2F-1.

Figure 23

a) GST pulldown

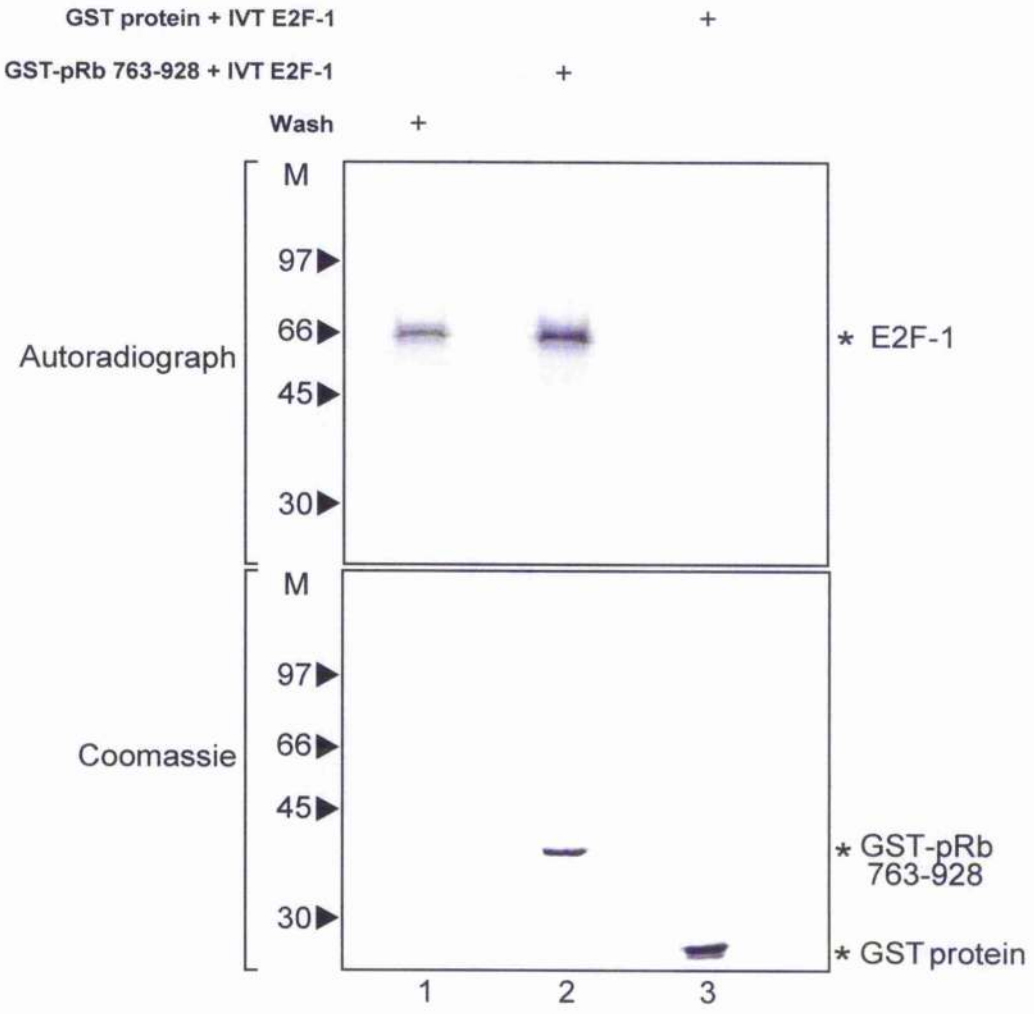

b) INPUTS

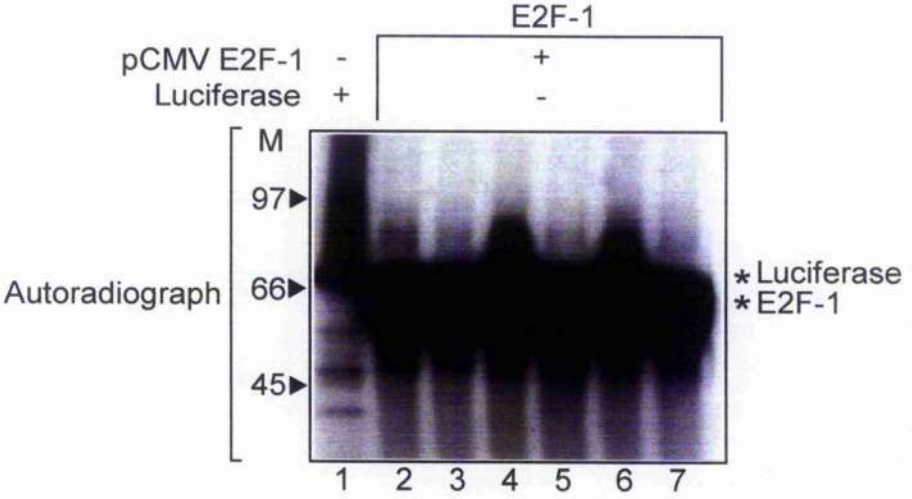

Figure 23: The C-terminal domain of pRb can bind E2F-1

^{35}S-Methionine labelled E2F-1 was incubated with 2 μg of GST-C-pRb 763-928 or GST protein.

a) Binding of GST-pRb 763-928 to ^{35}S-Methionine labelled E2F-1 was assayed by autoradiography, and GST-pRb 763-928 was visualised by Coomassie staining.

b) IVT ^{35}S-Methionine labelled E2F-1 input levels (10 % of extract used in the binding assay) were also visualized by autoradiography.

Figure 24

a)

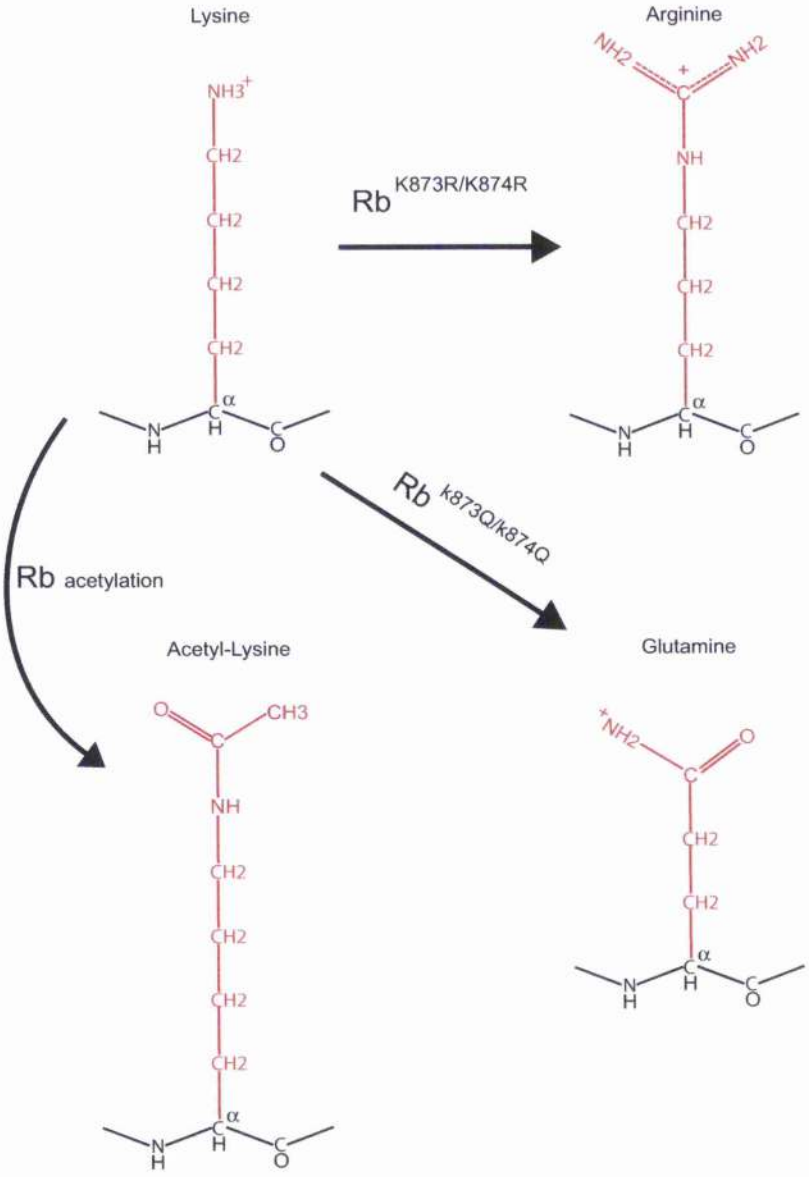

b)

	Charge	Polarity	Mass (Daltons)	v an der waals volume A^3
Lysine	+	Polar	128	169
Arginine	+	Polar	156	173
Glutamine	Neutral	Polar	128	143
Ac-lysine	Neutral	Polar	132	170

Adapted and reproduced from; The Merek Index, (ISBN 911910-28-X) & CRC handbook of chemistry and physics, (ISBN 0-8493-0458-X)

Figure 24: A structural comparison between K, R, Q and acetyl-K residues

a) Comparison of the chemical structures of K, R, Q and acetyl-K residues. The main chain is coloured black, with the variable side chains shown in red.

b) Table comparing the physical properties of K, R, Q and acetyl-K residues.

Figure 25

a)

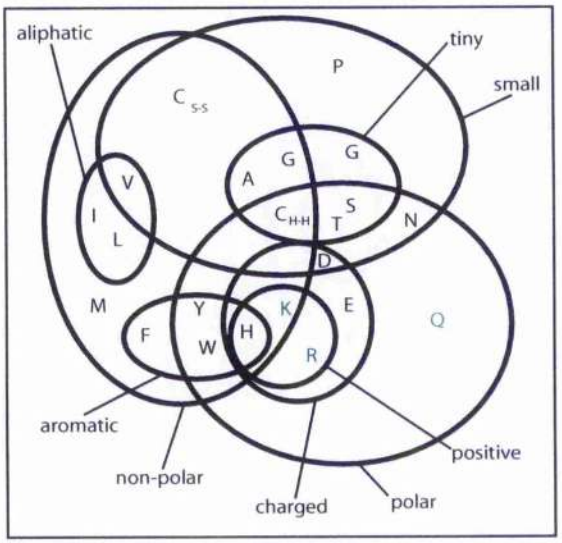

b)

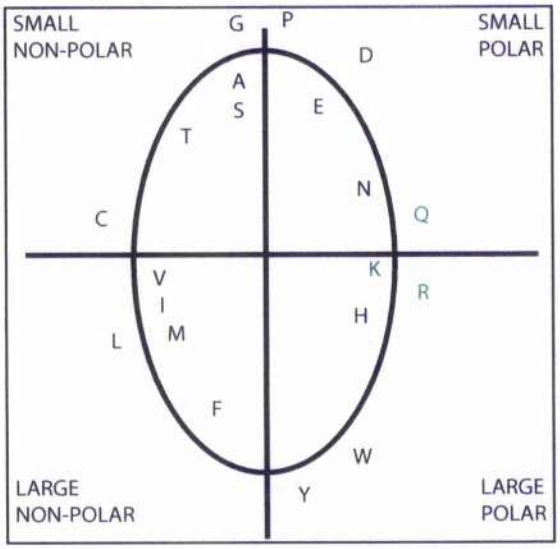

c)

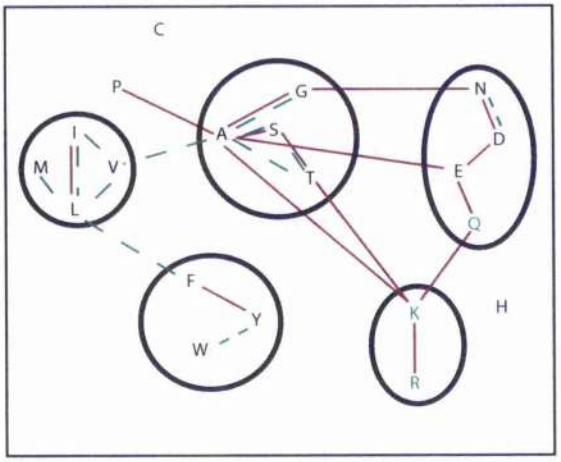

Reproduced from [245], [246], and [247].

Figure 25: Comparison of the physical properties of K, R and Q

a) Venn diagram showing the relationship of the 20 naturally occurring amino acids.

K, R and Q are polar residues. K and R carry a positive charge whilst Q is neutral in charge. Q substitution is thought to mimic K acetylation as both carry neutral charge.

b) A representation of amino acids by Dayhoff mutation odds matrix

Highlighted in green are K, Q and R residues. Left and right of the Y-axis indicate the degree of polarity (non-polar and polar properties respectively). Above and below the X-axis indicates representative size of amino acids (small to large respectively). R and Q are good candidates for substituting K residues due to their similar size and polarity.

c) Suggested amino acid substitutions for K acetylation

The diagram depicts the possible amino acid substitutions for solvent exposed amino acids (> 30 square Angstroms exposed to the solvent). Amino acids that are connected by a solid line can be substituted with 95 % confidence [247], based on statistics from fifty five proteins. pRb residues K873/874 are predicted to be exposed residues. Residues R and Q were selected due to their similar physical properties to K residues. R was selected for a residue that could not be acetylated. Q was selected as a

mutant that phenotypically mimics K acetylation, presumably due to similar structure, size and charge of an acetyl-lysine.

Figure 26

a)

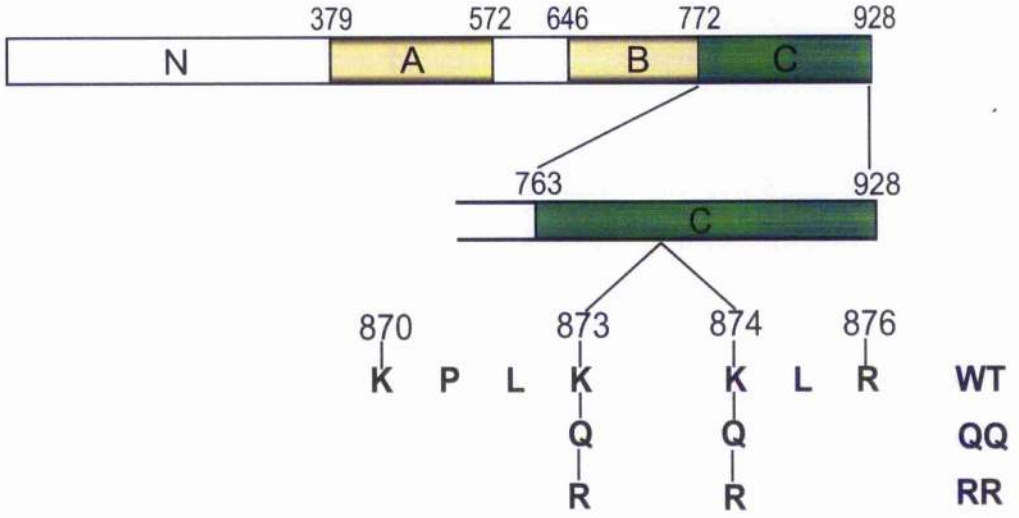
379
572
646
772
928
N
A
B
C
763
928
C
870
873
874
876
K P L K K L R WT
Q Q QQ
R R RR

Figure 26

b) PULL DOWN

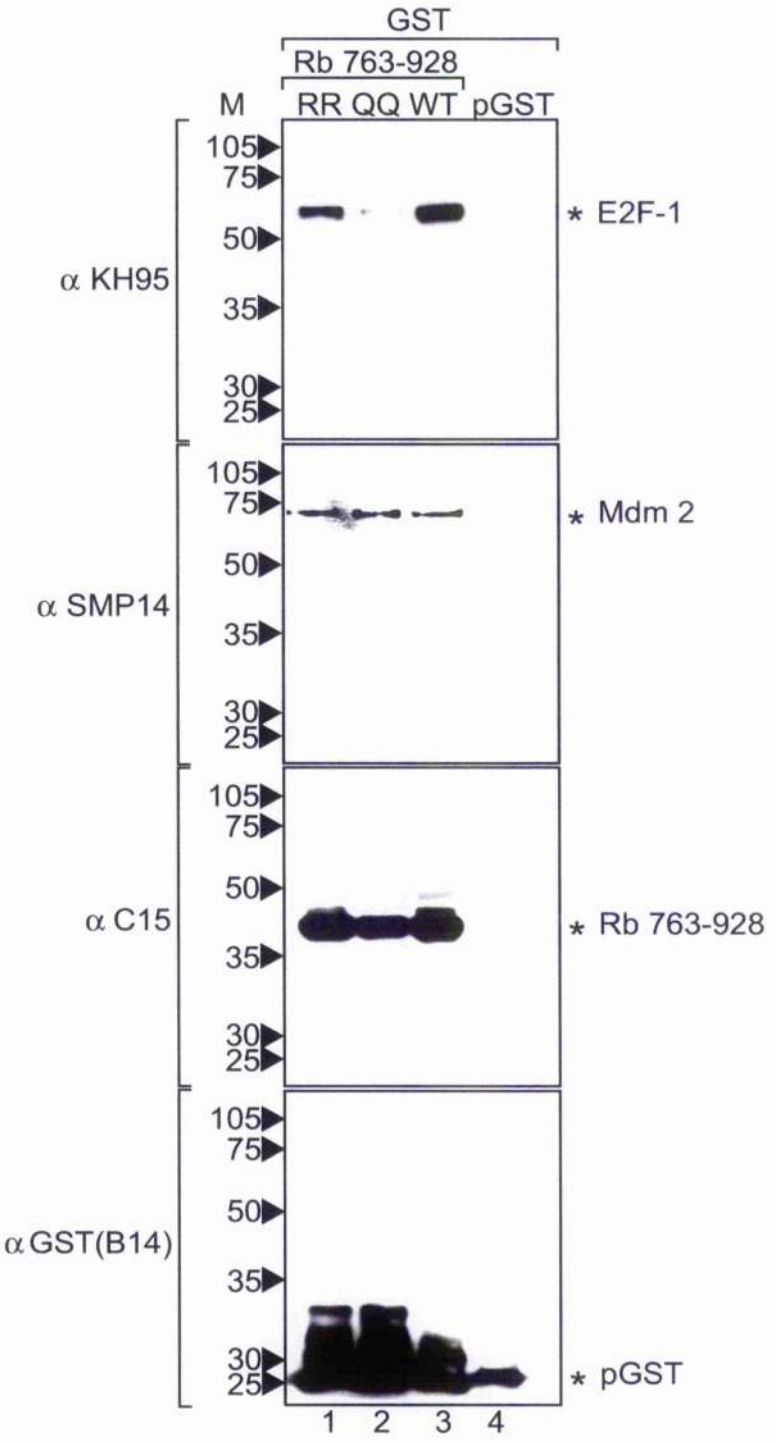

Figure 26

c) Inputs

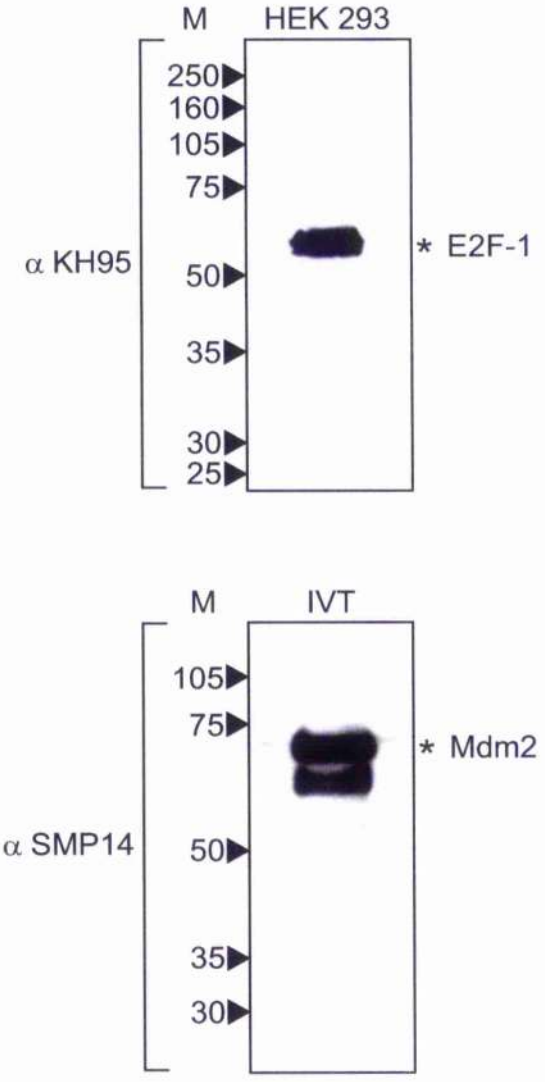

Figure 26: Mutating GST-C-pRb 763-928 residues K873/874 to Q inhibits binding to E2F-1

a) Depicts the GST-C-Rb 763-928 (wild-type, QQ and RR mutant) recombinant constructs used in this experiment.

b) Binding of GST-pRb 763-928, RR873/874 and QQ873/874 (1 µg) to E2F-1, Mdm2 and GST protein in HEK 293 cell extracts were assayed by immunoblotting with anti-E2F-1 (KH95), anti-Mdm2 (SMP-14) and anti-GST (B14).

c) Input levels of endogenous E2F-1 and Mdm2 (10 % of that used in pull downs) were visualised by immunoblotting.

THE ACETYLATION OF PRB AT RESIDUES K873/874 REDUCES THE E2F-1 INTERACTION IN CELLS.

Mutating residues K873/874 to Q reduces the C-pRb/E2F-1 interaction

HEK 293 cells were transiently transfected with constructs encoding HA-pRb wild-type (Figure 27a, lane 1), HA-C-pRb RR and QQ mutant derivatives (figure 27a, lanes 2 and 3), and HA-C-pRb wild-type (figure 27a, lanes 4 and 5). The cells were all co-transfected with pCMV E2F-1. Co-immunoprecipitation experiments were carried out as described (page 143). Briefly, the HA-pRb wild-type and HA-C-pRb mutant proteins were immunoprecipitated using the anti-HA antibody and samples were analysed using electrophoresis followed by immunoblotting for E2F-1 and C-pRb (Figure 27a).

Although more HA-C-pRb QQ mutant protein immunoprecipitated than wild-type or RR mutants, the HA-C-pRb QQ mutant protein showed much reduced interaction with E2F-1. Less HA-C-pRb RR mutant protein immunoprecipitated from extracts than the HA-C-pRb wild-type or HA-C-pRb QQ mutant proteins, but significantly more E2F-1 interacted with HA-C-pRb RR mutant protein than interacted with HA-C-pRb QQ mutant protein. The experiment contains a non-specific antibody control (Figure 27a, lane 5) and a non-transfection control (Figure 27a, lane 6).

Densitometric analysis was employed to compare the protein levels of E2F-1 and HA-C-pRb 763-928 mutant derivatives immunoprecipitated (in Lanes 1 to 4) (Figure 27b). Relative amounts of bound E2F-1 were adjusted by factoring in differences in immunoprecipitated HA-C-pRb 763-928. The HA-C-pRb QQ mutant derivative was only able to immunoprecipitate E2F-1 with 7 % efficiency of the wt HA-C-pRb 763-928. In contrast, the HA-C-pRb RR mutant derivative could immunoprecipitate E2F-1 0.8 times less efficiency than the wild-type HA-C-pRb 763-928 (Figure 27b).

The pcDNA3 2HA-pRb (763 to 928) mutated derivatives expressed equally well in HEK 293 cells (Figure 27c). pSG5L-HA-pRb (1-928) also expressed well in HEK 293

cells. In order to check the accuracy of the densitometric analysis, known amounts of BSA protein were analysed using electrophoresis and coomassic blue staining (Figure 27d, left panel). Using densitometry, the relative protein levels of the BSA bands were compared to the 1μg band (lane 1). Calculations of the amounts of BSA loaded in lanes 2, 3 and 4 are shown (Figure 27d, right panel).

Figure 27

a) IP

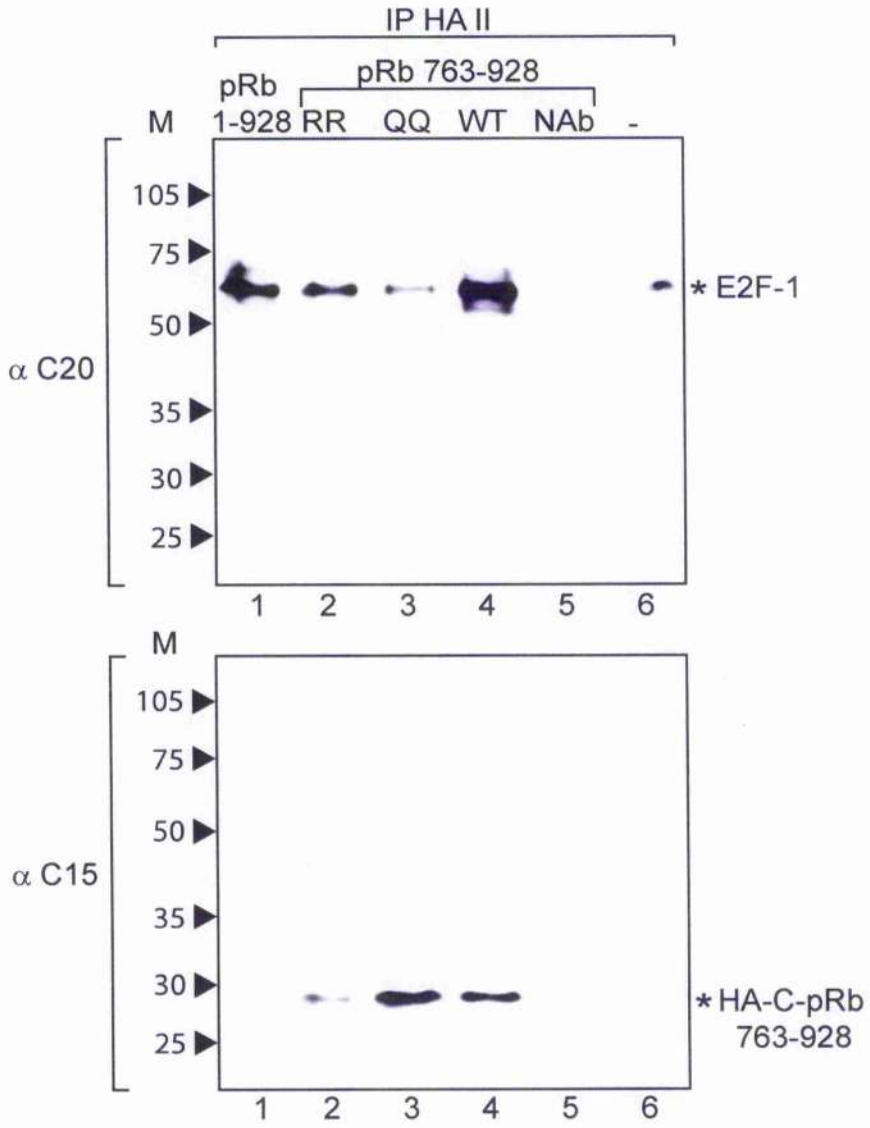

b) Densitometry

	RR	QQ	WT
HA-C-pRb levels	0.49	1.57	1
E2F-1 levels	0.4	0.11	1
E2F-1 adjusted for HA-C-pRb	0.82	0.07	1

Figure 27

c) Inputs

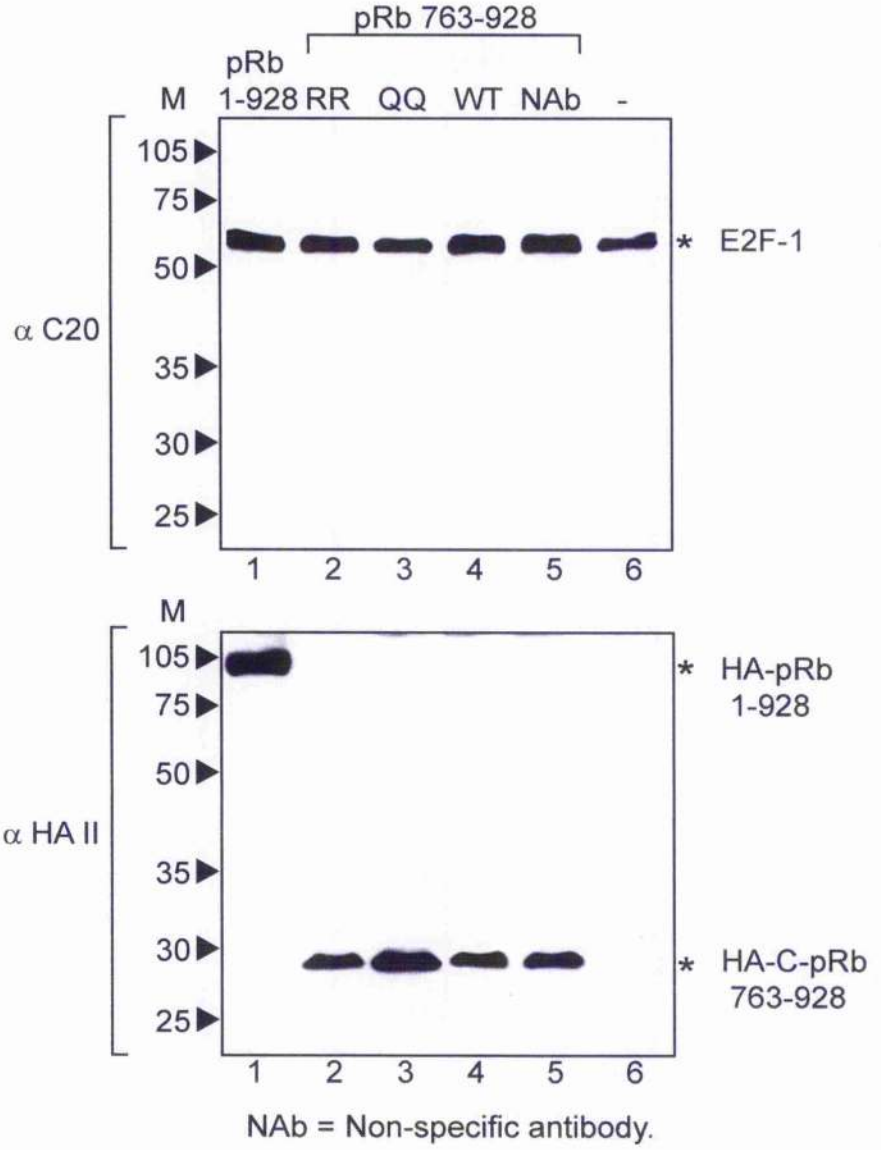

NAb = Non-specific antibody.

d) Densitometry standard.

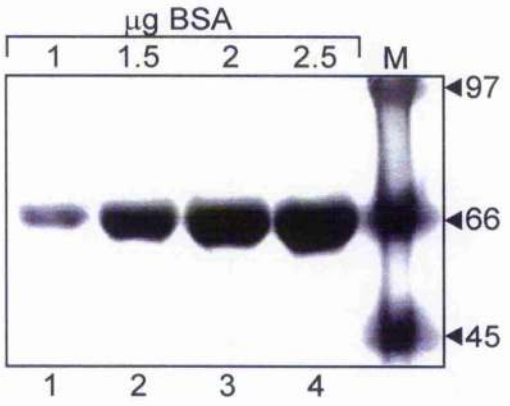

BSA (μg)	1	1.5	2	2.5
Relative levels	93	136	190	223
Calc BSA (μg)	1	1.46	2.04	2.4

Figure 27: E2F-1 interacts with C-Rb

Extracts were prepared from HEK 293 cells transfected with the following expression vectors; 2 μg of pcDNA3 HA-pRb 763-928 (wt, QQ, or RR) or 2 μg of pSG5L-HA-pRb 1-928. All samples were transfected with pCMV-β-gal (0.5 μg throughout).

a) Extracts were normalized and immunoprecipitated (IP) with anti-HA antibody (Lanes 1-4 and 6) or with goat-anti-rabbit antibody as non-specific antibody (NAb) (Lanes 5), and after electrophoresis, immunoblotted with anti-E2F-1 antibody (C20) (top panel) and anti-Rb C15 antibody (bottom panel).

b) Quantification of the protein levels in a). Protein levels are compared to HA-C-pRb 763-928 wt (Lane 4), which is given the nominal value of 1. The levels of both E2F-1 and HA-C-pRb mutant derivatives are shown. The levels of bound E2F-1 are adjusted to take into account the different levels of immunoprecipitated mutant HA-C-pRb 763-928 RR, QQ or wt.

c) Corresponding inputs showing 100 μg extract immunoblotted with anti-E2F-1(top panel) and anti-HA (bottom panel) antibodies.

d) Known amounts of BSA (1, 1.5, 2 and 2.5 μg) were resolved on an SDS PAGE gel and visualized with coomassie staining (left panel). Densitometry was used to measure the relative concentrations of BSA (right panel).

Mutating residues K873/874 to Q also reduces the FL-pRb/E2F-1 interaction

A similar experiment was carried out comparing the binding efficiencies of wild-type FL-pRb and FL-pRb mutant proteins to E2F-1. E1A bound pRb does not interact with the *trans*-activation domain of E2F-1 as it might do in tumour cell lines that are not transformed with adenovirus (such as U2OS, T98G or MCF-7 cell lines) [40]. Therefore it was reasoned that transfecting FL-pRb mutants into HEK 293 cells would allow the study of the pRb C-terminal domain and its interaction with E2F-1 in the context of FL-pRb.

HEK 293 cells were transiently transfected with constructs encoding Ha-pRb wt (Figure 28a, lanes 1, 3 and 6), HA-pRb-QQ mutant derivative (Figure 28a, lanes 4 and 7), and HA-pRb RR mutant derivative (Figure 28a, lanes 5 and 8). All cells were co-transfected with constructs encoding for E2F-1. FL-HA-pRb mutant derivatives were immunoprecipitated using the HA antibody and samples were analysed by electrophoresis followed by immunoblotting to detect immunoprecipitated HA-pRb mutant proteins and co-immunoprecipitated E2F-1 (Figure 28a). Lane 1 shows proteins immunoprecipitated using a non-specific antibody, and lane 2 shows proteins immunoprecipitated from the control extract. Significantly less E2F-1 immunoprecipitated with the FL HA-pRb QQ mutant in both un-treated cells (Figure 28a, Lane 4) and cells treated with etoposide (Figure 28a, Lane 7).

Densitometric analysis was employed to compare the protein levels of E2F-1 and HA-pRb mutant derivatives immunoprecipitated (in Lanes 3 to 5, and Lanes 6 to 8) (Figure 28b). Relative amounts of bound E2F-1 were adjusted by factoring in differences in immunoprecipitated HA-pRb. The HA-pRb QQ mutant derivative was only able to immunoprecipitate E2F-1 with 20 % of the efficiency observed with the wt HA-pRb (Figure 28b). In cells, the HA- pRb RR mutant derivative could immunoprecipitate E2F-1 with 11 % greater efficiency compared with the wt HA-pRb (Figure 28b). A more modest reduction in E2F-1 immunoprecipitation was observed if cells were treated with etoposide.

The HA-pRb QQ mutant bound E2F-1 with efficiency about 60 % of that compared to wt or RR HA-pRb mutant proteins.

Protein levels of E2F-1 immunoprecipitated with the FL HA-pRb wt and RR mutant proteins were similar. As expected [229], levels of E2F-1 immunoprecipitated with FL-pRb mutant proteins were higher in cells treated with etoposide (Figure 28c, Lanes 6 to 8).

The FL-HA-pRb 1-928 constructs (pSG5-L HA-pRb wt, QQ, and RR) were expressed equally well in HEK 293 cells (Figure 28c). Etoposide treated HEK 293 cells expressed greater levels of exogenous FL pRb mutant proteins than un-treated cells (Figure 28c). Protein levels of endogenous E2F-1 were consistent with that observed with DNA damage induced E2F-1 (Figure 28c) [229].

Figure 28

a) IP

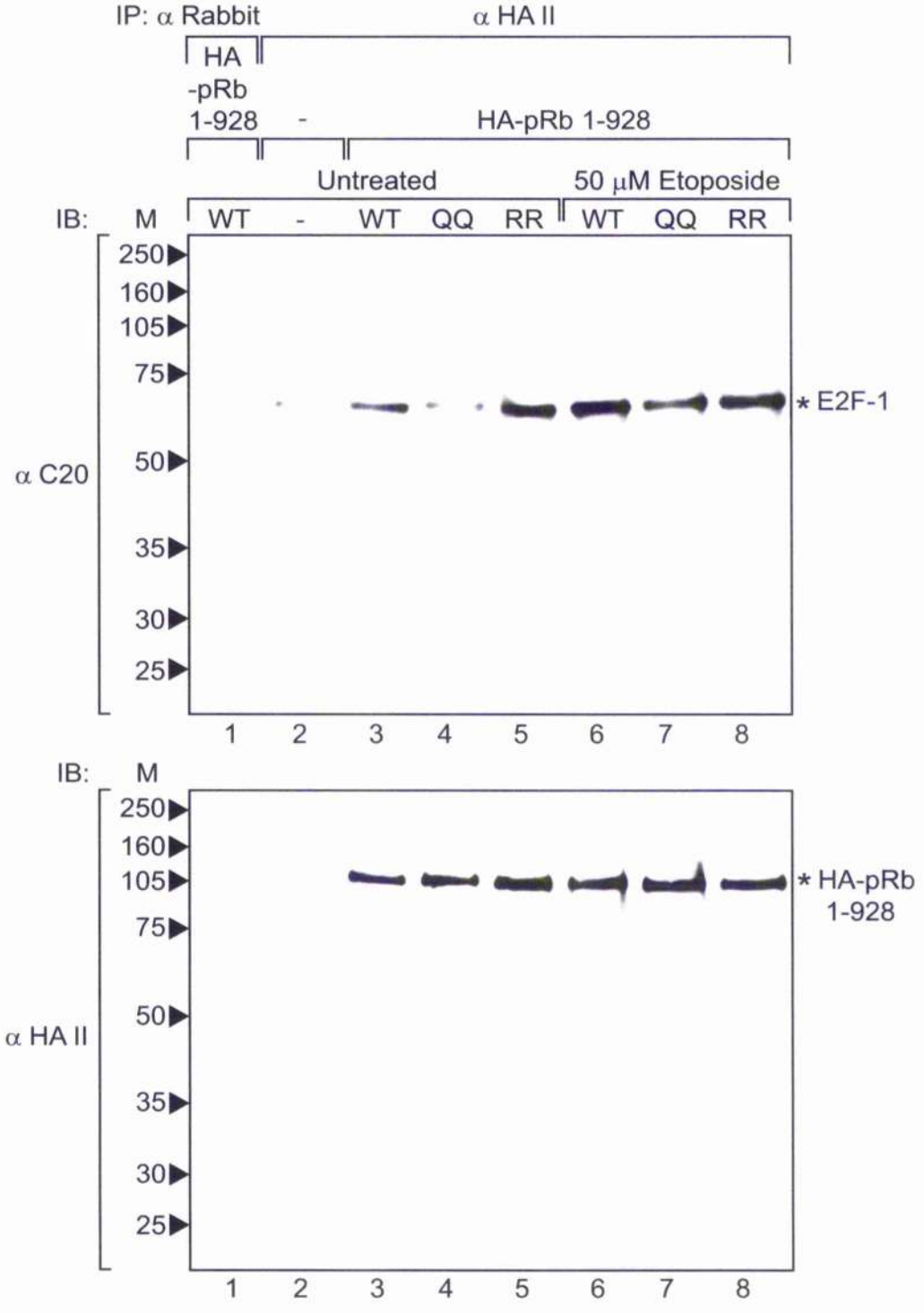

Figure 28

b) Densitometry

No treatment	WT	QQ	RR
HA-pRb levels	1	1.18	1.58
E2F-1 levels	1	0.24	1.58
E2F-1 adjusted for HA-pRb	1	0.20	1.11
Etoposide treatment	WT	QQ	RR
HA-pRb levels	1	1.26	1.09
E2F-1 levels	1	0.75	1.07
E2F-1 adjusted for HA-pRb	1	0.60	0.98

c) Inputs

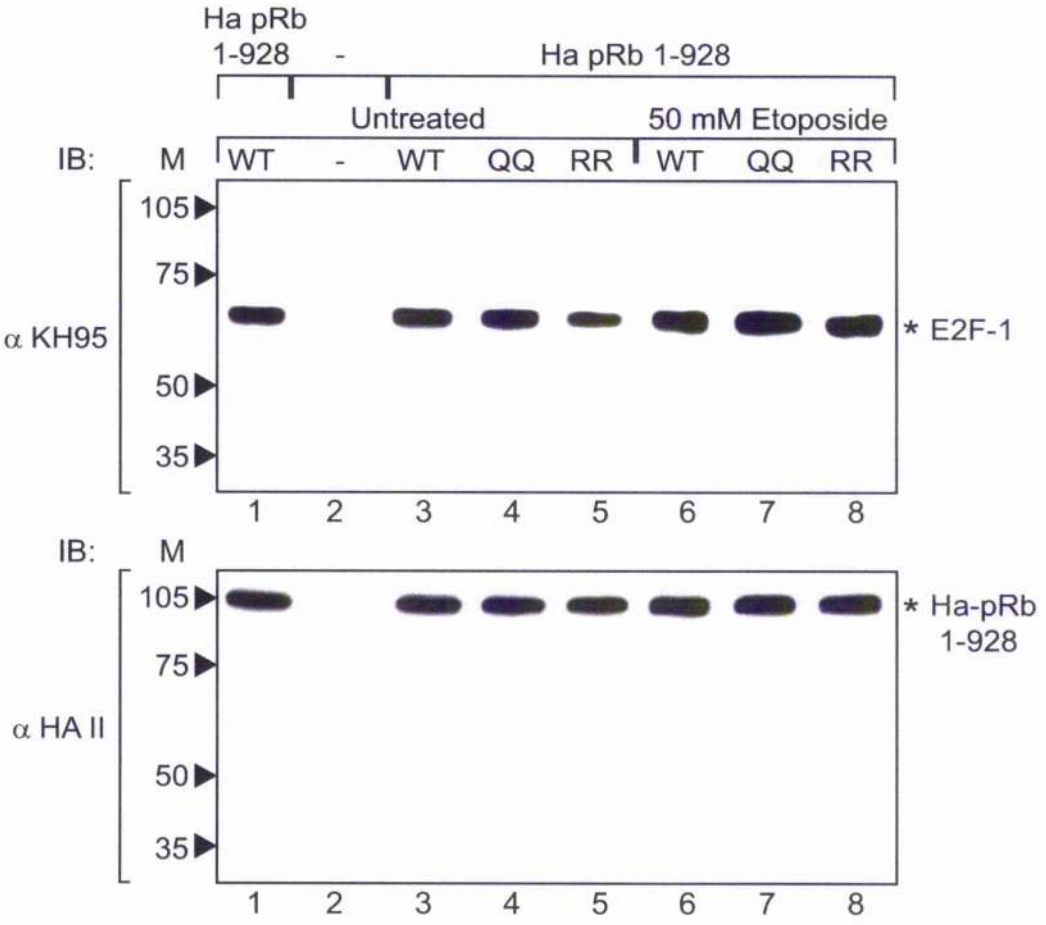

Figure 28: E2F-1 interacts with HA-pRb 1-928

Extracts were prepared from un-treated and etoposide treated HEK 293 cells transfected with expression vectors encoding pSG5L-HA-pRb 1-928 (wt, QQ, or RR) (2 μg). All samples were transfected with pCMV-β-gal (0.5 μg throughout).

a) Extracts were normalized and immunoprecipitated with anti-HA antibody (lanes 2 to 8), or with goat-anti-rabbit antibody as non-specific antibody (NAb) (lanes 1), and after electrophoresis, immunoblotted with anti-E2F-1 antibody (C20) and anti-HAII antibody.

b) Quantification of the protein levels in 'a'. Protein levels are compared to HA-pRb wt (Lane 4), which is given the nominal value of 1. The levels of both E2F-1 and HA-pRb mutant derivatives are shown. The levels of bound E2F-1 are adjusted to take into account the amount of mutant HA-pRb wt, QQ or RR in the pull down.

c) Corresponding inputs showing 100 μg extract immunoblotted with anti-E2F-1 KH95 antibody and anti-HA antibodies.

Mutating FL-pRb residues 873/874 to Q alters subcellular localization.

It was important to characterize the C-pRb mutant proteins intra-cellular localization. Using a specific antibody raised against acetylated K873/874 peptides (SK37), it was shown that acetylated pRb (at residues K873/874) underwent nuclear re-localization in response to etoposide treatment in U2OS cells [97]. The HA-C-pRb mutant constructs (pcDNA 2HA-pRb 763-923 wild-type, QQ and RR) were therefore transfected into U2OS cells. Cells were immunostained using the HA antibody to detect the exogenous protein. The three HA-C-pRb proteins localized into the nucleus of un-treated or etoposide treated U2OS cells (Figure 29a and 29b).

A characterization of the intra-cellular localization of FL-HA-pRb mutant derivative proteins was also investigated. The FL-HA-pRb mutant constructs (pSG5L-HA-pRb 1-928 wild-type, QQ and RR) were transfected into U2OS cells. Cells were immunostained using the HA antibody to detect the exogenous protein. The wild-type and RR mutants both localized to the nucleus (Figure 30; top and bottom rows, respectively). The FL HA-pRb QQ mutant localised mainly to the cytoplasm with small amounts of nuclear staining present (Figure 30; middle row).

DNA damage does not change the localization of wt, QQ or RR mutant FL-Rb

A similar experiment was carried out using U2OS cells treated with etoposide. Etoposide treatment had no obvious effect on the localization of FL-HA-pRb mutant proteins (Figure 31), since localization was similar to that observed in Figure 30. The nuclear localization of endogenous pRb in U2OS cells with and without etoposide treatment.

Figure 29

a)

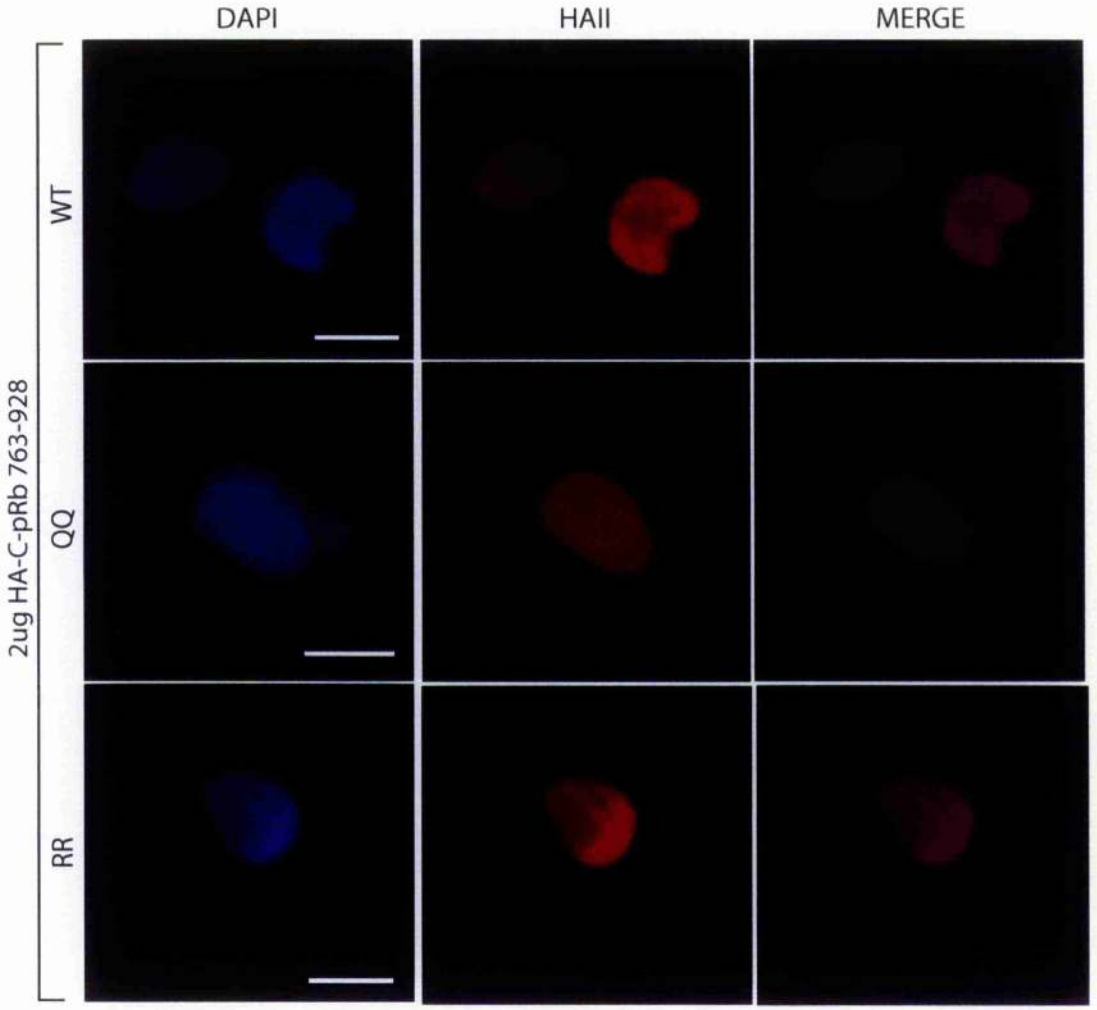

Figure 29

b)

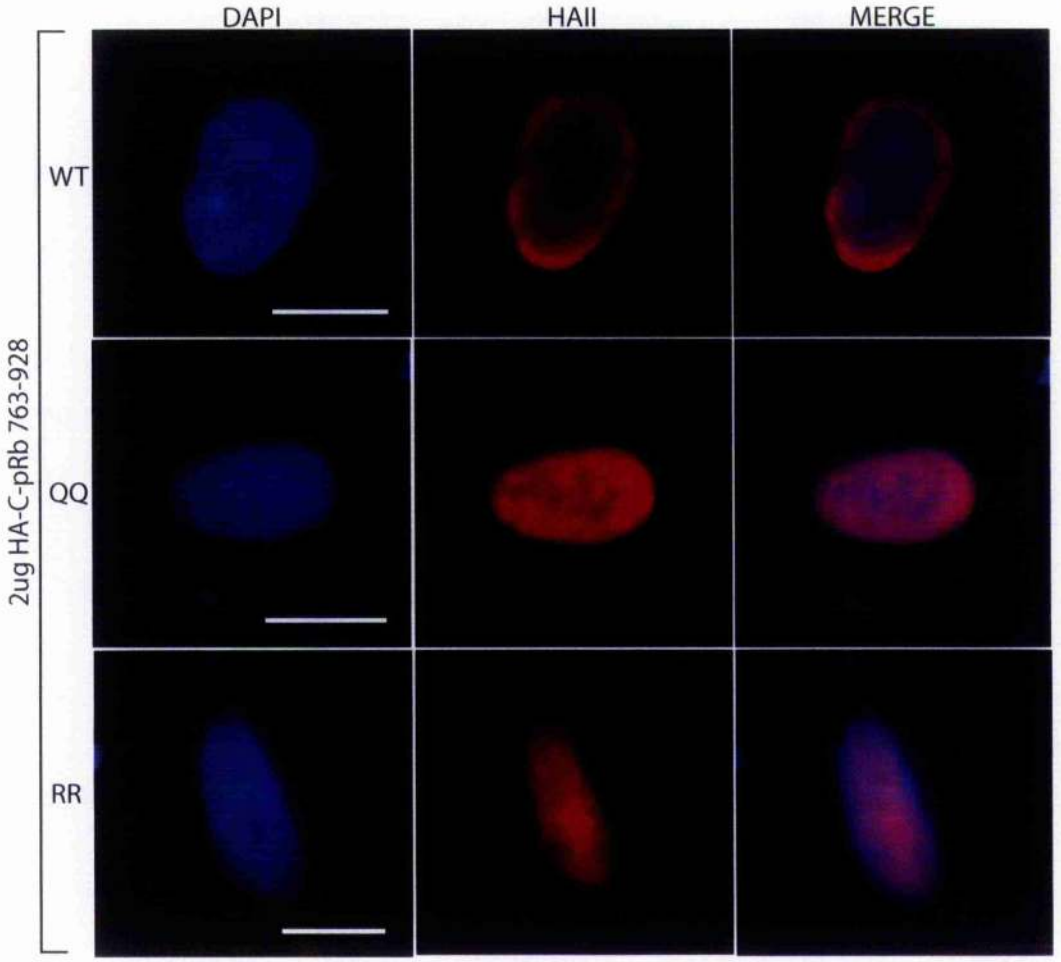

Figure 29: HA-C-pRb 763-928 (wt, QQ and RR mutants) localize to the nucleus of both un-treated and etoposide treated U2OS cells

U2OS cells were transfected with 2 μg of pcDNA3 2HA-Rb 763-928 wt or QQ or RR mutant DNA. After 48 h transfection, cells were immunostained using anti-HA antibody to detect the pRb mutant derivative proteins. All images are shown at 630 X magnification. Images were digitally manipulated for enlargement. A white bar at the bottom of the images represents 10μm.

a) U2OS cells un-treated and immunostained 48 h post-transfection.

b) U2OS cells treated with 50 μM etoposide for 8 h prior to immunostaining.

The nuclear localization of endogenous pRb in U2OS cells with and without etoposide treatment

As the exogenous C-pRb and FL-pRb mutant proteins (used in Figures 29-31) were over-expressed, it was reasoned that subtle changes in the intra-nuclear localization of pRb would not be detected by staining for the exogenous protein. Therefore, U2OS cells were stained with antibodies that detect endogenous pRb in both un-treated and etoposide treated cells (Figure 32). Cells were stained with IF8, or G3-245 (Figure 32a and 32b). Both pRb antibodies detected similar nuclear localization of pRb whether the cells were etoposide treated or not. There was no obvious change in nuclear localization under DNA damage conditions.

Figure 30

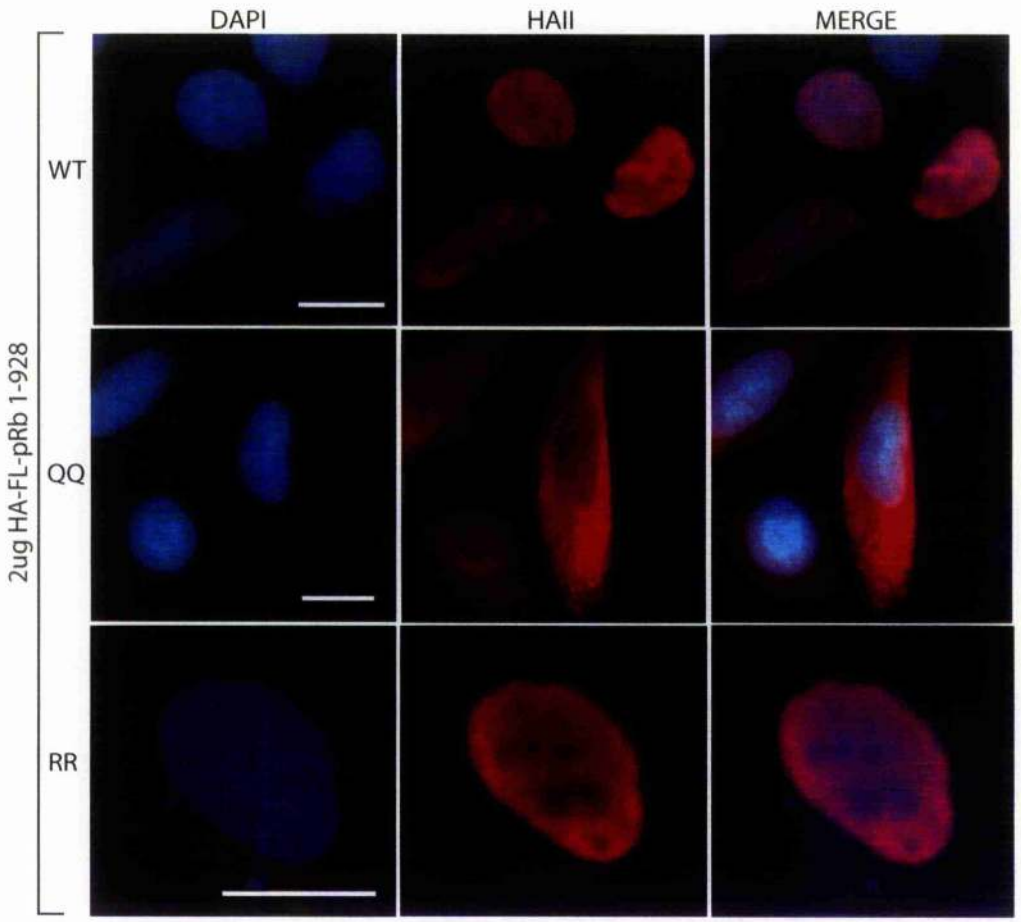

Figure 30: The localization of HA-pRb 1-928 (wt, QQ and RR) mutant proteins

U2OS cells were transfected with 2 μg of pSG5L-HA-pRb wt or QQ or RR mutant DNA. After 48 h transfection, cells were immunostained using anti-HA antibody to detect the mutant derivative proteins. All pictures are shown at 630X magnification. Images were digitally manipulated for enlargement. A white bar at the bottom of the images represents 10μm.

Figure 31

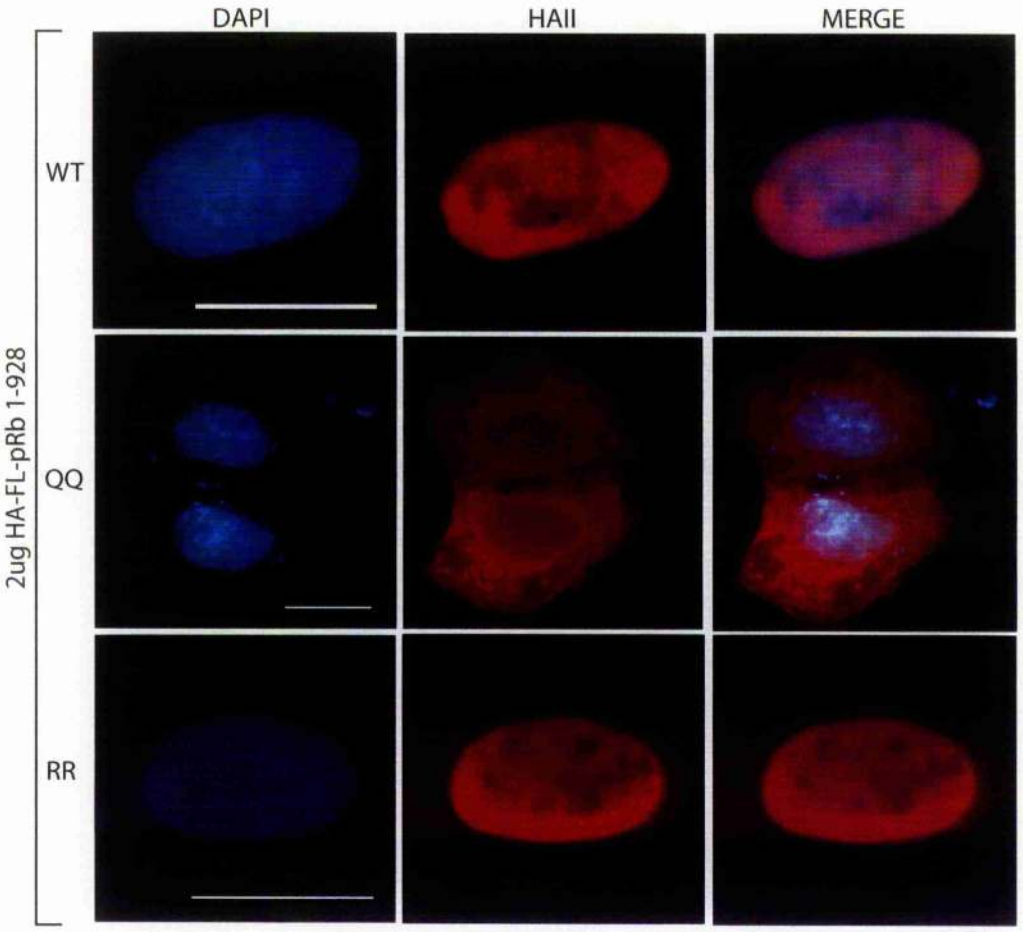

Figure 31: The localization of HA-pRb 1-928 (wt, QQ and RR) mutant proteins in response to etoposide treatment

U2OS cells were transfected with 2 μg of pSG5L-HA-pRb wt or QQ or RR mutant DNA. Cells were treated with 50 μM etoposide 40h post-transfection and immunostained 8h post-treatment. Cells were immunostained using anti-HA antibody to detect the mutant derivative proteins. All pictures are shown at 630X magnification. Images were digitally manipulated for enlargement. A white bar at the bottom of the images represents 10μm.

Figure 32

a)

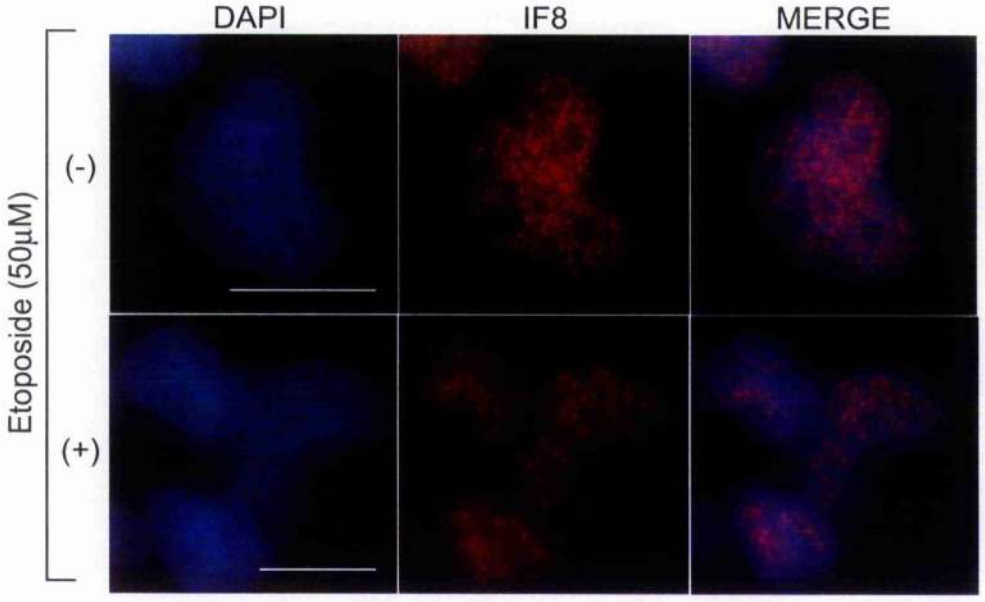
DAPI
IF8
MERGE
Etoposide (50μM)
(-)
(+)

b)

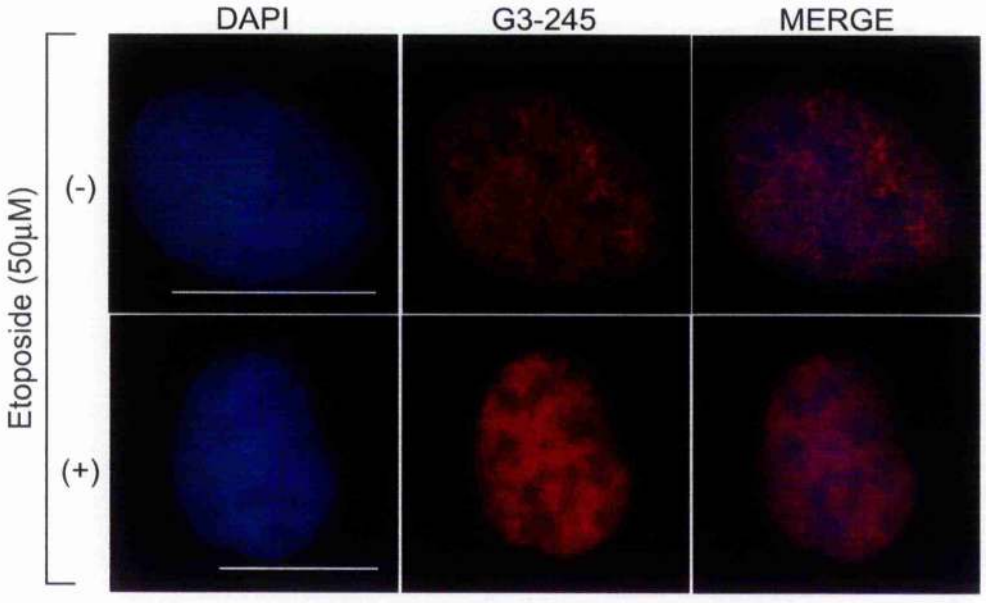
DAPI
G3-245
MERGE
Etoposide (50μM)
(-)
(+)

Figure 32: The localization of endogenous pRb with and without etoposide treatment

U2OS cells were treated without or with 50 μM etoposide 40h post-transfection and immunostained 8h post treatment. Cells were immunostained using either anti-IF8 antibody (raised against whole pRb) or G3-245 (which recognises an epitope between aa 322-344 of pRb). All pictures are shown at 630X magnification. Images were digitally manipulated for enlargement. A white bar at the bottom of the images represents 10μm.

ACETYLATION AT RESIDUES K873/874 OF PRB INCREASES THE INTERACTION BETWEEN THE C- AND N-TERMINAL DOMAINS OF PRB.

The N-pRb domain binds to the C-pRb *in vitro*

The regions in pRb used in this binding study are represented (Figure 33a). GST bound recombinant C-pRb 763-928 (wt, QQ and RR mutant protein) was used as bait for the nuclear extract containing N-pRb (Figure 33b). It was observed that the N-pRb bound to the C-pRb (Figure 33b, Lanes 3 and 4) but not to GST protein (Figure 33b, Lane 5). The middle panel shows the mutant protein levels of pRb 763-928 bound to the GST beads (Figure 33b, Lanes 1 to 4). The protein level of GST-pRb QQ mutant protein is approximately a fourth of GST-pRb wt or GST-pRb RR protein levels, but it still binds to the N-pRb (Figure 33b, Lane 3). The C-pRb RR mutant protein was not observed to specifically bind the N-pRb protein (Figure 33b, Lane 2). As a positive control, pRb 763-928 wt was shown to interact with HA-pRb 1-928 (Figure 33b, Lane 1).

Densitometric analysis was employed to compare the protein levels of HA-N-pRb 1-376 and GST-C-pRb 763-928 mutant derivatives (Figure 33c). Relative amounts of bound HA-N-pRb 1-376 were adjusted by factoring in differences in levels of GST-C-pRb 763-928 mutant derivatives bound to GST Sepharose beads. The GST-C-pRb QQ mutant derivative was able to pull down HA-N-pRb approximately 4 times more efficiently than the wild-type GST-C-pRb 763-928. In contrast, the assay did not detect any interaction between GST-C-pRb RR mutant derivative and HA-N-pRb. Interestingly, wild-type GST-C-pRb was able to pull down FL HA-pRb 3.3 fold more efficiently than its interaction with HA-N-pRb.

The pcDNA3 2HA N-pRb was transfected into HEK 293 cells, and nuclear extract harvested for use as a source of N-pRb for *in vitro* pull down assays (Figure 33d).

Figure 33

a)

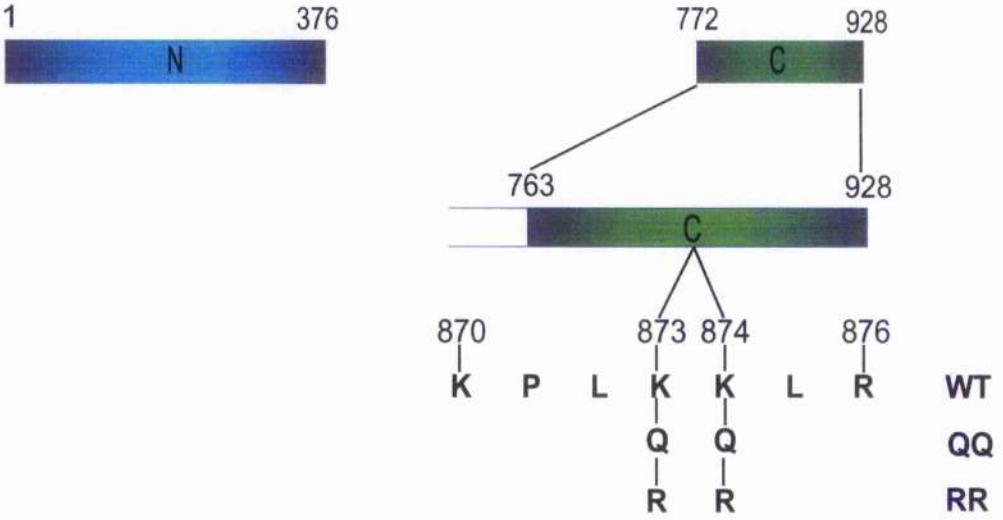

Figure 33

b)

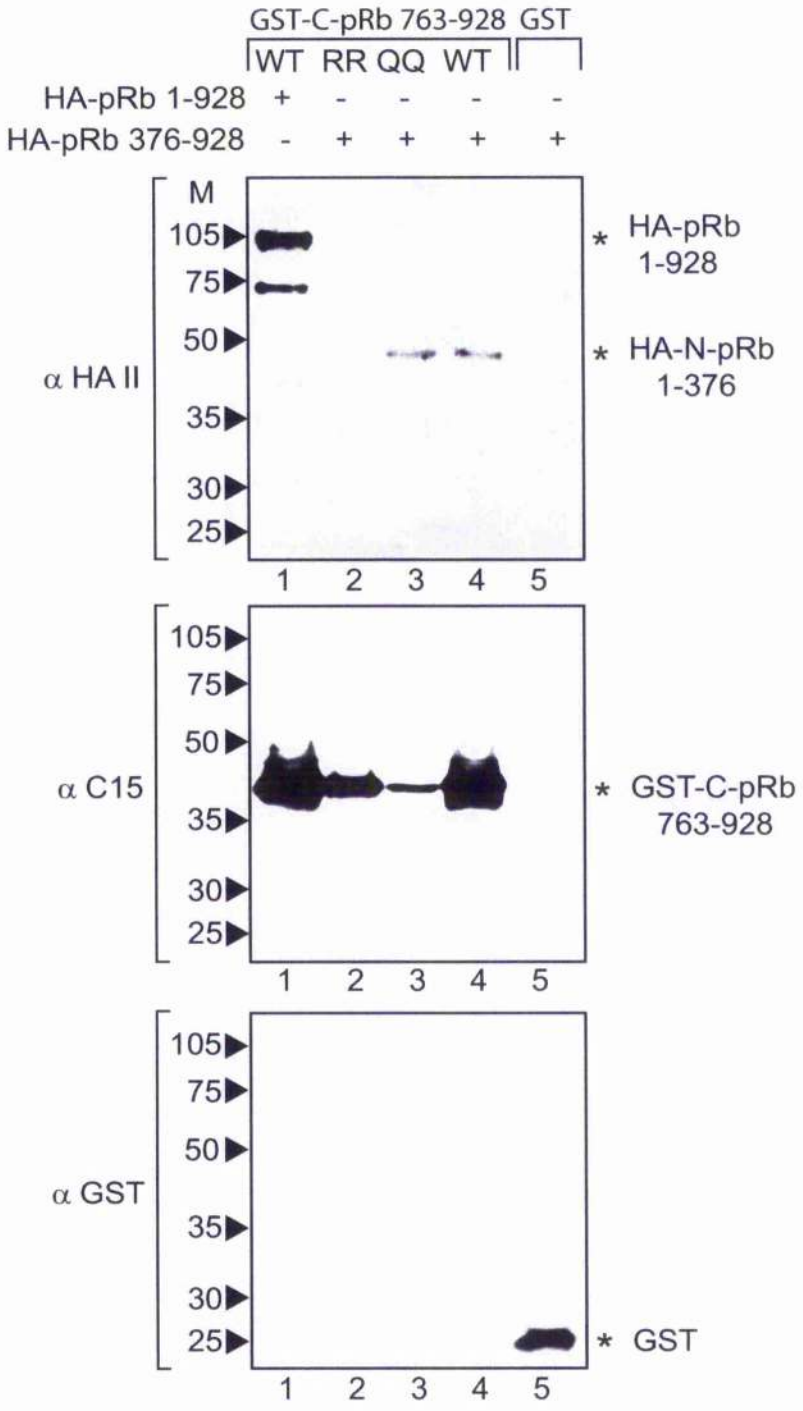

c)

	WT (FL)	RR	QQ	WT
GST-C-pRb levels	1	0.56	0.24	1
HA-N-pRb 1-376 levels	3.31	0	0.98	1
HA-N-pRb 1-376 adjusted for GST-C-pRb	3.31	0	4.08	1

Figure 33

d)

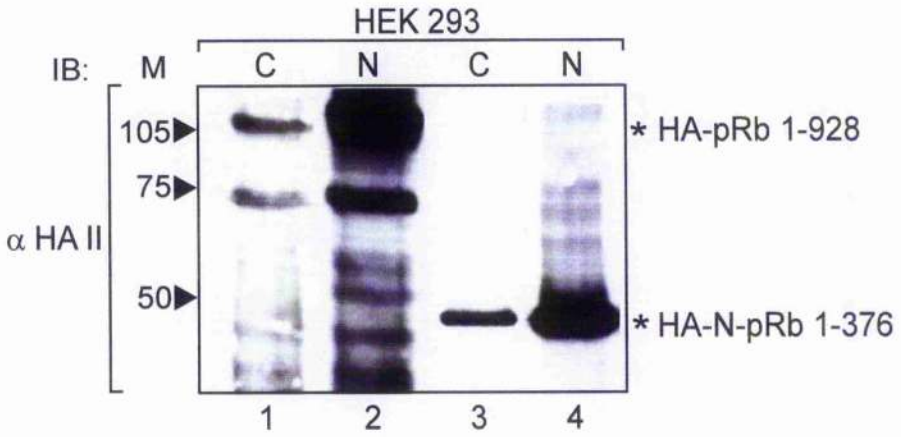

Figure 33: The N-terminal and C-terminal domains of pRb interact with each other *in vitro*

a) The diagram in part 'a' depicts the N-terminal domain and C-terminal domain constructs of pRb used in the pull down assays.

b) Part 'b' shows a GST *in vitro* pull down of wild-type HA-pRb and HA-N-pRb 1-376 (extracted from HEK 293 cells) by recombinant GST-C-pRb (763-928). Site directed mutagenesis was utilized to mutate GST-C-Rb residues 873/874 from K to R or Q (acetylation mimic). Anti-HA antibody was used to detect wild-type HA-pRb and HA-N-pRb 1-376. Levels of recombinant GST-C-pRb were assessed by immunoblotting using anti-C15 antibody that detects a peptide at the C-terminal domain of pRb.

c) Quantification of the protein levels in b). Protein levels are compared to GST-pRb 763-928 wt (Lane 4), which is given the nominal value of 1. The levels of both HA-N-pRb and GST-pRb mutant derivatives are shown. The levels of bound HA-N-pRb are adjusted to take into account the amount of mutant GST-pRb 763-928 wt, QQ or RR in the pull down.

d) HEK 293 cells were transfected with 2 μg of pSG5L-HA pRb 1-928 or 2 μg of pcDNA3-HA pRb 1-376. Nuclear and cytoplasmic extract (100 μg) was analysed by electrophoresis followed by immunoblotting using the anti-HA

antibody. Extract from lanes 2 and 4 were used as sources of HA-pRb 1-928 and HA-pRb 1-376 respectively in the GST *in vitro* pull down assay.

CHAPTER 4

DISCUSSION

GST-C-PRB 763-928 INTERACTS WITH E2F-1 *IN VITRO.*

The data presented here suggest that residues K873/874 maybe required for the C-terminal domain pRb/E2F-1 interaction. The K to Q substitution at K873/874 of the C-terminal domain in pRb appears to reduce the C-pRb/E2F-1 interaction *in vitro*. The concordant K to R substitution at the same residues appears to retain E2F-1 binding with almost equal level compared to the wild-type C-pRb. This result shows that acetylation of C-pRb at K873/874 reduces the affinity of C-pRb for E2F-1.

There are two main concerns in drawing conclusions from these experiments. The *in vitro* assays do not preclude that the microenvironment in cells may be different. The second concern surrounds the validity of using K to Q substitution to infer the effects of acetylation. However, the substitutions of K to Q or R were chosen on the basis of their similar physical properties (Figure 24 and 25) [247-249]. Other studies however have provided convincing results that K to Q substitution is a phenotypic mimic for acetylation [75, 177, 214]. In order to confirm my results, it would be necessary to develop a method for separating *in vitro* acetylated C-pRb from the non-acetylated form. A recent publication suggests a way that acetylated protein forms can be isolated from lysate with a purity of greater than 90 % [250]. Future work may use such techniques to obtain acetylated C-pRb for the *in vitro* binding assay studies.

There are a number of possibilities as to why the C-pRb QQ mutant does not interact with E2F-1. K873/874 of C-pRb does not form part of the consensus-binding site for interaction with E2F-1. The two regions that were observed to bind the marked box of

E2F-1 are residues 786-800 and residues 829-864 of pRb [98]. It is possible therefore that acetylation of K873/874 causes a conformational change in the C-terminal domain of pRb that affects one or both of the C-pRb binding regions, preventing them from interacting with the E2F-1 marked box region.

Mutation of K to Q changes the net charge of residues 873/874 from +1 to neutral, which mimics the change in charge resulting from K acetylation. K and R residues are both basic amino acids whereas Q residues are more electronegative (Figure 24a). The pRb 763-928 QQ and RR mutants were still able to bind Mdm2 protein. This result suggests that the K to Q/R mutation does not simply ablate the binding ability of the mutant proteins altogether, and also perhaps that another region of C-pRb is involved in binding Mdm2. Crystallographic studies could be utilised to compare the 'wild-type and QQ' C-pRb proteins. In summary, E2F-1 binds to the C-terminal domain of pRb 763-928, an interaction that is blocked by acetylation of pRb residues K873/874.

THE ACETYLATION OF PRB AT RESIDUES K873/874 REDUCES THE E2F-1 INTERACTION IN CELLS.

Mutating residues 873/874 to Q reduces the C-pRb/E2F-1 interaction

Using mammalian expression vectors encoding C-terminal domain pRb proteins (derived from GST C-pRb constructs used in Figure 26), it has been demonstrated that the C-Rb QQ mutant protein binds weakly to E2F-1 in HEK 293 cells. pRb phosphorylation is the only post-translational modification reported to control the pRb/E2F-1 interaction directly. Thus perhaps acetylating pRb in response to DNA damage releases the anti-apoptotic behaviour of pRb by interfering with its interaction with E2F-1. Acetylation of pRb at residues K873/874 is known to reduce pRb phosphorylation and facilitate cell cycle arrest [214].

HEK 293 cells are transformed with adenovirus, and express the E1A and E1B

oncoproteins [246], which are likely to interfere with the pRb small pocket/E2F-1 interaction. Therefore, the immunoprecipitations (in Figures 27 and 28) were likely to detect interactions between the C-terminal domain of pRb and the marked box region of E2F-1. Limited conclusions can be drawn from these data. Firstly endogenous E2F-1 contains the *trans*-activation domain, so pRb that is not in complex with E1A could potentially produce false positives *in vivo,* by binding to E2F-1 using the small pocket region (domains A and B). Secondly, the endogenous pRb present may interact with the C-pRb mutant proteins. Indeed, pRb is known to bind to itself via N-terminal domain/C-terminal domain interactions [135].

Further study in this area might utilise gel shift assays to compare complex formation of C-pRb wild-type/E2F-1/DP-1 with that of C-pRb QQ/E2F-1/DP-1. It might be expected that the C-pRb QQ mutant protein would cause less band shift complexes than the C-pRb wild-type protein, as the interaction between C-pRb QQ and E2F-1/DP-1 would be much weaker than that between wild-type C-pRb/E2F-1/DP-1.

The immunoprecipitation experiments in Figures 27 and 28 could be repeated using exogenously expressed E2F-1 (1-374)/DP-1 instead of relying on endogenous E2F-1/DP-1. This would prevent any HA-pRb pocket interactions with the *trans*-activation domain of endogenous E2F-1 because the two forms of E2F-1 would resolve differently on an SDS-PAGE gel.

Mutating residues K873/874 to Q also inhibits the FL-pRb/E2F-1 interaction

The immunoprecipitation of E2F-1 with FL-pRb was meant to confirm that pRb could bind E2F-1 using the small pocket interaction with the *trans*-activation domain of E2F-1. Therefore, the expected result was that the FL-pRb QQ mutant would bind E2F-1 as efficiently as FL-pRb wild-type derivative. It seems however that the FL-pRb QQ mutant binds E2F-1 less efficiently than the wild-type FL-pRb or FL-pRb RR mutants. This effect was mirrored in cells treated with etoposide.

There maybe several reasons for this. Firstly, the E1A concentration in HEK 293 cells could be significant enough to bind all exogenous FL pRb protein, thus preventing pRb small pocket interactions with E2F-1. Secondly, it is possible that mutating K residues 873/874 to Q might alter the localization of the FL-pRb QQ mutant protein but not alter the localization of the C-pRb QQ mutant protein. Thirdly, it might be that basic residues (like K or R) are necessary for successful interaction between the C-terminal domain of pRb and E2F-1 to occur. Perhaps neutralizing the charge on residues K873/874 by acetylation or Q substitution loosens the interaction between the C-terminal domain of pRb and E2F-1.

Localization of the pRb exogenous proteins

The C-terminal domain pRb mutant proteins all localized to the nucleus, even in cells treated with etoposide (Figure 29), as did the FL-pRb wild-type and RR mutant proteins. It is significant that the FL-pRb QQ protein localizes more to the cytoplasm than the nucleus. This result contradicts earlier data we published (Figure 4C [97]). However, subsequently we had cause to re-sequence this sample of FL-pRb QQ mutant construct, which was confirmed to be contaminated with FL-pRb wt DNA. The subcloning of the FL-pRb QQ mutant construct was repeated, and all subsequent immunostaining experiments in U2OS cells showed FL-pRb QQ mutant protein to localize more to the cytoplasm than the nucleus.

Using an anti-acetylated pRb antibody (SK37), we recently reported that DNA damage responsive acetylated pRb localizes to the nucleus (showing only limited cytoplasmic staining) [97]. This apparent contradiction between figure 1C of Markham *et al* 2006 [97] and Figures 30 and 31 of this thesis should be further investigated. Presently we have no definitive data indicating that treatment of U2OS cells with 10 μM etoposide induces acetylation of residues 873/874 simultaneously. In figure 1C of Markham *et al* 2006, U2OS cells were treated with 10 μM etoposide for 8 h. It is possible that longer

exposure to a greater concentration of etoposide might induce further acetylation, altering acetylated pRb subcellular localization to a mainly cytoplasmic distribution.

The Rb protein contains two regions that confer nuclear localization (the A/B pocket, and the C terminal domain). The A/B pocket when fused to the pECE-β-galactosidase construct (pECE-β-gal-Rb-A/B) confers nuclear/cytoplasmic localization upon the heterologous protein [251]. The C-terminal domain of pRb contains a bi-partite NLS that has been characterized as spanning residues 860-877 (Figure 8) [252]. It is likely that mutating the K residues at 873/874 is enough to ablate nuclear localization conferred by the bi-partite NLS. The K residues in the NLS are central to its function, and even mutating adjacent residues to a Q is enough to cause pRb to localize to both the cytoplasm and the nucleus [253]. The FL-pRb mutated at K873/874 to Q is nuclear/cytoplasmic, but the corresponding C-pRb QQ mutant is nuclear. It is possible that the N-terminal domain of pRb may interact with the C-terminal domain of pRb in context with the FL protein to influence its intra-cellular localization.

In summary, the C-pRb protein binds to E2F-1 in HEK 293 cells, an interaction that is blocked by mutating residues K873/874 to Q. This interaction is independent of endogenous pRb because HEK 293 cells express E1A that binds to the small pocket region of pRb and prevents its association with the *trans*-activation domain of E2F-1 [105, 246]. Exogenously expressed FL-HA-pRb also binds E2F-1, and its binding was blocked when residues K873/874 of pRb are mutated to Q. Although FL-pRb QQ mutant localizes mainly to the cytoplasm, this localization is unlikely to explain the loss of binding to E2F-1 as the truncated C-pRb QQ mutant localizes to the nucleus, but also exhibits low binding to E2F-1.

ACETYLATION AT RESIDUES K873/874 OF PRB INCREASES THE INTERACTION BETWEEN THE C- AND N-TERMINAL DOMAINS OF PRB.

The N-pRb binds to the C-pRb *in vitro*

The two-hybrid study by Sterner *et al* found that the N-terminal domain of pRb interacts with the C-terminal domain of pRb in yeast [100]. It has been confirmed using *in vitro* pull down assays that the HA-N-pRb (derived from HEK 293 nuclear extract) does indeed interact with the GST-C-pRb. *In vitro* pull down assays utilizing C33A cells (in which *Rb* is genetically inactivated) as the source of exogenous HA-N-pRb were unable to detect an interaction between HA-N-pRb and GST-C-pRb. Lysing C33A cells to separate nuclear and cytoplasmic fractions later confirmed that the exogenously expressed HA-N-pRb localized mostly to the cytoplasm, whereas in HEK 293 cells exogenously expressed HA-N-pRb localized mostly to the nucleus (Chapter 3, Figure 22).

One explanation is that HA-N-pRb interacts with endogenous nuclear wild-type pRb at the bridging region between the N-terminal domain and the A domain (residues 379-572), and that during the pull down, GST-C-pRb binds to the B domain (residues 646-772). In this hypothesis, the A/B pocket domain of pRb might act as a protein scaffold to facilitate a binding surface for the exogenous HA-N-pRb and GST-C-pRb to interact. This hypothesis is supported by the observation that HA-pRb FL binds much more efficiently to GST-C-pRb than the HA-N-pRb does (Figure 33b, Lane 1). The affinity that the HA-N-pRb and GST-C-pRb wild-type proteins have for each other is quite modest compared to the affinity that the HA-tagged exogenous proteins have for the regions of pRb that they neighbour. Testing this hypothesis might require crystallographic analysis to assess the binding affinities of pRb N-terminal and C-terminal domains for the A/B pocket.

The mutant derivative GST-C-pRb QQ showed enhanced *in vitro* binding to HA-N-pRb 1-376. In contrast, the GST-C-pRb RR mutant derivative showed greatly reduced *in*

vitro binding affinity to HA-N-pRb 1-376. This is a new observation. One interpretation is that the acetylation of residues K873/874 of GST-C-pRb promotes an increase in affinity between the N-terminal and C-terminal domains. However, it is also possible that the acetylation of residues K873/874 might cause a change in the conformation of the C-terminal domain of pRb, thereby causing it to bind against the face of the B domain of the pRb small pocket. Thus a flip in conformation might bring the N-terminal and C-terminal domains close enough together to interact. Again, crystallographic analysis would be very useful in determining the effect of acetylation on the binding properties of the C-terminal domain.

It has been shown that residues K873/874 are acetylated in response to etoposide treatment in a number of cell types [97]. Results presented here indicate that acetylation at residues K873/874 of the C-pRb increases its *in vitro* affinity for the N-pRb. The next step would be to test the binding affinity of N-pRb to C-pRb *in vivo*. It is possible that acetyl forms of N-pRb also induce a conformational change at the N-terminal domain end of pRb that promotes interaction between the C-terminal domain and the N-terminal domain. The next step would be to identify the acetylated K residues in the N-pRb by mass spectroscopy. N-pRb acetylation mutants could then be engineered (K to Q), and these mutants could be tested in binding assays and crystallographic analysis to assess the combined effect of acetylation of both the N-terminal and C-terminal domains on their binding to each other and to the A/B small pocket region.

In summary, the N-terminal domain of pRb binds to the C-terminal domain of pRb *in vitro*. The GST tagged C-pRb QQ mutant demonstrated 4-fold greater binding to the N-terminal domain of pRb comparative to C-pRb wild-type, indicating that acetylation of pRb at residues 873/874 might induce greater binding between the N-terminal and C-terminal domains of pRb.

CHAPTER 5

DISCUSSION

pRb is acetylated across multiple domains

There is now evidence that pRb is acetylated across four of its five domains (only the spacer has not been studied (aa 572-646)). *In vitro* data can be summarized as follows: The Retinoblastoma N-terminal (aa 1-376) and C-terminal (aa 763-928) domains are efficiently acetylated by Flag-p300 FL (Figure 35a). The A domain derivative of pRb (aa 379-572) does display acetylation *in vitro* by Flag-p300 FL, but it is barely detectable in gel based assays [214]. The B domain derivative of pRb (aa 646-792) does not show detectable *in vitro* acetylation (Figure 35-A) [214]. It is hypothesised that the A/B domains are more efficiently acetylated when they are interacting together [214]. A small polypeptide (aa 710 to 732) in the B domain (corresponding to exon 21) and which is conserved across species, can be acetylated at residue 713 [214].

Engineered GST-pRb derivatives spanning the C-terminal domain of pRb show that there are two regions of the C-terminal domain that are acetylated *in vitro* by Flag-p300 FL (residues 794-829 and residues 830-884) (Figure 35B(i)). However, mutating residues K873/874 to Q or R, completely ablates acetylation of GST-C-pRb 763-928, suggesting that acetylation of these residues is required for the acetylation of other residues in GST-pRb 794-829 [97, 214] (Figure 35B (ii)).

A study by Nguyen *et al* [53] showed that GST-pRb 379-928 wild-type is acetylated *in vitro* by Flag-P/CAF, but the pRb derivative mutated at residues K873/874 (GST-pRb 379-928 RR) is not acetylated by Flag-P/CAF. Further to this, Flag-p300 FL combined with Flag-P/CAF acetylates GST-pRb 379-928 wild-type more

Figure 34

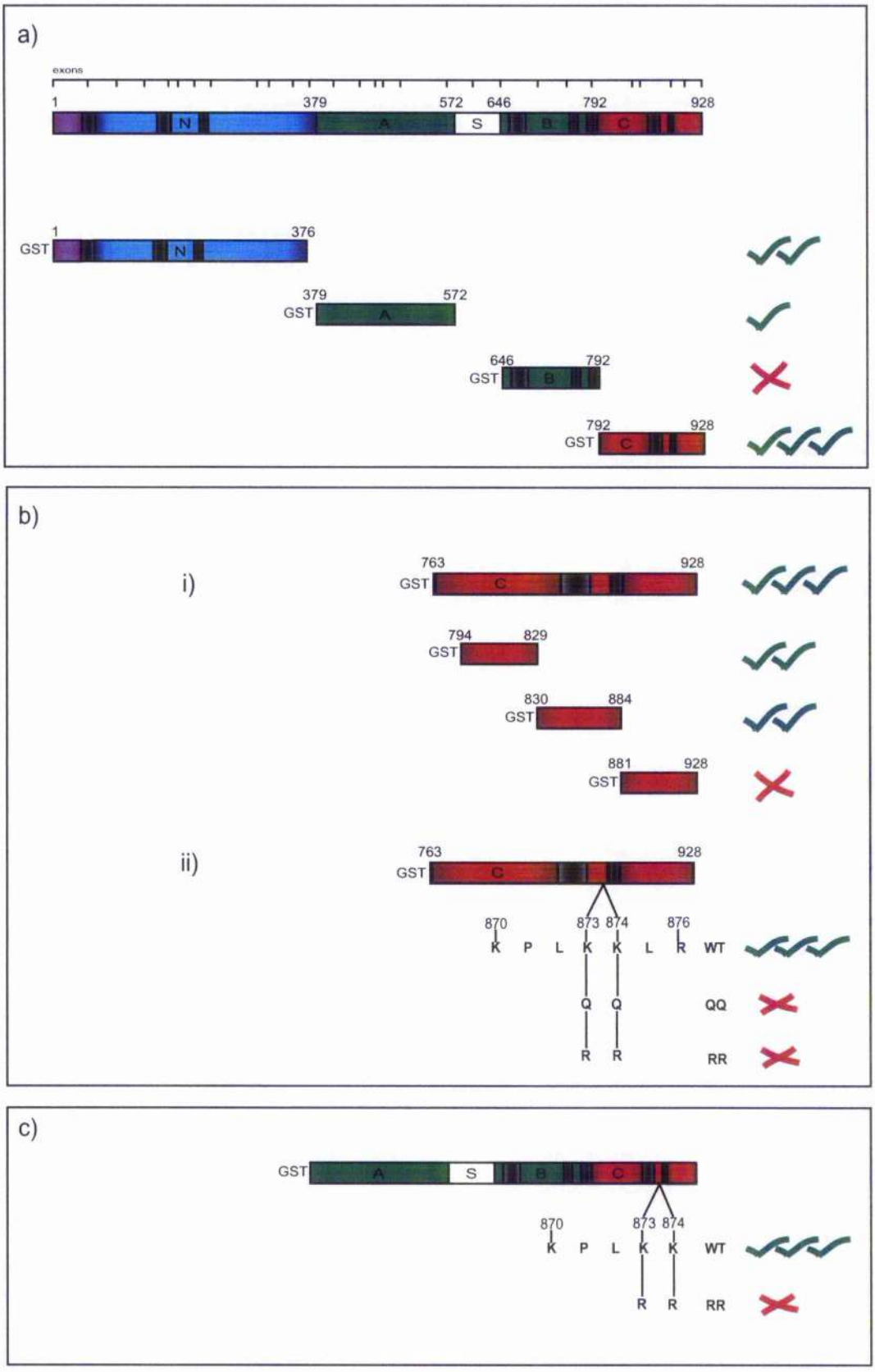

Adapted from [214] and Figure 14.

Chapter 5

Figure: 34 The *in vitro* acetylation of GST pRb derivatives

Both Flag-p300 FL and Flag-P/CAF acetylate the Rb protein in vitro.

a) Top shows a schematic representation of pRb 1-928. Below indicates which GST pRb domains are acetylated by Flag-p300. The derivatives are indicated by ticks or cross, indicating whether they are acetylated and their relative acetylation.

b) i) Shows GST pRb derivatives spanning the C-terminal domain of pRb (aa 763-928) that are acetylated by Flag-p300. Derivatives are indicated as acetylated or not as in a).

ii) Shows GST-pRb 763-928 wt, QQ and RR mutant derivatives (mutated at residues K873/874) that are acetylated by Flag-p300. Derivatives are indicated as acetylated or not as in a).

c) Shows GST pRb 379-928 wt, and RR mutant derivatives (mutated at residues 873/874) that are acetylated by Flag-P/CAF.

efficiently than either Flag-p300 FL or Flag-P/CAF could in isolation [53]. It is possible that p300 and P/CAF acetylate pRb more effectively in a complex. P/CAF is able to bind to pRb 379-928 [53], so perhaps P/CAF can recruit p300 to the pRb large pocket domain (residues 379-928).

Acetylation of a K residue alters its physical properties by neutralizing the positive charge of the K residue but maintaining its polar and steric properties (Chapter 4, Figure 24 and 25). The B domain of pRb is not highly acetylated [214]. This may be because six basic K residues in the B domain (K713, K720, K722, K729, K740 and K765) are required to hydrogen bond with acidic residues in the LXCXE peptide [41], an interaction that allows the LXCXE motif containing proteins to bind the pRb small pocket. It is interesting that Flag-p300 FL can acetylate residues in the N-terminal domain of pRb (Figure 36a and 36b) and residues across the pRb large pocket [214], but P/CAF is only able to acetylate residues K873/874 [53].

There are thirty-one K residues across the N-terminal domain of pRb (twenty three in the N sub-domain, and 8 in the R sub-domain) (Figure 36, parts a) and b)). Residue 136 is the only point mutation observed from the thirty one K residues in the N-terminal domain in a patient suffering from unilateral retinoblastoma (Figure 36a and 36c) [254]. The only other significant mutations affecting the N-terminal domain are discrete internal mutations resulting in the deletion of exons 4 and 8. Potential acetylation sites in these regions are highlighted (Figure 36d) [145]. Exons 4 and 8 encode protein sequence that is highly conserved among vertebrate species (bird, human, rodent, fish and amphibian) [111]. Also exon 8 contains S and T residues (position S250 and T252) that are phosphorylated by Cdks [146]. It may be therefore that acetylation of the N-terminal domain will affect its phosphorylation in a similar way to which acetylation at residues K873/874 reduce cyclin E/Cdk2 dependent phosphorylation, thus promoting cell cycle arrest [214].

Figure 35

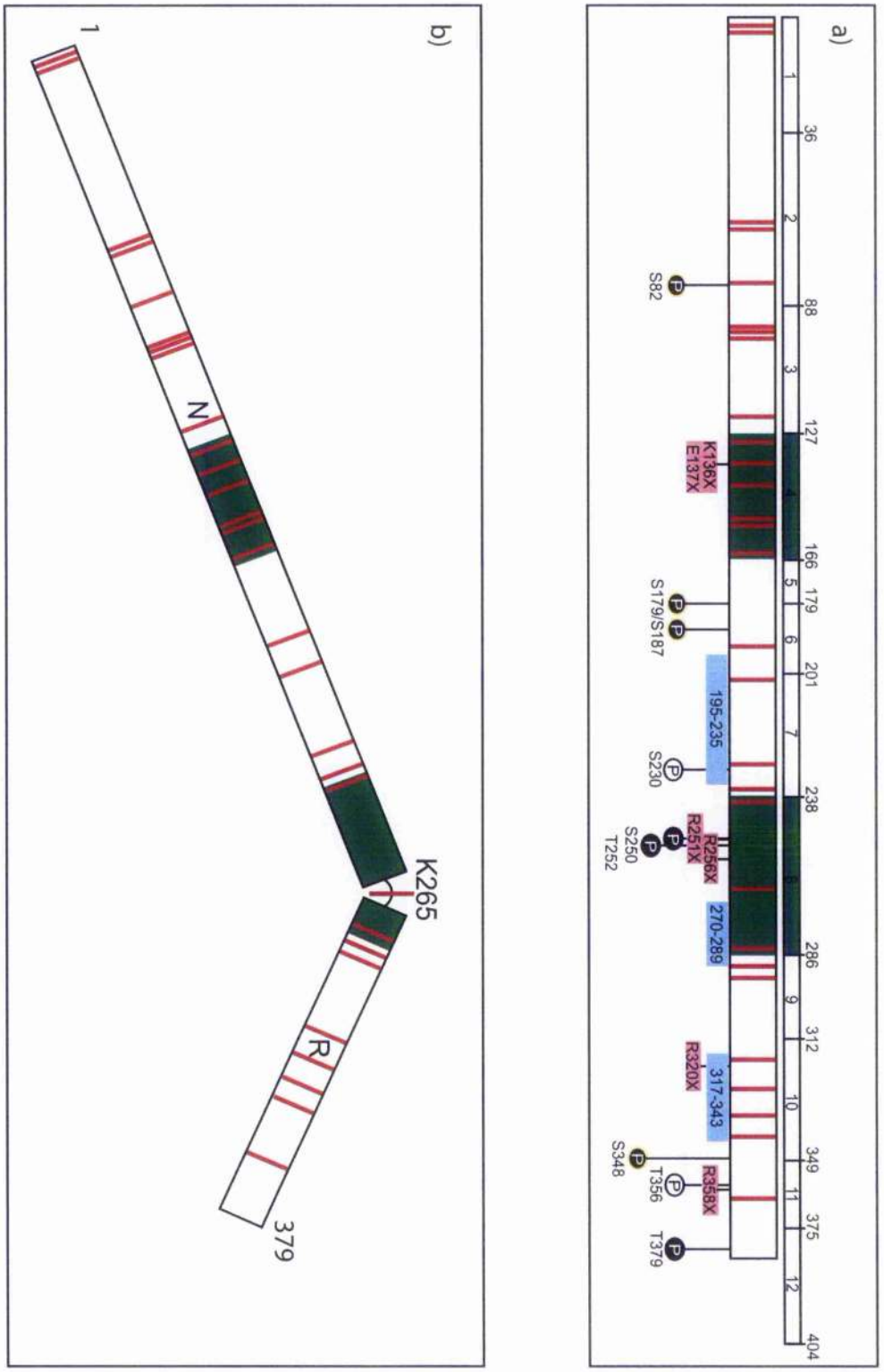

Adapted from [104], [111], [145], and http://rb1-lsdb.d-lohmann.de

Figure 35

c)

MPP KTPRK TA ATAAAAAAEPPAPPPPPPEEDPEQDSGPEDLPLVRLEF EETEEPDFTALCQ KLKIP DHVRERAWLTWE KVS SVDGVLGGYIQ KKKEL WGICIFIAAVDLDEMSFTFTELQ KNI EISVH KFF NLL KEI DTST KVD N AMSRLL KKYD VLFALFS KLE RTCELIYLTQPSSSISTEINSALVL KVS WI TFLLA KGE VLQMEDDLVISFQLMLCVLDYFI KLS PPMLL KEPYK TAVI PINGSPRTPRRGQNRSARIA KQL ENDTRIIEVLC KEH ECNIDEV KNV YF KNF IPFMNSLGLVTSNGLPEVENLS KRY EEIYL KNK DLDARLFLDHD KTL QTDSIDSFETQRTPR KSN LDEEVNVIPPHTPVR

d)

a) Exon 4

aa 126-ISVH KFF NLL KEI DTST KVD N
AMSRLL KKYD VLFALFS KLER-aa 166

b) Exon 8

aa 236-KEPYK TAVIPINGSPRTPRRGQN
RSARIA KQL ENDTRIIEVLC KEH ECNIDE- aa 287

e)

Protein	aa	Consensus Sequence	aa
Cdc25A	116	PA**L**K**R**SH**S**DSLDHD	129
Cdc25C	209	SG**L**Y**R**SP**S**MPENLN	222
E2F1	357	PL**L**S**R**MG**S**LRAPVD	371
BRCA1	981	PP**L**F**P**IK**S**FVKTKC	994
p53	13	PL**S**Q**E**TF**S**DLWKLL	26
C-Rb	804	IY**I**S**P**LK**S**PYKISE	817
C-Rb	888	SK**H**L**P**GE**S**KFQQKL	901
C-Rb	899	QK**L**A**E**MT**S**TRTRMQ	912
N-Rb	75	WL**T**W**E**KV**S**SVDGVL	88
N-Rb	172	IY**L**T**Q**PS**S**SISTEI	185
N-Rb	180	SI**S**T**E**IN**S**ALVLKV	193
N-Rb	340	DK**T**L**Q**TD**S**IDSFET	353

Figure 35: The N-terminal domain of pRb

a) Schematic of the N-terminal domain of pRb (residues 1-379). Directly above the schematic, mapped are regions encoded by each exon. Exons 4 (residues 127-166) and exon 8 (238-286) are shaded in green because they have been found deleted in some human cancers. The vertical lines in red represent the position of lysine residues across the N-terminal domain. Below the schematic, the three regions of the N-terminal domain that are highly conserved across species (residues 195-235, 270-289, and 317-343) are highlighted in blue. N-terminal domain point mutations found in human tumours are shown shaded in red. The locations of known Cdk phosphorylation sites are shown as black circles labelled P, and the location of possible Cdk sites are shown as white circles labelled P. The locations of possible Chk2 phosphorylation sites are depicted as black and yellow circles labelled P.

b) The N-terminal domain of pRb consists of two protease/caspase resistant sub-domains labelled N (1-263 approximately 30KDa) and R (263-379 approximately 10KDa). Secondary structural analysis predicts that the two domains are globular and connected by a hinge region.

c) There are thirty one potentially acetylated K residues in pRb 1-378. The potential acetylation sites in the N-terminal domain pRb protein sequence are highlighted in red. The K residue highlighted in green at aa position 136 is the

only known point mutation that has been observed from a patient with unilateral retinoblastoma (K to X).

d) Discrete N-terminal domain internal mutations that are naturally occurring mutant alleles in human tumours were assessed for their proximity to potential acetylation sites (shown in red).

e) The Chk2 consensus phosphorylation sites in various transcription factors (from Cdc25A to p53). The C-pRb and N-pRb are predicted sites of Chk2 phosphorylation.

Treating cells with etoposide induces the acetylation of both K 873/874 and the N-terminal domain of pRb

The N-terminal domain of pRb was acetylated in HEK 293 cells, and treating cells with etoposide induced greater levels of acetylation. A similar result is observed when comparing N-terminal domain acetylation with damage-inducible acetylation of residues K873/874 of pRb. Etoposide-inducible acetylation is so far detectable in six cell types (HEK 293, NIH 3T3, WI38, HCT15, AT fibroblasts, and F9 cells) [97]. Levels of pRb acetylation at residues K873/874 are increased upon treating WI38 cells and HEK 293 cells with TSA. Etoposide is known to activate the ATM damage response pathway [255], but curiously preliminary data suggest that ATM is not a requirement for damage-inducible pRb acetylation because it is detectable in AT cells (Darran O'Connor, personal communication).

Chan *et al* 2001 [214] studied the regulation of pRb acetylation during cell cycle progression. Immunoprecipitated endogenous pRb was immunoblotted with anti-acetylated K antisera. In T98G cells, which express wild-type pRb, cell cycle progression was monitored after serum-stimulating starved cells. Under these conditions, cells entered S-phase at 16–20 h when assayed by flow cytometry, suggesting that acetylated pRb accumulated at the G1/S phase transition.

Increased G1 arrest is observed in SAOS2 cells by exogenously expressing pRb 379-928 QQ mutant derivative, thereby mimicking the acetylation of pRb [214]. This observed increase in G1 arrest might result from the affect of acetylation at residues K873/874 on Cyclin A/E docking [256]. Cell cycle progression proceeds up until cyclin D/Cdk 4/6 phosphorylation of pRb. Acetylation at K residues 873/874 prevents Cyclin A/E from docking to the C-terminal domain of pRb [214], thereby preventing cells from entering the S-phase [256]. Cell cycle arrest also occurs prior to cells undergoing differentiation [53], entering senescence [257] or prior to apoptosis (reviewed by [245].

p300 and P/CAF may form a HAT complex to facilitate pRb acetylation

Acetylation of pRb at residues K873/874 is inducible in U937 cells under conditions of serum starvation [214]. This suggested that acetylation of pRb might be involved in regulating differentiation. A study by Nguyen *et al* 2004 [53] provided evidence that pRb undergoes acetylation upon cellular differentiation, including skeletal myogenesis. In addition to p300, P/CAF can mediate pRb acetylation as pRb interacts directly with the acetyl-transferase domain of P/CAF *in vitro* and can associate with P/CAF in differentiated cells. Significantly, by using a C-terminal domain acetylation-impaired mutant of pRb, they revealed that acetylation does not affect pRb-dependent growth arrest or the repression of E2F transcriptional activity. Instead, acetylation is required for pRb-mediated terminal cell cycle exit and the induction of late myogenic gene expression. It would be interesting to determine whether the N-terminal domain of pRb is required for pRb-mediated differentiation, and assess whether the N-terminal domain undergoes acetylation during differentiation.

E2F-1 *trans*-activates apoptotic genes, and genes required for G1/S-phase through two separate domains

The Rb protein plays an essential role in cell survival by regulating the activity of multiple apoptotic mediators (reviewed by [245]). pRb inhibits apoptosis by binding to the E2F-1 transcription factor, thereby preventing *trans*-activation of apoptotic genes by E2F-1 [240]. It was first proposed by Hsieh *et al* [240] that pRb may inhibit E2F-1 induced apoptosis by mechanisms other than steric suppression of the E2F-1 *trans*-activation domain (E2F-1 374-437). Over-expression of E2F-1 (in which the *trans*-activation domain has been deleted) can still induce E2F-1 dependent apoptosis [96, 240]. E2F-1 (132) is a point deletion mutant, defective for DNA binding. In reporter assays, this mutant failed to activate transcription and also failed to induce E2F-1-dependent apoptosis in SAOS2 cells

[240].

A significant increase in DNA-binding activity can be achieved when an E2F family member heterodimerizes with a DP family member. An increase in the DNA binding capacity of E2F-1 is accompanied by a dramatic increase in apoptosis (in cells over-expressing E2F-1/DP-1 or a cyclin A-binding-defective mutant of E2F-1 (E2FΔ24)) [258-260]. This stimulation of DNA-binding activity is reflected in the increase in E2F-dependent transcription when E2F-1 is co-transfected with DP-1 [261, 262]. Those particular studies were carried out around the same time as the discovery that E2F-1 over-expression induces apoptosis independently and concurrently with p53-dependent apoptosis [241-243].

pRb has two binding domains for E2F-1

Dick *et al* [96] created a mutant Rb (RbΔE2F-G) that had lost pocket/E2F binding but retained binding to viral oncoproteins such as E1A or HPV E7. Using RbΔE2F-G, they discovered that pRb contained two E2F-1 binding domains. Using binding assays they isolated a new E2F-1 binding domain to the C-terminal domain of pRb. Using gel shift assays, they showed that RbΔE2F-G caused a shift in E2F-1/DP-1 complex. In contrast to wild-type pRb, RbΔE2F-G failed to cause a shift in the E2F-4/DP-1 complex. What is of greater interest was their finding that increasing concentrations of RbΔE2F-G reduced the binding affinity of E2F-1/DP-1 for the DNA probe (where as the wild-type protein did not). This led to the suggestion that pRb (through its C-terminal domain) might inhibit E2F-1 *trans*-activation at pro-apoptotic promoters [96].

The interaction between RbΔE2F-G and E2F-1 may prevent E2F-1/DP-1 from binding DNA. This affect is *trans*-activation domain independent, and may explain why E2F-1 1-374 still causes E2F-1-dependent apoptosis, despite lacking a *trans*-activation domain. Thus, there are two E2F-1 binding domains (the A/B small pocket, and the C-terminal domain) interacting with two different regions of E2F-1 (the *trans*-activation

domain and the marked box domain (MB)). Does pRb inhibit promoters at S-phase genes and simultaneously allow E2F-1 to *trans*-activate apoptotic promoters? What are the upstream signals that determine whether pRb inhibits E2F-1 apoptosis or releases inhibition?

The previous model suggested that pRb interacted with the *trans*-activation domain of E2F-1 and prevented any of the transcription machinery from accessing E2F-1, thereby preventing expression. Repression was released through sequential phosphorylation of the C-terminal domain by cyclin D/Cdk 4/6 which facilitated phosphorylation of the B domain by cyclin (E/A)/Cdk2. This model seemed reasonable until the unexpected finding that the C-terminal domain of pRb (residues 792-928) can interact with the marked box region (MB) of E2F-1 [96].

Recent structural studies have shed light on how the two E2F-1 binding domains in pRb cooperate to repress E2F-1 *trans*-activation, and why this repression is lifted by phosphorylation of the C-terminal domain of pRb. It was discovered that the C-pRb/E2F-1 interaction was dependent on E2F-1 heterodimerizing with its DP-1 partner [96, 98]. There are two segments of C-pRb involved in the interaction with E2F-1 MB domain. The C-pRb ^{core} domain (residues 829-864) contributes the majority of the binding energy, binding to E2F-1 with a Kd of 5 μM. The C-pRb ^{nterm} domain (residues 786-800) also interacts with E2F-1 MB segment, increasing the affinity of C-pRb for E2F-1 MB by 36 fold (corresponding to a Kd of 110 nM).

This led to a revised model. In its active state, pRb binds E2F-1 MB using both C-pRb^{core} and C-pRb^{nterm} domains, and also pRb binds E2F-1 *trans*-activation domain via the small pocket. Cyclin D/Cdk4/6 first phosphorylates S788 and S795 of the C-pRb^{nterm} domain. This ablates the binding between C-pRb^{nterm} domain and E2F-1 MB domain. Further phosphorylation by cyclin D/Cdk4/6 allows access of cyclin E/A/Cdk2 to its docking site on C-pRb, and further phosphorylation of T821 and T826 by cyclin E/A/Cdk2 allows the release of E2F-1 [98]. Etoposide induced DNA damage responsive acetylation

of residues 873/874 will prevent cyclin E/A docking to the C-pRb^{core}, and thus arrest cells in G1/S phase.

Assuming no DNA damage, cyclin E/Cdk2 phosphorylates E2F-1, which stimulates transcription of cyclin E. This positive feedback loop sends the cell into S-phase [191]. This model is not the whole story as there are many more phosphorylation events during G1/S phase and S-phase. There are a total of sixteen Cdk phosphorylation sites across pRb that are phosphorylated during G1/S phase transition and S-phase (Chapter 1, Figure 8) (reviewed by [104]).

The effect of damage responsive acetylation on pRb, E2F-1 and p53

It is clear that acetylation at residues K873/874 of pRb can do more than just induce cell cycle arrest. Excitingly, the C-pRb 763-928 QQ mutant showed much reduced binding to E2F-1 both *in vitro* and *in vivo*. In contrast the C-pRb QQ mutant could still bind Mdm2, consistent with earlier reports suggesting that acetylation at K873/874 increased its affinity for Mdm2 [214]. Further to this, FL-pRb QQ mutant derivatives failed to efficiently bind E2F-1 in HEK 293 cells. Due to being transformed with adenovirus, HEK 293 cells over-express E1A. The reason for using HEK 293 cells was to allow a situation in which exogenous FL-pRb did not bind the *trans*-activation domain of E2F-1 efficiently. Thus any remaining binding would be attributable to the C-terminal domain of pRb and its interaction with E2F-1 MB. FL-pRb wild-type and FL-pRb RR mutant derivatives both bound E2F-1, but the FL-pRb QQ mutant did not. Therefore, it is suggested that damage-responsive acetylation at residues K873/874 of pRb prevents its association with the MB of E2F-1, thereby allowing *trans*-activation at apoptotic promoters.

It is likely that most of the pRb in the cell is not acetylated in response to DNA damage. Using an antibody specific for acetyl-K at residues 873/874, acetylated pRb *trans*locates from a diffuse nuclear staining (seen in un-treated cells) to punctate nuclear

speckles (in etoposide treated cells) [97]. However, staining with an endogenous pRb antibody showed no obvious difference in pRb intra-cellular location (Chapter 4, Figure 32). Indeed other reports confirm that pan-pRb antibodies do not detect *trans*location of pRb resulting from post-translational modification, and that specific antibodies are required (designed against specific modifications) in order to track changes in nuclear location [106, 107]. In a similar manner, not all E2F-1 is phosphorylated in response to etoposide induced DNA damage. Using a phospho-specific antibody against phospho-S364, a change in the intra-cellular location of Chk2 phosphorylated E2F-1 was observed [229]. E2F-1 phosphorylated by Chk2 *trans*locates from a diffuse nuclear staining (seen in un-treated cells) to punctate nuclear speckles (in etoposide treated cells), in a similar fashion to acetylated pRb staining in U2OS cells.

Presently, two other reports have described the DNA damage induced acetylation of the cell cycle transcription factors E2F-1 and p53 [75, 228]. These studies both report that treating cells with doxorubicin (for E2F-1) and IR (for p53) results in the induction of acetylation. Studies on E2F-1 demonstrate that residues 117, 121, and 125 are acetylated *in vivo* in response to doxorubicin treatment. This induction of acetylation occurs between 8 and 16h post treatment (induction of pRb acetylation by etoposide occurs between 4 and 24h post treatment [97]. TUNEL assays show that K to Q triple mutant derivatives of E2F-1 (at residues 117, 121, and 125) cause an increase in apoptosis in un-treated cells to a similar degree that E2F-1 wild-type causes when cells are treated with doxorubicin. E2F-1 is stabilized by DNA damage induced Chk2 phosphorylation of S364 [229] in parallel with DNA damage induced acetylation (at residues 117, 121, and 125).

A similar study on DNA damage inducible Chk1/2 phosphorylation of p53 more closely studied the link between Chk phosphorylation and DNA damage inducible acetylation [228]. p53 is phosphorylated by Chk1 and Chk2 S/T protein kinases at its N-terminal and C-terminal domains. Most of the Chk phosphorylation sites characterized so far map to the N-terminal domain of p53 and are thought to contribute to the DNA damage

induced stabilization of p53. This recent study characterized six Chk1/Chk2 sites in the C-terminal domain of p53. Chk-mediated phosphorylation of three sites (S366, S378, and T387) is induced by double-stranded breaks in DNA. Chk1 specifically phosphorylates T387, whilst Chk2 phosphorylates S366. Chk1 and Chk2 both phosphorylate S378.

Importantly, Chk1 and Chk2 have roles in regulating p53 acetylation. Using siRNA to knockdown Chk1/2, it is observed that levels of C-terminal p53 phosphorylation and acetylation of K382 is reduced [228]. This leads to a reduced activation of the *p21* and *Bax* genes in response to DNA damage. Reduced Chk kinase levels resulted in a reduction of DNA damage responsive p53 acetylation, and a corresponding drop in apoptosis was observed. Acetylation of p53 augments its affinity for DNA, thereby stimulating the *trans*-activation of p53 target genes [206, 263].

This study progressed further to characterize the affects of DNA damage induced Chk1/2 phosphorylation on p53. S/T to D mutants were engineered to mimic phosphorylation of S366 and T387. These mutants interact more efficiently with p300, and showed higher levels of K373 and K382 acetylation *in vivo*. The p53 S366D and T387D mutant derivatives bound more strongly to the p21 promoter and AIP1 promoters in ChIP assays. Phoshorylation by Chk1/Chk2 of S366 and T387 facilitates an increase in K373 and K382 acetylation and a corresponding increase in binding to p21 and AIP1 promoters, thus facilitating apoptosis [228].

The ATM/Chk2 pathway may activate DNA damage responsive acetylation of pRb

In response to DNA damage, E2F-1 and p53 are phosphorylated by Chk2, thereby leading to increases in their levels of acetylation.

Perhaps DNA damage inducible acetylation of pRb (at residues K873/874) is also controlled by Chk2 phophorylation. In this regard, preliminary results are encouraging. Recent work in our group has shown that the C-terminal domain of pRb is phosphorylated by Chk2 kinase *in vitro*. Further to this, expressing a Chk2 dominant negative construct in NIH3T3 cells ablates etoposide-induced acetylation (personal communication, Judith Soloway). There are several Chk2 consensus phosphorylation sites in the C-terminal of pRb (Figure 36e). The S residues are fairly near to residues K873/874 and may serve to directly recruit p300/P/CAF complex to pRb/E2F-1.

In HEK 293 cells, the N-terminal domain of pRb is also acetylated in response to DNA damage (Chapter 3, Figure 20). Close inspection of the N-terminal domain pRb protein sequence revealed the presence of four potential Chk2 consensus phosphorylation sites (Figure 36e). There are 6 potential acetylation sites neighbouring theses Chk2 consensus phosphorylation sites (Figure 36a), three of which are encoded for by exon 4 (KVD, KKYD and KLER), and one by exon 8 (KEPYK) (Figure 36d). Exon 4 and exon 8 of pRb have been found deleted in tumour-derived samples and both regions are highly conserved across species [111].

The reports on E2F-1 and p53 damage responsive acetylation suggest that it is Chk2 phosphorylation that causes a change in intra-cellular location of pRb/E2F in response to DNA damage. Both acetylated pRb and Chk2 phosphorylated E2F-1 are shown to translocate to distinct nuclear speckles [74, 97]. If Chk2 phosphorylation is confirmed as the upstream activator of pRb acetylation, it could be that pRb translocates to these nuclear speckles during damage in response to its phosphorylation by Chk2. Perhaps Chk phosphorylation may trigger E2F-1 and pRb to translocate during DNA damage. Also,

they may translocate whilst still in complex.

E2F-1 is primarily stabilized by ATM kinase. In response to DNA damage, activated ATM phosphorylates E2F-1 at S31 [73]. Degradation of E2F-1 was shown to be dependent on S31 binding to SCF/p45^{skp2} thereby mediating E2F-1 proteosomal degradation [264]. Upon ATM dependent E2F-1 stabilization, E2F-1 and E2F-2 can further activate ATM. Over-expressing E2F-1 and E2F-2 induce the phosphorylation of ATM [265]. Thus ATM activity is induced by E2F stabilization and can phosphorylate more Chk2 kinase.

Further to this, E2F-1 up regulates Chk2 kinase independently of ATM. In this way, a continued DNA damage response might cause a gradual increase in nuclear levels of E2F-1. This would lead to greater up-regulation of Chk2 increased ATM kinase activity [265]. This led to the hypothesis that at basal levels of E2F-1, its activity is blocked by pRb and is thus inactive, but upon mitogenic stimulation, E2F-1 induces G1/S phase transition. When E2F-1 levels are stabilized in response to DNA damage by ATM and Chk2, E2F-1 levels exceeded a threshold beyond which leads to E2F-1 dependent apoptosis [56].

Nuclear translocation of pRb/E2F-1 through Chk2 phosphorylation

It seems logical that phosphorylation by ATM and Chk2 might stabilize E2F-1 gradually, and that when the pRb/E2F-1 complex is sufficiently phosphorylated by Chk2, *trans*location to damage responsive promoters might occur. Once localized to apoptotic promoters, p300-P/CAF might be recruited to phospho-E2F-1/pRb and histone H4, resulting in their acetylation. Acetylation of the C-pRb then blocks C-pRb/E2F interaction, allowing the MB domain of E2F-1 to positively influence transcription. In the case of pRb there is good reason to suggest that Chk2 phophorylation might be involved in nuclear *trans*location. During the G1/S phase transition, sequential phosphorylation of C-pRb by cyclin D/Cdk4/6 and cyclin E/A/Cdk2 dissociates pRb from E2F-1. Chk2 phosphorylation

of pRb/E2F-1 complex may facilitate the nuclear *trans*location of the whole complex, rather than just pRb.

pRb contains two NLS, in the 'A/B pocket' and the 'C-terminal domain bi-partite NLS' (Chapter 1, Figure 8). The C-terminal domain of pRb contains the bi-partite NLS which spans residues 869-877 [252]. It is possible that Chk2 phosphorylation of the C-terminal domain (residues S895 and S906) might impact on the pRbC-terminal domain NLS. The K residues at 873/874 form a vital part of the bi-partite NLS (indeed it is bi-partite because it has two basic K patches that are required for its function) [253]. It was shown that mutating residues K873/874 of FL-pRb to Q caused widespread nuclear/cytoplasmic staining among populations of cells (Chapter 4 Figure 30 and 31). Mutating the C-pRb residues K873/874 to Q had no effect on the nuclear localization regardless of whether cells were treated with etoposide or not (Chapter 4 Figure 29A and 29B). The FL-pRb-QQ mutant protein may leave the nucleus due to a lack of Chk2 phosphorylation. However, no translocation event was observed with HA-C-pRb QQ mutant indicating that the influence of the A/B domain and the N-terminal domain of pRb can impact upon the intra-cellular localization of pRb.

This localization change of pRb/E2F in response to DNA damage might occur through a change in affinity of pRb for Lamins A/C and Lap2α. Both these proteins bind pRb and are components of nuclear intermediate filament complexes [266]. Lamin A/C might play a role in mediating the formation of the pRb foci because pRb is dispersed throughout the nucleus and fails to associate with E2F foci in their absence [267]. Recent studies find that nuclear anchorage of pRb also requires LAP2α [268].

Lamin A/C and LAP2α tether hypophosphorylated pRb to the nucleus. During S phase, pRb distributes to hundreds of small foci throughout the nucleus, which indicates that progressive phosphorylation of pRb results in dissociation from these matrix-associated sites of function. In response to intra-S phase DNA damage and activation of protein phosphatase 2A, hypophosphorylated pRb resumes a focal staining pattern that is

reminiscent of perinucleolar foci, and inhibits origins of DNA replication and prevents endoreduplication [269].

Maybe during DNA damage, a proportion of pRb is required to inhibit E2F-1 at S-phase promoters and promoters of genes involved in endoreduplication. If DNA damaging signals persist, cells would perhaps require activating E2F-1-dependent and p53-dependent apoptosis. How might pRb remain bound to S-phase promoters whilst at the same time be released from apoptotic promoters? Specific signals might be sent to pRb at damage responsive promoters that cause the release of pRb and the *trans*-activation of apoptotic genes, or alternatively signals might be sent to pRb causing it to re-localize to damage responsive promoters to displace repressive p107/E2F-4 complexes with activating pRb/E2F-1 complexes.

Activating pRb/E2F-1 complexes swap places with repressing p107/E2F-4 complexes at apoptotic promoters in response to DNA damage

Earlier, a study by Pediconi was cited concerning E2F-1 acetylation being linked to increased apoptosis [75]. As part of this study, ChIP assays were utilized to assess E2F/pocket protein complex promoter occupancy in un-treated and doxorubicin treated cells. This study indicates that under normal cell culture conditions, p107/E2F-4 complexes occupy and repress *p73*, whereas pRb/E2F-1 complexes occupy *TK* and *DHFR* promoters. Under doxorubicin treatment, the pRb/E2F-1 complex and the p107/E2F-4 complex swap promoters leading to acetylation of H4 at *p73* promoter and deacetylation of H4 at *TK* and *DHFR* promoters [75]. What this study doesn't address is how pRb/E2F complexes are able to translocate from one area of the nucleus to another. If Chk2 phosphorylation of pRb alters binding to Lamins or LAP2α, what proteins might chaperone pRb/E2F-1 complex to apoptotic promoters?

It is interesting that the N-terminal domain of pRb binds more efficiently to the GST-C-pRb QQ mutant derivative in GST pulldown assays. Perhaps DNA damage

responsive acetylation of pRb might induce conformational change in pRb tertiary structure, resulting in binding between the N-terminal and C-terminal domains. For instance, in response to DNA damage induced acetylation (maybe at apoptotic promoters), the N-terminal domain of pRb might bind to the C-terminal domain of pRb resulting in the loss of E2F-1 binding. The N-terminal domain is the largest domain in pRb, and it might be involved in determining what proteins can bind the C-terminal domain during DNA damage. The N-terminal domain of pRb might influence post-translational modification (for instance phosphorylation and de-phosphorylation), stability, and steady-state levels, as well as other auto-regulatory mechanisms of the pRb protein [140].

A model for how ATM/Chk2 pathway activates E2F-1-dependent apoptosis and p53-dependent apoptosis in response to DNA damage

Recent studies combined with work presented here on pRb acetylation have helped form a model of how ATM/Chk2 pathways facilitate E2F-1 and p53-dependent apoptosis. Routine cell cycle progression is shown (Figure 37). In response to mitogenic signalling, cyclin D/Cdk4/6 phosphorylates RbC^{nterm}, causing it to dissociate from E2F-1/DP-1. Subsequent phosphorylation of the pRb B domain by cyclin E/Cdk2 leads to the release of E2F-1, and promotes the *trans*-activation of E2F target genes [98].

Figure 36

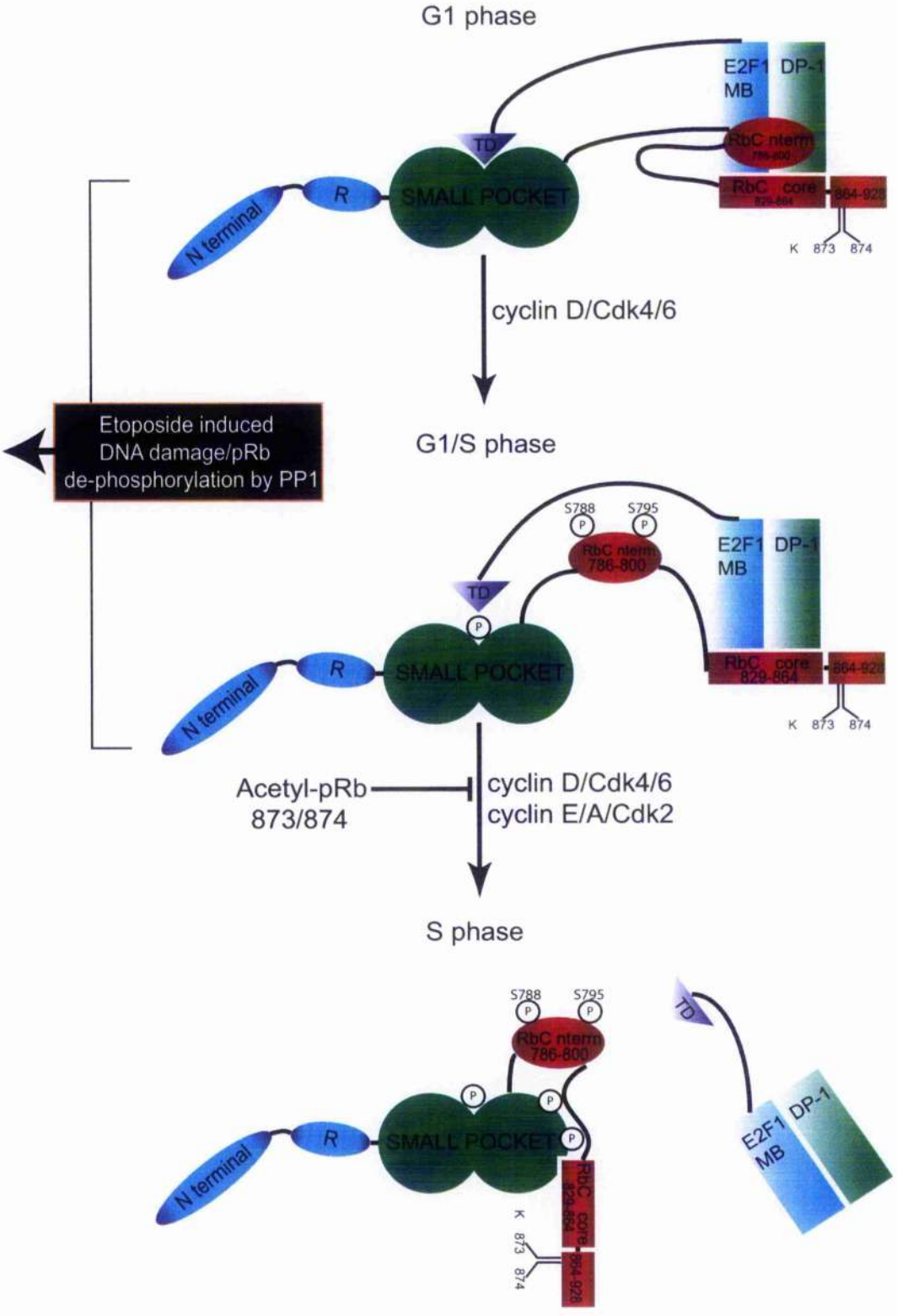
G1 phase
E2F1
MB
DP-1
TD
RbC nterm
786-800
SMALL POCKET
R
N terminal
RbC core
829-864
864-928
K 873 874
cyclin D/Cdk4/6
Etoposide induced
DNA damage/pRb
de-phosphorylation by PP1
G1/S phase
S788
S795
P
RbC nterm
786-800
E2F1
MB
DP-1
TD
SMALL POCKET
R
N terminal
RbC core
829-864
K 873 874
Acetyl-pRb
873/874
cyclin D/Cdk4/6
cyclin E/A/Cdk2
S phase
S788
S795
RbC nterm
786-800
SMALL POCKET
R
N terminal
K 873 874
TD
E2F1
MB
DP-1

Figure 36: Proposed model for pRb repression of E2F genes that control G1/S and S-phase

The diagram depicts the small pocket region of pRb (residues 379-792) bound to the *trans*-activation domain of E2F-1 and the C-terminal domain of pRb (792-928) bound to the marked box domain of E2F-1 and DP-1. Two regions of the C-terminal domain of pRb are involved in binding E2F-1 marked box (MB) (RbC^{core} (residues 829-864) and RbC^{nterm} (residues 786-800)). Initial phosphorylation of pRb by cyclin D/Cdk4/6 blocks the RbC^{nterm} interaction with E2F-1 MB. The activation of cyclin E/Cdk2 and further phosphorylation of the pRb small pocket blocks the RbC^{core} interaction with the MB and also the small pocket interaction with E2F-1 TD. The RbC^{core} region binds back onto the small pocket leaving E2F-1 to activate G1-S phase and S-phase genes. Hyper-phosphorylated pRb is de-phosphorylated by PP1 in response to etoposide treatment (see part B).

In response to etoposide induced DNA damage, PP1 de-phosphorylates pRb (Figure 38) [107]. Double stranded breaks in DNA are bound by the TIP60 HAT enzyme, which forms initial DNA repair complexes. Upon DNA damage, TIP60 rapidly acetylates ATM kinase, thereby activating it [72]. ATM kinase targets Chk2 kinase. Phosphorylation of Chk2 results in its activation, from where it targets a number of transcription factors including p53, E2F-1 and potentially pRb (Figure 38)[228, 229].

p53 and E2F-1 are targeted by ATM kinase (Reviewed in [270] [265]. In the case of E2F-1, ATM stabilizes the protein by preventing the binding of SCF/p45 ^{skp2} thereby preventing E2F-1 proteosomal degradation [264]. Further damage responsive phosphorylation of p53 and E2F-1 by Chk2 mediates a variety of effects. Chk2 phosphorylation induces p53 acetylation, which results in increased DNA binding and thereby up regulating *trans*-activation of cell cycle arrest genes (such as *p21*) and apoptotic genes (such as *Bax).* p53 acetylation also interferes with p53 ubiquitination, hence increasing its stability [228]. p53 mediates cell cycle arrest through *trans*-activation of *p21* and subsequent drop in pRb phosphorylation.

Chk2 phosphorylation of the pRb/E2F complexes may occur gradually, as stabilised E2F-1 up regulates Chk2 kinase expression, and ATM activation [265]. When E2F-1 protein is stabilized over a certain threshold level, phospho-pRb/E2F complex may *trans*locate to apoptotic promoters such as p73 and Apaf-1 (Figure 39) [75]. They would thereby displace the p107/E2F4 repressor complexes (which then *trans*locate to promoters of S-phase genes to repress the cell cycle) (Chapter 1, Figure 6). The Chk2 phosphorylated 'pRb/E2F complex' would promote the recruitment of the p300/P/CAF HAT complex. This complex would form scaffolds to facilitate transcription at apoptotic promoters. p300/P/CAF acetylates histone tails (such as histone H4) allowing the local unwinding of chromatin. p300/P/CAF then acetylates pRb (causing it to dissociate with E2F-1).

Figure 37

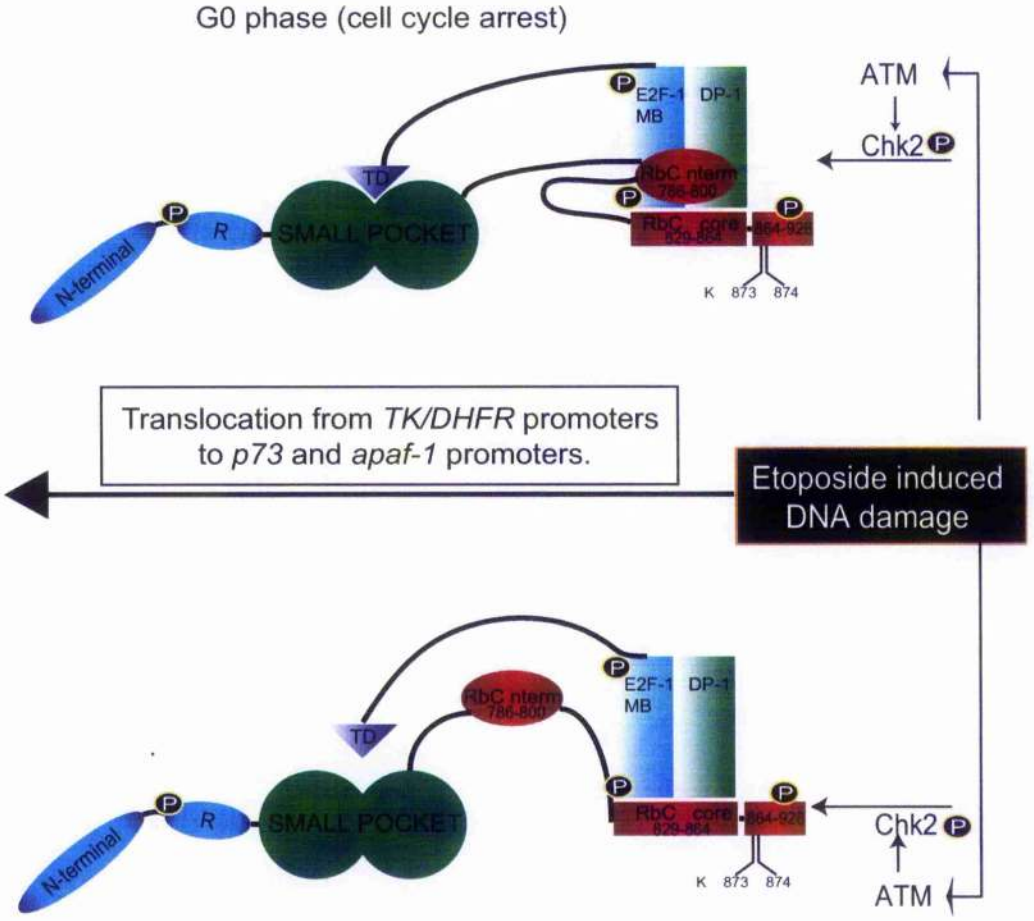
G0 phase (cell cycle arrest)
E2F-1
MB
DP-1
ATM
Chk2
TD
RbC nterm
786-800
RbC core
829-864
864-928
R
SMALL POCKET
N-terminal
K 873 874
Translocation from TK/DHFR promoters
to p73 and apaf-1 promoters.
Etoposide induced
DNA damage
E2F-1
MB
DP-1
RbC nterm
786-800
TD
R
SMALL POCKET
N-terminal
RbC core
829-864
K 873 874
Chk2
ATM

Figure: 37: Proposed model for stabilization of E2F-1 and pRb through phosphorylation by ATM/Chk2 and the recruitment of P/CAF/p300 complexes

The ATM/Chk2 pathway controls the damage responsive acetylation of pRb, E2F-1 and p53. ATM kinase, which phosphorylates and activates Chk2 kinase, phosphorylates E2F-1 at S31. In turn, Chk2 kinase phosphorylates E2F-1 at residue 364, thus contributing to its increased stability. The diagram depicts a model in which DNA inducible acetylation is dependent on Chk2 activation. Chk2 may phosphorylate pRb at is N-terminal domain, where several Chk2 kinase consensus phosphorylation sites occur (Figure 36c). It is suggested that Chk2 phosphorylation may recruit p300/P/CAF to pRb and E2F-1 to facilitate acetylation.

Figure 38

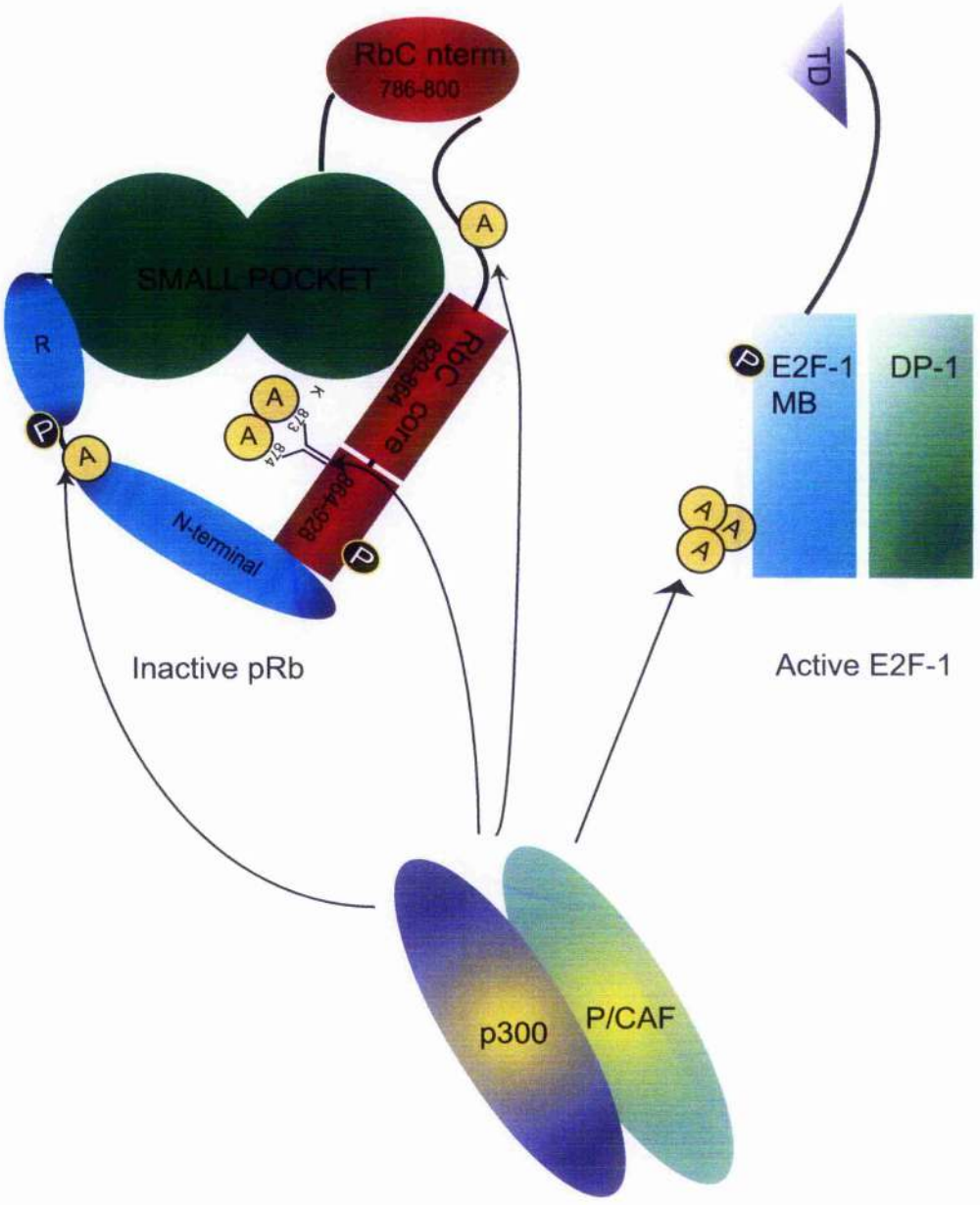
RbC nterm
786-800
SMALL POCKET
R
P
A
N-terminal
A
A
K
873
874
RBC Core
829-864
864-928
P
Inactive pRb
TD
P
E2F-1
MB
DP-1
A
A
A
Active E2F-1
p300
P/CAF

Figure: 38: Proposed model to explain pRb/E2F-1 translocation from S-phase promoters to apoptotic promoters

The phosphorylation model depicted in Figure 39 involves the recruitment of p300/P/CAF complexes that acetylate pRb and E2F-1. Acetylation of pRb at residues K873/874 and in the N-terminal domain may cause a change in conformation to block the binding of the C-terminal domain of pRb with the MB domain of E2F-1. The acetylation of residues K873/874 promotes binding of the N-terminal domain, which may alter the intra-cellular localization of pRb. Acetylation of E2F-1 in its DNA binding domain may serve to increase its affinity for DNA binding, thus promoting the *trans*-activation of genes involved with apoptosis.

E2F-1 is also acetylated thereby facilitating its DNA binding and stimulating transcription (Figure 39) [88].

Future prospectives

In the future, it would be useful to engineer other HAT enzymes into baculovirus in order to assess whether other HAT enzymes can acetylate pRb. Perhaps combining HAT enzymes in acetylation assays could shed light on potential transcription factor HAT complexes. For instance, it would be useful to study whether P/CAF can acetylate the N-terminal domain of pRb (both on its own and with p300), and to address whether p300/P/CAF complexes can from in response to DNA damage. It is likely that the *in vitro* acetylation of the A/B pocket would require an intact A/B interface. It would be interesting to study further the observations by Chan that K713 in the B pocket is acetylated *in vitro* [214]. Perhaps acetylation of K713 might disrupt binding of LXCXE proteins (such as HDAC enzymes and cyclin D).

The key steps in the study of N-terminal domain pRb acetylation include analysing the acetylated N-terminal domain pRb using mass spectroscopy to define which residues Flag-p300 FL acetylates. This data could be used to create mutant N-terminal domain pRb derivatives that mimic acetylation (K to Q) or prevent acetylation (K to R). Next, the link between Chk phosphorylation and acetylation could be studied. Utilizing *in vitro* kinase assays, potential Chk2 kinase consensus phosphorylation sites could be studied. Site-directed-mutagenesis could be used to assess which consensus sites are phosphorylated by Chk2 *in vitro*.

GST pulldown experiments showed that HA-N-pRb bound to GST-C-pRb QQ mutant derivative with approximately 4 fold greater binding affinity than to GST-C-pRb wt. Once the sites of acetylation have been mapped, it would be interesting to test N-terminal domain acetylation mimics for binding to the C-terminal domain of pRb. Perhaps the acetylation of the N-terminal domain of pRb will further increase the binding between

the two-pRb derivatives. Cdk enzymes phosphorylate pRb at residues 250 and 252 of the N-terminal domain. Perhaps acetylation might interfere with phosphorylation at these sites, and help facilitate G1 arrest. This can be assessed using N-pRb (K to Q) mutants.

In cells, it is necessary to test whether N-terminal domain acetylation is under the control of Chk2 phosphorylation. Using HCT15 cells (which do not express Chk2), dominant negative Chk2 mutant DNA could be exogenously expressed, and the levels of acetylation of HA-N-pRb 1-376 with or without damage could be compared with HCT15 cells expressing wild-type Chk2 protein. Also in cells, siRNA approaches could be utilized to study whether P/CAF is required for damage responsive acetylation of pRb. Already preliminary siRNA experiments in our group have concluded that p300 is required for acetylation at residues K873/874 (Darran O'Connor, personal communication). It is expected that P/CAF might complex with p300 to acetylate pRb.

The affect that pRb acetylation has on apoptosis should be investigated using the TUNEL assay. $Rb^{-/-}$ cells could be transiently transfected with pRb acetylation mutant constructs (K to Q) to compare levels of apoptosis with cells which are transfected with pRb acetylation dead mutant constructs (K to R). Protein levels of p73 and Apaf1 could be assessed in cells transfected with acetylated pRb mutants. Using $Rb^{-/-}$ cells, the ability of pRb acetylation mutants to activate *p73* reporter constructs could be studied under DNA damage conditions. Using FACS analysis, E2F-1 dependent apoptosis could be measured comparing cells transfected with wild-type pRb verses those transfected with acetylation mutants. The binding properties of pRb acetylation mutants could be further studied using gel shift assays, to assess their effect on E2F-1 binding to DNA.

In cells, the effect of Chk2 phosphorylation on pRb acetylation at residues K873/874 could be studied using 2D electrophoresis. Mutant derivatives of pRb in which potential Chk2 sites are either mutated to A or D (preventing or mimicking phosphorylation) could be transfected into cells and pRb acetylation at residues K873/874 measured using the acetyl-pRb SK37 antibody.

In cells transfected with dominant negative Chk2, the intra-cellular location of acetyl-pRb and phospho-E2F-1 could be assessed in the presence or absence of DNA damage in order to confirm whether Chk2 phosphorylation affects pRb/E2F location. In this regard, the binding of Lamin A/C and LAP2α proteins to acetyl-pRb mutants could be assessed in the presence and absence of DNA damage. In future it would be interesting to study the mechanisms behind pRb/E2F nuclear *trans*-location.

In conclusion, acetylation of pRb at residues K873/874 affects the binding of pRb with E2F-1 under DNA damage conditions. Future work should seek to assess the affect of the N-terminal domain of pRb (and its acetylation) on the interaction with E2F-1. In this regard crystallographic studies may well be required to further elucidate the precise nature of interactions between the C-terminal domain and the N-terminal domain of pRb. Understanding the mechanisms by which post-translational modification of pRb controls its anti-apoptotic function may lead to the identification of possible drug targets (such as HDAC inhibitors [271]) that utilize the cells apoptotic mechanisms to target tumour cells for death, leaving non-transformed cells unharmed.

References

1. Norbury, C. & Nurse, P., (1992). Animal cell cycles and their control. *Annu Rev Biochem,* **61**: p. 441-70.
2. Malumbres, M., Hunt, S. L., Sotillo, R., Martin, J., Odajima, J., Martin, A., Dubus, P., Ortega, S. & Barbacid, M., (2003). Driving the cell cycle to cancer. *Adv Exp Med Biol,* **532**: p. 1-11.
3. Hartwell, L. H. & Weinert, T. A., (1989). Checkpoints: controls that ensure the order of cell cycle events. *Science,* **246**: p. 629-34.
4. Pardee, A. B., (1974). A restriction point for control of normal animal cell proliferation. *Proc Natl Acad Sci U S A,* **71**: p. 1286-90.
5. Dannenberg, J. H., van Rossum, A., Schuijff, L. & te Riele, H., (2000). Ablation of the retinoblastoma gene family deregulates G(1) control causing immortalization and increased cell turnover under growth-restricting conditions. *Genes Dev,* **14**: p. 3051-64.
6. Marshall, B. G., Wangoo, A., O'Gaora, P., Cook, H. T., Shaw, R. J. & Young, D. B., (2001). Enhanced antimycobacterial response to recombinant Mycobacterium bovis BCG expressing latency-associated peptide. *Infect Immun,* **69**: p. 6676-82.
7. Schaeffer, H. J., Weber, M. J., (1999). Mitogen-Activated Protein Kinases: Specific Messages from Ubiquitous Messengers. *Molecular Cellular Biology,* **19**: p. 2435-2444.
8. Kolch, W., (2000). Meaningful relationships: the regulation of the Ras/Raf/MEK/ERK pathway by protein interactions. *Biochem J,* **351 Pt 2**: p. 289-305.
9. Han, Z. S., Enslen, H., Hu, X., Meng, X., Wu, I. H., Barrett, T., Davis, R. J. & Ip, Y. T., (1998). A conserved p38 mitogen-activated protein kinase pathway regulates

Drosophila immunity gene expression. *Mol Cell Biol,* **18**: p. 3527-39.

10. Lewis, T. S., Shapiro, P. S. & Ahn, N. G., (1998). Signal transduction through MAP kinase cascades. *Adv Cancer Res,* **74**: p. 49-139.

11. Robinson, M. J. & Cobb, M. H., (1997). Mitogen-activated protein kinase pathways. *Curr Opin Cell Biol,* **9**: p. 180-6.

12. Matsushime, H., Roussel, M. F., Ashmun, R. A. & Sherr, C. J., (1991). Colony-stimulating factor 1 regulates novel cyclins during the G1 phase of the cell cycle. *Cell,* **65**: p. 701-13.

13. Heldin, C. H. & Miyazono, K., (1995). [Transforming growth factor-beta. An interesting candidate for clinical use]. *Lakartidningen,* **92**: p. 1569-72.

14. Gao, N., Flynn, D. C., Zhang, Z., Zhong, X. S., Walker, V., Liu, K. J., Shi, X., Jiang, B. H., (2004). G1 cell cycle progression and the expression of G1 cyclins are regulated by P13K/AKT/mTOR/p70S6K1 signaling in human ovarian cancer cells. *Am J Physiol Cell Physiol,* **287**: p. 281-291.

15. Liu, J. J., Chao, J. R., Jiang, M. C., Ng, S. Y., Yen, J. J. & Yang-Yen, H. F., (1995). Ras transformation results in an elevated level of cyclin D1 and acceleration of G1 progression in NIH 3T3 cells. *Mol Cell Biol,* **15**: p. 3654-63.

16. Winston, J., Dong, F. & Pledger, W. J., (1996). Differential modulation of G1 cyclins and the Cdk inhibitor p27kip1 by platelet-derived growth factor and plasma factors in density-arrested fibroblasts. *J Biol Chem,* **271**: p. 11253-60.

17. Hashiba, M., Wetzig, J., v Baumgarten, R., Watanabe, S. & Baba, S., (1993). Influence of gravity on the eye movement response elicited by periodic lateral linear acceleration. *Microgravity Sci Technol,* **6**: p. 282-5.

18. Lukas, J., Pagano, M., Staskova, Z., Draetta, G. & Bartek, J., (1994). Cyclin D1 protein oscillates and is essential for cell cycle progression in human tumour cell lines. *Oncogene,* **9**: p. 707-18.

19. Quelle, D. E., Ashmun, R. A., Shurtleff, S. A., Kato, J. Y., Bar-Sagi, D., Roussel,

M. F. & Sherr, C. J., (1993). Overexpression of mouse D-type cyclins accelerates G1 phase in rodent fibroblasts. *Genes Dev,* **7**: p. 1559-71.

20. Serrano, M., Gomez-Lahoz, E., DePinho, R. A., Beach, D. & Bar-Sagi, D., (1995). Inhibition of ras-induced proliferation and cellular transformation by p16INK4. *Science,* **267**: p. 249-52.

21. Harper, J. W., Elledge, S. J., (1998). The role of Cdk7 in CAK function, a retro-retrospective. *Genes Dev,* **12**: p. 285-289.

22. Chiariello, M., Gomez, E. & Gutkind, J. S., (2000). Regulation of cyclin-dependent kinase (Cdk) 2 Thr-160 phosphorylation and activity by mitogen-activated protein kinase in late G1 phase. *Biochem J,* **349 Pt 3**: p. 869-76.

23. Wang, S., Ghosh, R. N. & Chellappan, S. P., (1998). Raf-1 physically interacts with Rb and regulates its function: a link between mitogenic signaling and cell cycle regulation. *Mol Cell Biol,* **18**: p. 7487-98.

24. Ekholm, S. V. & Reed, S. I., (2000). Regulation of G(1) cyclin-dependent kinases in the mammalian cell cycle. *Curr Opin Cell Biol,* **12**: p. 676-84.

25. Sherr, C. J., (2000). The Pezcoller lecture: cancer cell cycles revisited. *Cancer Res,* **60**: p. 3689-95.

26. Morgan, D. O., (1997). Cyclin-dependent kinases: engines, clocks, and microprocessors. *Annu Rev Cell Dev Biol,* **13**: p. 261-91.

27. Nigg, E. A., (1996). Cyclin-dependent kinase 7: at the cross-roads of transcription, DNA repair and cell cycle control? *Curr Opin Cell Biol,* **8**: p. 312-7.

28. Mailand, N., Falck, J., Lukas, C., Syljuasen, R. G., Welcker, M., Bartek, J. & Lukas, J., (2000). Rapid destruction of human Cdc25A in response to DNA damage. *Science,* **288**: p. 1425-9.

29. Sherr, C. J. & Roberts, J. M., (1999). CDK inhibitors: positive and negative regulators of G1-phase progression. *Genes Dev,* **13**: p. 1501-12.

30. Blain, S. W., Montalvo, E. & Massague, J., (1997). Differential interaction of the

cyclin-dependent kinase (Cdk) inhibitor p27Kip1 with cyclin A-Cdk2 and cyclin D2-Cdk4. *J Biol Chem,* **272**: p. 25863-72.

31. Friend, S. H., Bernards, R., Rogelj, S., Weinberg, R. A., Rapaport, J. M., Albert, D. M. & Dryja, T. P., (1986). A human DNA segment with properties of the gene that predisposes to retinoblastoma and osteosarcoma. *Nature,* **323**: p. 643-6.

32. Knudson, A. G., Jr., (1971). Mutation and cancer: statistical study of retinoblastoma. *Proc Natl Acad Sci U S A,* **68**: p. 820-3.

33. Yang, H., Williams, B. O., Hinds, P. W., Shih, T. S., Jacks, T., Bronson, R. T. & Livingston, D. M., (2002). Tumor suppression by a severely truncated species of retinoblastoma protein. *Mol Cell Biol,* **22**: p. 3103-10.

34. Morris, E. J. & Dyson, N. J., (2001). Retinoblastoma protein partners. *Adv Cancer Res,* **82**: p. 1-54.

35. Tommasi, S. & Pfeifer, G. P., (1995). In vivo structure of the human cdc2 promoter: release of a p130-E2F-4 complex from sequences immediately upstream of the transcription initiation site coincides with induction of cdc2 expression. *Mol Cell Biol,* **15**: p. 6901-13.

36. Zwicker, J., Liu, N., Engeland, K., Lucibello, F. C. & Muller, R., (1996). Cell cycle regulation of E2F site occupation in vivo. *Science,* **271**: p. 1595-7.

37. Lazzi, S., Bellan, C., De Falco, G., Cinti, C., Ferrari, F., Nyongo, A., Claudio, P. P., Tosi, G. M., Vatti, R., Gloghini, A., Carbone, A., Giordano, A., Leoncini, L. & Tosi, P., (2002). Expression of RB2/p130 tumor-suppressor gene in AIDS-related non-Hodgkin's lymphomas: implications for disease pathogenesis. *Hum Pathol,* **33**: p. 723-31.

38. Dyson, N., Howley, P. M., Munger, K. & Harlow, E., (1989). The human papilloma virus-16 E7 oncoprotein is able to bind to the retinoblastoma gene product. *Science,* **243**: p. 934-7.

39. Wang, H. G., Moran, E. & Yaciuk, P., (1995). E1A promotes association between

p300 and pRB in multimeric complexes required for normal biological activity. *J Virol,* **69**: p. 7917-24.

40. Kim, H. Y., Ahn, B. Y. & Cho, Y., (2001). Structural basis for the inactivation of retinoblastoma tumor suppressor by SV40 large T antigen. *Embo J,* **20**: p. 295-304.

41. Lee, J. O., Russo, A. A. & Pavletich, N. P., (1998). Structure of the retinoblastoma tumour-suppressor pocket domain bound to a peptide from HPV E7. *Nature,* **391**: p. 859-65.

42. Ichimura, K., Hanafusa, H., Takimoto, H., Ohgama, Y., Akagi, T. & Shimizu, K., (2000). Structure of the human retinoblastoma-related p107 gene and its intragenic deletion in a B-cell lymphoma cell line. *Gene,* **251**: p. 37-43.

43. Ewen, M. E., Xing, Y. G., Lawrence, J. B. & Livingston, D. M., (1991). Molecular cloning, chromosomal mapping, and expression of the cDNA for p107, a retinoblastoma gene product-related protein. *Cell,* **66**: p. 1155-64.

44. Helin, K., Holm, K., Niebuhr, A., Eiberg, H., Tommerup, N., Hougaard, S., Poulsen, H. S., Spang-Thomsen, M. & Norgaard, P., (1997). Loss of the retinoblastoma protein-related p130 protein in small cell lung carcinoma. *Proc Natl Acad Sci U S A,* **94**: p. 6933-8.

45. Claudio, P. P., Caputi, M. & Giordano, A., (2000). The RB2/p130 gene: the latest weapon in the war against lung cancer? *Clin Cancer Res,* **6**: p. 754-64.

46. Cinti, C., Leoncini, L., Nyongo, A., Ferrari, F., Lazzi, S., Bellan, C., Vatti, R., Zamparelli, A., Cevenini, G., Tosi, G. M., Claudio, P. P., Maraldi, N. M., Tosi, P. & Giordano, A., (2000). Genetic alterations of the retinoblastoma-related gene RB2/p130 identify different pathogenetic mechanisms in and among Burkitt's lymphoma subtypes. *Am J Pathol,* **156**: p. 751-60.

47. Baldi, A., Esposito, V., De Luca, A., Fu, Y., Meoli, I., Giordano, G. G., Caputi, M., Baldi, F. & Giordano, A., (1997). Differential expression of Rb2/p130 and p107 in normal human tissues and in primary lung cancer. *Clin Cancer Res,* **3**: p. 1691-7.

48. Susini, T., Baldi, F., Howard, C. M., Baldi, A., Taddei, G., Massi, D., Rapi, S., Savino, L., Massi, G. & Giordano, A., (1998). Expression of the retinoblastoma-related gene Rb2/p130 correlates with clinical outcome in endometrial cancer. *J Clin Oncol,* **16**: p. 1085-93.

49. Massaro-Giordano, M., Baldi, G., De Luca, A., Baldi, A. & Giordano, A., (1999). Differential expression of the retinoblastoma gene family members in choroidal melanoma: prognostic significance. *Clin Cancer Res,* **5**: p. 1455-8.

50. Tanaka, N., Odajima, T., Nakano, T., Kimijima, Y., Yamada, S., Ogi, K. & Kohama, G., (1999). Immunohistochemical investigation of new suppressor oncogene p130 in oral squamous cell carcinoma. *Oral Oncol,* **35**: p. 321-5.

51. Cobrinik, D., Lee, M. H., Hannon, G., Mulligan, G., Bronson, R. T., Dyson, N., Harlow, E., Beach, D., Weinberg, R. A. & Jacks, T., (1996). Shared role of the pRB-related p130 and p107 proteins in limb development. *Genes Dev,* **10**: p. 1633-44.

52. Lipinski, M. M. & Jacks, T., (1999). The retinoblastoma gene family in differentiation and development. *Oncogene,* **18**: p. 7873-82.

53. Nguyen, D. X., Baglia, L. A., Huang, S. M., Baker, C. M. & McCance, D. J., (2004). Acetylation regulates the differentiation-specific functions of the retinoblastoma protein. *Embo J,* **23**: p. 1609-18.

54. Chen, P. L., Riley, D. J., Chen, Y. & Lee, W. H., (1996). Retinoblastoma protein positively regulates terminal adipocyte differentiation through direct interaction with C/EBPs. *Genes Dev,* **10**: p. 2794-804.

55. Classon, M., Kennedy, B. K., Mulloy, R. & Harlow, E., (2000). Opposing roles of pRB and p107 in adipocyte differentiation. *Proc Natl Acad Sci U S A,* **97**: p. 10826-31.

56. Trimarchi, J. M. & Lees, J. A., (2002). Sibling rivalry in the E2F family. *Nat Rev Mol Cell Biol,* **3**: p. 11-20.

57. Stevaux, O. & Dyson, N. J., (2002). A revised picture of the E2F transcriptional network and RB function. *Curr Opin Cell Biol,* **14**: p. 684-91.

58. Helin, K., (1998). Regulation of cell proliferation by the E2F transcription factors. *Curr Opin Genet Dev,* **8**: p. 28-35.

59. Ogawa, H., Ishiguro, K., Gaubatz, S., Livingston, D. M. & Nakatani, Y., (2002). A complex with chromatin modifiers that occupies E2F- and Myc-responsive genes in G0 cells. *Science,* **296**: p. 1132-6.

60. de Bruin, A., Maiti, B., Jakoi, L., Timmers, C., Buerki, R. & Leone, G., (2003). Identification and characterization of E2F7, a novel mammalian E2F family member capable of blocking cellular proliferation. *J Biol Chem,* **278**: p. 42041-9.

61. Logan, N., Delavaine, L., Graham, A., Reilly, C., Wilson, J., Brummelkamp, T. R., Hijmans, E. M., Bernards, R. & La Thangue, N. B., (2004). E2F-7: a distinctive E2F family member with an unusual organization of DNA-binding domains. *Oncogene,* **23**: p. 5138-50.

62. Christensen, J., Cloos, P., Toftegaard, U., Klinkenberg, D., Bracken, A. P., Trinh, E., Heeran, M., Di Stefano, L. & Helin, K., (2005). Characterization of E2F8, a novel E2F-like cell-cycle regulated repressor of E2F-activated transcription. *Nucleic Acids Res,* **33**: p. 5458-70.

63. Logan, N., Graham, A., Zhao, X., Fisher, R., Maiti, B., Leone, G. & La Thangue, N. B., (2005). E2F-8: an E2F family member with a similar organization of DNA-binding domains to E2F-7. *Oncogene,* **24**: p. 5000-4.

64. Slansky, J. E., Farnham, P. J., (1996). Introduction to the E2F Family: Protein Structure and Gene Regulation. *Current Topics in Microbiology*: p. 1-30.

65. Fagan, R., Flint, K. J., Jones, N. , (1994). Phosphorylation of E2F-1 modulates its interactions with the retinoblastoma gene product and the adenoviral E4 19kDa protein. *Cell,* **78**: p. 799-811.

66. Harbour, J. W. & Dean, D. C., (2000). The Rb/E2F pathway: expanding roles and

emerging paradigms. *Genes Dev,* **14**: p. 2393-409.

67. Bremner, R., Cohen, B. L., Sopta, M., Hamel, P. A., Ingles, C. J., Gallie, B. L. & Phillips, R. A., (1995). Direct transcriptional repression by pRB and its reversal by specific cyclins. *Mol Cell Biol,* **15**: p. 3256-65.

68. Sellers, W. R., Rodgers, J. W. & Kaelin, W. G., Jr., (1995). A potent transrepression domain in the retinoblastoma protein induces a cell cycle arrest when bound to E2F sites. *Proc Natl Acad Sci U S A,* **92**: p. 11544-8.

69. Weintraub, S. J., Chow, K. N., Luo, R. X., Zhang, S. H., He, S. & Dean, D. C., (1995). Mechanism of active transcriptional repression by the retinoblastoma protein. *Nature,* **375**: p. 812-5.

70. Rayman, J. B., Takahashi, Y., Indjeian, V. B., Dannenberg, J. H., Catchpole, S., Watson, R. J., te Riele, H. & Dynlacht, B. D., (2002). E2F mediates cell cycle-dependent transcriptional repression in vivo by recruitment of an HDAC1/mSin3B corepressor complex. *Genes Dev,* **16**: p. 933-47.

71. Takahashi, Y., Rayman, J. B. & Dynlacht, B. D., (2000). Analysis of promoter binding by the E2F and pRB families in vivo: distinct E2F proteins mediate activation and repression. *Genes Dev,* **14**: p. 804-16.

72. Sun, Y., Jiang, X., Chen, S., Fernandes, N. & Price, B. D., (2005). A role for the Tip60 histone acetyltransferase in the acetylation and activation of ATM. *Proc Natl Acad Sci U S A,* **102**: p. 13182-7.

73. Lin, W. C., Lin, F. T. & Nevins, J. R., (2001). Selective induction of E2F1 in response to DNA damage, mediated by ATM-dependent phosphorylation. *Genes Dev,* **15**: p. 1833-44.

74. Stevens, C. & La Thangue, N. B., (2004). The emerging role of E2F-1 in the DNA damage response and checkpoint control. *DNA Repair,* **3**: p. 1071.

75. Pediconi, N., Ianari, A., Costanzo, A., Belloni, L., Gallo, R., Cimino, L., Porcellini, A., Screpanti, I., Balsano, C., Alesse, E., Gulino, A. & Levrero, M., (2003).

Differential regulation of E2F1 apoptotic target genes in response to DNA damage. *Nat Cell Biol,* **5**: p. 552-8.

76. Qin, X. Q., Chittenden, T., Livingston, D. M. & Kaelin, W. G., Jr., (1992). Identification of a growth suppression domain within the retinoblastoma gene product. *Genes Dev,* **6**: p. 953-64.

77. Harbour, J. W., (1998). Overview of RB gene mutations in patients with retinoblastoma. Implications for clinical genetic screening. *Ophthalmology,* **105**: p. 1442-7.

78. Horowitz, J. M., Yandell, D. W., Park, S. H., Canning, S., Whyte, P., Buchkovich, K., Harlow, E., Weinberg, R. A. & Dryja, T. P., (1989). Point mutational inactivation of the retinoblastoma antioncogene. *Science,* **243**: p. 937-40.

79. Whyte, P., Buchkovich, K. J., Horowitz, J. M., Friend, S. H., Raybuck, M., Weinberg, R. A. & Harlow, E., (1988). Association between an oncogene and an anti-oncogene: the adenovirus E1A proteins bind to the retinoblastoma gene product. *Nature,* **334**: p. 124-9.

80. Ludlow, J. W., DeCaprio, J. A., Huang, C. M., Lee, W. H., Paucha, E. & Livingston, D. M., (1989). SV40 large T antigen binds preferentially to an underphosphorylated member of the retinoblastoma susceptibility gene product family. *Cell,* **56**: p. 57-65.

81. Helin, K., Lees, J. A., Vidal, M., Dyson, N., Harlow, E. & Fattaey, A., (1992). A cDNA encoding a pRB-binding protein with properties of the transcription factor E2F. *Cell,* **70**: p. 337-50.

82. Hiebert, S. W., Chellappan, S. P., Horowitz, J. M. & Nevins, J. R., (1992). The interaction of RB with E2F coincides with an inhibition of the transcriptional activity of E2F. *Genes Dev,* **6**: p. 177-85.

83. Ferreira, R., Magnaghi-Jaulin, L., Robin, P., Harel-Bellan, A. & Trouche, D., (1998). The three members of the pocket proteins family share the ability to repress

E2F activity through recruitment of a histone deacetylase. *Proc Natl Acad Sci U S A,* **95**: p. 10493-8.

84. Brehm, A., Miska, E. A., McCance, D. J., Reid, J. L., Bannister, A. J. & Kouzarides, T., (1998). Retinoblastoma protein recruits histone deacetylase to repress transcription. *Nature,* **391**: p. 597-601.

85. Luo, R. X., Postigo, A. A. & Dean, D. C., (1998). Rb interacts with histone deacetylase to repress transcription. *Cell,* **92**: p. 463-73.

86. Lai, A., Lee, J. M., Yang, W. M., DeCaprio, J. A., Kaelin, W. G., Jr., Seto, E. & Branton, P. E., (1999). RBP1 recruits both histone deacetylase-dependent and -independent repression activities to retinoblastoma family proteins. *Mol Cell Biol,* **19**: p. 6632-41.

87. Trouche, D., Cook, A. & Kouzarides, T., (1996). The CBP co-activator stimulates E2F1/DP1 activity. *Nucleic Acids Res,* **24**: p. 4139-45.

88. Martinez-Balbas, M. A., Bauer, U. M., Nielsen, S. J., Brehm, A. & Kouzarides, T., (2000). Regulation of E2F1 activity by acetylation. *Embo J,* **19**: p. 662-71.

89. Weintraub, S. J., Prater, C. A. & Dean, D. C., (1992). Retinoblastoma protein switches the E2F site from positive to negative element. *Nature,* **358**: p. 259-61.

90. Hsiao, K. M., McMahon, S. L. & Farnham, P. J., (1994). Multiple DNA elements are required for the growth regulation of the mouse E2F1 promoter. *Genes Dev,* **8**: p. 1526-37.

91. Johnson, D. G., Schwarz, J. K., Cress, W. D. & Nevins, J. R., (1993). Expression of transcription factor E2F1 induces quiescent cells to enter S phase. *Nature,* **365**: p. 349-52.

92. Adnane, J., Shao, Z. & Robbins, P. D., (1995). The retinoblastoma susceptibility gene product represses transcription when directly bound to the promoter. *J Biol Chem,* **270**: p. 8837-43.

93. Neuman, E., Flemington, E. K., Sellers, W. R. & Kaelin, W. G., Jr., (1995).

Transcription of the E2F-1 gene is rendered cell cycle dependent by E2F DNA-binding sites within its promoter. *Mol Cell Biol,* **15**: p. 4660.

94. Chow, K. N., Starostik, P. & Dean, D. C., (1996). The Rb family contains a conserved cyclin-dependent-kinase-regulated transcriptional repressor motif. *Mol Cell Biol,* **16**: p. 7173-81.

95. Meloni, A. R., Smith, E. J. & Nevins, J. R., (1999). A mechanism for Rb/p130-mediated transcription repression involving recruitment of the CtBP corepressor. *Proc Natl Acad Sci U S A,* **96**: p. 9574-9.

96. Dick, F. A. & Dyson, N., (2003). pRB contains an E2F1-specific binding domain that allows E2F1-induced apoptosis to be regulated separately from other E2F activities. *Mol Cell,* **12**: p. 639-49.

97. Markham, D., Munro, S., Soloway, J., O'Connor D, P. & La Thangue, N. B., (2006). DNA-damage-responsive acetylation of pRb regulates binding to E2F-1. *EMBO Rep,* **7**: p. 192-8.

98. Rubin, S. M., Gall, A. L., Zheng, N. & Pavletich, N. P., (2005). Structure of the Rb C-terminal domain bound to E2F1-DP1: a mechanism for phosphorylation-induced E2F release. *Cell,* **123**: p. 1093-106.

99. Lees, E., Faha, B., Dulic, V., Reed, S. I. & Harlow, E., (1992). Cyclin E/cdk2 and cyclin A/cdk2 kinases associate with p107 and E2F in a temporally distinct manner. *Genes Dev,* **6**: p. 1874-85.

100. Sterner, J. M., Murata, Y., Kim, H. G., Kennett, S. B., Templeton, D. J. & Horowitz, J. M., (1995). Detection of a novel cell cycle-regulated kinase activity that associates with the amino terminus of the retinoblastoma protein in G2/M phases. *J Biol Chem,* **270**: p. 9281-8.

101. Ezhevsky, S. A., Nagahara, H., Vocero-Akbani, A. M., Gius, D. R., Wei, M. C. & Dowdy, S. F., (1997). Hypo-phosphorylation of the retinoblastoma protein (pRb) by cyclin D:Cdk4/6 complexes results in active pRb. *Proc Natl Acad Sci U S A,* **94**:

p. 10699-704.

102. Ren, S. & Rollins, B. J., (2004). Cyclin C/cdk3 promotes Rb-dependent G0 exit. *Cell,* **117**: p. 239-51.

103. Mittnacht, S., (1998). Control of pRB phosphorylation. *Curr Opin Genet Dev,* **8**: p. 21-7.

104. Adams, P. D., (2001). Regulation of the retinoblastoma tumor suppressor protein by cyclin/cdks. *Biochim Biophys Acta,* **1471**: p. M123-33.

105. Lee, C. & Cho, Y., (2002). Interactions of SV40 large T antigen and other viral proteins with retinoblastoma tumour suppressor. *Rev Med Virol,* **12**: p. 81-92.

106. Angus, S. P., Solomon, D. A., Kuschel, L., Hennigan, R. F. & Knudsen, E. S., (2003). Retinoblastoma tumor suppressor: analyses of dynamic behavior in living cells reveal multiple modes of regulation. *Mol Cell Biol,* **23**: p. 8172-88.

107. Barbie, D. A., Conlan, L. A. & Kennedy, B. K., (2005). Nuclear tumor suppressors in space and time. *Trends Cell Biol,* **15**: p. 378-85.

108. Dryja, T. P., Friend, S. & Weinberg, R. A., (1986). Genetic sequences that predispose to retinoblastoma and osteosarcoma. *Symp Fundam Cancer Res,* **39**: p. 115-9.

109. Inoue, A., Torigoe, T., Sogahata, K., Kamiguchi, K., Takahashi, S., Sawada, Y., Saijo, M., Taya, Y., Ishii, S., Sato, N. & Kikuchi, K., (1995). 70-kDa heat shock cognate protein interacts directly with the N-terminal region of the retinoblastoma gene product pRb. Identification of a novel region of pRb-mediating protein interaction. *J Biol Chem,* **270**: p. 22571-6.

110. Sterner, J. M., Dew-Knight, S., Musahl, C., Kornbluth, S. & Horowitz, J. M., (1998). Negative regulation of DNA replication by the retinoblastoma protein is mediated by its association with MCM7. *Mol Cell Biol,* **18**: p. 2748-57.

111. Goodrich, D. W., (2003). How the other half lives, the amino-terminal domain of the retinoblastoma tumor suppressor protein. *J Cell Physiol,* **197**: p. 169-80.

112. Kennedy, B. K., Barbie, D. A., Classon, M., Dyson, N. & Harlow, E., (2000). Nuclear organization of DNA replication in primary mammalian cells. *Genes Dev,* **14**: p. 2855-68.

113. Shen, W. J., Kim, H. S. & Tsai, S. Y., (1995). Stimulation of human insulin receptor gene expression by retinoblastoma gene product. *J Biol Chem,* **270**: p. 20525-9.

114. Kim, S. J., Lee, H. D., Robbins, P. D., Busam, K., Sporn, M. B. & Roberts, A. B., (1991). Regulation of transforming growth factor beta 1 gene expression by the product of the retinoblastoma-susceptibility gene. *Proc Natl Acad Sci U S A,* **88**: p. 3052-6.

115. Kim, S. J., Wagner, S., Liu, F., O'Reilly, M. A., Robbins, P. D. & Green, M. R., (1992). Retinoblastoma gene product activates expression of the human TGF-beta 2 gene through transcription factor ATF-2. *Nature,* **358**: p. 331-4.

116. Pietenpol, J. A., Munger, K., Howley, P. M., Stein, R. W. & Moses, H. L., (1991). Factor-binding element in the human c-myc promoter involved in transcriptional regulation by transforming growth factor beta 1 and by the retinoblastoma gene product. *Proc Natl Acad Sci U S A,* **88**: p. 10227-31.

117. Robbins, P. D., Horowitz, J. M. & Mulligan, R. C., (1990). Negative regulation of human c-fos expression by the retinoblastoma gene product. *Nature,* **346**: p. 668-71.

118. Yu, D., Matin, A. & Hung, M. C., (1992). The retinoblastoma gene product suppresses neu oncogene-induced transformation via transcriptional repression of neu. *J Biol Chem,* **267**: p. 10203-6.

119. Chen, P. L., Scully, P., Shew, J. Y., Wang, J. Y. & Lee, W. H., (1989). Phosphorylation of the retinoblastoma gene product is modulated during the cell cycle and cellular differentiation. *Cell,* **58**: p. 1193-8.

120. Qian, Y., Luckey, C., Horton, L., Esser, M. & Templeton, D. J., (1992). Biological

function of the retinoblastoma protein requires distinct domains for hyperphosphorylation and transcription factor binding. *Mol Cell Biol,* **12**: p. 5363-72.

121. Durfee, T., Mancini, M. A., Jones, D., Elledge, S. J. & Lee, W. H., (1994). The amino-terminal region of the retinoblastoma gene product binds a novel nuclear matrix protein that co-localizes to centers for RNA processing. *J Cell Biol,* **127**: p. 609-22.

122. Whitaker, L. L. & Hansen, M. F., (1997). Induction of apoptosis in Mv1Lu cells by expression of competitive RB1 mutants. *Oncogene,* **15**: p. 1069-77.

123. Doostzadeh-Cizeron, J., Evans, R., Yin, S. & Goodrich, D. W., (1999). Apoptosis induced by the nuclear death domain protein p84N5 is inhibited by association with Rb protein. *Mol Biol Cell,* **10**: p. 3251-61.

124. Takemura, M., Ohoka, F., Perpelescu, M., Ogawa, M., Matsushita, H., Takaba, T., Akiyama, T., Umekawa, H., Furuichi, Y., Cook, P. R. & Yoshida, S., (2002). Phosphorylation-dependent migration of retinoblastoma protein into the nucleolus triggered by binding to nucleophosmin/B23. *Exp Cell Res,* **276**: p. 233-41.

125. Xiao, Z. X., Chen, J., Levine, A. J., Modjtahedi, N., Xing, J., Sellers, W. R. & Livingston, D. M., (1995). Interaction between the retinoblastoma protein and the oncoprotein MDM2. *Nature,* **375**: p. 694-8.

126. White, R. J., (1997). Regulation of RNA polymerases I and III by the retinoblastoma protein: a mechanism for growth control? *Trends Biochem Sci,* **22**: p. 77-80.

127. Singh, P., Coe, J. & Hong, W., (1995). A role for retinoblastoma protein in potentiating transcriptional activation by the glucocorticoid receptor. *Nature,* **374**: p. 562-5.

128. Hinton, D. R., Hahn, J. A., Weiss, M. H. & Couldwell, W. T., (1998). Loss of Rb expression in an ACTH-secreting pituitary carcinoma. *Cancer Lett,* **126**: p. 209-14.

129. Batsche, E., Desroches, J., Bilodeau, S., Gauthier, Y. & Drouin, J., (2005). Rb enhances p160/SRC coactivator-dependent activity of nuclear receptors and hormone responsiveness. *J Biol Chem,* **280**: p. 19746-56.

130. Philips, A., Maira, M., Mullick, A., Chamberland, M., Lesage, S., Hugo, P. & Drouin, J., (1997). Antagonism between Nur77 and glucocorticoid receptor for control of transcription. *Mol Cell Biol,* **17**: p. 5952-9.

131. Murphy, E. P. & Conneely, O. M., (1997). Neuroendocrine regulation of the hypothalamic pituitary adrenal axis by the nurr1/nur77 subfamily of nuclear receptors. *Mol Endocrinol,* **11**: p. 39-47.

132. Maira, M., Martens, C., Philips, A. & Drouin, J., (1999). Heterodimerization between members of the Nur subfamily of orphan nuclear receptors as a novel mechanism for gene activation. *Mol Cell Biol,* **19**: p. 7549-57.

133. Maira, M., Couture, C., Le Martelot, G., Pulichino, A. M., Bilodeau, S. & Drouin, J., (2003). The T-box factor Tpit recruits SRC/p160 co-activators and mediates hormone action. *J Biol Chem,* **278**: p. 46523-32.

134. Rivera, O. J., Song, C. S., Centonze, V. E., Lechleiter, J. D., Chatterjee, B. & Roy, A. K., (2003). Role of the promyelocytic leukemia body in the dynamic interaction between the androgen receptor and steroid receptor coactivator-1 in living cells. *Mol Endocrinol,* **17**: p. 128-40.

135. Hensey, C. E., Hong, F., Durfee, T., Qian, Y. W., Lee, E. Y. & Lee, W. H., (1994). Identification of discrete structural domains in the retinoblastoma protein. Amino-terminal domain is required for its oligomerization. *J Biol Chem,* **269**: p. 1380-7.

136. Fattman, C. L., An, B. & Dou, Q. P., (1997). Characterization of interior cleavage of retinoblastoma protein in apoptosis. *J Cell Biochem,* **67**: p. 399-408.

137. Hogg, A., Bia, B., Onadim, Z. & Cowell, J. K., (1993). Molecular mechanisms of oncogenic mutations in tumors from patients with bilateral and unilateral retinoblastoma. *Proc Natl Acad Sci U S A,* **90**: p. 7351-5.

138. Otterson, G. A., Chen, W., Coxon, A. B., Khleif, S. N. & Kaye, F. J., (1997). Incomplete penetrance of familial retinoblastoma linked to germ-line mutations that result in partial loss of RB function. *Proc Natl Acad Sci U S A,* **94**: p. 12036-40.

139. Sellers, W. R., Novitch, B. G., Miyake, S., Heith, A., Otterson, G. A., Kaye, F. J., Lassar, A. B. & Kaelin, W. G., Jr., (1998). Stable binding to E2F is not required for the retinoblastoma protein to activate transcription, promote differentiation, and suppress tumor cell growth. *Genes Dev,* **12**: p. 95-106.

140. Xu, H. J., Xu, K., Zhou, Y., Li, J., Benedict, W. F. & Hu, S. X., (1994). Enhanced tumor cell growth suppression by an N-terminal truncated retinoblastoma protein. *Proc Natl Acad Sci U S A,* **91**: p. 9837-41.

141. Murakami, Y., Katahira, M., Makino, R., Hayashi, K., Hirohashi, S. & Sekiya, T., (1991). Inactivation of the retinoblastoma gene in a human lung carcinoma cell line detected by single-strand conformation polymorphism analysis of the polymerase chain reaction product of cDNA. *Oncogene,* **6**: p. 37-42.

142. Mihara, K., Cao, X. R., Yen, A., Chandler, S., Driscoll, B., Murphree, A. L., T'Ang, A. & Fung, Y. K., (1989). Cell cycle-dependent regulation of phosphorylation of the human retinoblastoma gene product. *Science,* **246**: p. 1300-3.

143. Rogalsky, V., Todorov, G. & Moran, D., (1993). Translocation of retinoblastoma protein associated with tumor cell growth inhibition. *Biochem Biophys Res Commun,* **192**: p. 1139-46.

144. Thomas, N. S., Burke, L. C., Bybee, A. & Linch, D. C., (1991). The phosphorylation state of the retinoblastoma (RB) protein in G0/G1 is dependent on growth status. *Oncogene,* **6**: p. 317-22.

145. Riley, D. J., Liu, C. Y. & Lee, W. H., (1997). Mutations of N-terminal regions render the retinoblastoma protein insufficient for functions in development and tumor suppression. *Mol Cell Biol,* **17**: p. 7342-52.

146. Connell-Crowley, L., Harper, J. W. & Goodrich, D. W., (1997). Cyclin D1/Cdk4 regulates retinoblastoma protein-mediated cell cycle arrest by site-specific phosphorylation. *Mol Biol Cell,* **8**: p. 287-301.

147. Vousden, K. H., (2000). p53: death star. *Cell,* **103**: p. 691-4.

148. Vousden, K. H. & Woude, G. F., (2000). The ins and outs of p53. *Nat Cell Biol,* **2**: p. E178-80.

149. Ries, S., Biederer, C., Woods, D., Shifman, O., Shirasawa, S., Sasazuki, T., McMahon, M., Oren, M. & McCormick, F., (2000). Opposing effects of Ras on p53: transcriptional activation of mdm2 and induction of p19ARF. *Cell,* **103**: p. 321-30.

150. Chan, H. M., La Thangue, N. B., (2001). p300/CBP proteins: HATs for transcriptional bridges and scaffolds. *J Cell Sci,* **114**: p. 2363-2373.

151. Petrij, F., Giles, R. H., Dauwerse, H. G., Saris, J. J., Hennekam, R. C., Masuno, M., Tommerup, N., van Ommen, G. J., Goodman, R. H., Peters, D. J. & et al., (1995). Rubinstein-Taybi syndrome caused by mutations in the transcriptional co-activator CBP. *Nature,* **376**: p. 348-51.

152. Muraoka, M., Konishi, M., Kikuchi-Yanoshita, R., Tanaka, K., Shitara, N., Chong, J. M., Iwama, T. & Miyaki, M., (1996). p300 gene alterations in colorectal and gastric carcinomas. *Oncogene,* **12**: p. 1565-9.

153. Sobulo, O. M., Borrow, J., Tomek, R., Reshmi, S., Harden, A., Schlegelberger, B., Housman, D., Doggett, N. A., Rowley, J. D. & Zeleznik-Le, N. J., (1997). MLL is fused to CBP, a histone acetyltransferase, in therapy-related acute myeloid leukemia with a t(11;16)(q23;p13.3). *Proc Natl Acad Sci U S A,* **94**: p. 8732-7.

154. Giles, R. H., (1998). Update CBP/p300 transgenic mice. *Trends Genet,* **14**: p. 214.

155. Gayther, S. A., Batley, S. J., Linger, L., Bannister, A., Thorpe, K., Chin, S. F., Daigo, Y., Russell, P., Wilson, A., Sowter, H. M., Delhanty, J. D., Ponder, B. A., Kouzarides, T. & Caldas, C., (2000). Mutations truncating the EP300 acetylase in

human cancers. *Nat Genet,* **24**: p. 300-3.

156. Kung, A. L., Rebel, V. I., Bronson, R. T., Ch'ng, L. E., Sieff, C. A., Livingston, D. M. & Yao, T. P., (2000). Gene dose-dependent control of hematopoiesis and hematologic tumor suppression by CBP. *Genes Dev,* **14**: p. 272-7.

157. Janknecht, R. & Nordheim, A., (1996). MAP kinase-dependent transcriptional coactivation by Elk-1 and its cofactor CBP. *Biochem Biophys Res Commun,* **228**: p. 831-7.

158. Giordano, A. & Avantaggiati, M. L., (1999). p300 and CBP: partners for life and death. *J Cell Physiol,* **181**: p. 218-30.

159. Goodman, R. H. & Smolik, S., (2000). CBP/p300 in cell growth, transformation, and development. *Genes Dev,* **14**: p. 1553-77.

160. Ngan, V., Goodman, R.H., (2001). CREB-binding Protein and p300 in Transcriptional Regulation. *J Biol Chem,* **276**: p. 13505-13508.

161. Arany, Z., Sellers, W. R., Livingston, D. M. & Eckner, R., (1994). E1A-associated p300 and CREB-associated CBP belong to a conserved family of coactivators. *Cell,* 77: p. 799-800.

162. Arany, Z., Newsome, D., Oldread, E., Livingston, D. M. & Eckner, R., (1995). A family of transcriptional adaptor proteins targeted by the E1A oncoprotein. *Nature,* **374**: p. 81-4.

163. Eckner, R., Ewen, M. E., Newsome, D., Gerdes, M., DeCaprio, J. A., Lawrence, J. B. & Livingston, D. M., (1994). Molecular cloning and functional analysis of the adenovirus E1A-associated 300-kD protein (p300) reveals a protein with properties of a transcriptional adaptor. *Genes Dev,* **8**: p. 869-84.

164. Eckner, R., Ludlow, J. W., Lill, N. L., Oldread, E., Arany, Z., Modjtahedi, N., DeCaprio, J. A., Livingston, D. M. & Morgan, J. A., (1996). Association of p300 and CBP with simian virus 40 large T antigen. *Mol Cell Biol,* **16**: p. 3454-64.

165. Whyte, P., Williamson, N. M. & Harlow, E., (1989). Cellular targets for

transformation by the adenovirus E1A proteins. *Cell,* **56**: p. 67-75.

166. Dyson, N. & Harlow, E., (1992). Adenovirus E1A targets key regulators of cell proliferation. *Cancer Surv,* **12**: p. 161-95.

167. Moran, E., (1993). DNA tumor virus transforming proteins and the cell cycle. *Curr Opin Genet Dev,* **3**: p. 63-70.

168. Missero, C., Calautti, E., Eckner, R., Chin, J., Tsai, L. H., Livingston, D. M. & Dotto, G. P., (1995). Involvement of the cell-cycle inhibitor Cip1/WAF1 and the E1A-associated p300 protein in terminal differentiation. *Proc Natl Acad Sci U S A,* **92**: p. 5451-5.

169. Yang, X. J., Ogryzko, V. V., Nishikawa, J., Howard, B. H. & Nakatani, Y., (1996). A p300/CBP-associated factor that competes with the adenoviral oncoprotein E1A. *Nature,* **382**: p. 319-24.

170. Stein, R. W., Corrigan, M., Yaciuk, P., Whelan, J. & Moran, E., (1990). Analysis of E1A-mediated growth regulation functions: binding of the 300-kilodalton cellular product correlates with E1A enhancer repression function and DNA synthesis-inducing activity. *J Virol,* **64**: p. 4421-7.

171. Eckner, R., Yao, T. P., Oldread, E. & Livingston, D. M., (1996). Interaction and functional collaboration of p300/CBP and bHLH proteins in muscle and B-cell differentiation. *Genes Dev,* **10**: p. 2478-90.

172. Puri, P. L., Avantaggiati, M. L., Balsano, C., Sang, N., Graessmann, A., Giordano, A. & Levrero, M., (1997). p300 is required for MyoD-dependent cell cycle arrest and muscle-specific gene transcription. *Embo J,* **16**: p. 369-83.

173. Puri, P. L., Sartorelli, V., Yang, X. J., Hamamori, Y., Ogryzko, V. V., Howard, B. H., Kedes, L., Wang, J. Y., Graessmann, A., Nakatani, Y. & Levrero, M., (1997). Differential roles of p300 and PCAF acetyltransferases in muscle differentiation. *Mol Cell,* **1**: p. 35-45.

174. Gu, W., Shi, X. L. & Roeder, R. G., (1997). Synergistic activation of transcription

by CBP and p53. *Nature,* **387**: p. 819-23.

175. Imhof, A., Yang, X. J., Ogryzko, V. V., Nakatani, Y., Wolffe, A. P. & Ge, H., (1997). Acetylation of general transcription factors by histone acetyltransferases. *Curr Biol,* **7**: p. 689-92.

176. Boyes, J., Byfield, P., Nakatani, Y. & Ogryzko, V., (1998). Regulation of activity of the transcription factor GATA-1 by acetylation. *Nature,* **396**: p. 594-8.

177. Zhang, W., Bone, J. R., Edmondson, D. G., Turner, B. M. & Roth, S. Y., (1998). Essential and redundant functions of histone acetylation revealed by mutation of target lysines and loss of the Gcn5p acetyltransferase. *Embo J,* **17**: p. 3155-67.

178. Bordoli, L., Husser, S., Luthi, U., Netsch, M., Osmani, H., Eckner, R., (2001). Functional analysis of the p300 acetyltransferase domain: the PHD finger of p300 but not of CBP is dispensable for enzymatic activity. *Nucleic Acids Res,* **29**: p. 4462-4471.

179. Bannister, A. J. & Kouzarides, T., (1996). The CBP co-activator is a histone acetyltransferase. *Nature,* **384**: p. 641-3.

180. Brownell, J. E. & Allis, C. D., (1996). Special HATs for special occasions: linking histone acetylation to chromatin assembly and gene activation. *Curr Opin Genet Dev,* **6**: p. 176-84.

181. Chrivia, J. C., Kwok, R. P., Lamb, N., Hagiwara, M., Montminy, M. R. & Goodman, R. H., (1993). Phosphorylated CREB binds specifically to the nuclear protein CBP. *Nature,* **365**: p. 855-9.

182. Chen, X. N. & Korenberg, J. R., (1995). Localization of human CREBBP (CREB binding protein) to 16p13.3 by fluorescence in situ hybridization. *Cytogenet Cell Genet,* **71**: p. 56-7.

183. Giles, R. H., Dauwerse, H. G., van Ommen, G. J. & Breuning, M. H., (1998). Do human chromosomal bands 16p13 and 22q11-13 share ancestral origins? *Am J Hum Genet,* **63**: p. 1240-2.

184. Dhalluin, C., Carlson, J. E., Zeng, L., He, C., Aggarwal, A. K. & Zhou, M. M., (1999). Structure and ligand of a histone acetyltransferase bromodomain. *Nature,* **399**: p. 491-6.

185. Dallas, P. B., Cheney, I. W., Liao, D. W., Bowrin, V., Byam, W., Pacchione, S., Kobayashi, R., Yaciuk, P. & Moran, E., (1998). p300/CREB binding protein-related protein p270 is a component of mammalian SWI/SNF complexes. *Mol Cell Biol,* **18**: p. 3596-603.

186. Yao, T. P., Oh, S. P., Fuchs, M., Zhou, N. D., Ch'ng, L. E., Newsome, D., Bronson, R. T., Li, E., Livingston, D. M. & Eckner, R., (1998). Gene dosage-dependent embryonic development and proliferation defects in mice lacking the transcriptional integrator p300. *Cell,* **93**: p. 361-72.

187. Tanaka, Y., Naruse, I., Maekawa, T., Masuya, H., Shiroishi, T. & Ishii, S., (1997). Abnormal skeletal patterning in embryos lacking a single Cbp allele: a partial similarity with Rubinstein-Taybi syndrome. *Proc Natl Acad Sci U S A,* **94**: p. 10215-20.

188. Sartorelli, V., Puri, P. L., Hamamori, Y., Ogryzko, V., Chung, G., Nakatani, Y., Wang, J. Y. & Kedes, L., (1999). Acetylation of MyoD directed by PCAF is necessary for the execution of the muscle program. *Mol Cell,* **4**: p. 725-34.

189. Shi, Y. & Mello, C., (1998). A CBP/p300 homolog specifies multiple differentiation pathways in Caenorhabditis elegans. *Genes Dev,* **12**: p. 943-55.

190. Grossman, S. R., Perez, M., Kung, A. L., Joseph, M., Mansur, C., Xiao, Z. X., Kumar, S., Howley, P. M. & Livingston, D. M., (1998). p300/MDM2 complexes participate in MDM2-mediated p53 degradation. *Mol Cell,* **2**: p. 405-15.

191. Morris, L., Allen, K. E. & La Thangue, N. B., (2000). Regulation of E2F transcription by cyclin E-Cdk2 kinase mediated through p300/CBP co-activators. *Nat Cell Biol,* **2**: p. 232-9.

192. Arany, Z., Huang, L. E., Eckner, R., Bhattacharya, S., Jiang, C., Goldberg, M. A.,

Bunn, H. F. & Livingston, D. M., (1996). An essential role for p300/CBP in the cellular response to hypoxia. *Proc Natl Acad Sci U S A,* **93**: p. 12969-73.

193. Carmeliet, P., Dor, Y., Herbert, J. M., Fukumura, D., Brusselmans, K., Dewerchin, M., Neeman, M., Bono, F., Abramovitch, R., Maxwell, P., Koch, C. J., Ratcliffe, P., Moons, L., Jain, R. K., Collen, D. & Keshert, E., (1998). Role of HIF-1alpha in hypoxia-mediated apoptosis, cell proliferation and tumour angiogenesis. *Nature,* **394**: p. 485-90.

194. Avantaggiati, M. L., Ogryzko, V., Gardner, K., Giordano, A., Levine, A. S. & Kelly, K., (1997). Recruitment of p300/CBP in p53-dependent signal pathways. *Cell,* **89**: p. 1175-84.

195. Yuan, Z. M., Huang, Y., Ishiko, T., Nakada, S., Utsugisawa, T., Shioya, H., Utsugisawa, Y., Shi, Y., Weichselbaum, R. & Kufe, D., (1999). Function for p300 and not CBP in the apoptotic response to DNA damage. *Oncogene,* **18**: p. 5714-7.

196. Shikama, N., Lee, C. W., France, S., Delavaine, L., Lyon, J., Krstic-Demonacos, M. & La Thangue, N. B., (1999). A novel cofactor for p300 that regulates the p53 response. *Mol Cell,* **4**: p. 365-76.

197. Eid, J. E., Kung, A. L., Scully, R. & Livingston, D. M., (2000). p300 interacts with the nuclear proto-oncoprotein SYT as part of the active control of cell adhesion. *Cell,* **102**: p. 839-48.

198. Clark, J., Rocques, P. J., Crew, A. J., Gill, S., Shipley, J., Chan, A. M., Gusterson, B. A. & Cooper, C. S., (1994). Identification of novel genes, SYT and SSX, involved in the t(X;18)(p11.2;q11.2) translocation found in human synovial sarcoma. *Nat Genet,* **7**: p. 502-8.

199. Kamei, Y., Xu, L., Heinzel, T., Torchia, J., Kurokawa, R., Gloss, B., Lin, S. C., Heyman, R. A., Rose, D. W., Glass, C. K. & Rosenfeld, M. G., (1996). A CBP integrator complex mediates transcriptional activation and AP-1 inhibition by nuclear receptors. *Cell,* **85**: p. 403-14.

200. Lee, C. W., Sorensen, T. S., Shikama, N. & La Thangue, N. B., (1998). Functional interplay between p53 and E2F through co-activator p300. *Oncogene,* **16**: p. 2695-710.

201. Ogryzko, V. V., Kotani, T., Zhang, X., Schiltz, R. L., Howard, T., Yang, X. J., Howard, B. H., Qin, J. & Nakatani, Y., (1998). Histone-like TAFs within the PCAF histone acetylase complex. *Cell,* **94**: p. 35-44.

202. Yao, T. P., Ku, G., Zhou, N., Scully, R. & Livingston, D. M., (1996). The nuclear hormone receptor coactivator SRC-1 is a specific target of p300. *Proc Natl Acad Sci U S A,* **93**: p. 10626-31.

203. Chen, H., Lin, R. J., Schiltz, R. L., Chakravarti, D., Nash, A., Nagy, L., Privalsky, M. L., Nakatani, Y. & Evans, R. M., (1997). Nuclear receptor coactivator ACTR is a novel histone acetyltransferase and forms a multimeric activation complex with P/CAF and CBP/p300. *Cell,* **90**: p. 569-80.

204. Kim, T. K., Kim, T. H. & Maniatis, T., (1998). Efficient recruitment of TFIIB and CBP-RNA polymerase II holoenzyme by an interferon-beta enhanceosome in vitro. *Proc Natl Acad Sci U S A,* **95**: p. 12191-6.

205. Munshi, N., Merika, M., Yie, J., Senger, K., Chen, G. & Thanos, D., (1998). Acetylation of HMG I(Y) by CBP turns off IFN beta expression by disrupting the enhanceosome. *Mol Cell,* **2**: p. 457-67.

206. Gu, W. & Roeder, R. G., (1997). Activation of p53 sequence-specific DNA binding by acetylation of the p53 C-terminal domain. *Cell,* **90**: p. 595-606.

207. Marzio, G., Wagener, C., Gutierrez, M. I., Cartwright, P., Helin, K. & Giacca, M., (2000). E2F family members are differentially regulated by reversible acetylation. *J Biol Chem,* **275**: p. 10887-92.

208. Tomita, A., Towatari, M., Tsuzuki, S., Hayakawa, F., Kosugi, H., Tamai, K., Miyazaki, T., Kinoshita, T. & Saito, H., (2000). c-Myb acetylation at the carboxyl-terminal conserved domain by transcriptional co-activator p300. *Oncogene,* **19**: p.

444-51.

209. Zhang, W. & Bieker, J. J., (1998). Acetylation and modulation of erythroid Kruppel-like factor (EKLF) activity by interaction with histone acetyltransferases. *Proc Natl Acad Sci U S A,* **95**: p. 9855-60.

210. Soutoglou, E., Katrakili, N. & Talianidis, I., (2000). Acetylation regulates transcription factor activity at multiple levels. *Mol Cell,* **5**: p. 745-51.

211. Li, Q., Herrler, M., Landsberger, N., Kaludov, N., Ogryzko, V. V., Nakatani, Y. & Wolffe, A. P., (1998). Xenopus NF-Y pre-sets chromatin to potentiate p300 and acetylation-responsive transcription from the Xenopus hsp70 promoter in vivo. *Embo J,* **17**: p. 6300-15.

212. Waltzer, L. & Bienz, M., (1998). Drosophila CBP represses the transcription factor TCF to antagonize Wingless signalling. *Nature,* **395**: p. 521-5.

213. Zhang, Q., Yao, H., Vo, N. & Goodman, R. H., (2000). Acetylation of adenovirus E1A regulates binding of the transcriptional corepressor CtBP. *Proc Natl Acad Sci U S A,* **97**: p. 14323-8.

214. Chan, H. M., Krstic-Demonacos, M., Smith, L., Demonacos, C. & La Thangue, N. B., (2001). Acetylation control of the retinoblastoma tumour-suppressor protein. *Nat Cell Biol,* **3**: p. 667-74.

215. Wade, P. A., Jones, P. L., Vermaak, D., Veenstra, G. J., Imhof, A., Sera, T., Tse, C., Ge, H., Shi, Y. B., Hansen, J. C. & Wolffe, A. P., (1998). Histone deacetylase directs the dominant silencing of transcription in chromatin: association with MeCP2 and the Mi-2 chromodomain SWI/SNF ATPase. *Cold Spring Harb Symp Quant Biol,* **63**: p. 435-45.

216. Ogryzko, V. V., Schiltz, R. L., Russanova, V., Howard, B. H. & Nakatani, Y., (1996). The transcriptional coactivators p300 and CBP are histone acetyltransferases. *Cell,* **87**: p. 953-9.

217. Mizzen, C., Kuo, M. H., Smith, E., Brownell, J., Zhou, J., Ohba, R., Wei, Y.,

Monaco, L., Sassone-Corsi, P. & Allis, C. D., (1998). Signaling to chromatin through histone modifications: how clear is the signal? *Cold Spring Harb Symp Quant Biol,* **63**: p. 469-81.

218. Durrin, L. K., Mann, R. K., Kayne, P. S. & Grunstein, M., (1991). Yeast histone H4 N-terminal sequence is required for promoter activation in vivo. *Cell,* **65**: p. 1023-31.

219. Mann, R. K. & Grunstein, M., (1992). Histone H3 N-terminal mutations allow hyperactivation of the yeast GAL1 gene in vivo. *Embo J,* **11**: p. 3297-306.

220. Tse, C., Fletcher, T. M. & Hansen, J. C., (1998). Enhanced transcription factor access to arrays of histone H3/H4 tetramer.DNA complexes in vitro: implications for replication and transcription. *Proc Natl Acad Sci U S A,* **95**: p. 12169-73.

221. Tse, C., Sera, T., Wolffe, A. P. & Hansen, J. C., (1998). Disruption of higher-order folding by core histone acetylation dramatically enhances transcription of nucleosomal arrays by RNA polymerase III. *Mol Cell Biol,* **18**: p. 4629-38.

222. Ito, T., Ikehara, T., Nakagawa, T., Kraus, W. L. & Muramatsu, M., (2000). p300-mediated acetylation facilitates the transfer of histone H2A-H2B dimers from nucleosomes to a histone chaperone. *Genes Dev,* **14**: p. 1899-907.

223. Bulger, M., Ito, T., Kamakaka, R. T. & Kadonaga, J. T., (1995). Assembly of regularly spaced nucleosome arrays by Drosophila chromatin assembly factor 1 and a 56-kDa histone-binding protein. *Proc Natl Acad Sci U S A,* **92**: p. 11726-30.

224. Lee, D. Y., Hayes, J. J., Pruss, D. & Wolffe, A. P., (1993). A positive role for histone acetylation in transcription factor access to nucleosomal DNA. *Cell,* **72**: p. 73-84.

225. Turner, B. M., (1991). Histone acetylation and control of gene expression. *J Cell Sci,* **99 (Pt 1)**: p. 13-20.

226. Nightingale, K. P., Wellinger, R. E., Sogo, J. M. & Becker, P. B., (1998). Histone acetylation facilitates RNA polymerase II transcription of the Drosophila hsp26

gene in chromatin. *Embo J,* **17**: p. 2865-76.

227. Li, Q., Imhof, A., Collingwood, T. N., Urnov, F. D. & Wolffe, A. P., (1999). p300 stimulates transcription instigated by ligand-bound thyroid hormone receptor at a step subsequent to chromatin disruption. *Embo J,* **18**: p. 5634-52.

228. Ou, Y. H., Chung, P. H., Sun, T. P. & Shieh, S. Y., (2005). p53 C-terminal phosphorylation by CHK1 and CHK2 participates in the regulation of DNA-damage-induced C-terminal acetylation. *Mol Biol Cell,* **16**: p. 1684-95.

229. Stevens, C., Smith, L. & La Thangue, N. B., (2003). Chk2 activates E2F-1 in response to DNA damage. *Nat Cell Biol,* **5**: p. 401.

230. Bandara, L. R., Adamczewski, J. P., Hunt, T. & La Thangue, N. B., (1991). Cyclin A and the retinoblastoma gene product complex with a common transcription factor. *Nature,* **352**: p. 249-51.

231. Siegert, J. L. & Robbins, P. D., (1999). Rb inhibits the intrinsic kinase activity of TATA-binding protein-associated factor TAFII250. *Mol Cell Biol,* **19**: p. 846-54.

232. Lee, E. Y., Chang, C. Y., Hu, N., Wang, Y. C., Lai, C. C., Herrup, K., Lee, W. H. & Bradley, A., (1992). Mice deficient for Rb are nonviable and show defects in neurogenesis and haematopoiesis. *Nature,* **359**: p. 288-94.

233. Bandara, L. R., Buck, V. M., Zamanian, M., Johnston, L. H. & La Thangue, N. B., (1993). Functional synergy between DP-1 and E2F-1 in the cell cycle-regulating transcription factor DRTF1/E2F. *Embo J,* **12**: p. 4317-24.

234. Loughran, O. & La Thangue, N. B., (2000). Apoptotic and growth-promoting activity of E2F modulated by MDM2. *Mol Cell Biol,* **20**: p. 2186-97.

235. Dignam, J. D., Martin, P. L., Shastry, B. S. & Roeder, R. G., (1983). Eukaryotic gene transcription with purified components. *Methods Enzymol,* **101**: p. 582-98.

236. Gonzalez, F. A., Seth, A., Raden, D. L., Bowman, D. S., Fay, F. S. & Davis, R. J., (1993). Serum-induced translocation of mitogen-activated protein kinase to the cell surface ruffling membrane and the nucleus. *J Cell Biol,* **122**: p. 1089-101.

237. Thompson, P. R., Wang, D., Wang, L., Fulco, M., Pediconi, N., Zhang, D., An, W., Ge, Q., Roeder, R. G., Wong, J., Levrero, M., Sartorelli, V., Cotter, R. J. & Cole, P. A., (2004). Regulation of the p300 HAT domain via a novel activation loop. *Nat Struct Mol Biol,* **11**: p. 308-15.

238. Takasaki, Y., Deng, J. S., Tan, E. M., (1981). A Nuclear antigen associated with cell proliferation and blast transformation. *Journal of Experi Medicine,* **154**: p. 1899-1909.

239. Schmitz, H. D., Dutine, C., Bereiter-Hahn, J. , (2003). Exportin 1- independent nuclear export of GAPDH. *Cell Biology International,* **27**: p. 511-517.

240. Hsieh, J. K., Fredersdorf, S., Kouzarides, T., Martin, K. & Lu, X., (1997). E2F1-induced apoptosis requires DNA binding but not transactivation and is inhibited by the retinoblastoma protein through direct interaction. *Genes Dev,* **11**: p. 1840-52.

241. Qin, X. Q., Livingston, D. M., Kaelin, W. G., Jr. & Adams, P. D., (1994). Deregulated transcription factor E2F-1 expression leads to S-phase entry and p53-mediated apoptosis. *Proc Natl Acad Sci U S A,* **91**: p. 10918-22.

242. Wu, X. & Levine, A. J., (1994). p53 and E2F-1 cooperate to mediate apoptosis. *Proc Natl Acad Sci U S A,* **91**: p. 3602-6.

243. Kowalik, T. F., DeGregori, J., Schwarz, J. K. & Nevins, J. R., (1995). E2F1 overexpression in quiescent fibroblasts leads to induction of cellular DNA synthesis and apoptosis. *J Virol,* **69**: p. 2491-500.

244. Field, S. J., Tsai, F. Y., Kuo, F., Zubiaga, A. M., Kaelin, W. G., Jr., Livingston, D. M., Orkin, S. H. & Greenberg, M. E., (1996). E2F-1 functions in mice to promote apoptosis and suppress proliferation. *Cell,* **85**: p. 549-61.

245. Fan, G. & Steer, C. J., (1999). The role of retinoblastoma protein in apoptosis. *Apoptosis,* **4**: p. 21-9.

246. Graham, F. L., Smiley, J., Russell, W. C. & Nairn, R., (1977). Characteristics of a human cell line transformed by DNA from human adenovirus type 5. *J Gen Virol,*

36: p. 59-74.

247. Bordo, D. & Argos, P., (1991). Suggestions for "safe" residue substitutions in site-directed mutagenesis. *J Mol Biol,* **217**: p. 721-9.

248. French, S., Robson, B, (1983). What is a conservative substitution? *J.Mol. Evol,* **19**: p. 171-175.

249. Taylor, W. R., (1986). The classification of amino acid conservation. *J Theor Biol,* **119**: p. 205-18.

250. Piluso, L. G., Wei, G., Li, A. G. & Liu, X., (2005). Purification of acetyl-p53 using p300 co-infection and the baculovirus expression system. *Protein Expr Purif,* **40**: p. 370-8.

251. Zacksenhaus, E., Bremner, R., Phillips, R. A. & Gallie, B. L., (1993). A bipartite nuclear localization signal in the retinoblastoma gene product and its importance for biological activity. *Mol Cell Biol,* **13**: p. 4588-99.

252. Hu, W., Kemp, B. E. & Jans, D. A., (2005). Kinetic properties of nuclear transport conferred by the retinoblastoma (Rb) NLS. *J Cell Biochem,* **95**: p. 782-93.

253. Zacksenhaus, E., Jiang, Z., Hei, Y. J., Phillips, R. A. & Gallie, B. L., (1999). Nuclear localization conferred by the pocket domain of the retinoblastoma gene product. *Biochim Biophys Acta,* **1451**: p. 288-96.

254. Klutz, M., Horsthemke, B. & Lohmann, D. R., (1999). RB1 gene mutations in peripheral blood DNA of patients with isolated unilateral retinoblastoma. *Am J Hum Genet,* **64**: p. 667-8.

255. Nakada, S., Katsuki, Y., Imoto, I., Yokoyama, T., Nagasawa, M., Inazawa, J. & Mizutani, S., (2006). Early G2/M checkpoint failure as a molecular mechanism underlying etoposide-induced chromosomal aberrations. *J Clin Invest,* **116**: p. 80-89.

256. Adams, P. D., Sellers, W. R., Sharma, S. K., Wu, A. D., Nalin, C. M. & Kaelin, W. G., Jr., (1996). Identification of a cyclin-cdk2 recognition motif present in

substrates and p21-like cyclin-dependent kinase inhibitors. *Mol Cell Biol,* **16**: p. 6623-33.

257. Sebastian, T., Malik, R., Thomas, S., Sage, J. & Johnson, P. F., (2005). C/EBPbeta cooperates with RB:E2F to implement Ras(V12)-induced cellular senescence. *Embo J,* **24**: p. 3301-12.

258. Hiebert, S. W., Packham, G., Strom, D. K., Haffner, R., Oren, M., Zambetti, G. & Cleveland, J. L., (1995). E2F-1:DP-1 induces p53 and overrides survival factors to trigger apoptosis. *Mol Cell Biol,* **15**: p. 6864-74.

259. Krek, W., Xu, G. & Livingston, D. M., (1995). Cyclin A-kinase regulation of E2F-1 DNA binding function underlies suppression of an S phase checkpoint. *Cell,* **83**: p. 1149-58.

260. Shan, B., Farmer, A. A. & Lee, W. H., (1996). The molecular basis of E2F-1/DP-1-induced S-phase entry and apoptosis. *Cell Growth Differ,* **7**: p. 689-97.

261. Lam, E. W. & La Thangue, N. B., (1994). DP and E2F proteins: coordinating transcription with cell cycle progression. *Curr Opin Cell Biol,* **6**: p. 859-66.

262. Wu, C. L., Zukerberg, L. R., Ngwu, C., Harlow, E. & Lees, J. A., (1995). In vivo association of E2F and DP family proteins. *Mol Cell Biol,* **15**: p. 2536-46.

263. Barlev, N. A., Liu, L., Chehab, N. H., Mansfield, K., Harris, K. G., Halazonetis, T. D. & Berger, S. L., (2001). Acetylation of p53 activates transcription through recruitment of coactivators/histone acetyltransferases. *Mol Cell,* **8**: p. 1243-54.

264. Marti, A., Wirbelauer, C., Scheffner, M. & Krek, W., (1999). Interaction between ubiquitin-protein ligase SCFSKP2 and E2F-1 underlies the regulation of E2F-1 degradation. *Nat Cell Biol,* **1**: p. 14-9.

265. Rogoff, H. A., Pickering, M. T., Frame, F. M., Debatis, M. E., Sanchez, Y., Jones, S. & Kowalik, T. F., (2004). Apoptosis associated with deregulated E2F activity is dependent on E2F1 and Atm/Nbs1/Chk2. *Mol Cell Biol,* **24**: p. 2968-77.

266. Smith, E. D., Kudlow, B. A., Frock, R. L. & Kennedy, B. K., (2005). A-type

nuclear lamins, progerias and other degenerative disorders. *Mech Ageing Dev,* **126**: p. 447-60.

267. Johnson, B. R., Nitta, R. T., Frock, R. L., Mounkes, L., Barbie, D. A., Stewart, C. L., Harlow, E. & Kennedy, B. K., (2004). A-type lamins regulate retinoblastoma protein function by promoting subnuclear localization and preventing proteasomal degradation. *Proc Natl Acad Sci U S A,* **101**: p. 9677-82.

268. Markiewicz, E., Dechat, T., Foisner, R., Quinlan, R. A. & Hutchison, C. J., (2002). Lamin A/C binding protein LAP2alpha is required for nuclear anchorage of retinoblastoma protein. *Mol Biol Cell,* **13**: p. 4401-13.

269. Avni, D., Yang, H., Martelli, F., Hofmann, F., ElShamy, W. M., Ganesan, S., Scully, R. & Livingston, D. M., (2003). Active localization of the retinoblastoma protein in chromatin and its response to S phase DNA damage. *Mol Cell,* **12**: p. 735-46.

270. Vousden, K. H. & Lu, X., (2002). Live or let die: the cell's response to p53. *Nat Rev Cancer,* **2**: p. 594-604.

271. Vigushin, D. M. & Coombes, R. C., (2002). Histone deacetylase inhibitors in cancer treatment. *Anticancer Drugs,* **13**: p. 1-13.